THE BIOLOGICAL SIGNIFICANCE OF OSTEOCYTE APOPTOSIS

By

GEORGIA KOGIANNI

A Thesis submitted for the degree of Doctor of Philosophy
The University of Edinburgh
September 2004

Thesis Abstract

The maintenance of the functional and structural integrity of our skeleton requires the accurate spatial targeting of the activity of bone forming and resorbing cells, such that functional adaptation occurs and microdamage is repaired. Osteocytes are thought to be ideal candidates for targeting the remodeling process to specific sites, although little evidence exists to support this. More recently they have been proposed to direct turnover through their apoptotic death. Work in this thesis has focused on identifying a biological role for osteocyte apoptosis, the identity of osteocyte-derived resorption targeting signals and addresses the design of methods to blockade the excess apoptosis observed during the use of glucocorticoids. High levels of osteocyte apoptosis have been seen to co-localise with sites of bone resorption and to precede the resorption event, raising the possibility that signals derived from dying osteocytes direct osteoclasts to bone requiring remodeling; however the mechanism underlying this phenomenon is unknown. Many osteoclastic activities have been shown previously to be controlled, not directly, but via signals produced by osteoblastic cells. For this reason I have studied the effects of osteocyte apoptotic bodies on osteoblastic cells. Apoptotic bodies derived from different cell types were also used to determine behavioural responses in osteoblast and other potential target cells. Osteoblasts were shown to undergo apoptosis upon contact with osteocyte apoptotic bodies, while apoptotic products derived from different cell types, did not induce osteoblast death. Furthermore, target cells other than osteoblasts, did not undergo apoptosis in the presence of osteocyte or other cell type apoptotic products. These data indicated a specific role for osteocyte apoptosis in the bone microenvironment that might be directing the behaviour of osteoblasts in the bone remodeling process. In addition, the demonstration of phenotypic specificity in the apoptotic body-derived signals points to a further level of physiological "meaning" to apoptosis. The physical interaction of apoptotic osteocytes with osteoblasts and the resultant osteoblast death were dependent on membrane changes in the apoptotic body and appeared to involve the phagocytic receptors CD14 and scavenger receptor A as evidenced by using gene knockout animal models.

Having identified an important potential role for apoptotic osteocytes in targeting osteoblast removal at sites of remodeling, mechanisms that could interfere with the induction of osteocyte apoptosis in response to Dexamethasone were investigated. Dexamethasone-induced apoptosis was associated with activation of the Fas death receptor and ERK1/2 pathways. Bisphosphonates suppressed the pro-apoptotic stimuli, independently of their detailed structure and their in vivo anti-resorptive potency. These data suggested that bisphosphonates could provide therapeutic approaches against excess osteocytic death observed in glucocorticoid-induced osteoporosis in order to maintain a balance between osteocyte viability and death, which might ultimately lead to stabilised bone turnover activity and better bone quality.

Declaration

I hereby declare that this thesis has been composed by myself and is the result of my own work. I was assisted through the donation of cellular material as clearly indicated throughout the text of the thesis. This work has neither been presented nor accepted in any previous application for a degree.

Georgia Kogianni
2004.

Acknowledgements

I would like to thank Prof. Hamish Simpson and Dr. Brendon Noble for the support and guidance during my PhD in the Musculoskeletal Research Unit.

I am particularly obliged to Dr. Brendon Noble for the encouragement and continuous support he has provided me with, throughout my studies. I am thankful for his critical and occasionally ruthless judgment and the enthusiastic and inspiring guidance that motivated me to carry out and complete these studies.

I would like to thank Dr. Val Mann and Steph Collishaw for their advice and assistance and all the people working in the group who have all made my time more enjoyable during my studies. Special thanks to my friends Christina, Popi and Makis, my mother Eleni and my brother Vassilis for their patience, support, optimism and loving care that helped me complete my PhD.

I am grateful to Dr. Simon Brown and Dr. Jerremy Duffield (University of Edinburgh, UK) for provision of human and murine haematopoietic cells. I would like to thank Dr. Sarah Howie (University of Edinburgh, UK) for provision of murine spleen cells and lymphocytes and Prof. Peter Nijweide (Leiden University, Netherlands) for provision of primary chicken osteocytes. I am particularly indebted to Prof. Chris Gregory, Dr. Andrew Devitt and Dr. Adam Lacy-Hulbert (University of Edinburgh, UK) for provision of transgenic mouse models and Prof. Mike Rogers (University of Aberdeen, UK) for providing bisphosphonate molecules.

With great admiration and love to my mother and brother

Contents

Figure index

Table index

Abbreviations

AB	apoptotic bodies
ABC-1	ATP-binding cassette-1
ACAMPs	apoptotic cell associated molecular patterns
ADP	adenosine monophosphate
$AgNO_3$	Silver Nitrate
ALN	Alendronate
APS	Ammonium persulphate
ANOVA	analysis of variance
AO	acridine orange
ATP	adenosine triphosphate
Bcl-2	B-cell lymphoma/leukemia-2
BMPs	bone morphogenetic proteins
BMUs	basic multicellular units
BP	bisphosphonate
bp	base pair
BrdU	5-bromo-2 deoxyuridine
BSA	bovine serum albumin
Ca^{2+}	Calcium ion
Caspases	cysteine aspartate proteases
Cbfa1	core-binding factor-1
cDNA	complementary DNA
CFU-GM	colony-forming unit for the granulocyte-macrophage series
CLO	Clodronate
CM	conditioned medium
CMFDA	5-choromethylfluorescein diacetate
CMTMR	5-(-6)-(((4-chloromethyl)benzoyl)amino)tetramethylrhodamine
CO_2	carbon dioxide
cx	connexin

DAPI	4',6-Diamidino-2-phenylindole
dATP	2'-deoxy-adenosine 5'-triphosphate
dCTP	2'-deoxy-cytidine 5'-triphosphate
dGTP	2'-deoxy-guanosine 5'-triphosphate
dUTP	2'-deoxy-uracil 5'-triphosphate
Dex	Dexamethasone
DFF45	DNA fragmentation factor 45
ICAD	Inhibitor of caspase activated deoxyribonuclease
DIG	Digoxigenin
DMEM	Dulbecco's Modified Eagle's Medium
DMSO	dimethyl sulfoxide
DNA	deoxyribonucleic acid
dNTP	deoxynucleoside triphosphate
ecNOS	endothelial cell NO synthase
EDTA	Ethylenediaminetetraacetic acid
EGTA	Ethylene-bis(oxyethylenenitrilo)tetraacetic acid
ECL	Enhanced Chemiluminscence
ERK	extracellular signal regulated kinase
FADD	FAS associated death domain-containing protein
FasL	Fas ligand
FasR	fas receptor
FBS	fetal bovine serum
FGF	fibroblast growth factor
FITC	fluorescein isothiocyanate
FPP	farnesyl diphosphate
g	acceleration of gravity
gm	gram
GCs	glucocorticoids
GLAST	glutamate and aspartate transporter
H-	hydrogen atom-
h	hour/s
H&E	Hematoxylin & Eosin

H_2O	water
H_2O_2	hydrogen peroxide
HCl	Hydrogen chloride
HNO_2	nitrous acid
IGF	insulin-like growth factor
Ihh	Indian Hedgehog
I-kB	inhibitor of kB
IL	interleukin
JNK	c-Jun N-terminal kinase
kDa	kilo dalton
l	litre
L-NAME	N-Nitro-L-arginine methylester hydrochloride
LPS	lipopolysaccharide
LRP5	low density lipoprotein-receptor related protein 5
M	molarity
MAb	monoclonal antibody
MACS	magnetic activated cell sorting
mAmps	milli ampers
MAPK	mitogen activated protein kinase
M-CSF	macrophage colony-stimulating factor
MEK1/2	MAPK/ERK kinase
MEM	Minimum Essential Medium Eagle
MEPE	matrix extracellular phosphoglycoprotein
mg	milligram
$MgCl_2$	magnesium chloride
MHC	major histocompatibility complex
ml	millilitre
mM	millimolar
mRNA	messenger ribonucleic acid
Na_3VO_4	sodium orthovanadate
NaAc	sodium acetate
NaCl	sodium chloride

NaF	sodium fluoride
N-BPs	nitrogen containing bisphosphonates
NCS	newborn calf serum
NED	N-(1-Naphthyl)-ethylenediamine
NF-kB	Nuclear factor kappa B
nanogram	ng
NGF	Nerve growth factor
NHI	National Health Insurance
nm	nanomolar
NO	nitric oxide
NT	nick translation
OAB	osteocyte apoptotic bodies
OF45	osteoblast/osteocyte factor 45
OH-	hydroxyl group
oxLDL	oxidised low density-lipoprotein
P	phosphate
P/S	penicillin/streptomycin
PAGE	polyacrylamide gel
PAM	pamidronate
PARP	poly(ADP-ribose) polymerase
PBMCs	peripheral blood monocytes
PBS	phosphate buffer saline
PCR	polymerase chain reaction
PT pore	permeability transition
PGE_2	prostaglandin E_2
PHEX	Phosphate regulating gene with Homologies to Endopeptidases on the X chromosome
PI	propidium iodide
PI3 kinase	phosphoinositide 3-OH-kinase
PMA	phorbol 12-myristate 13-acetate;
PMN	Polymorphonuclear
PMSF	phenyl- methylsulfonyl fluoride

PRR	pattern recognition receptor
PS	phosphatidylserine
PTH	parathyroid hormone
PTHrP	parathyroid hormone-related protein
PtSerR	PS receptors
PVDF	polyvinylidene difluoride
RANK	receptor for activation of nuclear factor kB
RANKL	RANK ligand
RGD	Arg-Gly-Glu
RNA	Ribonucleic acid
RPMI medium	Roswell Park Memorial Institute medium
RT	Room temperature
RT-PCR	Reverse Transcription-polymerase chain reaction
S.D	Standard deviation
SDS	sodium dodecyl sulphate
SRA	scavenger receptor A
TBS-T	tris buffer saline-tween 20
TEMED	N,N,N',N'-tetramethylethylenediamine
TESPA	3-aminopropylnethoxy-silane
TGF-α	transforming growth factor α
TGF-β	transforming growth factor-β
TLR	Toll-like receptors
TNFα	tumour necrosis factor α
TNFR	tumour necrosis factor receptor
TRADD	TNF associated death domain-containing protein
TRAFs	TNF-R-associated factors
TSP1	thrombospondin 1
WT	wild-type
αMEM	Modified Eagles Medium Alpha
μM	micromolar

SECTION 1

Introduction

CHAPTER 1

Bone

1.1 Introduction

Bone is a rigid form of connective tissue that supports locomotion as a site for muscle attachment, provides protection for vital organs, nurtures the bone marrow and stores ions such as calcium and phosphate that participate in serum homeostasis (Felsenfeld 1999, Rasmussen 1971, Einhorn 1996, Baron 1996). Bone is a dynamic tissue that has the ability to adapt its architecture as a result of continuous modelling and remodelling cycles throughout life according to structural and mechanical requirements (Wolff 1892, Turner 1992, Parfitt 1994). The processes of bone modelling and remodelling are regulated by a variety of osteotropic cytokines and hormones, which influence the activity of bone cells in order to maintain coupling between bone resorption and formation (Rodan 1992, Rodan and Fleisch 1996). Imbalances in these interactions result in abnormal turnover cycles, characterised by insufficient formation of bone resorbing or forming cells, increased resorptive or forming activity or abnormal formation of mineral crystals, leading to diseases such as osteoporosis, Paget's disease of bone, osteolytic and osteosclerotic bone diseases. (Russell et al. 2001, Rodan and Martin 2000, Helfrich 2003).

Repair of damage and adaptation of bone to specific architectural requirements, depends on the targeted activity of bone forming and resorbing cells (Parfitt 2002). Osteocytes have been proposed to act as the mechanosensors and transducers in bone (Lanyon 1993, Zhang et al. 1997, Noble et al. 2003); however very little is known about the mechanism by which osteocytes direct the activity of bone resorbing or forming cells, resulting in targeted remodelling of bone according to structural and mechanical requirements. The aim of this thesis was to investigate the apoptosis of osteocytes and discuss the significance of this death on the targeted remodelling and the regulation of bone homeostasis. This section outlines the basic structural and functional organisation of bone and describes aspects of osteocyte function. In addition, it summarises the basic pathways of apoptosis and describes the current knowledge on apoptotic bone cell death.

1.2 Bone structure and modelling

Bones consist of hydroxyapatite crystals, collagenous and non-collagenous proteins and can be categorised into flat bones formed by intramembranous ossification, and long bones comprised of trabecular and cortical bone, which are formed by endochondral ossification (Carter and Orr 1992, Parfitt 1994, Baron 1996). Cortical bone encloses the medullary cavity and is composed of osteons oriented in the direction of maximal stress, surrounded by lamellae and interstitial bone, while macroscopically, trabecular bone has a spongy appearance and consists of a network of thin bone bridges oriented to resist mechanical loading (Einhorn 1996, Weiner et al. 1999, Sikavitsas et al. 2001). Spaces between trabeculae are filled with bone marrow (Baron 1996). During intramembranous ossification, mesenchymal cells differentiate into preosteoblasts and osteoblasts, which synthesise woven bone that is characterised by irregular calcification and arrangement of collagen fibres, and high osteocyte cell density, which is then progressively replaced by lamellar bone (Turner 1992, Weiner and Wagner 1998, Sikavitsas et al. 2001). During endochondral ossification, mesenchymal cells differentiate into prechondroblasts and chondroblasts that secrete cartilaginous matrix. Chondroblasts become embedded in their own matrix and turn into chondrocytes, which engender longitudinal growth (Parfitt 1976, Carter et al 1996). As chondroblasts continue to proliferate, more chondrocytes are formed which move away from the proliferative zone and become larger, while the matrix that surrounds them starts to calcify. This process is controlled by factors such as parathyroid hormone-related protein (PTHrP), Indian Hedgehog (Ihh) and bone morphogenetic proteins (BMPs) (Strewler 2001). Osteoclasts then, resorb the calcified matrix, while osteoblasts form the woven bone. (Parfitt 1994, Weiner and Wagner 1998, Boyde 1980).

1.3 Bone remodelling

Bone remodelling or turnover is the process by which old or damaged bone is replaced by new bone (Mundy 1995). Bone turnover occurs in basic multicellular units (BMUs) (Frost 1969) and involves a sequence of events, which include formation and activation of osteoclasts which carry out bone resorption, recruitment of osteoblasts which secrete new bone that eventually becomes mineralised, thus

completing the remodelling process, while that particular site returns to a quiescent state (Parfitt 1994, Parfitt 2002) (**Figure 1**).

Wolff's law has stated that changes in the form and function of bone are followed by specific changes in the internal bone architecture and external conformation, in accordance with quantitative laws (Wolff 1892). This law has provided the fundamental basis for understanding the skeleton in both physiological and pathological conditions and indicates that bone has the ability to sense structural and mechanical requirements, repair any damage occurring as a result of everyday use and adapt its architecture to maintain a constant reliability level, as a result of continuous modelling and remodelling cycles throughout life (Turner 1992, Parfitt 1994). Bone turnover can be non-site dependent or directed against specific sites (Parfitt 2002). Non-targeted remodelling could occur for example in order to restore mineral balance, while the maintenance of structural and mechanical integrity in bone is largely dependent on targeted remodelling (Burr 2002). The latter requires a method to direct the activity of bone resorbing and bone forming cells to specific sites, as it has been demonstrated by several studies which induced microdamage by loading canine (Burr and Martin 1993) or rat bone (Verborgt et al. 2000, Noble et al. 2003), which was followed by increased remodelling activity. However, targeted turnover also requires a method to detect the specific mechanical requirements, which is further discussed in §1.5.3 and §2.8.4.

1.4 Bone forming and resorbing cells

Osteoclasts are large, multinucleated cells, formed by the fusion of mononuclear progenitors (the CFU-GM, colony-forming unit for the granulocyte-macrophage series) in the bone marrow, which have the capacity in response to appropriate stimuli, to differentiate into a granulocyte, monocyte or osteoclast (Felix et al. 1994, Mundy 1996). The osteoclast is characterised by a ruffled border that polarises the cell on the bone surface (Mostov and Werb 1997). Acidification of bone is induced by an electrogenic proton ATPase, whereas the abundant Golgi complexes and a large endoplasmic reticulum compartment produce and process lysosomal and

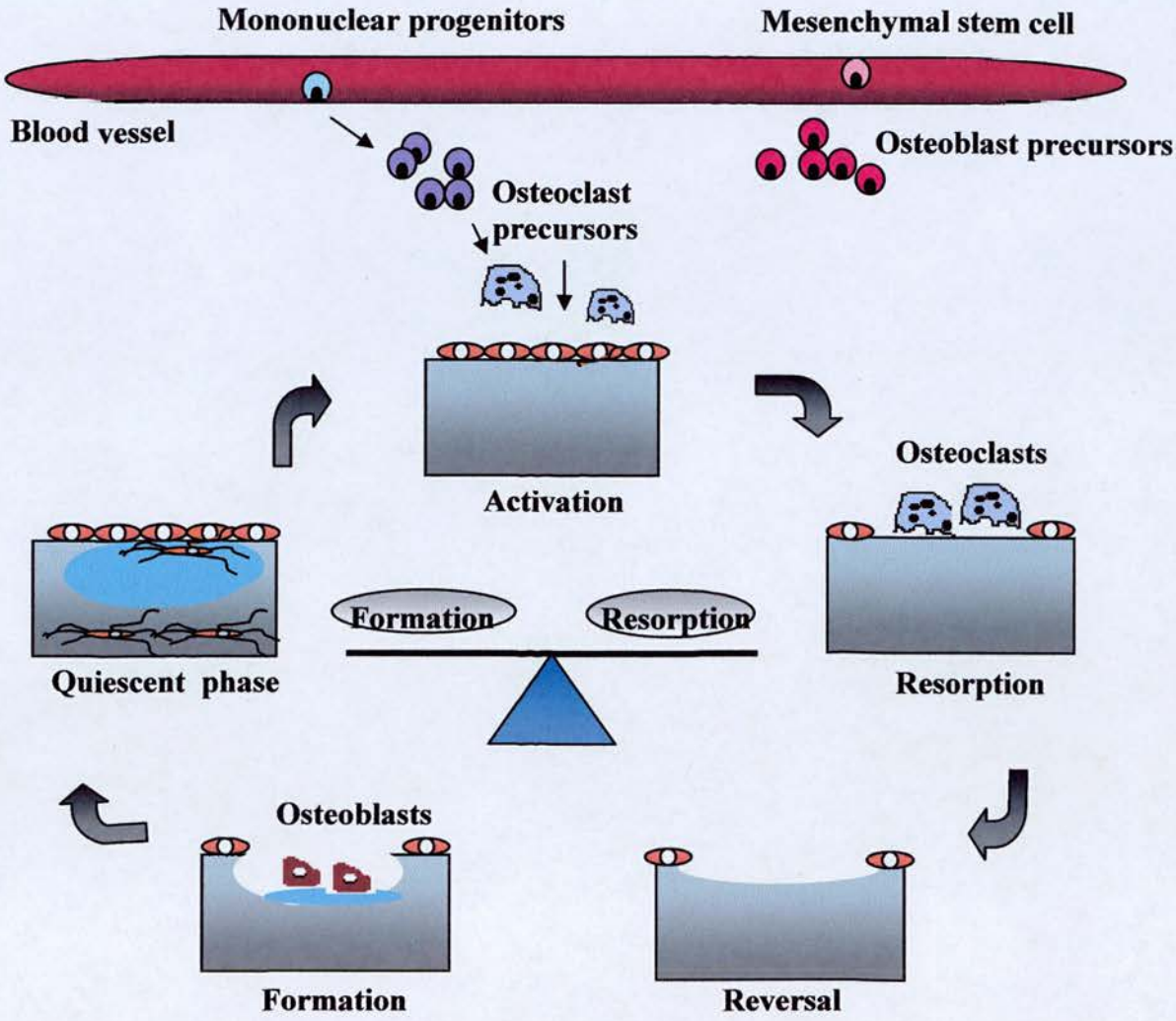

Figure 1. Representation of bone turnover cycle. Osteoclasts are activated to resorb bone at a particular bone surface, followed by bone formation by osteoblasts, in a sequence of events known as activation-resorption-reversal-formation process.

proteolytic enzymes, which are secreted via the ruffled border in the localised environment and carry out bone degradation (Teitelbaum 2000). As members of the monocyte/macrophage family of phagocytes described in §2.7, osteoclasts readily phagocytose bone minerals through the protrusion of pseudopodia around the particles followed by endophagosome formation and lysosomal degradation (Wenisch et al. 2003, Wang et al. 1997). In addition, it has been proposed that osteoclasts phagocytose apoptotic cells as demonstrated by the appearance of apoptotic fragments possibly derived from osteoblasts and/or osteocytes in large vacuoles within osteoclasts, in alveolar bone of young rats (Boabaid et al. 2001, Cerri et al. 2003).

Formation and differentiation of osteoclast precursors is under the control of several factors, including PTH, tumour necrosis factor α (TNFα), transforming growth factor α (TGF-α), interleukin-1 (IL-1) and 1,25-dihydroxyvitamin D_3 (Blair 1998). However, osteoclastogenesis particularly depends on a soluble product known as the macrophage colony-stimulating factor (M-CSF) and the receptor for activation of nuclear factor kB (RANK) ligand, also known as osteoprotegerin ligand, which requires contact with osteoblast progenitor cells and marrow stromal cells (Kong et al. 1999, Miyamoto et al. 2000). These latter cells express the membrane-bound molecule RANKL and OPG, a soluble decoy receptor that competes with RANK for RANKL regulating osteoclast formation (Lacey et al. 2000, Teitelbaum 2000).

Osteoblasts are derived from bone marrow stromal cells or connective tissue mesenchymal stem cells (Prockop 1997), and can appear as flat cells or be characterised by a round nucleus, multiple Golgi stacks, and a well-developed endoplasmic reticulum (Puzas 1996). In addition they are characterised by cytoplasmic processes extending into the osteoid tissue, with which they communicate with osteocytes in their canaliculi and gap junctions to communicate with other osteoblasts (Baron 1996, Schiller et al. 2000). Central to osteoblast differentiation is the transcription factor core-binding factor-1 (Cbfa1), expressed in mesenchymal cells destined to become chondrocytes or osteoblasts (Harada et al. 1999, Ducy et al. 2000) and Indian Hedgehog, which regulates expression of PTH

and PTHrP controlling chondrocyte hypertrophy. Other growth factors involved in osteogenesis include the BMPs, TGF-β and members of the fibroblast growth factor family (FGF) and the insulin-like growth factor (IGF) family (Harada and Rodan 2003, Siddhanti and Quarles 1994). These factors are expressed during proliferation of progenitor cells, along with matrix components, such as type I collagen and fibronectin (Ducy et al. 2000, Puzas 1996). At the same time, gene products appear that are associated with a mature matrix, such as alkaline phosphatase and matrix gla-protein, followed by products such as osteopontin and osteocalcin which result in hydroxyapatite accumulation and completion of mineralisation (Yamaguchi et al. 2000, Puzas 1996). Osteoblastic activity is also influenced by hormones such as PTH, 1,25-dihydroxyvitamin D_3, glucocorticoid hormones and gonadal steroids (Strewler 2001). Recent studies have identified a role for LRP5 (low density lipoprotein-receptor related protein 5), in the transcription control of bone formation, also linked to Wnt signalling involved in developmental processes, as gain of function mutation led to high bone mass while loss of function led to osteoporosis-pseudoglioma syndrome (Little et al. 2002, Boyden et al. 2002). Furthermore, studies have identified the gene Sclerostin (SOST), encoding for a protein that binds BMPs and suppresses their activity in bone, decreasing bone formation (Balemans et al. 2001, Brunkow et al. 2001). Finally, evidence have suggested a role for the central nervous system in the regulation of bone formation, as leptin deficiency induced high bone mass independently of its anti-appetite effects (Ducy et al. 2000, Corral et al. 1998). At the end of the secretion period, mature osteoblasts are found on the bone surface in clusters of cuboidal cells, as bone lining cells, undergo apoptosis or become osteocytes (Jilka et al. 1998, Karsdal et al. 2002).

1.5 Osteocytes

1.5.1 Definition and morphology

Osteocytes are terminally differentiated, postmitotic cells that reside in lacunae within the matrix of both cancellous and cortical bone (Aarden et al. 1994, Sikavitsas et al. 2001). Osteocytes are formed from bone surface osteoblasts that have become encased by their own matrix production, which eventually calcifies (Aarden et al. 1996). It has been suggested that a limited number of osteoblasts can become

osteocytes (Palumbo et al. 1990a,b); however the signals that direct this differentiation have not been identified yet. During their differentiation, osteocytes acquire long dendritic-like processes, which extend through the matrix via the canaliculi and form a communication network between other osteocytes and osteoblasts lining the bone surface (Aarden et al 1996, Palumbo et al. 1990a,b Noble et al 2000). Canaliculi are small channels, formed around previously existing osteoblast processes and allow the diffusion of nutrients and waste products in and out of the tissue.

Osteocytes have smaller cell volume than osteoblastic cells; however, they possess most of the ultrastructural characteristics of an osteoblast including many mitochondria and ribosomes and well-developed Golgi apparatus and endoplasmic reticulum (**Figure 2 and Figure 3**) (Aarden et al. 1994). Osteocytes are embedded in hard matrix and therefore are difficult to investigate. Very few studies using primary osteocytes are available to date. Nijweide et al. have developed an antibody termed mAb OB7.3 (see §1.5.3.3) that reacted specifically with avian osteocytes (Nijweide and Mulder 1986). Isolation from chicken calvariae and investigation of these cells in culture revealed that osteocytes remain postmitotic following their extraction and retain some of the osteoblastic characteristics, such as alkaline phosphatase activity and PTH receptors (Van der Plaas et al. 1994). Recently, an osteocytic-like cell line called MLO-Y4, derived from murine long bones was developed enabling the investigation of several signal transduction pathways, as discussed in §1.5.3. MLO-Y4 osteocyte-like cells were isolated from transgenic mice, in which the SV40 large T-antigen expression was under the control of the osteocalcin promoter (Kato et al. 1997). The cells were able to proliferate and express large amounts of osteocalcin (Kato et al. 1997), a characteristic of osteocytes (Mikuni-Takagaki et al. 1995), which possibly prevents mineralisation of the tissue around the cell body. The cell line is also characterised by long cytoplasmic processes (**Figure 3**), low alkaline phosphatase activity, low collagen type I mRNA expression, osteopontin and connexin 43 mRNA expression, which is important for communication between cells (Kato et al. 1997). Because of the abundance of osteocytes in bone and the communication network that they form, several functions have been proposed for

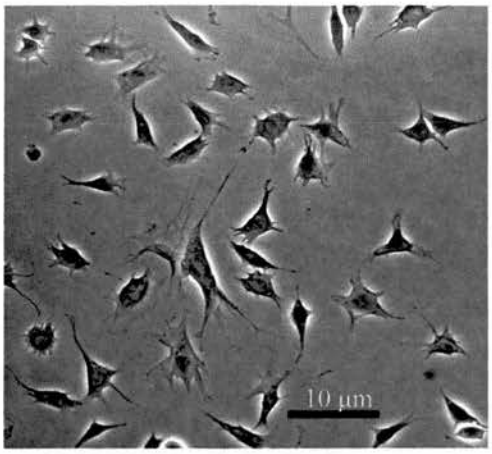

Figure 2. MLO-Y4 osteocytes in culture. Representative image of the MLO-Y4 osteocyte-like cell line, isolated and characterised by Kato et al. 1997, demonstrating large cytoplasmic extensions which enable contact between neighbour osteocytes. Image was taken using phase contrast light microscopy. Bar = 10 µm.

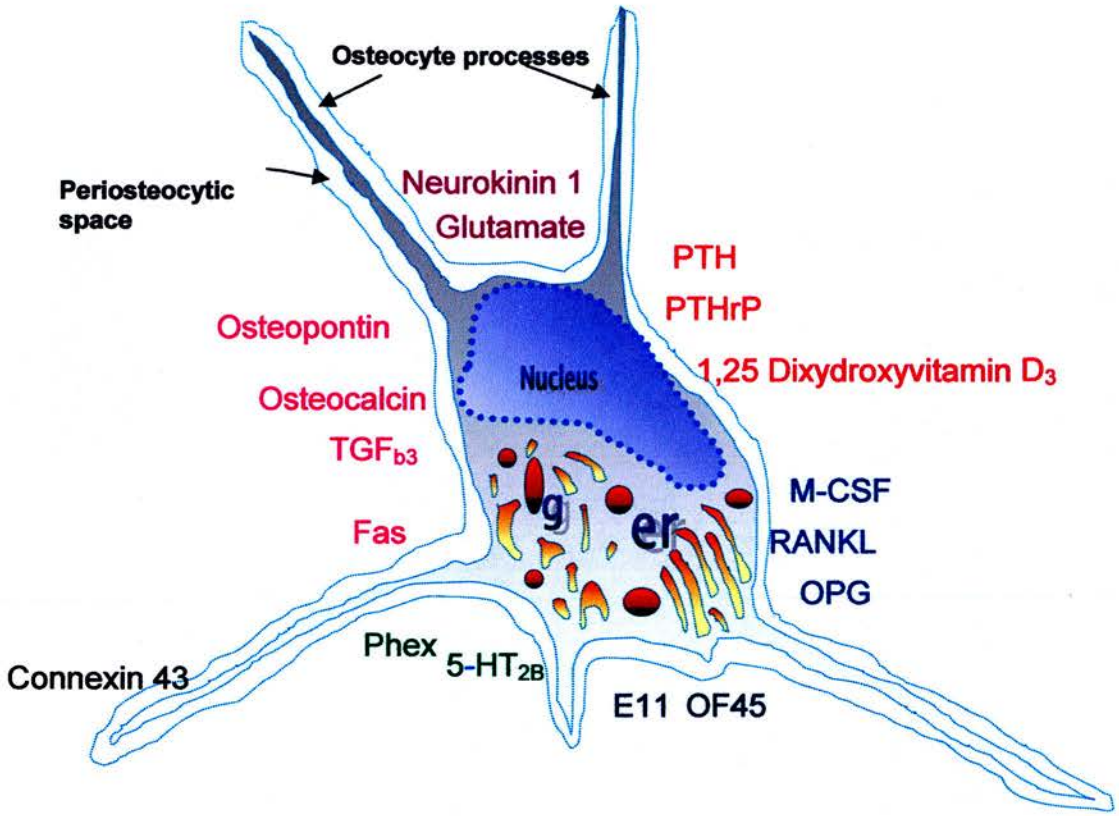

Figure 3. The osteocyte. The osteocyte contains a large Golgi apparatus (g), a well developed endoplasmic reticuclum (er) and a basal nucleus. The osteocyte expresses molecules involved in the targeting of bone formation and resorption and are under the influence of hormones, neuronal factors and mechanical stimuli.

these cells, as discussed in §1.5.2. Therefore it is important to investigate further and characterise osteocytes, either through the establishment of new cell lines at various differentiation stages or the development of antibodies against specific antigens, discussed in §1.5.3.3 enabling the routine isolation of osteocytes following the sequential digestion of bones from different species.

1.5.2 Function of osteocytes

Several theories have been proposed concerning the function of osteocytes and their contribution to the process of bone remodelling. Osteocytes were initially thought to contribute to the removal of bone matrix by resorbing calcified bone around them, a phenomenon known as osteocyte osteolysis (Belanger et al. 1963, Parfitt 1976). This belief was probably based on the size of the lacunae in particular diseases or to the production of proteolytic enzymes, such as collagenase, capable of degrading bone matrix. Later evidence however, suggested that osteocytes are not able to resorb bone (Boyde 1980, Marotti et al. 1990, Van der Plaas et al. 1994). Osteocytes have also been proposed to contribute to the mineralisation process, by secreting non-collagenous proteins, such as osteocalcin and osteopontin (Ikeda et al. 1996). Furthermore, osteocytes have been reported to produce inhibitory signals that decrease the apposition rate of osteoblasts during refilling of BMUs and enable the recruitment of osteoblasts to become osteocytes (Marotti 1996, Martin 2000).

Despite the evidence that enable osteocytes to contribute to the processes of bone resorption and formation, these theories can not justify the existence of the extensive network that these cells form within the bone matrix. Experiments in the last decade have led to the conclusion that osteocytes sense the amount of strain applied in the local environment either through changes in fluid flow or cell deformations (Lanyon 1993, Zhang et al. 1997, Noble et al. 2003). Osteocytes were shown to interact with osteoblasts via gap junctions, as evidenced by the passage of calcein dye between MLO-Y4 osteocytes and MC3T3-E1 osteoblasts, while mechanical deformation of osteocyte cell membrane induced calcium signals in neighbouring osteocytes and osteoblasts, suggesting that osteocytes are capable of communicating a mechanical response (Yellowley et al. 2000). A reduced incidence of bone resorption has been

correlated with osteonecrosis, characterised by death of bone cells (Kenzora et al. 1978), while examination of the lacunar occupancy at different stages of the remodelling cycle, revealed that forming as well as resorbing osteons contained higher osteocyte density and lacunar occupancy, compared to quiescent osteons (Power et al. 2002). Other studies have demonstrated a decline in the osteocyte lacunar density in human cortical bone, in association with microcracks and increased porosity observed in aging (Vashishth et al. 2000). Finally, studies have shown that apoptosis of osteocytes preceded bone resorption in rat ulna bone, in response to mechanical loading (Noble et al. 2003). In summary, these findings suggest that osteocytes constitute a signalling network capable of influencing the remodelling activity of bone, following mechanical stimulation and might also provide a candidate signal through their apoptosis for specific site-directed remodelling, which forms the hypothesis tested in section 2. The nature of the control that osteocytes exert on the remodelling process might also be explained by examining the response of osteocytes to hormonal or mechanically derived stimuli. (**Figure 3**).

1.5.3 Hormonal and neuronal-related factors

Osteocytes are affected by a number of hormones and cytokines that are known to regulate bone homeostasis. Estrogen loss induced by either gonadotrophin-releasing hormone analogs or ovariectomy, increased the proportion of apoptotic osteocytes, which could be reversed following estrogen administration (Tomkinson et al. 1997 and 1998), while glucocorticoid treatment also affected the viability of osteocytes in the human and mouse (Weinstein et al. 1998 and 2000). Immunohistochemical studies revealed the presence of receptors on osteocytes for mineralocorticoids, glucocorticoids (Beavan et al. 2001) and $1,25(OH)_2D_3$ (Boivin et al. 1987). In addition, osteocytes have demonstrated PTHrP and PTH binding (Rao et al. 1983, Fermor et al. 1995), which were shown to alter cx43 expression and induce apoptosis, regulating possibly osteocyte communication and survival (Divieti et al. 2001).

Osteocytes also express receptors associated with the nervous system, such as neurokinin-1 receptors, which bind to substance P released from axons of sensory neurons and possibly regulate osteoclastic resorption (Goto et al. 1998). In addition, they express the glutamate and aspartate transporter (GLAST) gene and mRNA, which have been shown to be down-regulated in response to mechanical loading, suggesting a paracrine role of glutamate in the communication between osteocytes and osteoblasts (Mason et al. 1997). Binding of serotonin to the receptor 5-HT_{2B} reduced production of nitric oxide (NO) from mechanically stimulated mouse osteoblasts, whereas the highest expression of 5-HT_{2B} mRNA was found in osteocytes, suggesting a role for serotonin in the modulation of mechanical stimuli in bone (Westbroek et al. 2001).

1.5.4 Mechanotransduction and the osteocyte

Several studies have investigated signal transduction pathways in osteocytes in response to mechanical loading. Pulsating fluid flow was shown to increase intracellular Ca^{++} concentration, which further increased prostaglandin E_2 (PGE_2) production in isolated chicken osteocytes (Ajubi et al. 1999) and in MLO-Y4 osteocytes (Hakeda et al. 2000). PGE_2 production was associated with increased levels of cx43 protein, in a cAMP-PKA-dependent manner (Cheng et al. 2001, Cherian et al. 2003), while fluid shear stress led to rearrangement of Cx43 and Cx45, disruption of junctional communication and disconnection of bone cells (Thi et al. 2003). These studies have indicated that in response to mechanical loading, osteocytes could possibly transmit a metabolic signal, which could influence local bone remodelling, since it has been shown that PGE_2 is able to sustain recruitment and maturation of osteoclasts and proliferation and differentiation of osteoblasts (Suda et al. 1995, Samoto et al. 2003). Release of PGE_2 from chicken osteocytes was shown to be preceded by NO release from activated endothelial cell NO synthase (ecNOS) (Klein-Nulend et al. 1995 and 1998). In addition, a reduced expression of ecNOS on osteocytes has been observed in association with femoral neck fracture, suggesting the importance of NO in directing osteoclast resorption depths and orientation, in response to different magnitude strains sensed by the osteocytes (Loveridge et al. 2002, Burger et al. 2003). Furthermore, in mouse alveolar

osteocytes mechanical loading increased production of dentin matrix protein 1 (Gluhak-Heinrich 2003), while osteopontin production was associated with increased number of osteoclasts and resorption pits on the site of pressure, indicating a role for osteopontin in initiation of resorption (Terai et al. 1999).

1.5.5 Factors that affect osteocytic phenotype

Recent studies have identified a gene known as E11, which encodes for a 17.4 kDa protein, a type I transmembrane protein, preferentially expressed in mature osteoblasts, preosteocytes and osteocytes, at regions of the cell membrane in contact with the matrix. Expression was increased during intramembranous and endochondral bone formation and during the early stages of fracture healing (Wetterwald et al. 1996, Hadjiargyrou et al. 2001). Several studies have identified E11 as an osteoblastic lineage differentiation marker, expressed in preosteoblasts, mature osteoblasts, preosteocytes, mature osteocytes, osteoblastic cell lines and MLO-Y4 osteocyte-like cells (Lian et al. 1999, Bonewald et al. 2000). However, Schulze et al. showed that E11 is present only on osteocytic cell membranes as well as their processes, in calvariae, acting as a late osteogenic marker (Schulze et al. 1999).

E11 is identical in amino acid sequence to a protein called podoplanin, in glomerular epithelial cells (podocytes), which is involved in maintaining the shape of podocyte foot processes and glomerular permeability, and also RT140, a protein isolated from rat type I lung alveolar epithelial cells (Breiteneder-Geleff et al. 1997, Matsui et al. 1999, Vanderbilt et al.1999). In addition, E11 shares 87% sequence homology to the murine protein OTS-8 which has been reported to bind to the cell surface receptor CD44, involved in cell adhesion and migration in tumour vascular endothelial cells (Nose et al. 1990, Ohizumi et al. 2000). CD44 was also shown to be expressed during fracture healing (Yamazaki et al. 1999). These findings imply that E11 is associated with the formation and maintenance of osteoblastic and octeocytic cellular processes, as well as in the adhesion of these cells to the bone matrix during fracture repair.

Osteocytes within trabecular and cortical rat bone were found to express high levels of a bone-specific cDNA termed OF45 (osteoblast/osteocyte factor 45), encoding for an RGD-containing protein (Petersen et al. 2000). Studies in the rat mandible using *in situ* mRNA localization demonstrated OF45 expression in mature osteoblasts and in osteocytes throughout ossification in the skeleton, hence it may represent an important marker of the osteocyte phenotype (Igarashi et al. 2002). Skeletal examination in OF45 knockout animals showed increased bone mass due to increased osteoblast numbers and activity, while osteoclast recruitment and numbers were not affected (Gowen et al. 2003). The authors have suggested that OF45 mRNA is associated with differentiation into the osteocyte phenotype, possibly involved in the regulation of bone mineralisation. The mouse OF45 gene sequence is homologous to the human MEPE gene, implicated in oncogenic osteomalacia and has been proposed as a downstream target in the phosphate pathway regulated by the PHEX endoprotease (Gowen et al. 2003, MacDougall et al. 2001). Interestingly, it has been shown that the PHEX protein is the target of the antibody mAb OB7.3 (Westbroek et al. 2002), which is specifically used to isolate chicken osteocytes (Nijweide and Mulder 1986). These observations suggest that osteocytes participate in phosphate handling and regulation of mineralisation, since mutations in the PHEX gene result in bone mineralization abnormalities and X-linked hypopshosphataemia (Sabbagh et al. 2003).

1.5.6 Osteocyte-derived factors that affect osteoclast survival and function

Most of the studies described above propose that osteocytes are implicated in the regulation of bone turnover events by acting as sensors and transducers of mechanical-derived stimuli (§1.5.3.2) and by expressing osteotropic factors (§1.5.3.1 and 1.5.3.3). However, little is known about any direct effects of osteocyte-derived factors on osteoclast recruitment and function. Studies have suggested that release of TGF-β from MLO-Y4 osteocytes exerts direct inhibitory effects on osteoclast resorption, in an estrogen-dependent manner (Heino et al. 2002), while generation of ecNOS and NO by osteocytes directs orientation and depth of resorption by osteoclasts (Loveridge et al. 2002, Burger et al. 2003).

In addition, MLO-Y4 osteocytes have recently been suggested to support osteoclastogenesis in co-culture experiments with spleen or marrow mouse cells, via the production of RANKL (Zhao et al. 2002). The authors proposed that direct contact is required between osteocytes and osteoclasts, in order to promote osteoclastogenesis; however, this hypothesis has not yet been supported by *in vivo* data that would show osteocytic cellular processes reaching the bone marrow and interacting with osteoclast precursors. Ahuja et al. have shown that CD40L, which serves as a survival factor for dendritic cells, protected MLO-Y4 osteocytes against the antiapoptotic actions of Dexamethasone, TNFα or etoposide. The authors have also suggested that CD40 may increase OPG production, as it does in B-lymphocytes and that it may regulate production of matrix metalloproteinases by osteocytes and osteoblasts participating in bone turnover (Ahuja et al. 2003).

1.6. Summary

Bone undergoes multiple cycles of remodelling during a lifetime in order to adapt to specific requirements of strength and shape, according to Wolff's law (1892). Osteocytes have been proposed to maintain bone quality by sensing mechanical loading and transmitting signals that possibly target the activity of bone effector cells, osteoclasts and osteoblasts through the canalicular network. In particular, the bone resorptive activity of osteoclasts has been correlated with the incidence of osteocyte apoptosis close to those areas (Noble et al. 1997). Apoptosis of osteocytes is discussed in §2.8.4 and is investigated in detail in sections 2 and 3, which address the possible biological significance of osteocyte apoptosis.

CHAPTER 2

Apoptosis

2.1 Introduction

Cell death is an essential phenomenon conserved throughout evolution, and can be characterised as necrotic cell death, which refers to the morphology seen when cells or tissues die from severe and sudden injury and apoptotic cell death, which is the focus of this section. Apoptosis can be initiated by a variety of stimuli and appears to be an essential homeostatic mechanism for the healthy development and maintenance of tissues (Kerr et al. 1972, Levine et al. 1994, Cotman and Anderson 1995). Recent evidence has suggested that apoptosis of cells, rather than being a silent event leading to the disposal of unwanted cells, could also result in specific immunosuppressive or pro-inflammatory responses, when they interact with monocytes/macrophages (Gao et al. 1998, Chen et al. 2001, Voll et al. 1997, Fadok et al. 1998), or dendritic cells (Stuart et al. 2002, Albert et al. 1998, Belone et al. 1997, Inaba et al. 1998, Albert et al. 2001). These findings raise interesting issues as to the consequences of phagocytosis of different apoptotic cells by various phagocytes, which is the focus of section 2. This chapter outlines the basic apoptotic events and describes in vivo and in vitro cases of apoptosis of bone cells.

2.2 Definition of apoptosis

Most of the knowledge concerning the genetic control of apoptosis comes from studies on the nematode, Caenorhabditis elegans (Ellis and Horvitz 1986). Apoptosis is the result of the induction of an internal suicide program and is characterised by membrane blebbing, chromatin condensation, DNA cleavage and packaging of cellular contents into apoptotic bodies. The contents of dying cells are eliminated by phagocytosis, so that they do not generate an inflammatory response within the body (**Figure 4**) (Kerr et al. 1972, Savill 1997). Apoptosis could be divided into four stages, the initiating phase, the decision and execution phase and phagocytosis (Dragovich et al. 1998). The roles of the Bcl-2 proteins, caspases and death receptors throughout this four stage sequence are summarised in the following paragraphs.

2.3 Caspases (Cysteine ASpartate ProteASES)

Caspases disassemble the cell's structure, terminate DNA replication, attack the nucleus, prevent repair mechanisms and prepare the cell for phagocytosis

(Thornberry et al. 1998). Caspases include the initiator caspases (caspases 1, 2, 8, 9, 10), activated by functional changes occurring in the mitochondria and death receptors, and effector caspases (caspases 3, 6, 7), which are mediators of the execution phase, activating the DFF45 enzyme in humans or ICAD in mice (Dragovich et al. 1998). These are Ca^{++}/Mg^{+} dependent endonucleases, cleaving DNA into oligomers of 180bp (Guchellaar et al. 1997). Other caspase targets include the lamins, p21 activated kinase-2, gelsolin, PARP and replication factor C, implicated in repair mechanisms (Thornberry et al. 1998, Allen et al. 1998).

2.4 Bcl-2 family of proteins and implication of mitochondria in apoptosis.

During apoptosis, functional and structural changes occur in mitochondria, due to disruption of the regulation of the permeability transition (PT) pore, a complex of proteins located between the mitochondrial membranes (Kroemer 1997). Opening of the PT pore induces changes in the mitochondrial inner transmembrane potential $\Delta\psi m$ and results in the generation of ceramide, reactive oxygen species and NO (Green et al., 1998, Decaudin et al., 1998). These events lead to cytochrome c release, disruption of the electron transfer chain and activation of caspase-9, which in turn activates caspase-3 (Decaudin et al. 1998, Allen et al. 1998). The Bcl-2 family of proteins includes the anti-apoptotic proteins the Bcl-2, Bcl-x_L, Bag, Mcl-1 and A1 and the pro-apoptotic proteins Bcl-x_s, Bax, Bad, Bid and Bak,. The levels of these proteins on the outer mitochondrial membrane and their ability to form homodimers or heterodimers, regulate opening of the PT pore and the apoptotic threshold of the cell. (Adams et al. 1998, Kroemer 1997).

2.5 Death Receptors

Death receptors are members of the TNF/NGF superfamily and include Fas and TNF Receptors 1 and 2 (**Figure 5**), Death Receptor-3 and TRAIL receptors 1, 2, 3, and 4 (Ashkenazi et al. 1998). Binding of Fas L to Fas R or TNF L to TNF R1 causes receptor oligomerisation (**Figure 5**). Death receptors interact through a death domain with adapter molecules, such as FAS- or TNF-associated death domain-containing protein (FADD or TRADD). Following this interaction, FADD interacts with

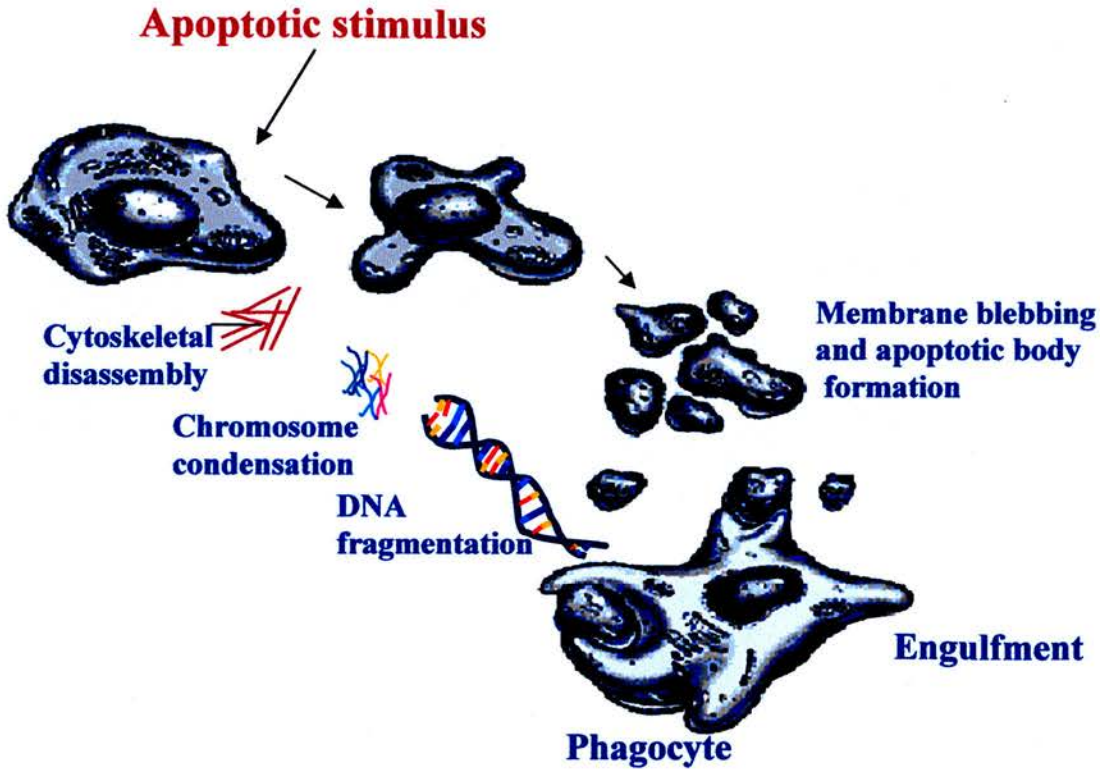

Figure 4. The four stages of apoptosis: 1) Exposure to an apoptotic stimulus, 2) Decision to initiate survival or apoptotic cascades, 3) execution phase, characterised by cytoplasmic and chromatin condensation, fragmentation of DNA and membrane blebbing and 4) Clearance phase involving the engulfment of the apoptotic bodies by a nearby phagocyte, in order to avoid inflammation

caspase-8 or caspase-10, activating the apoptotic cascade (Wehrli et al 2000). Fas signalling can be inhibited by inhibitors of caspase-8 and downstream effector caspases, or Bcl-2 proteins (Ashkenazi et al. 1998). TNF-R1 could also interact with TRAFs (TNF-R-associated factors) and activate the JNK pathway, initiating transcription of survival proteins (Rothe et al. 1995, Kitson et al. 1996, Ashkenazi et al. 1998) (**Figure 5**). TNF and Fas receptors can also activate the sphingomyelin pathway, which produces ceramide and initiates apoptosis through the JNK pathway (Verheij et al. 1996).

2. 6 Membrane blebbing

Apoptotic cells fragment into membrane-bound bodies, which are rapidly ingested by phagocytes, such as macrophages, or by neighbouring cells. The force that drives the formation of apoptotic bodies is produced by actin-myosin II cytoskeletal structures (Mills et al. 1999). Inhibition of the Rho kinase ROCK has been shown to prevent formation of membrane blebs (Coleman et al. 2001), while activation of ROCK resulted in stabilisation of actin-myosin interactions (Amano et al. 2001) and generation of a hydrodynamic force, which leads to cell contraction. In addition caspases cleave regulatory proteins, reducing the interaction between the plasma membrane and the cytosleleton, leading to bleb protrusion (Fedier and Keeler 1997).

2.7 Phagocytosis

Phagocytosis is a rapid and efficient process that prevents leakage of contents that would initiate an inflammatory response and which requires recognition of the apoptotic bodies by phagocytes, in order to engulf them and degrade them, without disturbing neighbouring living cells (Savill 1997) (**Figure 6**). Carbohydrate and glycoprotein changes on the apoptotic cell membrane have been shown to enable recognition of the apoptotic cells by the macrophage lectin receptors. (Savill et al 1992, Henson et al. 2001). Other markers on the apoptotic cell surface include thrombospondin 1 (TSP1) binding sites and phosphatidylserine (PS). PS is a phospholipid normally present on the inner leaflet of the membrane and is exposed through a Ca^{++}-dependent movement involving activation of a phospholipid scramblase and downregulation of an ATP-dependent aminophospholipid

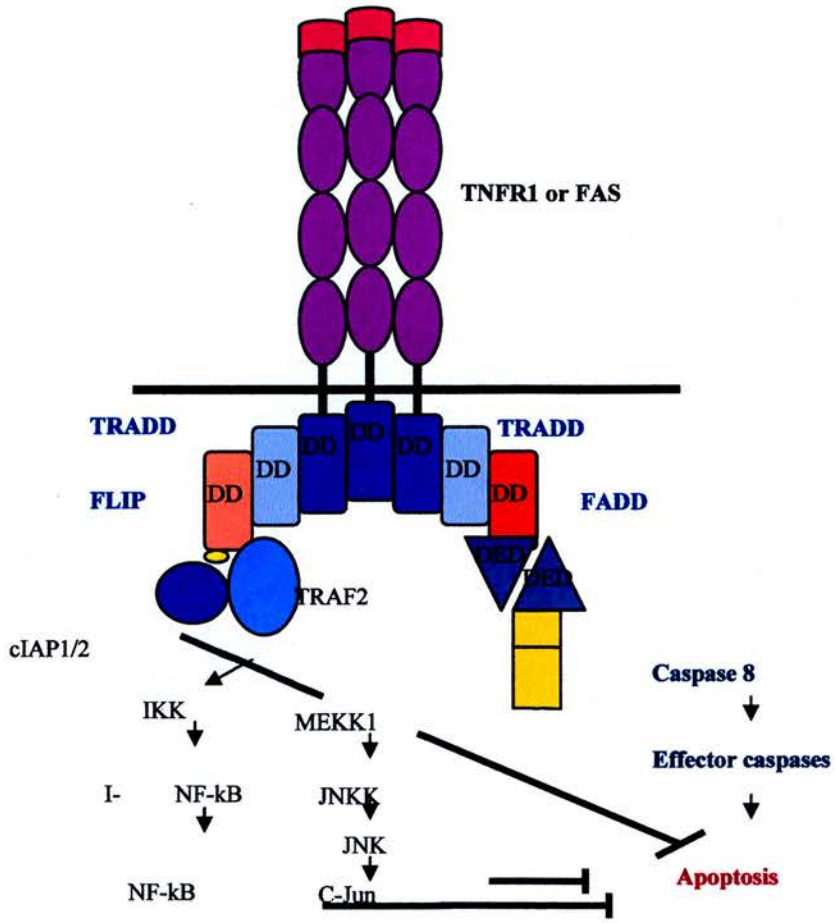

Figure 5. Death receptor signalling. Binding of Fas L to Fas R or TNF L to TNF R1 causes receptor oligomerisation. The receptor interacts with adapter molecules, such as FADD or TRADD, which interact with caspase-8 activating the apoptotic cascade. Signalling from these receptors can be inhibited by caspase-8 inhibitors, Bcl-2 proteins or by x-linked inhibitors of apoptosis (x-IAP). TNF-R1 also interacts with TRAFs (TNF-R-associated factors), which activate the inhibitor of kB (I-kB) resulting in NF-kB activation and transcription of survival proteins. (Rothe et al. 1995), or it can induce pro-survival signals through the JNK MAPK pathway.

→ = stimulatory effect, ⊣ = inhibitory effect.

translocase. Inhibition of phospholipid translocation has been shown to prevent phagocytosis (Fadok et al. 2001). PS exposure occurs at the early stages of apoptosis, as demonstrated by PS binding with Annexin V FITC, a rapid, sensitive and quantitative assay (Shouman et al. 1998).

Phagocytic receptors (**Figure 6**) are also involved in the uptake of apoptotic cells, such as the lectin and PS receptors (PtSerR) (Fadok et al. 2000) mentioned above. Macrophages employ CD36 and $\alpha_v\beta_3$ integrin, which bind to apoptotic neutrophils, eosinophils and lymphocytes through TSP1, as demonstrated by inhibition studies, using monoclonal antibodies and RGD peptides (Savill et al. 1992). Scavenger receptors of class A and class B and the ABC-1 membrane transporter have also been shown to participate in the uptake of apoptotic cells (Platt et al. 1996, Henson et al. 2001). Other recognition molecules include the CD14, which has the ability to interact with lipopolysaccharride on bacteria and also to induce apoptotic cell tethering and uptake, in a noninflammatory manner (Devitt et al. 1998). CD14, identified by the monoclonal antibody 61D3, has been proposed to act as a pattern recognition receptor, interacting with a series of apoptotic cell associated molecular patterns (ACAMPs) (Flora and Gregory 1994, Gregory 2000). Following recognition of apoptotic bodies, phagocytes undertake pseudopodia extension possibly through the involvement of PI3 kinase (Cox et al. 1999) and finally engulf apoptotic cells. Studies in C. Elegans have identified two pathways implicated in engulfment, which induce cytoskeletal changes, polymerisation of F actin and formation of a phagocytic cup (Coleman et al. 2002, Leverrier et al. 2001, Henson et al. 2001, Tosello-Trampont et al. 2001). Apoptotic body uptake is followed by endosomal fusion and lysosomal degradation, brought about by F-actin dissociation and depolymerisation (Bengtson et al. 1993).

2.8 Apoptosis in Bone

In bone tissue, necrosis occurs following exposure to radiation, steroid use and ischemia, leading to the formation of patches of dead bone, separated from healthy

Phagocyte

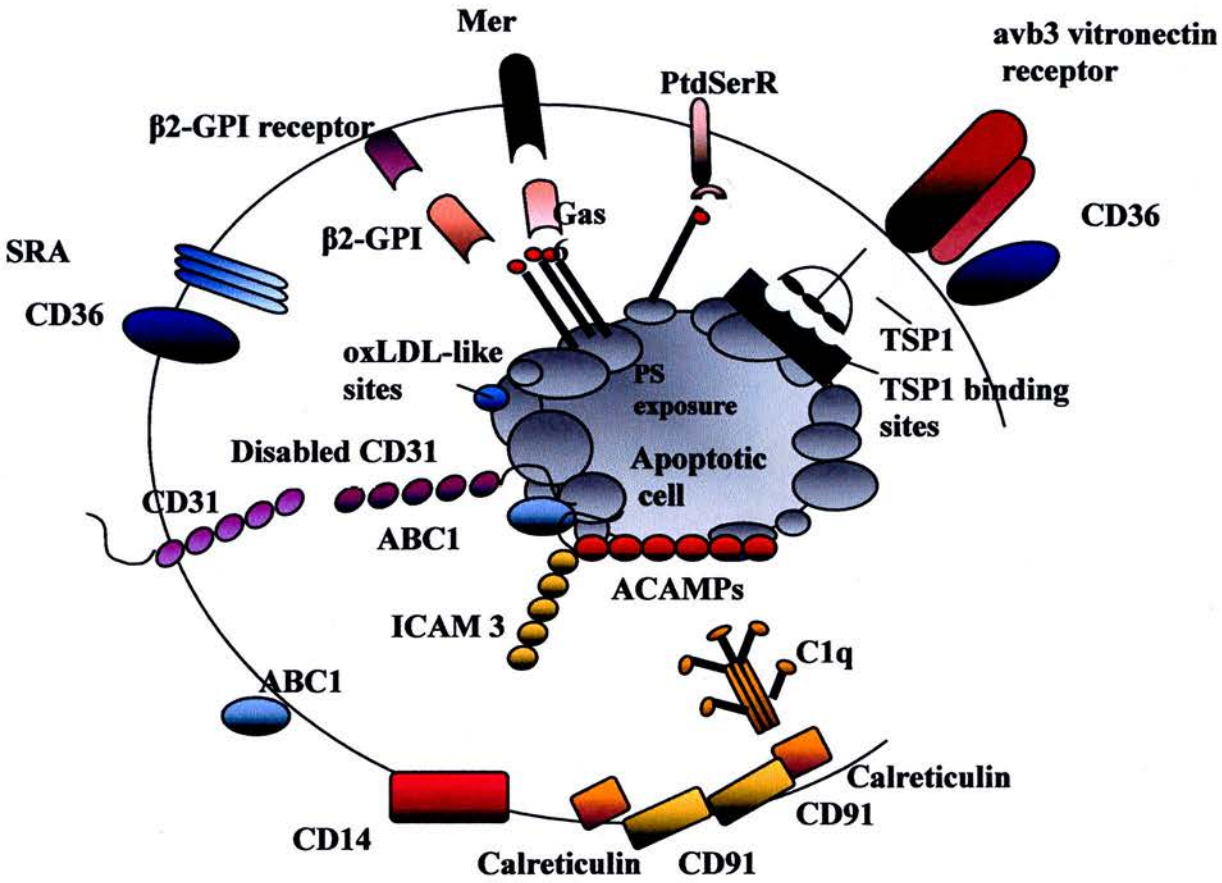

Figure 6. Mechanisms involved in the recognition of apoptotic cells by phagocytes. Apoptotic cell changes include exposure of PS which is recognised by the PS receptor on phagocytes, receptors for β2-glycoprotein and the Mer kinase receptor for Gas6. In addition, scavenger receptors like CD36 and SRA recognise oxidised sites on apoptotic cells, while CD36 may also enhance engulfment through formation of CD36-TSP1-avβ3 vitronectin receptor complex. ABC1 is implicated in the rearrangement of phospholipids in both the prey and the phagocyte. The CD91-calreticulin system is implicated in innate recognition, through binding to C1q, while CD14 is implicated both in the recognition of self- and non-self components. (Image adapted from Savill et al. 2002, *Nat Rev*, page 967).

bone (Sugimoto et al. 1993, Wong et al. 1987). In addition, evidence is available for apoptotic bone cell death during development and bone turnover as well as in disease situations, as discussed below in further detail.

2.8.1 Chondrocyte apoptosis

During endochondral ossification and fracture healing, when cartilaginous tissue is replaced by woven bone, chondrocytes become hypertrophic and undergo programmed cell death, characterised by DNA fragmentation, condensation of the nuclei and cell shrinkage (Lee et al. 1998). Hypertrophic chondrocytes that undergo apoptosis have been suggested to signal to osteoclasts for their removal (Bronckers et al. 2000), although the mechanism is unclear.

2.8.2 Osteoclast apoptosis

Osteoclasts have been shown to undergo apoptosis following completion of the resorption. The process is characterised by cytoplasmic and nuclear condensation and DNA fragmentation into nucleosomal-sized units (Roodman et al. 1996). Estrogen exerts anti-resorptive activities through induction of osteoclast apoptosis, either directly through estrogen receptor mediated pathways (Kameda et al. 1997), or indirectly through the production of TGF-β from osteoblasts (Hughes et al. 1996). In addition, bisphosphonates are well known anti-osteoclastic agents (reviewed in section 3), which inhibit osteoclast survival and function following different routes, depending on the absence or presence of a nitrogen group (Papapoulos 1997, Rodan 1998, Rogers et al. 1999). Glucocorticoids exert different effects on osteoclastic activity, in different species. Glucocorticoids stimulate human and murine bone resorption (Conaway et al. 1996, Hamdy 1997), whereas in rats (Tobias and Chambers 1989, Dempster et al. 1997), glucocorticoids resulted in increased bone mass and induction of osteoclast apoptosis.

Further studies have shown that Ca^{++} concentrations, at levels similar to those produced during demineralisation, induce osteoclast apoptosis (Lorget et al. 2000), while vitamin K_2 also inhibited resorption through induction of osteoclast apoptotic death (Kameda et al. 1996). Finally, mice "knockout" for the Bcl-2 gene had an

osteopetrotic phenotype, implying that Bcl-2 levels might control osteoclast survival and resorptive activity in active pits (McGill et al. 2002, Glantschnig et al. 2002). Previous studies on Bcl-$2^{-/-}$ mice however, did not observe an osteopetrotic phenotype but increased numbers of osteoblasts and disorganised appearance of collagen fibres (Boot-Handford et al. 1998).

2.8.3 Osteoblast apoptosis

Osteoblast apoptosis has been evidenced by several *in vitro* studies. The Fas/FasL death receptor pathway has been implicated in apoptosis of both human and murine osteoblasts either through interaction with T cells (Kawakami et al. 1997) or exposure to pro-inflammatory cytokines such as TNF-α, IL-1 and IFN-γ (Ozeki et al. 2002). In addition, okadaic acid and caryculin A induce apoptosis in osteoblasts *in vitro*, providing a possible role for protein phosphatases in regulation of osteoblastic activity (Morimoto et al. 1997).

Inorganic phosphate has been shown to induce osteoblast apoptosis, which appeared to be enhanced by increasing concentrations of Ca^{++}, suggesting that these two ions, which are major components of the bone extracellular matrix, act as local apoptogens for osteoblasts (Adams et al. 2001). Landry et al. observed *in vivo* formation of osteoblast apoptotic bodies in the callus of rat tibia, which was proposed as a mechanism for eliminating excess osteoblasts from the injury site, following callus formation (Landry et al. 1997). Furthermore, apoptosis of mature osteoblasts has been shown to be influenced by cytokines and growth factors present in the bone microenvironment such as IL-6 and TGF-β (Jilka et al. 1998), while survival and differentiation of osteoblasts into osteocytes, was dependent on matrix metalloproteinase activity and activation of latent TGF-β by MMPs, which was mediated through the p44/42 MAPK pathway (Karsdal et al. 2002).

2.8.4 Osteocyte apoptosis

Death of osteocytes *in vivo*, was initially described by Frost, who observed an increasing incidence of empty lacunae with increasing age (Frost 1960). Osteocyte death appeared to occur in most types of bone, and could be associated with a range

of diseases, including osteoporosis and osteoarthritis (Dunstan 1993). The mechanism, by which osteocytes died under these conditions, was initially thought to be due to necrosis. However, recent evidence suggests that osteocytes are capable of apoptosis. Studies using both pathological and healthy human bone have provided some insights into the apoptotic morphology of an osteocyte, suggesting the presence of DNA fragmentation, intact nuclear envelope, chromatin condensation and cell shrinkage (Noble et al. 1997). More recent studies in the ribs of premature infants have identified the presence of tissue transglutaminase in apoptotic osteocytes, as well as high expression of the anti-apoptotic protein Bcl-2, which appeared to correlate with regions of low osteocyte apoptosis (Stevens et al. 2000). In addition, osteocytes in the immediate vicinity of the microdamage site were shown to express the pro-apoptotic protein Bax whereas, Bcl-2 was expressed at some distance from microcracks, on osteocytes that appeared to create a wall around the apoptotic osteocytes in the microcracks (Verborgt. et al. 2002), suggesting that the expression pattern of anti-apoptotic and pro-apoptotic factors on osteocytes might be directing the resorption process to specific areas following microdamage.

Several studies have reported that there may be an association between osteocyte apoptosis and the regulation of bone turnover. For example, the viability of osteocytes is affected by the presence or absence of hormones, which influence the maintenance of bone homeostasis such as glucocorticoids (Weinstein et al. 1998 and 2000) or estrogen (Tomkinson et al. 1997 and 1998).

In addition, evidence is accumulating on the role of osteocyte apoptosis on the targeted remodelling in response to mechanical stimuli and microdamage. Large numbers of apoptotic osteocytes were found to surround resorption areas induced by fatigue microdamage (Verborgt et al. 2000) or during orthodontic tooth movement (Hamaya et al. 2002). More recently a direct association was demonstrated between osteocyte apoptosis and mechanical loading, which was immediately followed by intracortical remodelling, providing the first evidence that apoptotic death of osteocytes might be an important mechanism for specific site-directed remodelling (Noble et al 2003).

2.9 Summary

Apoptosis is an essential homeostatic mechanism for the healthy development and maintenance of tissues. Various diseases occur when apoptotic mechanisms malfunction, including cancers, autoimmune disorders or neurodegenerative diseases (Levine et al. 1994, Miyashita et al. 1994, Thompson 1995, Cotman and Anderson 1995). Apoptosis has been described in osteoblasts and osteoclasts, as well as osteocytes, during bone growth and remodelling, in response to factors produced as a normal consequence of the transition between bone resorption, reversal and bone formation. These findings indicate that apoptosis is an important, routine mechanism in the maintenance of bone homeostasis which forms the hypothesis investigated in section 2 in which I demonstrate that products derived from the apoptosis of osteocytes are capable of modifying the behaviour of bone effector cells.

SECTION 2

The biological significance of osteocyte apoptosis

Introduction to Section 2

Advanced age has been associated with imbalances between bone resorption and formation and a substantial loss in bone mass, compared to the skeleton of young individuals (Riggs et al. 1982). In addition, ageing has been correlated with increased incidence of empty lacunae, indicating that there is an age-related dependency in the viability of osteocytes (Frost 1960). Osteocytes have been proposed to receive mechanical signals and to initiate biochemical responses that direct bone resorption and formation, allowing bone to adapt to specific shape and strength requirements (Noble et al. 2003), indicating that the quality of bone is very closely associated with the presence of osteocytes and the communication network that they form through their cytoplasmic processes, within the bone matrix (Dunstan et al. 1993). Studies have shown that forming as well as resorbing osteons contain higher osteocyte density and lacunar occupancy, compared to quiescent osteons, suggesting that osteocytes might contribute to the process of bone remodelling (Power et al. 2002). The process by which osteocytes control bone turnover is not understood yet. However, there is accumulating evidence that controlled death of osteocytes through apoptosis, might be providing the signals that direct turnover, since it has been observed in close association with resorbing areas and most importantly prior to initiation of bone resorption (Noble et al. 1997, Verborgt et al. 2000, Noble et al. 2003).

All these observations suggest that death of osteocytes via apoptosis is of significance to the maintenance of bone homeostasis. This section focuses on the effects of osteocyte apoptosis on cells of the osteogenic and other lineages as well as on mechanisms that might mediate these effects.

CHAPTER 3

Apoptotic osteocytes induce specific responses to different target cells

3.1 Abstract

Osteocyte apoptosis has been associated with targeting of the activity of specific bone resorbing cell types. High levels of osteocyte apoptosis have been evidenced prior to initiation of bone resorption raising the possibility that signals derived from these dying cells direct osteoclasts to bone requiring remodelling (Noble et al. 2003). Here we hypothesise that products form apoptotic osteocytes will significantly alter the behaviour of osteoblastic cells. In particular this study has attempted to identify the significance of osteocyte apoptosis by characterizing the responses of bone cells and a variety of other target cells from various tissues, to the presence of osteocyte apoptotic products.

TE85 human osteoblasts and primary mouse osteoblasts were shown to undergo apoptosis in the presence of osteocyte apoptotic bodies compared to untreated osteoblast cultures ($p = 0.001$ and $p = 0.0001$, respectively). Soluble apoptotic factors as well as healthy or necrotic osteocyte products did not affect osteoblast viability, pointing to the presence of a specific apoptotic body associated factor expressed during osteocyte apoptosis, with death-inducing activity in osteoblasts. Apoptotic bodies produced from other (non-osteocyte) cell types and lineages failed to induce osteoblast apoptosis. In addition, different cell types used as target cells, did not undergo apoptosis when challenged with osteocytic and a range of other cell apoptotic products, indicating that there is phenotypic specificity in the death-inducing signal delivered by apoptotic osteocytes to osteoblasts. Furthermore, in macrophage cultures, prolonged incubation with osteocyte apoptotic bodies and their conditioned medium increased cell number and induced morphological changes, compared to control cultures.

This study provides evidence that apoptotic osteocytes are capable of being recognized by different cell types and could carry a message able to elicit specific responses, depending on the cell they encounter. Such phenotypic recognition of apoptotic products provides a further level of "meaning" to apoptosis in general.

3.2 Introduction

Apoptosis, a form of programmed cell death conserved throughout evolution, represents an essential part of life for a multicellular organism, fulfilling a need to abolish supernumerary, hazardous or misplaced cells (Wylie et al. 1980). Everyday, about 10 billion cells undergo apoptosis in our bodies and are effectively phagocytosed by the macrophages residing in tissues or by neighboring cells acting as semi-professional phagocytes (Savill 1997). Phagocytosis of dying cells is a safe way of removing cells; however it might also suppress inflammation and modulate immune responses (Savill et al. 2002). Recent studies have shown that apoptotic cells can either directly exert immunosuppressive effects, by secreting IL-10 (Gao et al. 1998) or decrease production of pro-inflammatory cytokines such as IL-12, IL-1 and TNFα, and increase production of IL-10 or TGF-β, when engulfed by activated monocytes (Voll et al. 1997, Fadok et al. 1998). In addition, antigens on the apoptotic cell membrane have been suggested to access the cytoplasm and be cross-presented on MHC I and MHC II molecules on macrophages, inducing dendritic cell maturation, and regulation of immune responses (Belone et al. 1997, Inaba et al. 1998). Apoptotic bodies may provide the catalytic surface for thrombin generation, and lead to immunogenic responses, since changes in phospholipids and PS exposure lead to coagulation events and generation of antibodies against phospholipids, in the presence of cells normally found in circulating plasma (Casciola-Rosen et al. 1996).

Although most apoptotic cells share common characteristics (Kerr et al. 1972), cell-specific membrane antigens are present on the surface of apoptotic bodies derived from peripheral blood (Aupeix et al. 1997), highlighting the possibility that phagocytes might recognise the cellular source of the apoptotic body and respond differently to its ingestion. These findings imply that apoptotic cells could carry a message able to elicit specific responses, depending on the cell they were derived from and the phagocyte that engulfs them.

Bone is a rigid structural tissue, in which precise targeted activity of the effector cells maintains its size and shape/strength. Association has been established between apoptosis of the osteocytes and the targeting of the activity of specific bone resorbing

cell types. Verborgt et al. observed large numbers of apoptotic osteocytes surrounding resorption areas that were induced by fatigue microdamage (Verborgt et al. 2000), while Noble et al. have demonstrated that very high levels of osteocyte apoptosis were evident prior to initiation of bone resorption (Noble et al. 1997), directing osteoclasts to bone requiring remodelling (Noble et al. 2003).

Bone appears as an ideal system for studying the geographically localised phenotypes arising from the specific effects of phagocytosis of apoptotic vesicles. This chapter examines whether osteocyte apoptosis might influence directly the bone effector cells, and provides sufficient evidence that apoptotic osteocytes are capable of inducing specific responses to bone cells and to a variety of other target cells from various tissues.

3.3 Materials and Methods

All chemicals were purchased from Sigma, UK and all tissue culture reagents were purchased from Invitrogen, UK, unless otherwise stated. Tissue culture well plates and petri dishes were purchased from Corning, UK. Tissue culture procedures were performed in a laminar flow hood (class 2) receiving HEPA-filtered air, using sterile equipment.

3.3.1 Culture of cell lines

The murine long-bone derived osteocyte-like MLO-Y4 cell line was cultured in Modified Eagles Medium Alpha (αMEM) supplemented with 5% fetal bovine serum (FBS), 5% newborn calf serum (NCS), 1% penicillin/streptomycin (P/S) and 1% L-glutamine (Kato et al. 1997). The TE85 human osteosarcoma cell line was cultured in Minimum Essential Medium Eagle (MEM) supplemented with 10% FBS, 1% P/S and 1% L-glutamine (McAllister et al. 1971). The murine monocyte cell line IC21 was maintained in RPMI supplemented with 10% FBS, 1% P/S and 1% L-glutamine (Mauel and Defendi, 1971). The T hybridoma cell line DO11 10 was provided by Dr Sarah Howie and maintained in RPMI supplemented with 10% FBS, 1% P/S and 1% L-glutamine as described by Underhill et al. 1999.

Cells were grown in continuous monolayer culture in sterile 75 cm^2 tissue culture flasks. For MLO-Y4 osteocytes, flasks were coated with 0.1 M collagen type I from rat tail prior to use. Growth media were stored at 4 ^{o}C and warmed to 37 ^{o}C prior to use. Cells were maintained in an incubator at 37 ^{o}C in a 95% humidified atmosphere of O_2:CO_2 in the ratio of 95%: 5%. Subculturing was performed twice weekly upon reaching 90% of confluency, maintaining the cells in the log phase of proliferation. For adherent cultures (MLO-Y4, TE85 and IC21 cell cultures) the monolayer of cells was detached with addition of 1 ml of trypsin solution at 2.5 gm/l for 5-10 minutes, followed by addition of 10 ml of growth medium. 1 ml of cell suspension was added to a new flask containing 9 ml of fresh growth medium and placed in an incubator for maintenance. Non-adherent cultures (T hybridoma cells) were subcultured twice weekly by adding 1 ml of cell suspension to 29 ml of fresh growth medium and placed in an incubator for maintenance.

3.3.2 Isolation of primary mouse cell cultures.

Osteoblast and osteocyte cultures were isolated from 3-6 week-old female mice, killed by CO_2 asphyxiation. The mice were used at this age due to higher availability within the university unit, while a wider range of ages did not indicate any age-related differences in the responses studied in this thesis. Using sterile dissection equipment, calvarial bones were removed. Following removal of the periosteum, bones were digested in trypsin for 10 minutes at 37 °C. Bone tissue was then sequentially digested in collagenase at a concentration of 0.75 mg/ml for 25 minutes, which was repeated 10 times. After each individual digestion, cells were collected by centrifugation at 500 g for 5 minutes and digestions were characterized as described in §3.3.3, so that digestions 2-5, which stained positive for alkaline phosphatase, as described in §3.3.3.2, were combined to provide the osteoblast population, while digestions 6-10 provided the osteocyte population as described in §3.3.3.1. Cultures were maintained in 24 or 96 well plates in αMEM supplemented with 5% FBS and 5% NCS for 8-10 days prior to experimental use. Bone marrow stromal cells were isolated from 3-6 week old female mice as described by Thomson et al. 1993.Using sterile equipment, femurs were removed and growth plates were cut open using a scalpel to expose the marrow cavity. The bone marrow was removed by flushing the cavity with αMEM using a syringe needle. Cells were maintained in same growth medium (αMEM supplemented with 5% FBS and 5% NCS) for 5 days prior to experimental use. Polymorphonuclear (PMN) cells and peripheral blood monocytes (PBMCs) were supplied by Dr. Simon Brown and were cultured in Iscove's Modified Eagle Medium supplemented with 10% FBS. Murine bone marrow macrophages were prepared by Dr Jeremy Duffield and maintained in DMEM F12 supplemented with 10% FBS, as described by Duffield et al. 2000. $CD4^+$ T lymphocytes and spleen cell were isolated by Dr Sarah Howie and maintained in RPMI supplemented with 10% FBS, as described by Eagar et al. 2004.

3.3.3 Characterization of primary calvarial cultures

3.3.3.1 Proliferative capacity (5-bromo-2 deoxyuridine, BrdU)

In order to distinguish between proliferating fibroblasts, osteoblasts and non-proliferating osteocyte cultures, cells from each collagenase digestion were analysed

using BrdU incorporation into newly synthesized DNA (Thomson et al. 1993). Cultures were transferred to growth medium supplemented with 0.1% serum for 24 h, to reduce proliferation and to synchronize cells to Go of the cell cycle. Cells were then incubated with 50 μM BrdU, an analogue of thymidine which is taken up into the DNA of cycling cells and 50 μM deoxycytidine, which inhibits DNA methylation and results in heterochromatin decondensation, in normal 10% growth medium for 16 h, and were fixed in 4% paraformaldehyde for 10 minutes. Cells were then washed in H_2O and incubated with 3 M HCl in order to permeabilise cells, for 30 minutes. Cells were washed thoroughly in PBS and incubated with anti-BrdU antibody (DAKO) at 1:200, in the presence of 0.5% Tween 20 and 0.5% BSA, for 1 h at 37 °C, followed by incubation in goat anti-mouse FITC antibody at 1:50 in the presence of 0.5% Tween 20 and 1% goat serum, for 1 h at 37 °C. Cells were washed in PBS, mounted in fluorescence medium and analyzed by fluorescence microscopy. Results were expressed as a percentage of proliferating BrdU positive cells against total number of cells identified by DAPI nuclear staining.

3.3.3.2 Alkaline phosphatase Immunostaining

Alkaline phosphatase belongs to a family of proteins that are attached to the plasma membrane via a glycosyl-phosphatidinositol linkage (Noda 1987) and catalyses the hydrolysis of phosphate monoesters:

$R\text{-}O\text{-}PO_3^{-} + H_2O \text{ ----> } R\text{-}OH + HPO^{4-}$

Alkaline phosphatase is widely used as a marker of the osteoblast phenotype and has been proposed to participate in bone mineralization (Waymire et al. 1995). Alkaline phosphatase was detected in primary osteoblast cultures using light microscopy. Cultures were washed in PBS and fixed in 4% paraformaldehyde for 10 minutes. Cells were washed in PBS and were incubated with alkaline phosphatase staining solution, consisting of 1 mg/ml Napthol-ASMX-mix and 1 mg/ml Fast Blue in 0.4% $MgCl_2$ solution, made in distilled water. The reaction mixture was filtered through a 0.2 μm sterile syringe filter prior to addition to cultures for 15 minutes at 37 °C. The reaction was inhibited by washing the cultures in PBS, followed by 1% Acetic acid solution. Osteoblasts expressing alkaline phosphatase were detected against total number of cells in cultures identified by nuclear DAPI staining.

3.3.3.3 Mineralised nodule formation (Von Kossa stain)

Primary osteoblasts were induced to form mineralised nodules in confluent cultures by addition of mineralisation solution containing 10 nM 1,25 dihydroxyvitamin D_3, 100nM Dexamethasone (Calbiochem, UK), 50 μg/ml Ascorbic acid and 10mM β-glycerol phosphate in normal growth medium (Noble et al. 1995). The mixture was filtered through a 0.2 μm sterile syringe filter prior to addition to cultures and was replaced every 3 days for 3 weeks, after which time bone nodules were visible under the light microscope in osteogenic cultures. After the mineralisation period, bone nodules were identified using Von Kossa staining (Bills et al. 1974). Cultures were fixed in 4% paraformaldehyde followed by incubation in 5% Silver Nitrate ($AgNO_3$) solution, exposed under strong light for 30 minutes at room temperature. Treatment with silver solution replaces calcium and phosphates ions as they become reduced, forming insoluble silver salts. The silver deposit becomes densely black after prolonged exposure to light.

$CaCO_3 + 2\ AgNO_3 \rightarrow Ag_2CO_3 + CaNO_3$

Ag_2CO_3 (light treated) $\rightarrow Ag_2O + CO_2$

(Seen as black)

Cultures were then washed in PBS and incubated in 3% sodium thiosulphate solution for 5 minutes, followed by Eosin staining for 3 minutes.

3.3.4 Induction of apoptosis and characterization of apoptotic bodies by Annexin-V FITC binding and PI staining.

3.3.4.1 Production and characterisation of osteocyte apoptotic bodies.

A range of methods of apoptosis induction was used in order to determine any specificity in response to osteocyte apoptotic products due to the specific mode of engendering apoptosis. Osteocytes (primary and MLO-Y4 cell line) were either incubated in 0.1% FBS media for 7-10 days, or in the presence of 0.4 mM H_2O_2 or 10^{-6} M Dexamethasone for 4-5 hours, at 37 °C. Following induction of apoptosis, osteocyte cultures were characterized by fluorescein isothiocyanate (FITC) conjugated Annexin-V and propidium iodide (PI) staining, in order to distinguish between viable (FITC negative, PI negative), early apoptotic (FITC positive, PI negative) and late apoptotic (FITC positive, PI positive) or necrotic cells (FITC negative, PI positive). In addition, a sample from the supernatant of each culture was

collected every hour during incubation with Dex and H_2O_2, or every 2 days during incubation in low serum media and apoptotic bodies were characterised by Annexin-V-FITC and PI staining to reveal the presence of early and late apoptotic changes.

3.3.4.2 Production and characterization of other apoptotic bodies

Apoptotic bodies derived from T hybridoma cells, IC21 monocyte-like cells and osteoblast precursor cells were produced in low serum medium for 7-10 days at 37 ^{o}C, and characterized by Annexin-V-FITC and PI staining. PMN and PBMC-derived apoptotic bodies were provided by Dr. Simon Brown.

3.3.5 Production of non-apoptotic osteocyte products

3.3.5.1 Induction of osteocyte necrosis and isolation of necrotic vesicles

Osteocytes were incubated in the presence of 0.8 mM H_2O_2 for 3 hours at 37 ^{o}C, to produce necrotic vesicles. Following induction of necrosis, osteocyte cultures were characterized by Annexin-V-FITC and PI, as described in §3.3.10.1 to distinguish between viable (FITC negative, PI negative), early apoptotic (FITC positive, PI negative) and late apoptotic or necrotic cells (FITC positive, PI positive and FITC negative, PI positive). To investigate the effect of medium that nourished necrotic vesicles, osteocyte cultures were incubated in 0.1% FBS media for more than 14 days. Medium was collected following isolation of the vesicles by centrifugation at 13,000 g and removal of cell debris by passing through a 0.2 μm sterile syringe filter. More than 80% of the vesicles stained positive only for PI (indicative of necrotic but not apoptotic cells) and were resuspended in growth medium appropriate for the target cultures, according to their density, prior to presenting to target cell cultures.

3.3.5.2 Production and isolation of osteocyte lysis products

Osteocytes were incubated in solution containing 2 mM Tris-HCl, 2 mM EDTA, 2 mM EGTA and 0.1% Triton-X for 15 minutes on ice. Following lysis of cells, cell fragments were collected by centrifugation at 3,000 g for 10 minutes. The pellet was resuspended in αMEM medium and presented to target cell cultures at density described in §3.3.8.

3.3.6 Purification of apoptotic bodies by Annexin V-biotin-streptavidin complex.

Apoptotic bodies were purified on the basis of phosphatidylserine (PS) exposure on the outer leaflet of the cell membrane, since this is one of the early changes that take place in the apoptotic cell membranes, which can be visualised following binding to FITC labelled Annexin V protein (Figure 7). The procedure followed comprised modifications of the technique by Brown et al 2002. Following induction of apoptosis, cells were incubated with CellTracker Orange dye (to facilitate their identification at later experimental stages) (as described in §3.3.5), at 1 μg/ml or with DAPI at 2.5 ng/ml for 20 minutes and washed in PBS to remove excess dye. Apoptotic products were collected in universal tubes and incubated with 0.3 M of biotinylated Annexin V (Roche, UK) at a density of 100,000 cells/ml, on ice for 5 minutes followed by incubation with 100 μl Streptavidin superparamagnetic beads for 10 minutes on ice. Apoptotic products expressing PS were purified with the use of a magnetic sorting device (magnetic activated cell sorting-MACS) (DAKO, UK) and were washed in Hanks' Buffered Saline Solution to dissociate the apoptotic body-magnetic bead complex. Prior to presenting vesicles to target cell cultures, they were resuspended in growth medium appropriate for the target cultures, at measured apoptotic body density. Samples of apoptotic bodies were also cytospan and stained with Hematoxylin & Eosin, as described in §3.3.10.4 to characterize formation of apoptotic body-magnetic bead complexes (Figure 8).

3.3.7 Visualization of apoptotic body and target cell morphology using fluorescence microscopy.

Apoptotic bodies were readily visualised with Orange Cell Tracker CMTMR (5-(-6)-(((4-chloromethyl)benzoyl)amino)tetramethylrhodamine, which becomes absorbed at 540 nm and emitted at 566 nm (Molecular Probes), while target osteoblasts were visualised with Green Cell Tracker CMFDA (5-choromethylfluorescein diacetate), absorbed at 492 nm and emitted at 516 nm (Molecular Probes). Orange Cell Tracker and Green Cell Tracker pass freely through the cell membrane and react with intracellular thiols in glutathione S-transferase mediated reaction, producing a cell impermeant fluorescent dye-thioether which can be retained for a long time, since it

can be fixed with aldehydes. Orange Cell Tracker does not require enzymatic cleavage by esterases to activate its fluorescence, while Green Cell Tracker is non-fluorescent and colorless until inside the cytoplasm, where esterases cleave off its acetate groups, releasing a highly fluorescent product. Cell were incubated for 20 minutes with either compound at a concentration of 1 μg/ml in DMSO followed by thorough washing to remove excess unconjugated probe. In addition, both the target cells and phagocytic prey were stained with DAPI (4',6-Diamidino-2-phenylindole), which is stimulated at 344 nm and emitted at 488 nm. DAPI is rapidly taken up by cells, and forms fluorescent complexes with double-stranded DNA. Binding to DNA enhances the fluorescence of DAPI because it is a highly energetic interaction or because it forms stable hydrogen bonds with the minor groove of the double helix as well. The exact staining method with either the Cell Tracker or DAPI varies according to experimental requirements and is indicated for individual experiments in the figure legends.

3.3.8 Phagocytosis assay

Phagocytosis was determined using minor modifications of the technique by Tosello-Trampont et al. 2001. Briefly, target cells were plated at a density of 30,000 cells/well for primary osteoblasts, 15,000 cell/well for TE85 human osteoblasts, 20,000 cells/well for bone marrow stromal cells, 30,000 cells/well for primary bone marrow macrophages, 200,000 cells/well for primary $CD4^+$ T lymphocytes and 20,000 cells/well for T hybridoma lymphocytes, in 96 well plates (Corning, UK). For apoptotic products, density varied according to target cell density in order to achieve an average of 5x more apoptotic bodies than cells in a well (5 bodies/per target cell) (Fadok et al. 1998, Moodley et al. 2003). Target cells were stained with CellTracker Green dye at 1 μg/ml for 20 minutes or with DAPI at 2.5 ng/ml for 20 min at 37 °C, and were washed in PBS to remove excess dye prior to incubation with apoptotic bodies for the time points (range of 1 h-48 h) indicated in the figure legends. Media conditioned by both healthy and apoptotic prey cell cultures were also collected and presented to target cell cultures after centrifugation at 13,000 g and purification through a 0.2 μm sterile syringe filter, to remove solid cellular material.

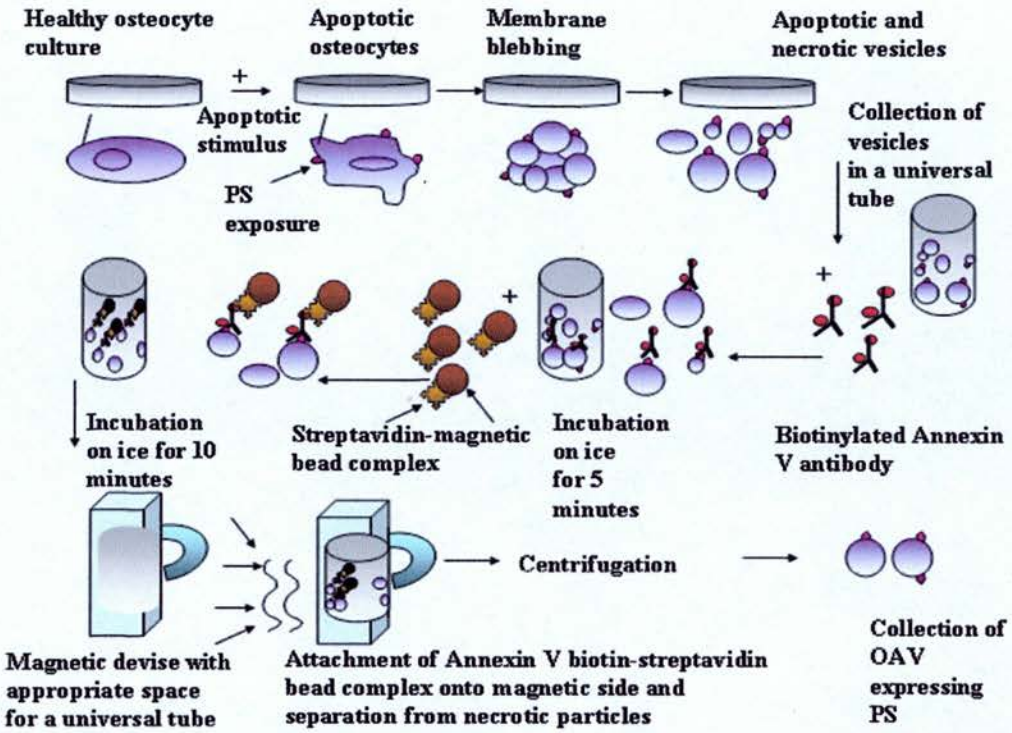

Figure 7. Purification of osteocyte apoptotic bodies displaying phosphatidyl serine. Osteocytes in cultures were incubated with agents inducing apoptosis. Primary and secondary apoptotic products as well as necrotic products were collected in universal tubes and incubated with 0.3 M of biotinylated Annexin V on ice for 5 minutes, followed by incubation with 100 µl Streptavidin superparamagnetic beads for 10 minutes on ice. Apoptotic vesicles expressing PS on the surface were purified with the use of a magnetic device, washed in Hanks' Buffered Saline Solution and were centrifuged to dissociate the apoptotic body-magnetic bead complex, prior to presenting to target cell cultures.

A

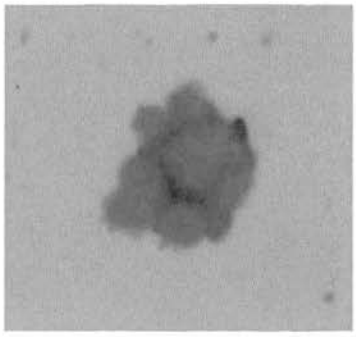

B

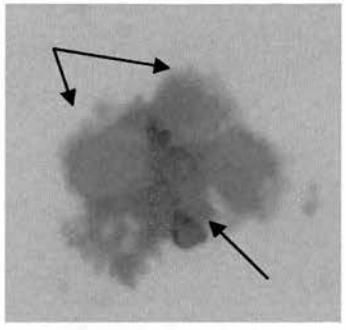

Figure 8. Purification of osteocyte apoptotic bodies. **A**. Apoptotic osteocyte displaying apoptotic bodies. **B**. Apoptotic bodies were purified on the basis of phosphatidyl serine (PS) exposure, as one of the early changes that take place in the apoptotic cell membranes, which can be identified following binding to Annexin V protein, through the formation of Annexin-V-biotin-streptavidin complex with the use of a magnetic device. Samples were cytospan and stained with H&E.

Experiments were carried out a minimum of 3 times, and each treatment group was represented by 3 wells in each independent experiment. Cells were observed in 3 fields per well resulting in 9 fields per treatment group. Control treatments comprised vehicle treatments using the medium in which vesicles were resuspended, which was the growth medium used for each target cell culture. For experiments investigating the response of target cells to media that nourished apoptotic vesicles (CM), vehicle treatments include the addition of an equal volume of growth medium used to maintain the cells producing the particular apoptotic vesicles.

3.3.9 Interaction and Engulfment assays

Following incubation of target cells with apoptotic bodies for the appropriate time intervals, indicated in the figure legends, medium was removed and cultures were washed twice in ice-cold PBS to remove apoptotic bodies with low affinity interactions with the target cells. For estimation of engulfment of apoptotic bodies by target cells, cultures were washed for 2 minutes in trypsin at 2.5 gm/l, so that the apoptotic bodies would be removed from the surface of target cells and after appropriate staining, as described above, would only appear inside target cells. Engulfment was expressed as percentage of cells with 0, 1, 2, 3, 4 or more apoptotic bodies. Experiments were carried out a minimum of 3 times, and each treatment group was represented by 3 wells in each independent experiment. Cells were observed in 3 fields per well resulting in 9 fields per treatment group.

3.3.10 Determination of Apoptotic State

A range of techniques were used to assess the apoptotic state, for all the independent experimental culture setups. Cells were observed in 3 fields per well (x20 magnification lens, approximately 40-100 cells per field) resulting in 9 fields per treatment group. Identical magnifications were used for all apoptosis estimates allowing similar numbers of cells to be counted per field in all experiments.

3.3.10.1 Annexin-V-FITC Assay

One of the earliest changes that occur in cells undergoing apoptosis is the appearance of negatively charged phospholipids on the outer leaflet of the membrane bilayer,

which can be detected with fluorescently labelled Annexin V; a Ca^{2+}-dependent phospholipid binding protein with high affinity for phosphatidyl serine (PS) (Martin et al. 1995). Cells were washed in PBS and incubated with Annexin-V-FITC at a concentration of 1 μg/ml for 15 minutes at RT, followed by PI at 2.5 ng/ml to identify necrotic cells in the culture. Analysis by fluorescence microscopy, allowed discrimination between viable (FITC negative, PI negative), apoptotic (FITC positive) or necrotic cells (FITC negative). Apoptotic cells were expressed as the percentage of the ratio of annexin positive and PI negative cells estimated from 9 fields (3 wells per treatment and 3 fields per well) over the total number of cells estimated from those fields. Total number of cells was estimated using brightfield microscopy.

$$\text{Percentage of apoptotic cells} = \frac{\text{Average number of apoptotic cells from 9 fields}}{\text{Average number of cells from 9 fields}} \times 100$$

3.3.10.2 DNA fragmentation using in situ Nick Translation

The percentage of target cells demonstrating DNA breaks was investigated on samples fixed in 4% paraformaldehyde, using a sensitive DNA nick translation technique detecting single DNA breaks (Noble et al. 1997). In situ nick translation staining allows the determination of early DNA breaks, prior to the loss of any DNA content or morphological variations and prior to plasma membrane permeabilisation (Petit et al 1995). Positive controls were established through pre-treatment with DNaseI (Roche, UK) at 0.2 mg/ml in PBS, for 30 minutes. Cells were exposed to nick translation mixture which consisted of 3 μM Digoxigenin (DIG) labelled dUTP (DIG-11-dUTP), 3 μM each of dATP, dGTP, dCTP, 50 mM Tris HCl, pH 7.5, 5 mM $MgCl_2$ and 0.1 mM dithiotreitol and 0.5 μl/100 μl DNA polymerase for 1 hour at 37 ^{o}C, in a humidified chamber (Roche, UK). Negative controls were established by omitting from the NT mixture. Wells were washed in PBS and incubated for 1 hour at RT with FITC-labelled anti-DIG antibody (Roche, UK) and 5% normal sheep serum. Wells were washed in PBS, counter stained with PI at 2.5 ng/ml and mounted in DAKO mounting medium (DAKO, UK). Target cells staining positive for FITC label and PI, were considered as cells containing fragmented DNA. The ratio of total

cells (PI positive) to apoptotic (FITC positive) was determined using fluorescence microscopy and digital image capture.

$$\text{Percentage of apoptotic cells} = \frac{\text{Average number of FITC cells from 9 fields}}{\text{Average number of PI cells from 9 fields}} \times 100$$

3.3.10.3 DAPI staining for healthy and apoptotic cell morphology

DAPI (4',6-Diamidino-2-phenylindole) staining reveals chromatin condensation, shrinkage of nuclei and the fragmentation of the nuclear material into smaller blebs, representing late stages during the apoptotic cascades (Cowden et al. 1981). Following experimental treatment, cells were fixed in 4% paraformaldehyde, washed in PBS and air-dried. Cells were then incubated with DAPI at 2.5 ng/ml for 20 minutes, washed in PBS and examined by fluorescence microscopy and digital image capture. Healthy cells were characterised by intact nucleus and normal cytoplasmic appearance. Results were expressed as the percentage of the ratio of apoptotic to non-apoptotic cells

$$\text{Percentage of apoptotic cells} = \frac{\text{Average number of apoptotic cells from 9 fields}}{\text{Average number of cells from 9 fields}} \times 100$$

3.3.10.4 Cytospin and H&E staining

For non-adherent CD4+ T lymphocyte and T hybridoma cell cultures, apoptotic and healthy morphology were investigated, in addition to the above methods, with Haematoxylin & Eosin staining. H&E staining enabled the visualisation of nuclei as they stain deep blue-black with haematoxylin detecting morphological nuclear changes during late stages of apoptosis, while the cytoplasm is stained pink after counterstaining with eosin. Following completion of the experiment, samples of 100 µl were collected from the supernatant of experimental samples and were placed into cytospin chambers. Samples were cytospan onto slides after being centrifuged for 3 minutes at 300 rpm. Samples were immediately fixed for 5 minutes in methanol and were stained with H&E for 2 minutes, after which samples were thoroughly washed in distilled water. Samples were left to air-dry and were mounted in pertex mounting medium (CellPath, UK). Apoptotic and healthy morphology were characterized under the light microscope.

3.3.11 Inhibition of apoptosis using caspase inhibitors

Caspases are involved at various stages in apoptotic cascades, mediating either death receptor pathways or cleavage of intracellular components in order to disassemble the cell's structure (Thornberry et al. 1998). In order to determine whether osteoblast apoptosis in response to OAB was a caspase-dependent process, target cells were incubated with caspase 3/7 inhibitor (Glaxosmithkline, USA), a non-peptide selective inhibitor of caspases 3 and 7 based on sulphanylamide derivatives (Lee et al. 2000), mediating mainly end-stage cytoskeletal and nuclear changes in the apoptotic cell at 1 μM for 1 hour prior to addition of apoptotic bodies.

3.3.12 Statistical Analysis

All statistical analyses were performed using quantitative data analysis with SPSS release 10.1 for Windows. The distribution of the data within the sampling population they were obtained from was determined by applying the Kolmogorov-Smirnov test. In cases where the randomly selected sample data were shown to have a normal (Gaussian) distribution (95% of data would fall within plus or minus 1.96 standard deviations from the mean value) parametric statistical tests such as two-tailed Analysis of Variance (ANOVA) and the post-hoc Tukey test and Dunnett test were performed directly to determine statistical significance between the treatment groups. For comparison between percentages or proportions, the square root of each proportion was transformed into its arcsine, which enabled the distribution of the data to be nearly normal allowing therefore the use of parametric tests. The Tukey test was used to compare more than two means at once since this reduces the error associated with multiple t-tests (Zar 1984), while the Dunnett test was used to compare the control mean to all the other group means (Zar 1984). In order to determine the functional dependence of one variable (e.g. the proportion of apoptotic osteoblasts) on another (number of OAB phagocytosed), simple linear regression analysis was used and the correlation coefficient and slope of the regression line) were calculated to determine the significance of the regression. Results are expressed as means ± S.D. $p<0.05$ was considered to be statistically significant.

3.4 Results

3.4.1 Characterization of osteocyte apoptotic bodies (OAB) and bodies derived from other cells types

Osteocytes were induced to undergo apoptosis as described in §3.3.4 **(Figure 9A and 9C**) and OAB were collected and characterized based on the exposure of PS on the plasma membrane detected with fluorescently labeled Annexin V. The staining was combined with PI to allow differentiation between apoptotic, secondary necrotic and necrotic vesicles. Following incubation with Dex and H_2O_2 for 4-5 hours or in low serum media for 7-10 days, more than 80% of the vesicles collected from the supernatant of cultures were positive for Annexin V (**Figure 9B and 9D**). OAB were spherical vesicles, which varied in diameter ranging between 0.02 μm to 0.5 μm. (**Figure 10**). Although the presence of necrotic osteocyte debris in the primary extraction was considered negligible, since less than 5% were positive for PI (indicative of necrotic cells and/or late stage leaky apoptotic particles), osteocyte apoptotic bodies were further purified based on the exposure of Annexin V, (by MACS, as described in §3.3.6) to ensure the absence of necrotic factors (**Figure 10**). In a similar manner to OAB, vesicles derived from T hybridoma cells, IC21 monocytes and fibroblastic/osteoblast precursor cells were characterised and stained for PS exposure with Annexin V FITC and further purified by MACS (**Figure 11**).

3.4.2 Characterization of primary osteoblast and osteocyte cultures

Cultures obtained from calvarial digestions number 2-5 had the morphological characteristics of osteoblasts, with cuboidal appearance and polarized nuclei (Baron 1996). In addition osteoblast cultures were characterized as positive for alkaline phosphatase staining (**Figure 12A**) and formation of bone nodules (**Figure 12B**), which are indicative of osteoblast function (Wong et al. 1983, Lomri et al. 1988). Osteocyte cultures were isolated from calvarial digestions above number 6 and characterised based on proliferation, since primary osteocytes are non-proliferating cells, identified by BrdU staining as described in §3.3.3. The majority of the cells did not stain positive for BrdU (**Figure 12C**), while they also had the characteristic morphology of osteocytes, with long cytoplasmic processes and relatively small cell body (**Figure 12D**).

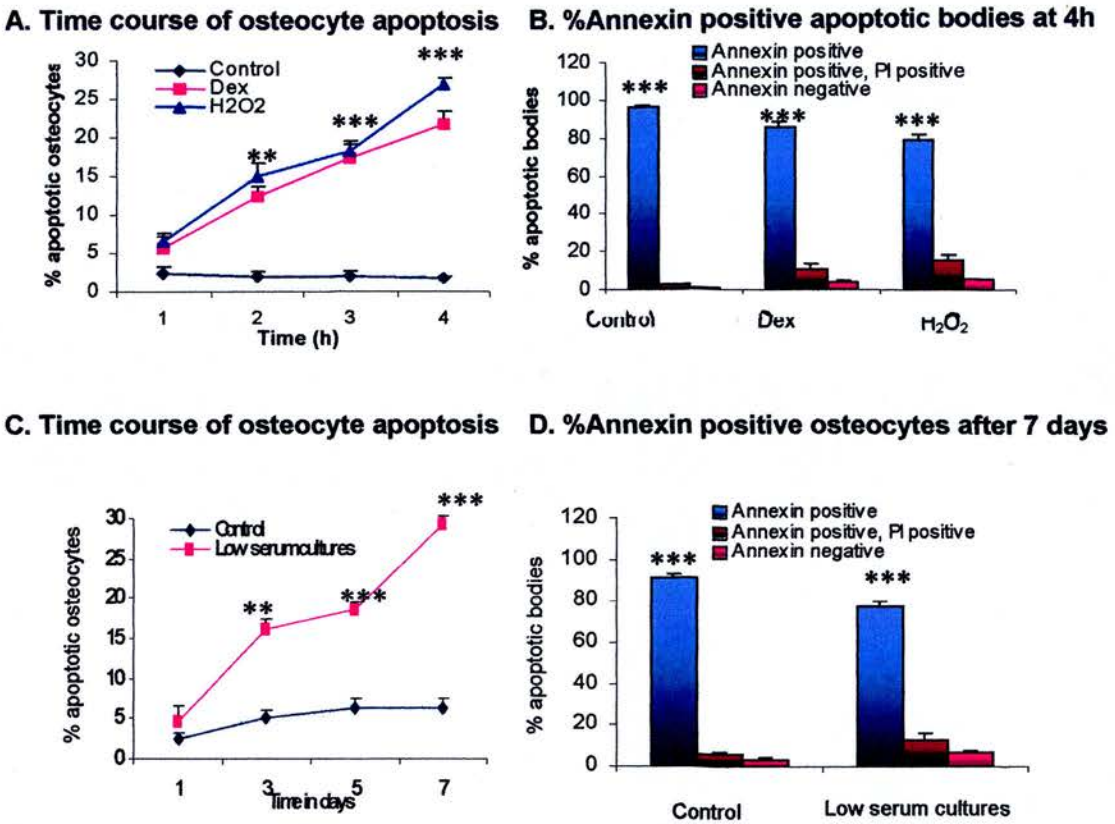

Figure 9. Characterisation of osteocyte apoptotic bodies (OAB). OAB were obtained from cultures incubated in low serum or in the presence of Dex at 10^{-6} M and 0.4 mM H_2O_2. **A**. Time course induction of osteocyte apoptosis in the presence of Dex at 10^{-6} M and H_2O_2. **B**. Mean percentages of apoptotic vesicles collected from the supernatant of apoptotic osteocyte cultures, staining positive for Annexin V and PI after 5 hours incubation with Dex or H_2O_2. **C**. Time course induction of osteocyte apoptosis incubated in low serum growth medium. **D**. Mean percentages of apoptotic vesicles collected from the supernatant of apoptotic osteocyte cultures staining positive for Annexin V and PI after 7 days incubation in low serum. Error bars represent ± S.D. *** = $p<0.0001$, ** = $p<0.001$, compared to (A, C) control cultures and (B, D) Annexin negative vesicles. Annexin positive = early apoptotic, Annexin positive, PI positive = late apoptotic or secondary necrotic bodies and Annexin negative = necrotic bodies.

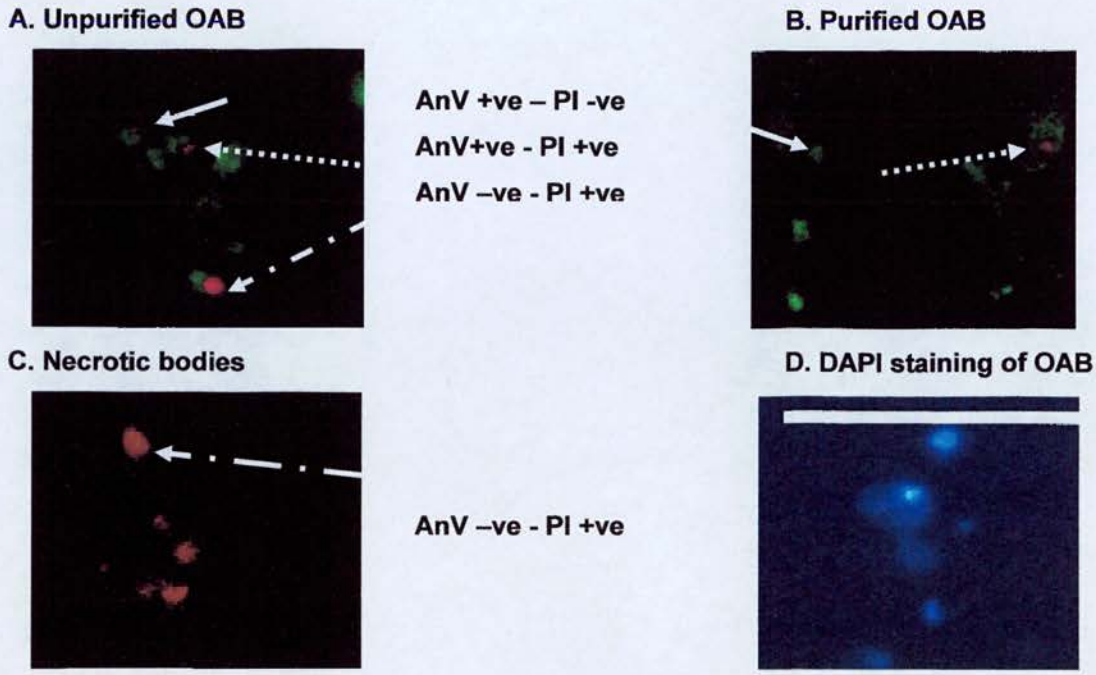

Figure 10. Osteocyte Apoptotic Bodies. OAB were stained with Annexin V-FITC (green) to indicate exposure of phosphatidyl serine on the plasma membrane, and counterstained with PI (red) to indicate late apoptosis or necrosis. **A**.Unpurified bodies contained early apoptotic (AnV+ve -PI-ve), late apoptotic (AnV+ve –PI+ve) or necrotic bodies (AnV-ve –PI+ve) **B**. Purified bodies contained early apoptotic (AnV+ve -PI-ve) and late apoptotic bodies (AnV+ve –PI+ve) and **C**. Necrotic bodies (AnV-ve –PI+ve). **D**. DAPI staining of OAB to show the presence of nuclear osteocyte fragments...Bar =10 μm

——→ =AnV+ve -PI-ve ·····→= AnV+ve –PI+ve —·→ =AnV-ve–PI+ve

A. T hybridoma cell cultures

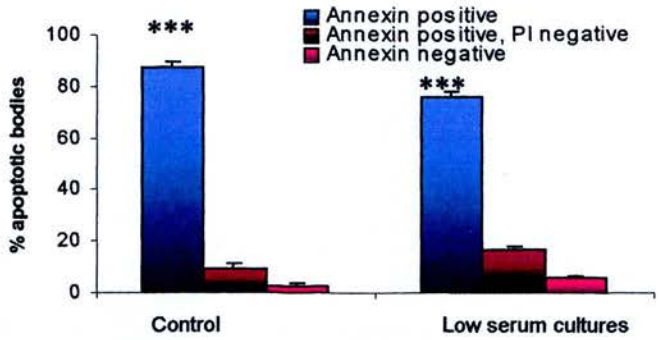

B. IC-21 cell cultures

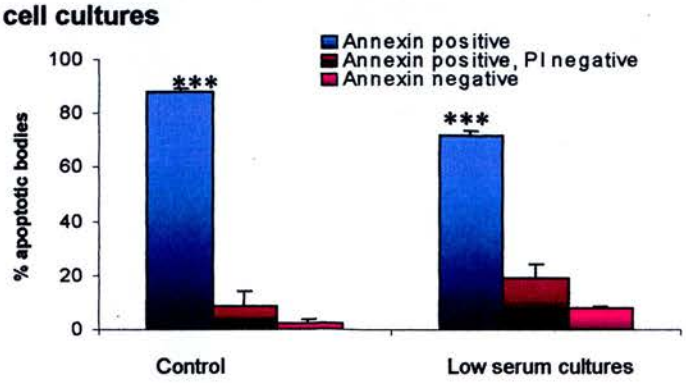

C. Fibroblast/osteoblast precursor cultures

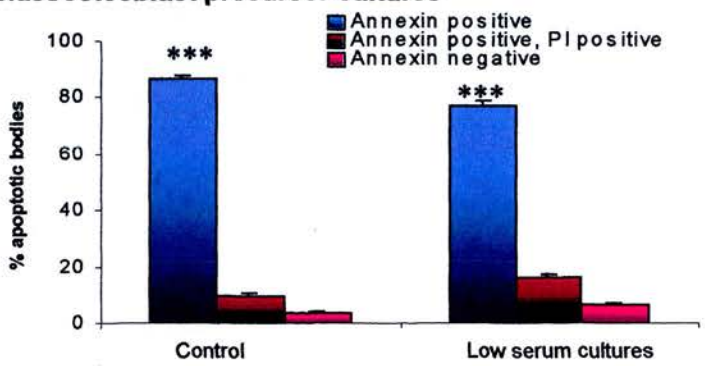

Figure 11. Characterisation of apoptotic bodies from other cell types. Apoptotic products were obtained from cultures incubated in growth medium containing 0.1% FBS serum for 7 days. Graphs represent mean percentages of apoptotic bodies ± SD, collected from the supernatant of apoptotic cultures **A**. T hybridoma cell cultures, **B**. IC21 cell cultures and **C**. fibroblast/osteoblast precursor cultures staining positive for Annexin V and PI after 7 days incubation in low serum. Error bars represent ± SD. *** = $p<0.0001$, compared to Annexin negative bodies. Annexin V positive = early apoptotic, Annexin V positive, PI positive = late apoptotic or secondary necrotic bodies and Annexin V negative = necrotic bodies.

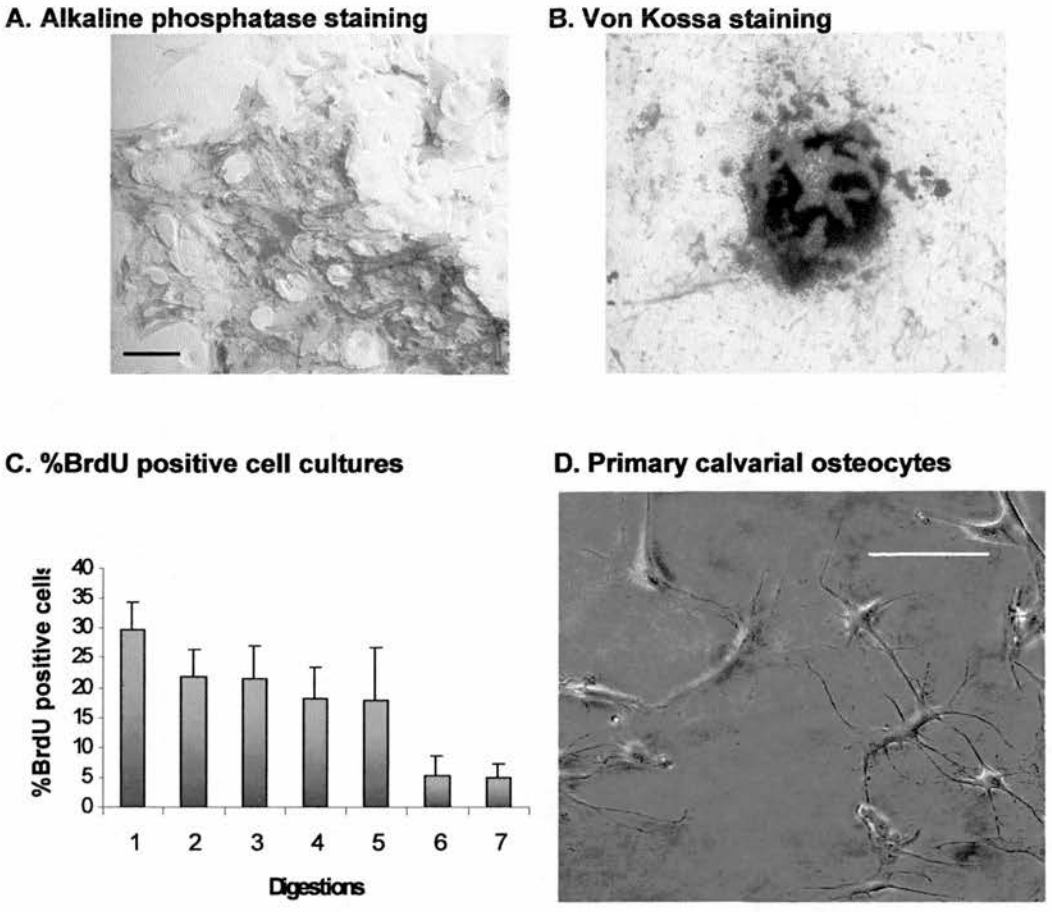

Figure 12. Isolation of primary osteoblast and osteocyte cultures by sequential digestions of mouse calvariae. Osteoblast cultures were characterised by **A.** Alkaline phosphatase staining and **B.** Formation of mineralised nodules identified by Von Kossa staining. **C.** Estimation of mean percentages of BrdU positive cells. **D.** Osteocyte cultures were isolated from digestions above number 6, which did not contain many proliferating cells, compared to cultures isolated from the first 5 digestions. Osteocyte cultures did not display mineralization in vitro using von kossa staining, while they were characterised by very low alkaline phosphatase activity. Osteoblast cultures were isolated from digestions 2-5, while digestion 1 contained mostly fibroblasts. Bar = 10 μm.

3.4.3 Apoptotic osteocytes induce osteoblast apoptosis

Since osteocytes are located close to the surface-resident osteoblasts in bone, osteocyte apoptotic bodies (OAB) were initially presented to TE85 human osteoblasts and primary mouse osteoblasts in culture for various time periods. Following incubation with apoptotic osteocytes, both types of osteoblasts were shown to undergo apoptosis (**Figure 13A and 14A**). In vivo studies have shown that control levels of apoptosis in osteoblasts would be around 0.66% and would increase for example to 2% (Weinstein 1998) and 19% (Plotkin 1999) following prednisolone treatment for 27 and 56 days respectively. In this thesis, mean percentage of apoptotic osteoblasts was increased from 2 ± 0.1% S.D. in untreated TE85 osteoblasts cultures and 2.6 ± 0.6% S.D. in untreated primary mouse osteoblast cultures to 20 ± 0.9 % S.D. and 24.5 ± 3.5% S.D. respectively in the presence of OAB ($p < 0.0001$ compared to control cultures in both cases), as evidenced by DAPI staining of cultures. Induction of apoptosis was accompanied by significant cell loss (**Figure 13B and 14B**) by 5 hours and 24 hours of incubation, whereas by 48 hours both increased apoptosis and cell reduction were minimised, compared to control cultures, indicating further proliferation of surviving cells.

Osteoblast apoptosis at 24 hours incubation with OAB was further characterised by externalisation of PS as evidenced by Annexin-V FITC staining (15 ± 2% S.D. compared to 0.31 ± 0.31% S.D. in untreated cultures) (**Figure 15A-15C**). In addition, Nick Translation identified fragmented DNA (**Figure 16A**), while DAPI staining showed chromatin condensation (**Figure 16B**). Confocal microscopy showed that numerous OAB were localised on the surface or inside osteoblasts which appeared apoptotic (**Figure 17A**). In addition, estimation of the percentage of apoptotic osteoblasts associated with OAB either engulfed or bound to their surface showed that osteoblasts appeared more likely to be apoptotic the more OAB were associated with them (**Figure 17B**). Indeed, regression analysis showed that there was a significant ($p = 0.039$) dependency of the proportion of apoptotic osteoblasts on the number of OAB phagocytosed by osteoblasts that appeared apoptotic (**Figure 17B**).

A. % Apoptotic osteoblasts

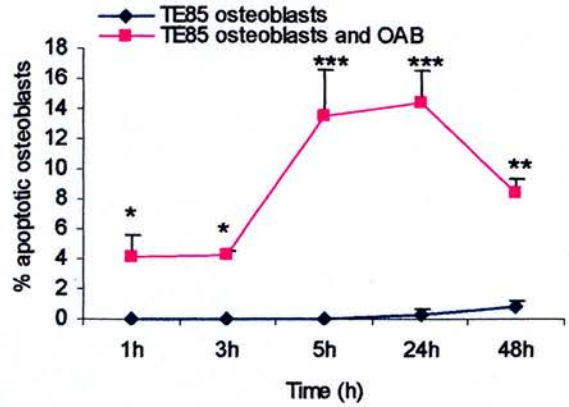

B. Number of cells per field

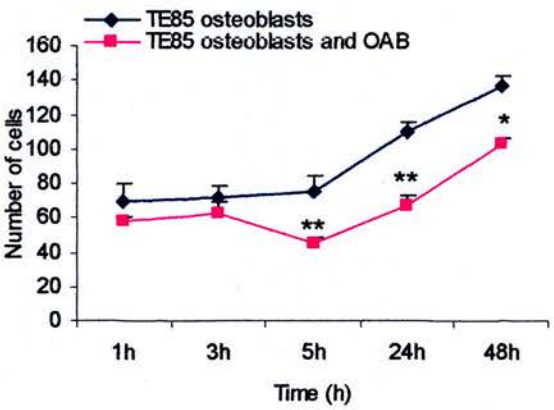

Figure 13. TE85 osteoblast apoptosis in relation to time. Osteoblast cultures were incubated in the presence of OAB for 1-48 h. Apoptotic osteoblasts were evidenced by DAPI nuclear staining and fluorescence microscopy. Graphs represent **A**. Mean percentages of apoptotic osteoblasts and **B**. Number of osteoblasts in culture, in relation to time, in the presence of OAB. *** = $p < 0.0001$, ** = $p < 0.001$, * = $p < 0.05$, compared to control. Error bars represent ± S.D. Control cultures represent treatment with vehicle for OAB (αMEM).

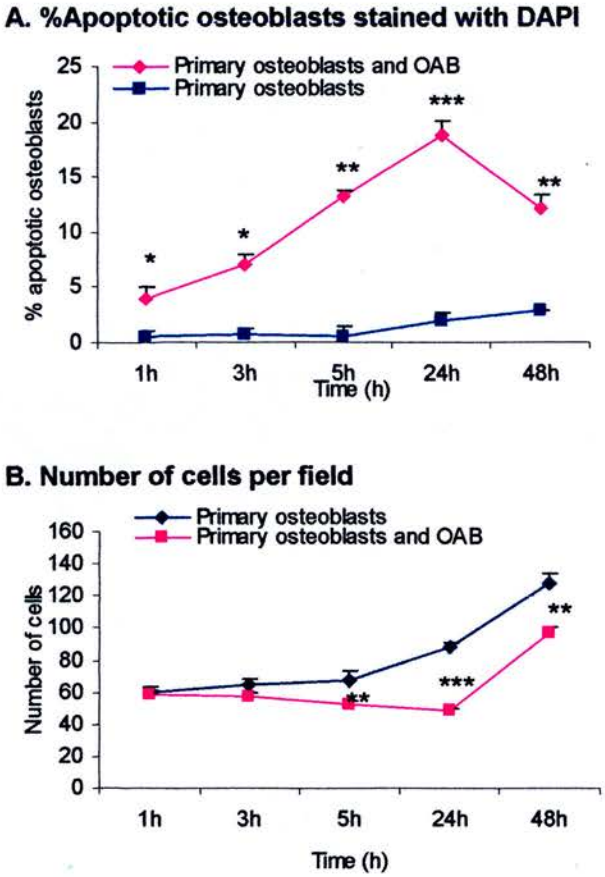

Figure 14. Primary mouse osteoblast apoptosis in relation to time. Osteoblast cultures were incubated in the presence of osteocyte apoptotic bodies for 1-48 h. Apoptotic osteoblasts were evidenced by DAPI nuclear staining. **A**. Mean percentages of apoptotic osteoblasts **B**. Osteoblast cell number in cultures, in relation to time, in the presence of osteocyte apoptotic bodies. *** = $p < 0.0001$, ** = $p < 0.001$, * = $p < 0.05$, compared to control. Error bars represent ± SD. Control cultures represent treatment with vehicle for OAB (αMEM).

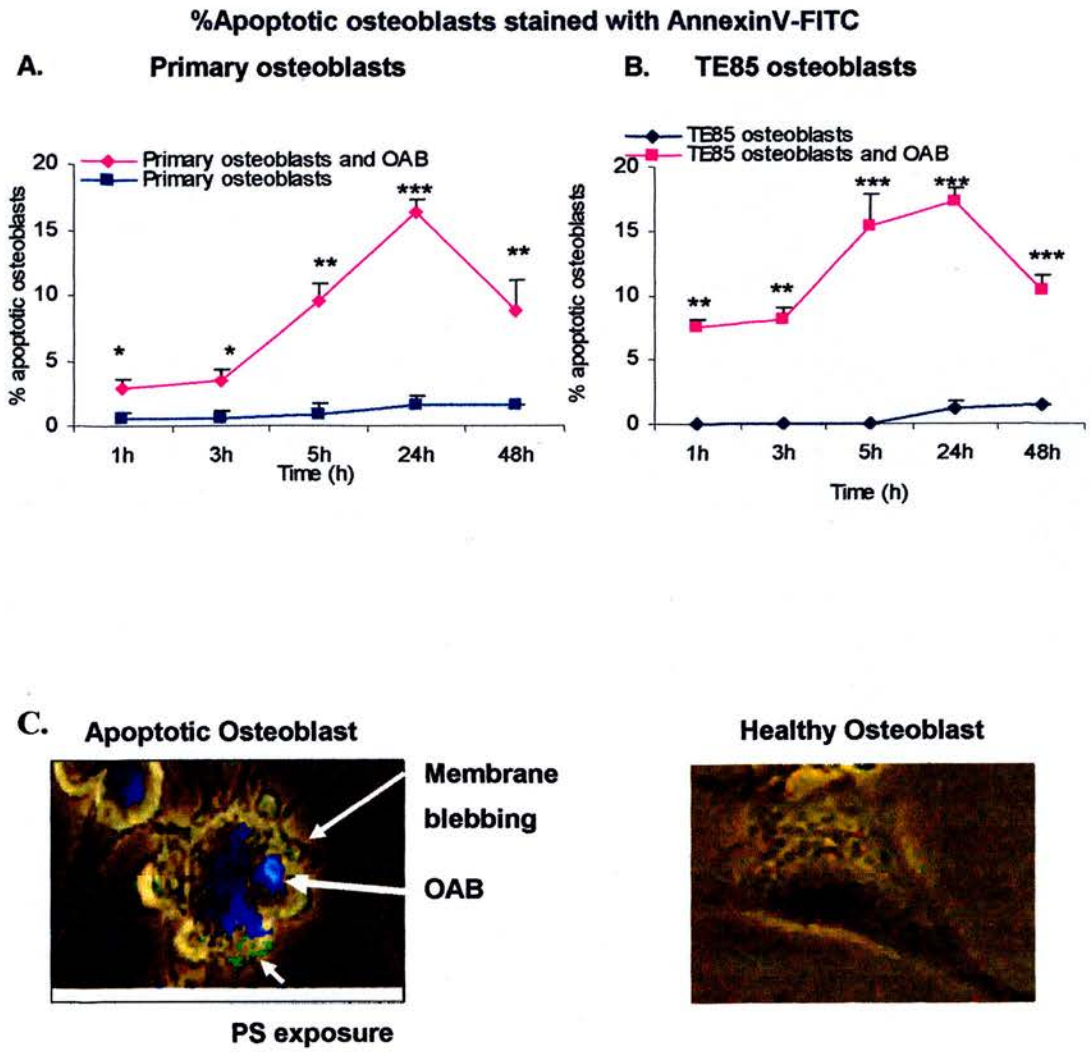

Figure 15. Osteoblast apoptosis in the presence of osteocyte apoptotic bodies. Osteoblast cultures were fed with OAB and apoptosis was evidenced in a time course of 1-48 hours by Annexin-V FITC binding and fluorescence microscopy. Graphs represent mean percentages of apoptotic **A**. TE85 osteoblasts and **B**. primary osteoblasts ± SD, in the presence of OAB. *** = $p < 0.0001$, ** = $p < 0.001$, * = $p < 0.05$, compared to control. Control cultures represent treatment with vehicle for OAB (αMEM). **C**. Apoptotic osteoblast (left image) exhibiting membrane blebbing and PS exposure evidenced by Annexin-V FITC staining (green), having phagocytosed OAB (DAPI blue) and healthy osteoblast not exposed to OAB (right image). Bar = 10 μm

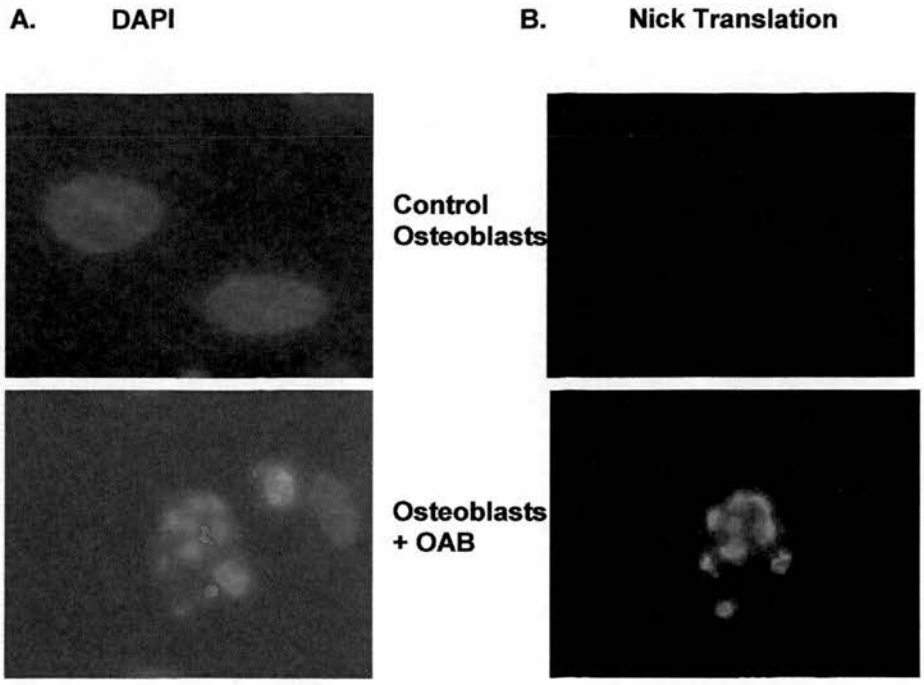

Figure 16. Osteoblast apoptosis in the presence of osteocyte apoptotic bodies. Primary osteoblast cultures were incubated in the absence (top panel) and presence (top panel) of OAB and apoptosis was evidenced after 24 hours incubation with **A**. DAPI nuclear staining and **B**. Nick Translation DNA staining which identified formation of apoptotic bodies and fragmented DNA, in contact with OAB. (Green = NT staining, Blue =DAPI staining and Red =OAB).

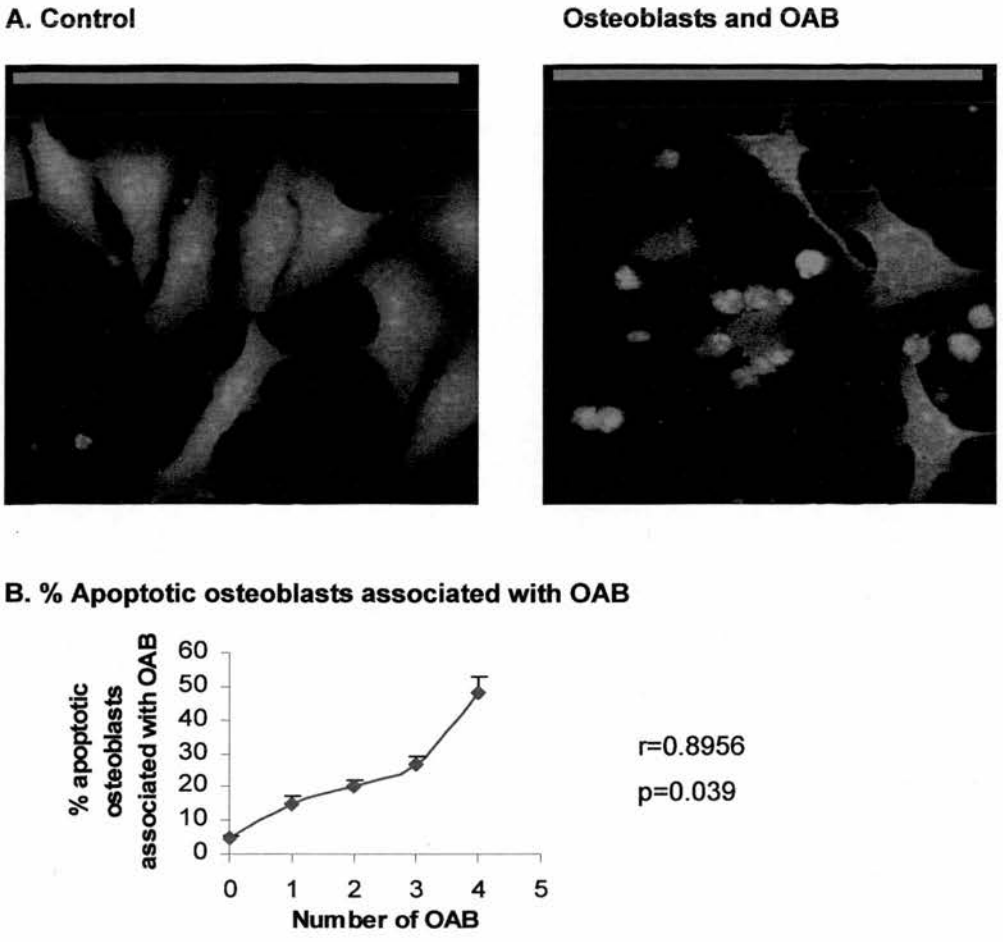

Figure 17. Osteoblast apoptosis in the presence of osteocyte apoptotic bodies. **A**. Representative images of confocal microscopy of osteoblast cultures (Green Cell tracker) fed with osteocyte apoptotic bodies (Orange Cell tracker). Left panel shows control osteoblast cultures and right panel shows cultures fed with OAB. Bar = 20 μm. **B**. Osteoblasts were incubated with OAB and the percentage of apoptotic osteoblasts that carried none, 1, 2, 3 or ≥ 4 OAB was determined. Error bars represent ± S.D., n=3, r = correlation coefficient.

3.4.4 Induction of osteoblast apoptosis is dependent on caspases 3 and 7

In order to determine whether OAB-induced osteoblast apoptosis involved activation of caspases to mediate end-stage cytoskeletal and nuclear fragmentation, a selective inhibitor of caspases 3 and 7 based on sulphanylamide derivatives (Lee et al. 2000) was used to treat osteoblast cultures prior to presentation of OAB. Treatment with caspase 3,7 inhibitor prevented DNA breakdown and formation of membrane blebs as evidenced by Nick translation (**Figure 18A**) and DAPI (**Figure 18B**) staining of osteoblast cultures, in the presence of OAB ($p = 0.01$ and $p = 0.003$, respectively compared to treatment with OAB alone).

3.4.5 Induction of osteoblast apoptosis is independent of the stimulus that induced osteocyte apoptosis

To characterise the ability of apoptotic osteocytes to induce osteoblast apoptosis, OAB were prepared by stimulation with different inducers of apoptosis, including absence of growth factors, Dex and H_2O_2 as described in §3.3.4 (**Figure 19**). DAPI staining of osteoblast cultures, 24 hours after incubation with OAB, showed that osteoblasts efficiently phagocytosed OAB. Mean percentages of apoptotic osteoblasts were significantly increased compared to control cultures ($p < 0.0001$ in all cases) independently of the stimulus that induced apoptotic osteocyte death.

3.4.6 Soluble osteocyte apoptotic products do not affect osteoblast survival

In order to determine the effect of soluble rather than apoptotic body-associated apoptotic products on osteoblast survival, medium that nourished the apoptotic osteocytes was introduced to osteoblast cultures. Estimation of mean percentages of apoptotic osteoblasts by DAPI staining of cultures indicated that soluble apoptotic products failed to induce osteoblast apoptosis ($p > 0.05$ compared to control) (**Figure 20**). In addition, medium that conditioned healthy osteocyte cultures had no effect on osteoblast survival, indicating that osteoblasts were only sensitive to the presence of osteocyte apoptotic bodies (**Figure 20 and 21**).

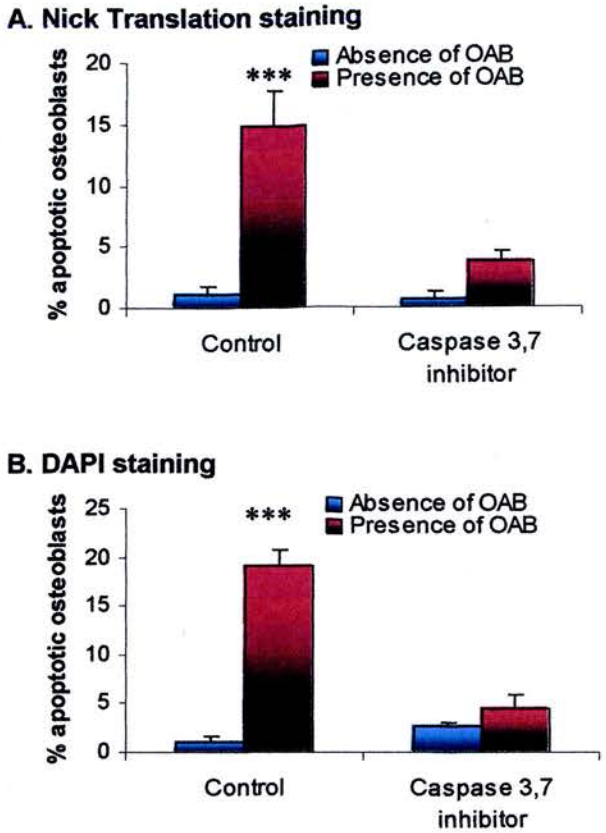

Figure 18. Caspase 3, 7-dependent induction of osteoblast apoptosis. Incubation of osteoblast cultures with an inhibitor of caspases 3 and 7 reduced mean percentages of apoptosis in the presence of OAB as estimated by **A**. Nick Translation staining and **B**. DAPI staining of cultures. Control treatments represent vehicle treatments for the medium in which OAB were prepared (αMEM) and percentages of apoptotic osteoblasts are statistically indifferent from untreated cultures (0.97 ± 0.1 S.D., $p > 0.05$) and vehicle cultures (DMSO) for caspase inhibitors (0.97 ± 0.65 S.D.). Error bars represent ± SD. *** = $p < 0.0001$, ** = $p < 0.001$, compared to control cultures.

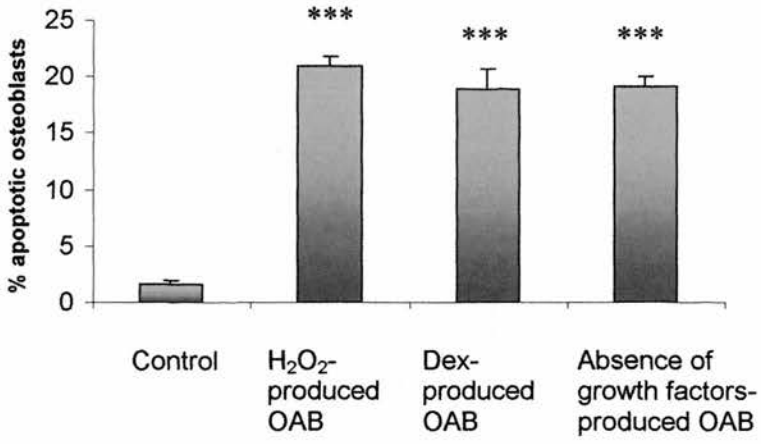

Figure 19. Osteoblasts undergo apoptosis in the presence of apoptotic osteocytes independently of the stimulus that induced apoptotic osteocyte death. OAB were prepared in response to absence of growth factors, Dexamethasone and H_2O_2, and were fed to TE85 osteoblasts in culture. Graphs represent mean percentages of apoptotic osteoblasts ± S.D., as estimated with DAPI staining of cultures. *** = $p < 0.0001$, compared to control. Control cultures represent treatment with vehicle for OAB (αMEM) and are similar to untreated cultures in percentages of apoptotic osteocytes (1.12 ± 0.33 S.D., $p > 0.05$).

3.4.7 Non-apoptotic osteocyte products do not induce osteoblast apoptosis

Osteoblast viability was also investigated in the presence of necrotic osteocyte products, lysed osteocyte products and streptavidin beads (**Figure 21**). Estimation of mean percentages of apoptotic osteoblasts by DAPI staining of cultures showed that necrotic or lysed vesicles did not induce osteoblast apoptosis, compared to control cultures ($p > 0.05$), pointing to differences between the responses induced by healthy, necrotic and apoptotic osteocytes on osteoblast cultures (**Figure 21**). In addition, streptavidin beads did not affect osteoblast viability compared to control cultures ($p > 0.05$). Osteoblast cell loss and apoptosis were observed however, following incubation with soluble factors released from cultures containing large numbers of necrotic osteocytes (**Figure 21**).

3.4.8 Apoptotic products from other cells fail to induce osteoblast apoptosis.

In light of the close proximity of osteoblasts to cells in the bone marrow, besides bone cells, apoptotic products derived from a variety of marrow cell phenotypes as well as from distant tissues were compared to osteocyte apoptotic bodies, in terms of their response on osteoblasts. Primary osteoblast cultures were incubated with apoptotic products of mesenchymal (primary calvarial osteocytes and MLO-Y4 long-bone osteocytes, periosteal fibroblasts and renal fibroblasts) and haematopoietic origin (IC21 monocytes and T hybridoma cells) and also the conditioned media in which they were produced (**Figure 22A**). Apoptosis, estimated by DAPI staining was observed only in the presence of OAB ($p = 0.0001$ compared to control), while the media that nourished apoptotic osteocytes as well as apoptotic products either soluble or membrane-bound derived from other cell types, did not affect osteoblast survival, compared to control cultures ($p > 0.05$ in all cases, compared to control).

In addition, incubation of TE85 human osteoblasts with a range of apoptotic cell products of haematopoietic origin, including primary human PMNs and PBMCs, indicated again that apoptotic osteoblast death occurred only in the presence of OAB (**Figure 22B**).

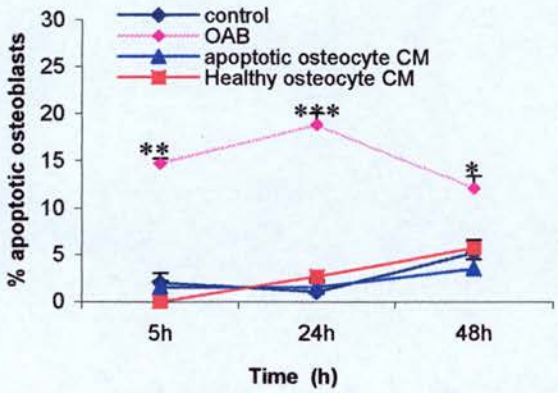

Figure 20. Soluble osteocyte apoptotic products do not induce osteoblast apoptosis. Time course of primary mouse osteoblast cultures incubated in the presence of OAB and their conditioned medium (CM). Graphs represent mean percentages of apoptotic osteoblasts ± SD as evidenced by DAPI staining of cultures. Results indicated that apoptotic osteocyte CM did not increase mean percentages of apoptosis or osteoblast cell numbers, compared to control cultures. *** = $p < 0.0001$, ** = $p < 0.001$, * = $p < 0.05$, compared to control. Control cultures represent treatment with vehicle for OAB (αMEM).

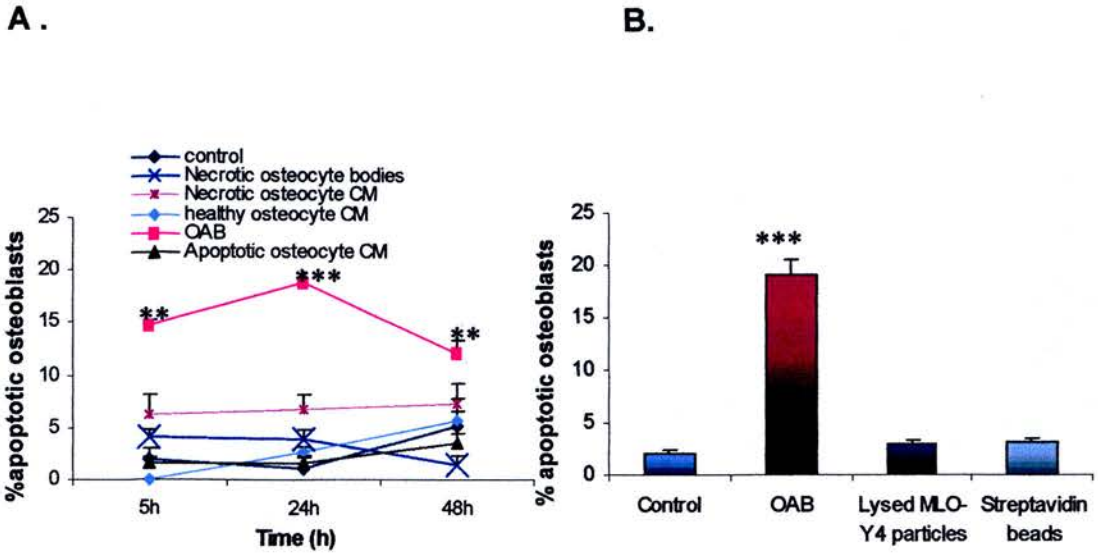

Figure 21. Osteocyte necrotic vesicles do not induce osteoblast apoptosis. A. Time course of primary mouse osteoblast apoptosis in culture in the presence of necrotic osteocyte vesicles, their conditioned medium (necrotic CM), medium that nourished healthy osteocyte cultures and OAB. **B**. Incubation of primary osteoblasts with lysed MLO-Y4 particles and streptavidin magnetic beads for 24 hours. Graphs represent mean percentages of apoptotic osteoblasts ± S.D., as evidenced by DAPI staining of cultures. Control cultures represent treatment with vehicle for OAB (αMEM).

3.4.9 Different target cell phenotypes do not undergo apoptosis in the presence of apoptotic osteocyte products

Seeking additional evidence for the specificity in the response observed in osteoblast cultures, other potential target cell systems were investigated in the presence of osteocyte apoptotic bodies (**Figure 23 and 24**).

3.4.9.1 Macrophages

Bone marrow macrophages were incubated with a range of different apoptotic bodies derived from osteocytes, IC21 monocytes and T hybridoma cells. Mean percentages of apoptotic macrophages were not significant with any of the different apoptotic cell sources, compared to untreated macrophage cultures ($p > 0.05$), indicating that apoptotic osteocytes do not induce apoptosis in macrophage cultures (**Figure 23B and 24B**). In contrast, both OAB and their conditioned media increased number of macrophages in culture and induced changes in macrophage morphology, which acquired long dendritic processes, by 72 and 96 hours of incubation ($p = 0.0001$, compared to control cultures) (**Figure 25**). Soluble factors released from healthy osteocytes did not affect macrophage numbers in culture and did not alter cell morphology.

3.4.9.2 $CD4^+$ T lymphocytes and T hybridoma cells

T lymphocyte-lymphoma mouse cells (**Figure 23C and 24C**) and $CD4^+$ T helper lymphocytes (**Figure 23D and 24D**) did not undergo apoptosis in the presence of OAB ($p > 0.05$, compared to control cultures, in both cell types), or other apoptotic bodies and their conditioned media. In both types of lymphocyte cultures however, cells were physically associated more commonly with osteocyte apoptotic bodies than with other apoptotic bodies.

3.4.9.3 Spleen cells

No reduction in cell number or induction of apoptosis by apoptotic osteocyte products was observed in mouse spleen cells ($p > 0.05$ compared to control cultures) (**Figure 24E**), indicating that apoptotic osteocytes might deliver specific signals and initiate different or no responses to non-osteocytic target cell systems.

A. Primary osteoblasts

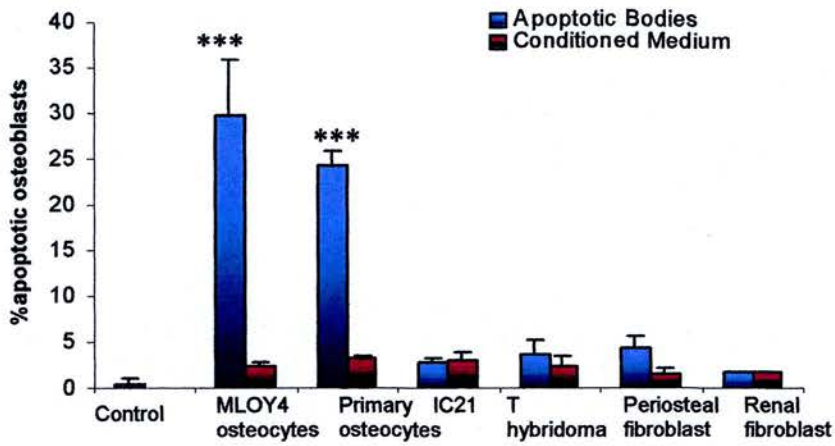

B. TE85 osteoblasts

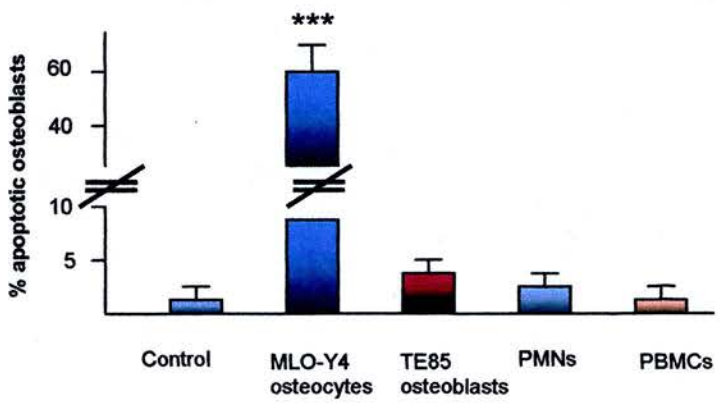

Figure 22. Apoptotic bodies derived from different cell types, do not induce osteoblast apoptosis. Osteoblasts were incubated with a range of apoptotic vesicles produced from different cell types for 24 hours. Graphs represent mean percentages of apoptotic osteoblasts ± S.D., as evidenced by DAPI staining of cultures **A**. mean percentages of apoptotic primary osteoblasts fed with MLO-Y4 osteocyte apoptotic bodies, primary OAB, IC21 monocyte, T hybridoma, periosteal and renal fibroblast apoptotic bodies (AB), and their conditioned media. **B**. mean percentages of TE85 human osteoblasts incubated with AB derived from MLO-Y4 osteocyte, TE85 osteoblasts, PBMCs and PMNs. Control cultures represent treatment with vehicle for OAB and are similar to untreated cultures in percentages of apoptotic osteocytes (0.58 ± 0.58% S.D. and 1.15 ± 0.3% S.D. for primary and TE85 osteoblasts respectively). Error bars represent ± S.D. *** = $p < 0.0001$, compared to control cultures (Dunnets test).

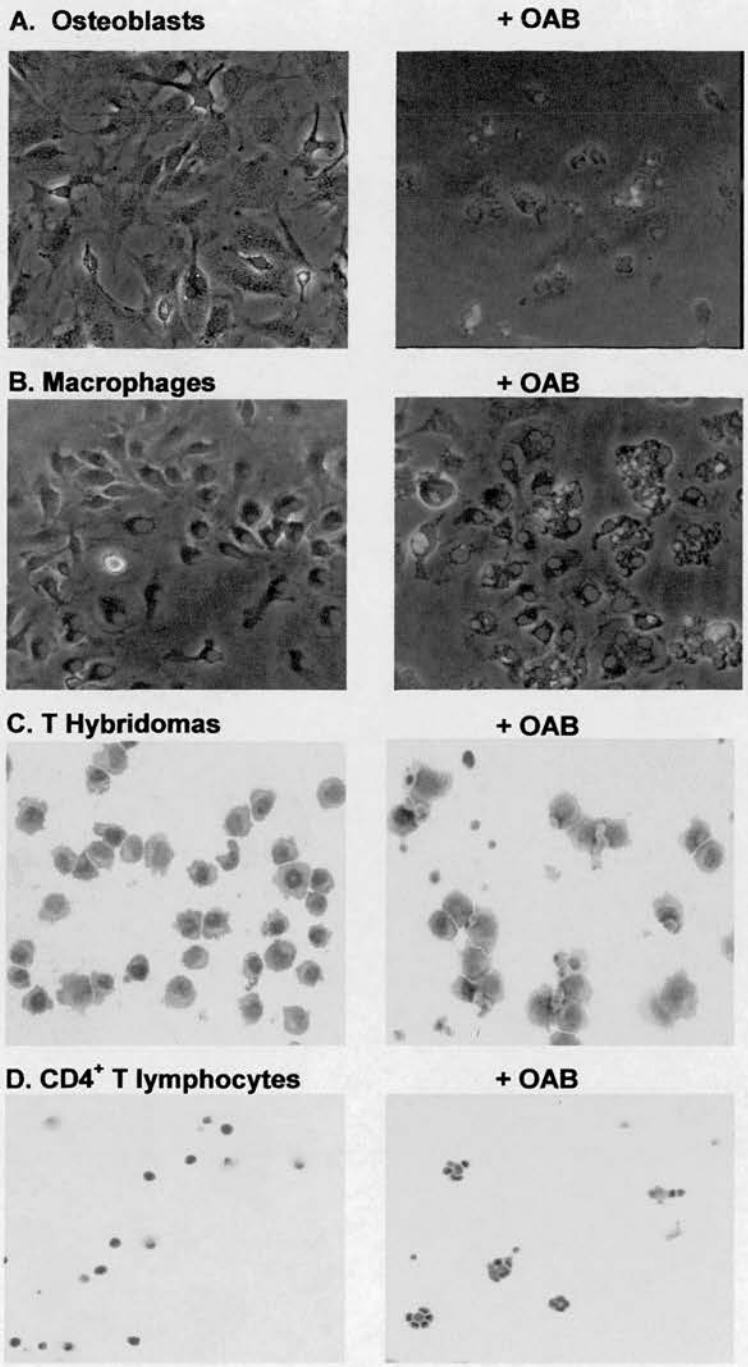

Figure 23. Response of various cell systems to osteocyte apoptotic bodies after 24h of incubation. **A**. primary osteoblasts, and **B**. macrophages, observed using combined images of phase contrast microscopy and fluorescence microscopy (DAPI blue = cell nuclei and Orange Cell Tracker = OAB). **C.** T hybridomas and **D**. $CD4^+$ T lymphocyte cultures incubated in the presence and absence of OAB for 24 hours. 20x magn.

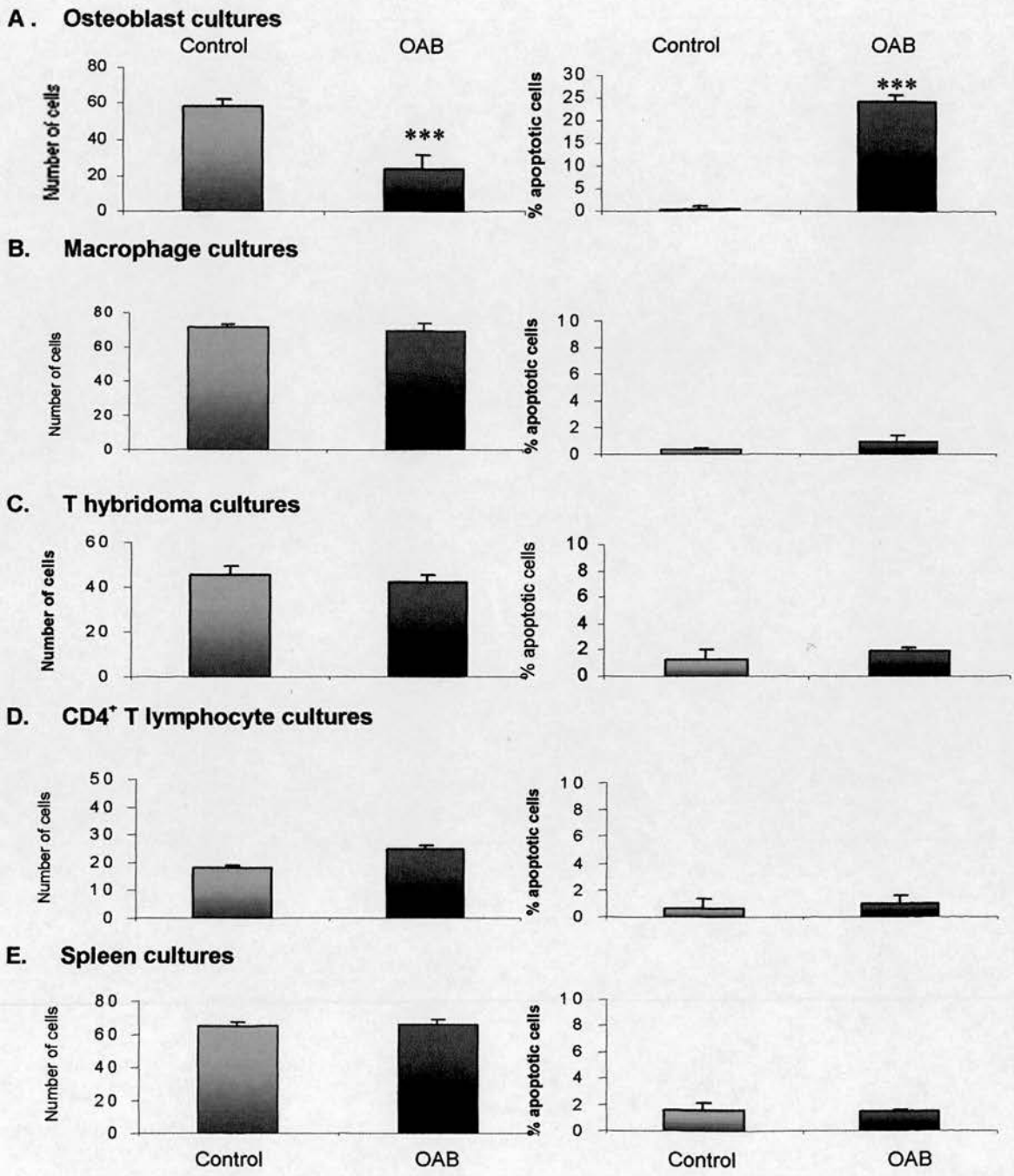

Figure 24. Different target cells do not undergo apoptosis in response to OAB. Target cells were incubated with OAB for 24 hours. Graphs show mean number of cells and percentages of apoptotic cells ± SD as estimated by DAPI staining of cultures **A**. Osteoblast, **B.** Macrophages, **C.** T hybridomas, **D.** $CD4^+$ T lymphocytes and **E.** Spleen cells. Error bars represent ± S.D. *** = $p < 0.0001$, ** = $p < 0.001$, compared to control cultures.

A. Number of macrophages per field

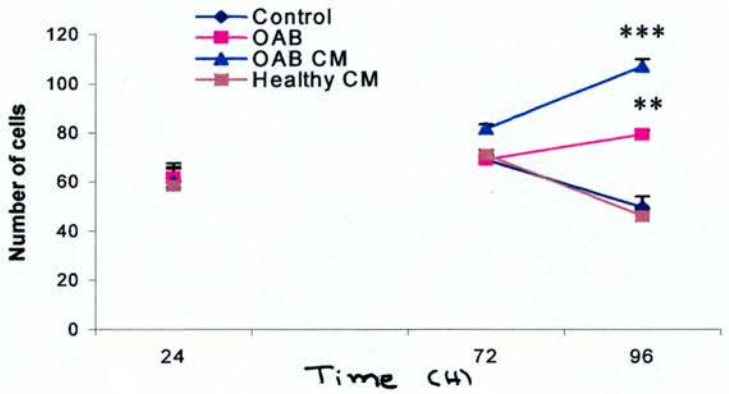

B. Macrophage cultures in response to AOB treatment after 72 hours

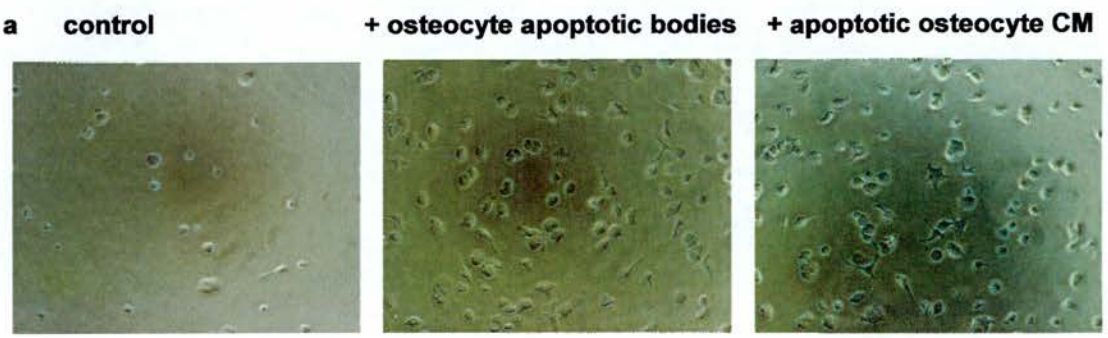

Figure 25. Increase in cell number in macrophage cultures in response to osteocyte apoptotic bodies. Macrophage cultures were incubated with OAB for 24 to 96 h. **A**. Estimation of number of cells in cultures revealed that OAB and their conditioned media (CM) significantly increased cells numbers, after 72 h and 96 h of incubation. **B**. Representative images of macrophage cultures showing increased number of cells in culture and morphological changes after 72 h of incubation with OAB and CM. Error bars represent ± S.D. *** = $p < 0.0001$, compared to control cultures . 20x magnification.

3.5 Discussion

This study has identified several aspects of osteocyte function relevant to the biological significance of osteocyte apoptosis in bone and has shown that apoptotic osteocytes are capable of inducing specific and unique responses in the different target cell systems investigated. Osteoblasts, both primary cells and a cell line, were shown to undergo apoptosis following phagocytosis of osteocyte apoptotic bodies produced either from primary murine osteocyte-like cultures or MLO-Y4 osteocyte cell line cultures. OAB-induced apoptosis of osteoblasts was characterised by externalisation of phosphatidylserine on the outer leaflet of the plasma membrane, cytoplasmic and nuclear condensation, fragmentation of the DNA and formation of apoptotic bodies. In addition, induction of osteoblast apoptosis was shown to be caspase-dependent. Treatment of osteoblast cultures with a non-peptide selective inhibitor of caspases 3 and 7 mediating mainly end-stage cytoskeletal and nuclear changes in the apoptotic pathways, based on sulphanylamide derivatives (Lee et al. 2000), managed to prevent osteoblast apoptosis indicating that blockade of these two caspases was sufficient to prevent apoptotic death. Soluble factors released during osteocyte apoptosis did not induce the same response as apoptotic bodies, indicating that a membrane-bound or OAB resident factor is responsible for initiation of osteoblast apoptosis. In addition, healthy or necrotic osteocytes were not able to induce osteoblast apoptosis pointing to the existence of a specific factor or factors expressed during the process of osteocyte apoptosis and persisting after the production of apoptotic bodies.

Significant osteoblast cell loss and apoptotic death of about 15% were observed as early as 5 hours after addition of OAB, and reached a peak after 24 hours of incubation. However, at 48 hours after treatment, both apoptosis and loss of cell number were reduced compared to values at 24 hours possibly due to the transient nature of the apoptotic response and the proliferation of the healthy cells remaining in the cultures after OAB challenge, respectively. Alternatively the reduced apoptotic response could be due to limitations of *in vitro* culture systems related to movement and distribution of the apoptotic bodies to new target cells. It is possible that having being delivered in the cultures, apoptotic bodies land on a proportion of cells that

subsequently die, but they do not ever encounter other cells due to the static nature of the cell culture environment. On the other hand, our time lapse microscopy data which included image capture in control and OAB-treated osteoblast cultures, every 10 minutes for 24 hours using a Nikon ECLIPSE TE2000-U time-lapse microscope, suggest that this is not the case since we witnessed significant (Brownian / thermal motion derived) movement of apoptotic bodies within the cultures.

Phagocytosis of OAB and the subsequent death of osteoblasts did not appear to be dependent on the stimulus that induced apoptosis in the osteocyte cell cultures. OAB prepared in response to treatment with three different apoptosis-inducing stimuli, namely Dexamethasone, H_2O_2 and serum deprived conditions, were equally efficiently engulfed by osteoblasts and induced similar levels of osteoblast apoptotic death. Studies by others have shown however that the efficient recognition and engulfment of apoptotic epithelial cells by homotypic neighbors was dependent on the stimulus that triggered apoptotic death (Wiegand et al. 2001). These current data suggest that it is unlikely that the different pathways leading to apoptosis of osteocytes engendered by different apoptotic stimuli, determine the efficiency of phagocytosis by osteoblasts and the subsequent induction of osteoblast apoptosis. A possible explanation for this finding could be that the death inducing factor/factors associated with OAB are produced at a late stage in the pathway to death, at a point downstream of the stimulus dependent on the specificity of the pathways. Alternatively, the factor responsible for the efficient phagocytosis of OAB by osteoblasts and the induction of osteoblast apoptosis might not be related to apoptotic characteristics per se but it might be specifically related to the osteocytic nature of the apoptotic bodies. This would seem unlikely since similar outcomes could not be derived from live or necrotic cells. However, it remains possible that it is an osteocyte derived factor which is either normally unlikely to be delivered to an osteoblast or that is exposed to the external environment during the formation of apoptotic bodies that is likely responsible for the effect. Actually, it is likely to be both apoptotic and osteocyte specific molecules involved, as suggested by the data discussed in the following paragraphs.

The current studies demonstrate the clear ability of osteoblasts to phagocytose apoptotic bodies from a variety of cell sources. Despite the osteoblast not being traditionally viewed as an important phagocyte in bone, there are examples of this behaviour in literature. A number of studies have previously reported that osteoblasts are capable of phagocytosing non-biological particles, which affect their viability and function (for review see Vermes et al. 2001). For example, it has been shown that MG63 osteoblasts and primary human osteoblast-like cells phagocytose particles smaller than 3 μm, which are frequently generated during wear of surgical implants (Lohmann et al. 2000, Lohmann et al. 2002). Phagocytosis of these non-biological particles induced alterations in osteoblast cell morphology, proliferation and differentiation as well as production of PGE_2 in a concentration and particle-dependent manner, inhibiting bone formation and contributing possibly to aseptic loosening of orthopaedic implants. Other studies have also shown that titanium particles derived from prosthetic devices induced cytotoxic effects on osteoblasts, which affected the adhesive properties of osteoblasts (Kwon et al. 2001), their viability (Pioletti et al. 1999) and proliferation (O'Connor et al. 2004) with particles ranging between 1.5 to 4 μm inducing the greatest effect as soon as 4 hours after introduction to cultures. Phagocytosis of these particles resulted both in necrotic and apoptotic cell death and the release of products that were cytotoxic when presented to other osteoblast cultures (Pioletti et al. 1999). Furthermore osteoblasts were observed to acquire a phagocytic phenotype upon engulfment of titanium alloy particles, resulting in the expression of the macrophage marker CD68, associated with fine granules in the cytoplasm (Heinemann et al. 2000).

Besides engulfing non-biological particles, osteoblasts have also been reported to phagocytose apoptotic bodies (Landry et al. 1997). Apoptotic bodies produced from osteoblasts in the callus of rat tibia that were fractured following a surgical operation were phagocytosed by homotypic cells. This observation was proposed to be a mechanism for eliminating excess osteoblasts from the injury site, following callus formation (Landry et al. 1997). These studies demonstrate that osteoblasts are capable of phagocytosis of biological and non-biological particles, both in vivo and in vitro conditions. Although phagocytosis of non-biological particles has been

reported to affect osteoblast function and viability, induction of apoptosis upon phagocytosis of biological particles by osteoblasts has not been previously reported. The specificity of the response seen in these experiments would explain why this is the case.

In the current studies, a comparison was carried out between the response of osteoblast cultures to apoptotic bodies produced from different cell types of mesenchymal (primary calvarial osteocytes and MLO-Y4 long-bone osteocytes, periosteal fibroblasts and renal fibroblasts) and haematopoietic origin (IC21 monocytes and T hybridoma cells). The findings indicated that osteoblasts phagocytosed apoptotic bodies efficiently from all cell phenotypes presented to them, suggesting that osteoblasts are capable of efficiently binding, recognising and engulfing apoptotic bodies derived from cells of various origins. However, of great significance to these studies was the observation that osteoblasts only underwent apoptosis following interaction with osteocyte apoptotic bodies, while uptake of other apoptotic bodies used in this study did not affect viability or osteoblast cell number in cultures. These data pointed to the existence of a very specific difference between the response of osteoblasts to OAB rather than other apoptotic bodies. The specificity of the response could possibly be attributed to the presence of an osteocytic specific factor delivered by OAB to osteoblasts and that is responsible for the induction of osteoblast apoptosis. The possible identity of these factors is dealt with in chapter 4.

Detailed investigation of the *in vitro* cultures following completion of delivery of the phagocytic meals and subsequent target cell response allowed the study of the importance of the physical interaction with and /or phagocytosis of the apoptotic bodies by the osteoblastic rather than other target cells in the ensuing response. The data suggested there was a higher probability of individual osteoblasts being apoptotic when they were physically associated with apoptotic bodies. In addition, it was shown that the majority of apoptotic osteoblasts were associated with more than four apoptotic bodies. Quantification of the phagocytic index in other studies has also shown that not all phagocytes in a culture interact with the same number of apoptotic

bodies, as phagocytes have appeared to interact more frequently on average with more than two (Sexton et al. 2001), three (Hanamaya et al. 2002) or more than four apoptotic bodies (Hamon et al. 2000). These findings have indicated that the induction of apoptosis was also related to the number of apoptotic bodies interacting with the target osteoblasts and that there was a requirement for a threshold amount of osteocyte apoptotic bodies that would interact with osteoblasts and engender their apoptotic death. In fact it might be possible that phagocytosis of osteocyte apoptotic bodies by osteoblasts was necessary for induction of osteoblast apoptosis, since most of the OAB interacting with apoptotic osteoblasts appeared to be engulfed, rather than bound on the surface of the apoptotic cells. Other studies have also reported the dependency on engulfment of apoptotic bodies by phagocytes in order to obtain particular responses. For example, production of TGF-β by human stellate cells (Canbay et al. 2003a) as well as generation of TNF-α and Fas by Kupffer cells (Canbay et al. 2003b) and the subsequent induction of their fibrogenic activity appeared to depend upon engulfment of hepatocyte apoptotic bodies.

Additional support for the specificity of the signal delivered by OAB to osteoblasts as well as the requirement of phagocytosis in the ensuing response was obtained through the comparison of the response induced by OAB in osteoblasts with that induced in other cell types used as target cells, such as macrophages, spleen cells, $CD4^+$ T lymphocytes and T hybridoma cells. Having established that OAB induce death in osteoblasts, these studies sought to determine whether OAB might induce the same response in all cell types. Macrophages appeared readily to bind and phagocytose multiple osteocyte apoptotic bodies, without however undergoing any apoptotic changes. In spleen cell cultures, osteocyte apoptotic bodies were also readily engulfed by cells with a macrophage-like and dendritic cell-like appearance, however without any evidence of apoptosis in the target cell cultures. In addition, I used primary $CD4^+$ T lymphocytes and a T hybridoma cell line, which have been shown not to demonstrate phagocytic capacity and presented them with OAB in culture. In the presence of OAB, both lymphocytic cell types did not undergo any apoptotic changes, despite close interaction of the OAB with the cells (see below).

Physical interaction of osteocyte apoptotic bodies with all the target cells used in this study indicated the existence of mechanisms involved in recognition, binding and/or phagocytosis of osteocyte apoptotic bodies. This finding would imply that OAB are associated with specific apoptotic changes in molecules expressed on their plasma membrane which are implicated in their efficient recognition, binding and engulfment by phagocytes. Such changes are likely to be of the type shown to be characteristic of a large number of apoptotic cells types (for review see §2.7). For example, OAB were clearly demonstrated to express phosphatidyl serine on the outer leaflet of the plasma membrane, as shown by binding of fluorescently labelled Annexin V, while their purification was also enabled by biotinylated Annexin V-streptavidin magnetic bead-conjugates. The role of phosphatidyl serine in recognition of osteocyte apoptotic bodies by phagocytes, as well as the involvement of other classical apoptotic cell recognition features such as loss of terminal sialic acid residues or the requirement of Ca^{2+} in the phagocytic process are investigated in more detail in chapter 4. Interestingly, it was also observed that a proportion of osteoblasts in cell culture would not be physically associated with any OAB, which might not necessarily be attributed to lack of movement of apoptotic bodies, as discussed above, but possibly to the fact that there exist subsets of osteoblasts incapable of binding OAB, since the primary osteoblast cultures are of course representative of a mixed population at different stages in the osteoblast lineage. In addition, it might be possible that binding of multiple OAB on a single osteoblast could be enabling the binding of additional OAB on the same cell. This phenomenon could be due to altered signaling mechanisms on osteoblasts following the binding of OAB, associated with possible changes induced in phagocytes in order to bind and internalise apoptotic bodies. Studies by others have also suggested that there is a requirement for alterations in membrane-related molecules, such as phosphatidyl serine, in both the phagocyte and the prey in order for efficient recognition and engulfment to occur (Marguet et al. 1999). These possibilities are investigated in chapter 4.

Data obtained from the different target cell systems used in this study suggested that neither engulfment of OAB by phagocytes, as observed in macrophage and spleen

cell cultures, nor binding as observed in the lymphocyte cultures are alone sufficient to induce apoptotic death in these target cells. The comparison between the response of osteoblasts and that of the other target cells to OAB, indicated that non-osteoblast lineage related cell phenotypes did not undergo apoptosis in response to osteocytic and a range of other cell apoptotic bodies. These data indicated a clear specificity in this system, in which unique recognition mechanisms are involved between OAB and osteoblasts, allowing OAB to induce apoptosis only to osteoblasts, while osteoblasts only undergo apoptosis in response to OAB. This would tend to suggest that not only do OAB carry a potent osteoblast death inducing signal but that this signal is not recognised in cell phenotypes other than those of the osteoblastic lineage. The relevance of such specificity to the functioning bone environment is likely to be large. The ability to send out apoptotic body derived death signals to specific cell types would represent an elegant signaling pathway in bone. The significance of this specificity is discussed further in the following paragraphs, while the identification of unique factors on OAB implicated in the ensuing response, is the subject investigated in chapter 4 and also of further work currently undertaken in our laboratory.

Although interaction of OAB with target cells other than osteoblasts did not lead to apoptotic death, morphological behavioural changes were observed in some of these cell types. For example, $CD4^+$ T lymphocytes appeared closely arranged around apoptotic osteocytes, with multiple lymphocytes physically interacting with a single osteocyte. This behaviour was in distinct contrast to that demonstrated by lymphocytes when they were challenged with apoptotic products produced by other lymphocytes and hybridoma cells. In T hybridoma cultures, cells were seen forming a phagocytic cap at multiple sites of interaction with apoptotic osteocytes, indicating clearly a preference for lymphocytes to physically interact with apoptotic osteocyte bodies. Furthermore, prolonged incubation of macrophages with apoptotic osteocytes and/or their conditioned medium resulted in an increase in cell number and a change in morphology, including the formation of long cytoplasmic extensions which resembled dendritic cell processes, compared to control cultures. Although not determined experimentally, macrophages appeared morphologically activated and

were characterised by the presence of large vacuoles in the cytoplasm, with single cells being physically associated with up to 20 OAB either internalised or bound on the cell surface. This might indicate that OAB promote at some level a pro-inflammatory response by modulating the behavior of macrophages. Engulfment of apoptotic cells by splenic macrophages has been shown to lead to infiltration of neutrophils (Lorimore et al. 2001), possibly through the release of the neutrophil chemoattractant molecules IL-8 and FasL (Kurosaka et al. 1998, Brown and Savill, 1999). In addition, inefficient clearance of apoptotic cells has been suggested to contribute to the inflammatory response observed in acute lung injury (Mantell et al. 1997), indicating that induction of pro-inflammatory responses following ingestion of intact apoptotic bodies might be directing the activity of macrophages to specific sites in order to efficiently clear apoptotic cells from these sites. For example, macrophages have been reported to accumulate at sites of inflammation in bone in response to chemoattractant molecules (Rahimi et al. 1995) and to carry out bone resorption following release of IL-1 and TNF-α and production of matrix metalloproteinase-1 in response to LPS (Hong et al. 2004). However, further investigation is required in order to determine whether OAB promote pro-inflammatory responses or the release of anti-inflammatory cytokines such as TGF-β1 and IL-10 in osteoblasts in a similar way to that seen in macrophages (Voll et al. 1997, Newman et al. 1982, Fadok et al. 1998, Huyhn et al. 2002), following their engulfment by macrophages. The appearance of dendritic-like cells following incubation of macrophages with OAB is being followed up in the laboratory and demonstrated the ability of apoptotic osteocytes to induce a specific response, other than apoptosis in a particular cell phenotype since it was not observed upon addition of apoptotic bodies and soluble apoptotic products derived from other cell types, such as IC21 monocytes and T hybridoma cells. Dendritic cells are known to modify and present antigens to cells of the immune system, while engulfment of apoptotic cells by dendritic cells has been shown to exert anti-inflammatory effects by suppressing their maturation (Stuart et al. 2002). In addition, it has also been suggested that antigens on the apoptotic cell membrane could access the cytoplasm and be cross-presented on MHC I and MHC II molecules on macrophages, inducing dendritic cell maturation, and regulation of immune responses (Bellone et al. 1997,

Inaba et al. 1998). At present, it is not clear how production of dendritic-like cells in the presence of OAB might contribute in the bone resorption process or in the modulation of the local immune system, while there is also no evidence to suggest or relate the possibility that OAB might travel any further than the osteoblasts on the bone surface.

This phenomenon, along with the induction of apoptosis specifically in osteoblastic cells, (which is the main response induced by OAB investigated in this thesis), might imply the possible existence of a range of phenotype specific molecular patterns carried by apoptotic bodies from a range of cell types. Such as possibility would be supported by the work of Aupeix et al. in which they demonstrated phenotype specific molecular markers on apoptotic bodies generated during AIDS (Aupeix et al. 1997). In these studies, apoptotic bodies could by way of their molecular signatures be traced back to their cell of origin. These observations imply that it is possible for apoptotic bodies, which carry on their surfaces specific cell-type antigens to elicit specific cell/tissue-related responses, depending on the cell they were derived from and the phagocyte that engulfs them, assigning novel functional significance to the circulation of apoptotic bodies derived from various tissues in peripheral blood as demonstrated by Aupeix et al. Overall, the possibility that a wide range of apoptotic and target cell signaling combinations might exist provides further significance and physiological meaning to the apoptotic process as a whole. We might now consider that there is not one but many cell phenotype dependent outcomes related to a cell's death and phagocytic removal from a tissue.

Prior to initiation of resorption, osteoblasts lining the bone surface are removed in order to expose the underlying bone mineral to osteoclasts, resulting in the activation of a quiescent bone surface (Parfitt 1994). In addition, osteoblasts produce signals such as RANKL that can both induce osteoclast maturation and mediate osteoclast formation in the presence of MCSF-1 (Lacey et al. 2000, Kong et al. 1999), and the soluble decoy receptor OPG, which inhibits differentiation and activation of osteoclasts by competing against RANKL (Yasuda et al. 1999), indicating that osteoblasts participate directly in the activation of bone turnover. Interestingly,

apoptosis of osteocytes has been reported to target the activity of osteoclasts, the bone resorbing cells, by directing them to sites that require to be resorbed in order to maintain the appropriate structure and strength of bone (Noble et al. 2003). However, the mechanisms underlying this phenomenon remain unclear. Data provided in this thesis show that apoptotic osteocytes induce the apoptotic death of osteoblasts *in vitro* and *ex vivo*. In normal physiology, apoptosis in osteoblasts has been suggested to contribute to the maintenance of the osteocytic population, since following the end of the bone formation period in the turnover process, osteoblasts have been observed to undergo apoptosis or to become incorporated into the mineralising bone matrix and differentiate into osteocytes (Parfitt 1994). Induction of osteoblast apoptosis upon interaction with apoptotic osteocyte products, as suggested in this thesis, is of particular importance for the bone tissue microenvironment, since osteocytes are in close contact with osteoblasts (the bone forming cells) through the canalicular system. In addition, osteocytic processes have been shown to be in contact with osteoblasts via gap junctions (Doty 1981, Shapiro 1997), while removal of lining cells from the bone surface could possibly allow osteocytes to come in contact with cells in the bone marrow (Kamioka et al. 2001). Palazzini et al. have suggested that a functional syncytium is present between the cells of osteogenic origin, which is enabled by the presence of gap junctions, allowing osteocytes to communicate with cells in the vascular endothelium, through contact with osteoblasts and stromal cells, indicating that signals passing through this network could be regulating the function of these cells.

Since osteocytes are located within the bone matrix, we should consider how osteocyte apoptotic bodies could induce the apoptotic death of bone surface resident osteoblasts *in vivo*. It might be possible that osteocyte apoptotic bodies could be delivered through the syncytial network to neighbor osteocytes and osteoblasts inducing apoptosis. Recent studies have shown that tracer molecules like reactive red, microperoxidase and horseradish peroxidase ranging between 1-6 nm in size, could readily pass through the lacuno-canalicular system, while transport of ferritin which is 10 nm in size, could not be achieved, in rat long bone, in the absence of mechanical loading, possibly due to the theoretical presence of fiber matrix of 7 nm

pore size in the lacuno-canalicular channels (Wang et al. 2004). Osteocyte apoptotic bodies produced in these studies ranged in size between 0.02 μm to 0.5 μm, indicating that it might be possible for some osteocyte apoptotic bodies to be transported through the canaliculi which are approximately 0.2 μm radius. Although there are no studies available to show presence of apoptotic bodies in canaliculi, we have noted their presence in our laboratory. Transport could also possibly be increased by mechanical loading (Wang et al. 2000). In addition, there might be alterations in the lacuno-canalicular channels in response to death of an osteocyte, which might be allowing more communication between neighbour cells. Alternatively, if apoptotic bodies could not be delivered through the canalicular system, apoptotic osteocytes could be inducing the bystander death of other osteocytes reaching eventually osteoblasts on the surface. In conclusion, data provided in this chapter, suggest that osteocyte apoptotic death might play a primary role in the maintenance of bone quality, through initiation of bone turnover at particular areas through the induction of apoptosis in osteoblasts lining the bone surface. Death of the osteoblasts might possibly provide the signals for initiation of resorption by osteoclasts or alternatively facilitate the removal of anti-resorptive signals, such as OPG. Induction of apoptosis only to cells of osteoblast origin indicates that identification and subsequent manipulation of the signals responsible for osteoblast apoptosis could possibly allow the initiation of turnover at sites of interest without however altering the viability of non-osteoblast lineage cells present in the bone microenvironment. In addition, these data raise interesting issues with regard to the functional significance of apoptosis, other than in developmental and inflammatory processes, indicating that functional activity of cells in tissues might be regulated through encounter of apoptotic bodies derived from homotypic cells, cells that are close by or at distant sites, following their circulation in peripheral blood.

CHAPTER 4

Mechanisms of phagocytosis of osteocyte apoptotic bodies and induction of osteoblast apoptosis

4.1 Abstract

Phagocytosis of apoptotic cells is an efficient and complex process that requires specific changes to occur on the apoptotic cell membrane as well as co-operation between phagocyte receptors in order to achieve recognition and phagocytosis. Data in chapter 3 demonstrated that osteocyte apoptotic bodies can induce apoptosis in osteoblasts but not in other target cells investigated. This study attempts to identify mechanisms by which osteoblasts recognise OAB and undergo apoptosis.

OAB-induced osteoblast apoptosis was shown to be caspase-driven and associated with increased presence of the Fas death receptor on osteoblast cell membranes. In addition, initiation of osteoblast apoptosis was shown to depend on some level upon physical interaction with OAB. Agents that interfered with membrane composition on the osteoblast reduced the uptake of osteocyte apoptotic bodies and the induction of osteoblast apoptosis indicating that the osteoblast response to OAB was a Ca^{2+}-dependent process that required specific phospholipid and carbohydrate changes in both the phagocyte and the prey. Furthermore, OAB appeared to increase the production of nitric oxide in osteoblast cultures. Gene knockout animal models demonstrated partial blockade of ingestion but not apoptosis in the absence of scavenger receptor A (SRA). In addition, absence of CD14 in osteoblasts derived from knock out mice not only impaired the uptake of OAB, but also reduced osteoblast apoptosis by 50% possibly indicating that CD14 is acting at initial recognition stages, which enable the activation of pathways that lead to osteoblast apoptosis.

4.2 Introduction

Phagocytosis is a complex process that involves multiple changes on the apoptotic cell surface to allow rapid and efficient recognition by the phagocytes. Changes on the apoptotic cell membrane commonly involve loss of terminal sialic acid residues from glycoproteins such as N-acetylglucosamine, galactose and N-acetylgalactosamine, which become recognised by the macrophage lectin receptors. (Savill et al. 2000). Other apoptotic markers involved in the recognition process include anionic sites such as thrombospondin 1 (TSP1) binding sites and phosphatidyl serine (PS) (Fadok et al. 1998), which becomes exposed on the outer leaflet of the plasma membrane through a calcium dependent mechanism that involves activation of a phospholipid scramblase and downregulation of an ATP-dependent aminophospholipid translocase (Savill 1997).

Professional phagocytes usually engage different receptors to recognise and engulf apoptotic cells, at different phases of the apoptotic program, so that a variety of first-line and back-up mechanisms arise to ensure rapid clearance (Gregory 2000). The scavenger receptors A (SRA) and CD36, act as endocytic receptors in the clearance of oxidised low density-lipoprotein (oxLDL), while they have also been implicated in the mechanism of uptake of apoptotic cells (Platt et al. 1996, Platt et al. 1998). CD36 binds to oxidised residues on apoptotic cells. In addition it co-operates with the vitronectin receptor $a_v\beta_3$ and the bridging molecule, TSP1, via the TPS1- $\alpha_v\beta_3$ interaction, which can be inhibited by antibodies and RGD (Arg-Gly-Glu) peptides, preventing both recognition of apoptotic cells by phagocytes and adhesion of TSP to phagocytes. (Savill et al. 1992).

Other recognition mechanisms involve the ABC-1 membrane transporter, (Luciani and Chimini 1996) and CD14, which may be found in soluble form in the plasma or as a membrane-bound receptor on the macrophage cell surface. CD14 interacts with LPS on bacteria, but also mediates tethering and uptake of apoptotic cells, in a non-inflammatory manner. CD14 has been proposed to act as a pattern recognition receptor (PRR), interacting with a series of apoptotic cell associated molecular patterns (ACAMPs). (Guchelaar et al. 1997, Gregory 2000).

As discussed in chapter 3, osteocyte apoptotic bodies induce apoptosis in osteoblast cultures. Confocal microscopy of osteoblast cultures (**Figure 17**) indicated that OAB both bind onto the surface of osteoblasts and become engulfed by them. This study attempts to investigate mechanisms involved in the recognition and engulfment of the apoptotic osteocyte by phagocytic osteoblasts, and to identify molecules that might be implicated in the induction of osteoblast apoptosis. In addition, we have attempted to identify the molecular "reason" for phenotypic specificity in the apoptotic body/phagocyte interaction with a view to clarifying any further "meaning" to apoptotic body production.

4.3 Materials and Methods

Unless otherwise stated, all chemicals were purchased from Sigma, UK and all culture reagents were purchased from Invitrogen, UK. Tissue culture well plates and petri dishes were purchased from Corning, UK. Tissue culture procedures were performed in a laminar flow hood (class 2) receiving HEPA-filtered air, using sterile equipment.

4.3.1 Cell line culture

Cell line culture was carried out as described in §3.3.1. Briefly, MLO-Y4 osteocyte-like cells were cultured in αMEM supplemented with 5% fetal bovine serum (FBS), 5% newborn calf serum (NCS), 1% penicillin/streptomycin (P/S) and 1% L-glutamine while TE85 osteosarcoma cells were cultured in MEM supplemented with 10% FBS, 1% P/S and 1% L-glutamine.

4.3.2 Isolation of primary mouse osteoblast and osteocyte cultures.

Osteoblast and osteocyte cultures were isolated from 3-6 week old female mice as described in §3.3.2, and killed by CO_2 asphyxiation in a closed chamber. Briefly, calvarial bones were digested in trypsin at 2.5 gm/l for 10 minutes at 37 ^{o}C, followed by 10 sequential collagenase digestions at a concentration of 0.75 mg/ml, which provided the osteoblast and osteocyte populations as described in § 3.3.2. Murine bone marrow macrophages were supplied by Dr Jeremy Duffield and maintained in DMEM F12 supplemented with 10% FBS as described by Duffield et al. 2000.

Isolation of primary osteoblasts from CD14 and SRA transgenic mice

CD14 knockout mice were supplied by Prof. Chris Gregory and were generated as described by Haziot et al. 1996. Briefly, the CD14 gene was disrupted by removal of a 272 bp segment including the CD14 initiation codon in exon 1, the 97 bp intron and 172 bp of the coding region in exon 2, and by replacement with a neomycin resistance gene. This replacement resulted in a frame-shift mutation in the remaining CD14 sequence. The construct was electroporated to W9.5 ES cells and cells carrying the disrupted gene were injected to C57BL/6 mice blastocysts. Male chimaeras were bred with wild-type mice and offspring interbred to produce

homozygous CD14-deficient mice. Scavenger receptor A (SRA) knockout mice were supplied by Dr. Adam Lacy-Hulbert. Mice deficient in type I and II SR-A were generated by homologous recombination as described by Suzuki et al. 1997. The mice were bred onto the 129/ICR genetic background. Brother-sister matings were subsequently used to create homozygous receptor-deficient and wild-type mice on the same genetic background. All mice used in this study were housed in the animal facility (Edinburgh, UK) and were used between 2 and 8 week of age. Osteoblast cultures from the transgenic mice were isolated as described above.

4.3.3 Isolation of mouse calvariae for *ex vivo* experimental conditions

Mouse calvariae were aseptically isolated from 3 pure C57BL/6 mice and 3 CD14 knockout mice. Calvariae were carefully broken across the suture line in order to provide controls from each animal for each of the treatments and were kept in individual wells in a 24-well plate in aMEM medium supplemented with 10% FBS, 1% P/S and 1% l-glutamine. OAB from MLO-Y4 osteocytes were presented to the calvariae for 24 hours at 37 ^{o}C. After that period, the bones were submerged immediately in 5% polyvinyl alcohol and snap frozen in a hexane-chilling bath before being stored at -70 ^{o}C prior to cryostat sectioning. Cryostat sections of 8μm thickness were cut from the chilled material and transferred to 3-aminopropylnethoxy-silane (TESPA) coated slides to aid adhesion of the bone section to the slide by creating a highly charged surface. Three sections were used per treatment group (per half scull).

4.3.4 Characterization of primary calvarial cultures

4.3.4.1 Proliferative capacity (5-bromo-2 deoxyuridine, BrdU)

Proliferating fibroblasts, osteoblasts and non-proliferating osteocyte cultures were distinguished using BrdU incorporation into newly synthesized DNA, as described in §3.3.3.1.

4.3.4.2 Alkaline phosphatase Immunostaining

Alkaline phosphatase is widely used as a marker of the osteoblast phenotype and has been proposed to participate in bone mineralization (Waymire et al. 1995). Alkaline

phosphatase was detected in primary osteoblast cultures following incubation in Napthol-ASMX-mix and Fast Blue using light microscopy, as described in §3.3.3.2. Osteoblasts expressing alkaline phosphatase were detected against total number of cells in cultures identified by nuclear DAPI staining.

4.3.4.3 Mineralised nodule formation (Von Kossa stain)

Primary osteoblasts were induced to form mineralised nodules in confluent cultures, by addition of mineralisation solution for 3 weeks (Noble et al. 1995), followed by incubation in silver nitrate solution and exposure to light, as described in §3.3.3.3.

4.3.5 Induction of osteocyte apoptosis and characterization of apoptotic bodies by Annexin-V FITC binding and PI staining.

Osteocyte apoptotic bodies (OAB) were produced and characterised as described in chapter 3. Briefly, osteocytes were either incubated in 0.1% FBS media for 7-10 days, or in the presence of 0.4 mM H_2O_2 or Dexamethasone at 10^{-6} M for 4-5 hours, at 37 °C. Apoptotic osteocyte cultures were characterized by Annexin-V-FITC and Propidium Iodide staining, in order to distinguish between viable (FITC negative, PI negative), early apoptotic (FITC positive, PI negative) and late apoptotic or necrotic cells (FITC negative, PI positive), as described in §3.3.4.1.

4.3.6 Induction of osteocyte necrosis and isolation of necrotic vesicles by Annexin-V FITC binding and PI staining.

Necrotic osteocyte vesicles as well as the medium that nourished the necrotic vesicles was produced by incubating osteocyte cultures in 0.8 mM H_2O_2 for 3-5 hours at 37 °C, as described in §3.3.5.1.

4.3.7 Purification of apoptotic bodies by Annexin-biotin-streptavidin complex.

Apoptotic bodies were purified on the basis of phosphatidylserine (PS) exposure on the outer leaflet of the cell membrane, (**Figure 7**) as described in §3.3.6. Briefly, apoptotic cells were incubated in biotinylated Annexin V and Streptavidin magnetic beads, which enabled the purification of apoptotic bodies expressing PS with the use

of a magnetic sorting device. Apoptotic bodies were then resuspended in growth medium appropriate for the target cultures, at measured apoptotic body density.

4.3.8 Visualization of apoptotic body and target cell morphology with fluorescence staining.

Apoptotic bodies were readily visualised with Orange Cell Tracker CMTMR which becomes absorbed at 540 nm and emitted at 566 nm (Molecular Probes), while target osteoblasts were visualised with Green Cell Tracker CMFDA absorbed at 492 nm and emitted at 516 nm (Molecular Probes), as described in §3.3.7. In addition, both the target cells and phagocytic prey were stained with DAPI, which is stimulated at 344 nm and emitted at 488 nm, as described in §3.3.10.3. The exact staining method with either the Cell Tracker or DAPI varies according to experimental requirements and is indicated for individual experiments in the figure legends.

4.3.9 Phagocytosis assay

Phagocytosis was determined as described in §3.3.8. Briefly, target cells stained with CellTracker Green dye or DAPI were plated at a density of 30,000 cells/well for primary osteoblasts, 15,000 cell/well for TE85 human osteoblasts and 30,000 cells/well for primary bone marrow macrophages, in 96 well plates. Apoptotic products and media conditioned by both healthy and apoptotic prey cell cultures were collected and presented to target cell cultures as described in §3.3.8.

4.3.10 Interaction and Engulfment assays

Following incubation of target cells with apoptotic bodies for the appropriate time intervals indicated in the figure legends, medium was removed and cultures were analysed for low affinity interactions with apoptotic bodies or for engulfment of apoptotic bodies by target cells, as described in §3.3.9. Cells were observed in 3 fields per well resulting in 9 fields per treatment group.

4.3.11 Inhibition of phagocytosis

The process of phagocytosis involves alterations in the plasma membrane composition, such as exposure of negatively charged phospholipids on the outer

leaflet of the membrane and loss of terminal sialic acid residues, which enable recognition of apoptotic cells by phagocytes (Savill 1997), which also undergo membrane and cytoskeletal changes in order for engulfment to occur.

4.3.11.1 Inhibitors of plasma membrane components

Glyburide

Glyburide is a sulfonylurea compound that has been used to affect phagocytosis due to its ability to interfere with phospholipid efflux by inhibiting ABCA1 transporter activity (Becq et al. 1997, Marguet et al. 1999). Target cell cultures and osteocytes, prior to production of apoptotic bodies were incubated with glyburide for 4 h at 50 µM in DMSO. Target cultures were then presented with OAB, in order to determine the involvement of phospholipid changes in the interaction of target cells with OAB.

Oligomycin

Oligomycin is an inhibitor of the mitochondrial FoF1-ATPase but has also been shown to affect Ca^{2+}-dependent transbilayer movement of phospholipids (Cho et al. 1997, Catz et al. 1998, Marguet et al. 1999). Target cell cultures and osteocytes, prior to production of apoptotic bodies, were incubated with Oligomycin for 4 h at 6 µM in DMSO, in order to determine the involvement of phospholipid changes and the requirement of Ca^{2+} in the interaction of target cells with OAB.

Ethylenediaminetetraacetic acid (EDTA)

EDTA is a synthetic amino acid that forms chelates with both transition metal ions and main-group ions. EDTA binds Ca^{2+} and prevents its availability. EDTA has been widely used to reduce the availability of Ca^{2+} resulting in decreased phagocytosis (Yuan et al. 2001). OAB were incubated with EDTA at 5 mM in PBS for 5 minutes followed by incubation with OAB, in order to determine the requirement of Ca^{2+} in the interaction of target cells with OAB.

Trypsin

Trypsin is a widely used proteolytic enzyme that has also been shown to prevent glycoprotein-dependent recognition and engulfment by macrophages (Leiro et al. 1997). OAB were incubated with trypsin at 2.5 gm/l for 10 minutes in order to determine the dependency of interaction of OAB with target cells on peptide-containing molecules.

N-acetylglucosamine

N-acetylglucosamine is a cationic amino sugar that can competitively bind to lectin receptors on the macrophage which recognise modified surface glycoproteins on apoptotic cells (Dini et al. 1995). Target cells were incubated with N-acetylglucosamine for 1 hour at 1 mg/ml, prior to incubation with OAB, in order to determine the involvement of glycoprotein moieties on recognition of OAB by phagocytes.

4.3.11.2 Inhibitors of cytoskeletal components

Nocodazole

Nocodazole induces depolymerisation of microtubules and has been shown to interfere with engulfment of apoptotic cells by macrophages (Cannon and Swanson 1992). Target cells were incubated with Nocodazole for 15 minutes at 7 μM in DMSO, prior to incubation with OAB, in order to investigate the cytoskeletal changes on target cells upon engulfment of OAB.

4.3.12 Inhibition of nitric oxide (NO) production by phagocytes and OAB

NO is involved in the phagocytic process by macrophages (Corradin et al. 1991) while in addition it is produced by osteoblasts, osteoclasts and osteocytes and plays a central role in the regulation of bone turnover (van't Hof et al. 1997). Target cells and OAB were incubated with the nitric oxide synthase inhibitor L-NAME for 30 minutes at 0.1 mM prior to preparation of phagocytic meals in order to study the effect of nitric oxide upon engulfment of OAB by phagocytes.

4.3.13 Determination of Apoptotic State

A range of techniques were used to assess the apoptotic state as described in chapter 3. Cells were observed in 3 fields per well (x20 magnification lens, approximately 40-100 cells per field) resulting in 9 fields per treatment group. Identical magnifications were used for all apoptosis estimates allowing similar numbers of cells to be counted per field in all experiments.

4.3.13.1 Annexin-V-FITC Assay

The appearance of phosphatidylserine (PS) on the outer leaflet of the membrane bilayer can be detected with fluorescently labelled Annexin V; (Martin et al 1995). Cells were incubated with Annexin-V-FITC followed by propidium iodide (PI) as described in §3.3.10.1 in order to distinguish between viable (FITC negative, PI negative), early apoptotic (FITC positive, PI negative) and late apoptotic or necrotic cells (FITC negative, PI positive).

4.3.13.2 DNA fragmentation using in situ Nick Translation

The percentage of target cells demonstrating DNA breaks was investigated using in situ nick translation staining (Noble et al. 1997), which allows the determination of DNA breaks following the incorporation of DIG-labelled dUTP as described in §3.3.10.2. The ratio of total cells (PI positive) to apoptotic (FITC positive) was determined using fluorescence microscopy and digital image capture.

4.3.13.3 DAPI staining for healthy and apoptotic cell morphology

DAPI (4',6-Diamidino-2-phenylindole) staining which reveals chromatin condensation and nuclear fragmentation was performed as described in §3.3.10.3.

4.3.14 Nitrite assay (Griess assay)

In aqueous solutions, nitric oxide (NO) rapidly degrades to nitrate and nitrite making direct measurement of this compound difficult. Spectrophotometric quantitation of nitrite using Griess Reagent is straightforward and sensitive, but it might cause a possible underestimation of NO. Initially nitrate is reduced to nitrite, which is converted to nitrous acid (HNO_2) which then diazotizes sulfanilamide. This sulfanilamide-diazonium salt is then reacted with N-(1-Naphthyl)-ethylenediamine (NED) to produce a chromophore which is measured at 540 nm. This assay was modified from a previously described method (Green et al. 1982) in order to measure nitrite in up to 200 µl of biological fluids. Concentration of nitrite in the samples and blank controls was calculated against a series of sodium nitrite (1 mM) dilutions providing two standard curves of 0-100 µM (1:10 dilution) and 0-10 µM (1:100) dilution respectively. Samples were pipetted onto a microtitre plate and were

incubated with the Griess reagent made up with equal volumes of Reagent A (2% sulphanilamide in orthophosphoric acid) and Reagent B (0.2% N-l-napthyl ethylenediamine dihydrochloride, NED, in H_2O). The assay colour was left to develop at room temperature for 15 minutes and the concentrations were estimated using a microplate reader at 540 nm. Dilutions, where appropriate were made in the same medium used in the experimental samples.

4.3.15 Inhibition of apoptosis using caspase 8 inhibitor

Caspases are involved at various stages in apoptotic cascades, mediating either death receptor pathways or cleavage of intracellular components in order to disassemble the cell's structure (Thornberry et al. 1998). In order to determine whether osteoblast apoptosis in response to OAB involved the activation of death receptor pathways target cells were incubated with caspase 8 inhibitor II Z-IETD-FMK (Calbiochem, UK) (Martin et al. 1998), which is activated mainly by death receptors, at 1 μM for 1 hour prior to addition of apoptotic bodies.

4.3.16 Determination of Fas expression by immunocytochemical staining

The Fas pathway is a death receptor pathway that mediates apoptosis in cells of the immune system (Ashkenazi et al. 1998); in addition, osteoblasts have also been shown to undergo apoptosis in response to Fas activation (Kawakami et al. 1997, Ozeki et al. 2002). Immunocytochemical staining for Fas was used in order to determine the percentage of target cells that were expressing Fas on the cell surface in response to OAB. Following incubation with various agents, cells in 24-well plates were fixed in 4% paraformaldehyde and subsequently washed in PBS. Cells were incubated for 5 minutes with 0.1% SDS, and were washed in PBS thoroughly. Cells were then nourished for 20 minutes in goat serum followed by 1 h incubation with anti-Fas monoclonal antibody (BD Transduction labs, UK) at RT. After washing in PBS, cells were incubated with secondary anti-mouse FITC antibody for 1 hour and were counter-stained with PI. Cells were visualised by fluorescence microscopy and digital image capture. The ratio of total cells (PI positive) to Fas positive (FITC positive) was detected based on 9 fields from a total of 3 wells.

4.3.17 Reverse Transcription-polymerase chain reaction

Total RNA was isolated from cultures of MLO-Y4 cells using RNA-B™ (Biogenesis) according to the manufacturer's instruction. cDNA was synthesized from 3 μg of total RNA using oligo dT primers, and RNA was converted into cDNA by SuperScript II RNaseH⁻ reverse transcriptase first strand synthesis system for RT-PCR (Invitrogen). The PCR reaction was performed using Qiagen Taq PCR core kit (10X reaction buffer, Taq 5 u/μl, Q buffer and dNTP 10 mM each) in a total of 25 μl reaction containing 5 μM each forward and reverse primers. Mouse CD14 specific primers were designed against sequence accession number BC057889 and mouse β-Actin specific primers against sequence accession number X03765 from HGMP database as shown below. The resulting PCR products for CD14 and Actin were 290 bp and 290 bp respectively. The PCR reaction was carried out for 40 cycles with PTC-200 Peltier thermal cycler (MJ Research). PCR conditions were denaturation at 94 °C for 4 minutes, annealing at 57 °C for 1 minute and extension at 72 °C for 1 minute and 30 seconds. The PCR products were analysed in 1.2% agarose gel containing ethidium bromide. Primer Sequences:

CD14 forward 5'-GCGAGCTAGACGAGGAAAGTT-3'
CD14 reverse 5'-AAGAGTCAGTTCCTGGAGGCC-3'
Actin forward 5'-CAAGGTGTGATGGTGGGAATG-3'
Actin reverse 5'-GCTACGTACATGGCTGGGGTG-3'

PCR products were cut from the gel, the DNA gel extracted using Qiagen Kit and sequencing was carried out by the sequencing service (Edinburgh University) who use Big Dye version 2 run on a ABI 3730 capillary sequencing machine.

4.3.18 Statistical Analysis

Statistical analysis was performed with SPSS release 11.5 for Windows, using Analysis of Variance (ANOVA), Tukey test and Dunnett test for comparison between the treatment groups or simple regression analysis as described in §3.3.11. Results are expressed as means ± S.D. $p < 0.05$ was considered to be statistically significant.

4.4 Results

4.4.1 Characterization of osteocyte apoptotic bodies (OAB)

Osteocyte apoptotic bodies, ranging between 0.02-0.5 μm in diameter were isolated from osteocyte apoptotic cultures as described in §4.3.7 and 3.4.1

4.4.2 Characterization of primary osteoblast and osteocyte cultures

Osteoblast and osteocyte cultures obtained from murine calvaria were characterised as described in §3.3.3 and 3.4.2

4.4.3 Modification of binding/ingestion of OAB by phagocytes

In order to identify molecules that might be implicated in the interaction of osteoblasts with OAB, the latter were treated with several compounds that modify plasma membrane composition.

4.4.3.1 EDTA

EDTA is Ca^{2+} chelator that has been widely used to reduce the availability of Ca^{2+} resulting in decreased phagocytosis (Yuan et al. 2001). OAB were incubated in EDTA and introduced to osteoblast cultures for 24 h. Mean percentages of apoptotic osteoblasts estimated by Nick Translation (**Figure 26A**) and DAPI (**Figure 26B**) staining of cultures, were significantly reduced following incubation of apoptotic osteocytes with EDTA ($p = 0.008$, compared to cultures fed with OAB). In addition, treatment of OAB with EDTA significantly reduced their interaction both with osteoblasts and macrophages (**Figure 27A and 27B**) ($p = 0.001$ and $p = 0.03$ respectively compared to cultures fed with OAB), indicating that the availability of Ca^{2+} is important in mediating the interaction between apoptotic osteocytes and phagocytes.

4.4.3.2 Trypsin

OAB were incubated with the proteolytic enzyme trypsin prior to introduction to osteoblast cultures for 24 h, in order to determine the importance of binding of OAB to osteoblasts on protein-protein interactions. Mean percentages of apoptotic osteoblasts estimated by Nick Translation (**Figure 26A**) and DAPI (**Figure 26B**)

staining of cultures, were significantly reduced following incubation of apoptotic osteocytes with trypsin ($p = 0.001$ respectively, compared to cultures fed with OAB). Furthermore, incubation of OAB with trypsin significantly reduced phagocytosis of OAB by osteoblasts (**Figure 27A**) ($p = 0.03$) and macrophages (**Figure 27B**) ($p = 0.002$), compared to cultures treated with OAB alone, indicating possibly a glycoprotein-dependent binding and engulfment of OAB by phagocytes.

4.4.3.3 Glyburide

Glyburide, is a potent sulfonylurea compound that can inhibit ABCA1 transporter activity, block ATP-sensitive potassium channel (Becq et al. 1997), induces membrane depolarisation, and affects phospholipid efflux and PS externalisation (Marguet et al. 1999). The compound has been used to effectively block PS externalisation in a number of studies (Zha et al. 2001, Marguet et al. 1999, Hamon et al. 2000). Treatment of osteoblast cultures with glyburide prior to incubation with OAB, reduced the percentage of apoptotic osteoblasts (**Figure 28C**) by 4-fold, compared to cultures incubated with OAB alone as shown by DAPI staining ($p = 0.02$) (**Figure 29A**) and Nick Translation staining (**Figure 29B**). In addition, estimation of the mean percentages of osteoblasts and macrophages physically associated with OAB showed a significant reduction in cultures pre-treated with Glyburide ($p = 0.001$) (**Figure 30**), indicating that phospholipid changes and/or ABCA-1 transporter activity is mediating the interaction of osteoblasts with OAB which results in osteoblast apoptosis.

4.4.3.4 Oligomycin

Oligomycin is an antibiotic which inhibits the mitochondrial FoF"-ATPase and the Na+,K+-ATPase, and has also been shown to interfere with Ca^{2+}-influx mediated by store-operated channels (Cho et al. 1997) and to impair Ca^{2+}-induced transmembrane randomization of phospholipids (Marguet et al. 1999). The compound has been used previously to modify phospholipid activity in a number of studies (Catz et al. 1998, Marguet et al. 1999, Kamp et al. 2001). Pre-treatment of osteoblast cultures with oligomycin also resulted in decreased percentage of apoptotic osteoblasts in response to OAB (**Figure 28D**) as shown by DAPI staining (**Figure 29A**) ($p = 0.001$,

compared to cultures incubated with OAB alone) and Nick Translation staining (**Figure 29B**). Reduced osteoblast apoptosis was associated with reduced interaction between osteoblasts and OAB ($p = 0.0009$) (**Figure 30A**), while similar reduction was observed in the physical association of OAB with macrophage cultures pre-treated with Oligomycin ($p = 0.0004$) (**Figure 30B**), further supporting the importance of phospholipid asymmetry in the phagocyte for the recognition of OAB.

The mean percentage of apoptotic osteoblasts was also reduced when osteocytes rather than osteoblasts were pre-treated with glyburide and oligomycin prior to production of OAB ($p = 0.01$ and $p = 0.002$, respectively compared to treatment with OAB alone) (**Figure 29A and 29B**) pointing to the fact that phospholipid changes in both the target osteoblast and the osteocytic prey could affect induction of osteoblast apoptosis.

4.4.3.5 N-acetylglucosamine

Osteoblast cultures were incubated with N-acetylglucosamine, a compound which competitively binds to cell surface glycoproteins, in the presence of OAB, since it has been shown that loss of terminal sialic acid residues from cell surface glycoproteins is involved in the recognition of the apoptotic cells by lectin receptors. (Tarnowski et al. 1987, Savill et al. 2000). Incubation of osteoblast cultures with N-acetylglucosamine reduced the mean percentage of osteoblast apoptosis compared to cultures incubated with OAB alone estimated by DAPI staining ($p = 0.001$) **(Figure 29C)** and Nick Translation staining (**Figure 29D**). Treatment of osteoblast and macrophage cultures with N-acetylglucosamine also decreased the percentages of phagocytes physically associated with OAB, compared to cultures incubated with OAB alone ($p = 0.0001$ and $p = 0.0003$, respectively) (**Figure 30A and 30B**).

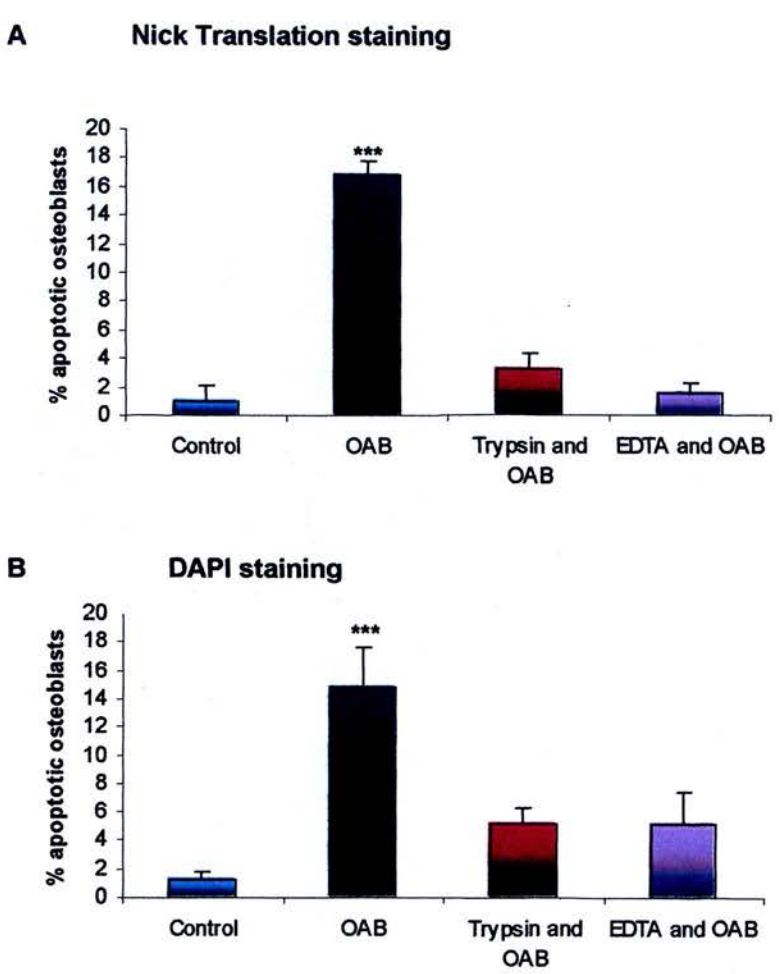

Figure 26. Ca++ and protein-dependent induction of osteoblast apoptosis. Osteoblast cultures were incubated with OAB that were pre-treated with Trypsin and EDTA. Graphs represent mean percentages of cells associated with OAB after 24 hours of incubation, estimated by **A**. Nick Translation staining and **B**. DAPI staining of cultures. Control treatments represent vehicle treatments for the medium in which OAB were prepared (αMEM) and percentages of apoptotic osteoblasts are statistically indifferent from untreated cultures (1.27 ± 0.64 S.D., $p > 0.05$). Error bars represent ± S.D. *** = $p < 0.0001$, ** = $p < 0.001$, compared to control cultures (Dunnetts test).

A % Phagocytosis in osteoblast cultures

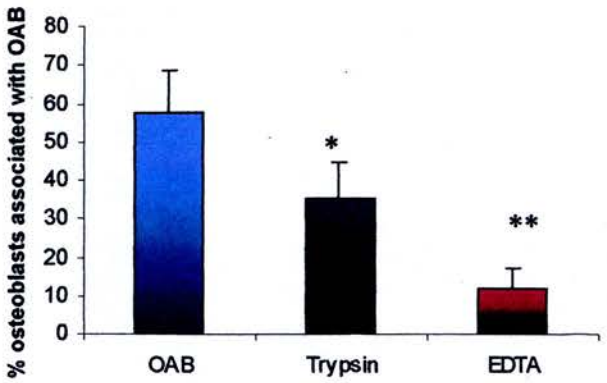

B % Phagocytosis in macrophage cultures

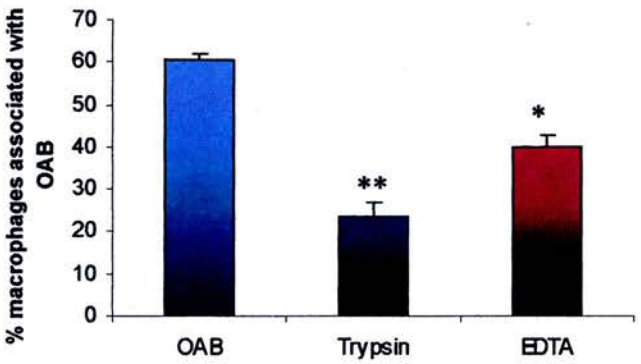

Figure 27. Ca++ and protein-dependent interaction of OAB with target cells. Osteoblast and macrophage cultures were incubated for 24 h with OAB that were pre-treated with Trypsin and EDTA. Association between OAB and **A.** osteoblasts and **B.** macrophages was estimated using combined images of fluorescence staining of both the phagocyte and the prey. Error bars represent ± S.D. ** = $p < 0.0001$, * = $p < 0.001$, compared to cultures incubated with OAB (Dunnetts test).

4.4.4 Modification of engulfment of OAB by phagocytes with Nocodazole

Incubation of osteoblast cultures with nocodazole, an agent that induces depolymerisation of actin filaments and impairs engulfment of apoptotic bodies (Cannon and Swanson 1992) also reduced OAB-induced pro-apoptotic activity (**Figure 28E**) as shown by DAPI staining ($p = 0.0001$) (**Figure 29C**) and Nick Translation staining (**Figure 29D**). In addition, upon pre-treatment of osteoblasts with Nocodazole, physical interaction between OAB and osteoblasts was also reduced ($p = 0.0003$) compared to treatment with OAB alone, indicating that blockade of the upstream binding and engulfment of OAB might be sufficient to regulate the apoptosis inducing activity of OAB. (**Figure 30A**). Furthermore, pre-treatment of macrophage cultures with nocodazole also reduced the mean percentages of phagocytosis of OAB by macrophages ($p = 0.0002$) compared to treatment with OAB alone (**Figure 30B**).

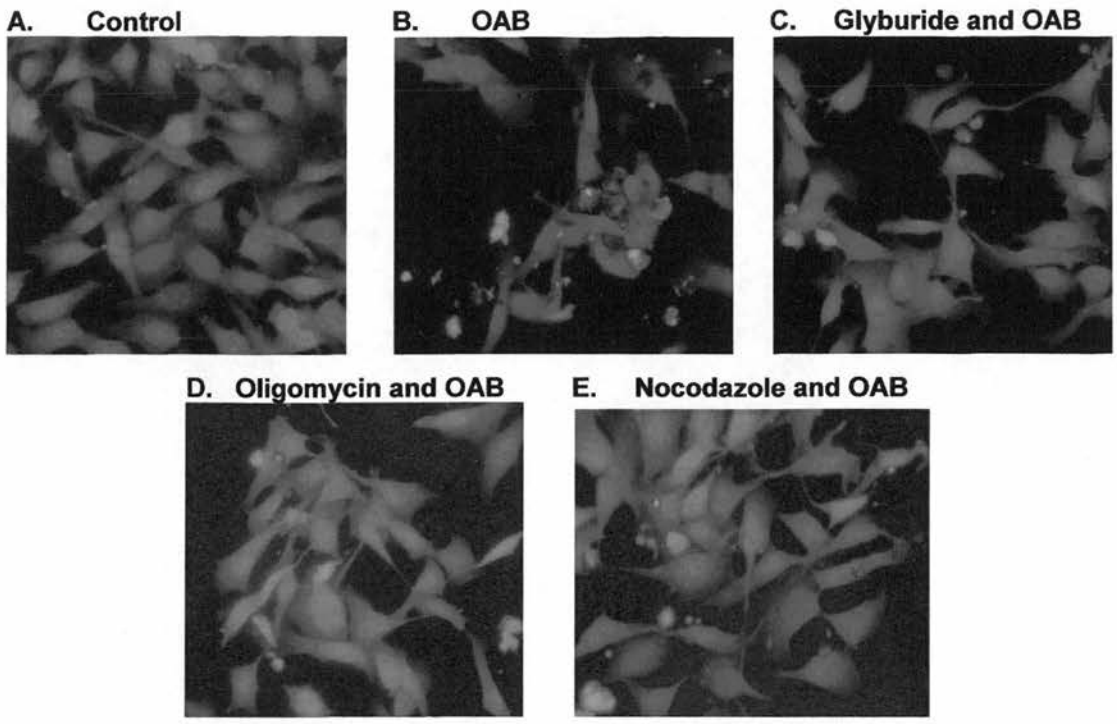

Figure 28. Inhibition of phagocytosis prevents osteoblast apoptosis. Osteoblast cultures were treated with agents and incubated with OAB for 24 hours. **A.** control cultures, **B.** cultures in presence of OAB, and cultures treated with **C.** Glyburide, **D.** Oligomycin and **E.** Nocodazole in the presence of OAB. Control treatments represent vehicle treatments for the medium in which OAB were prepared (αMEM). Green = target osteoblast cultures, Red = OAB. 20x magnification.

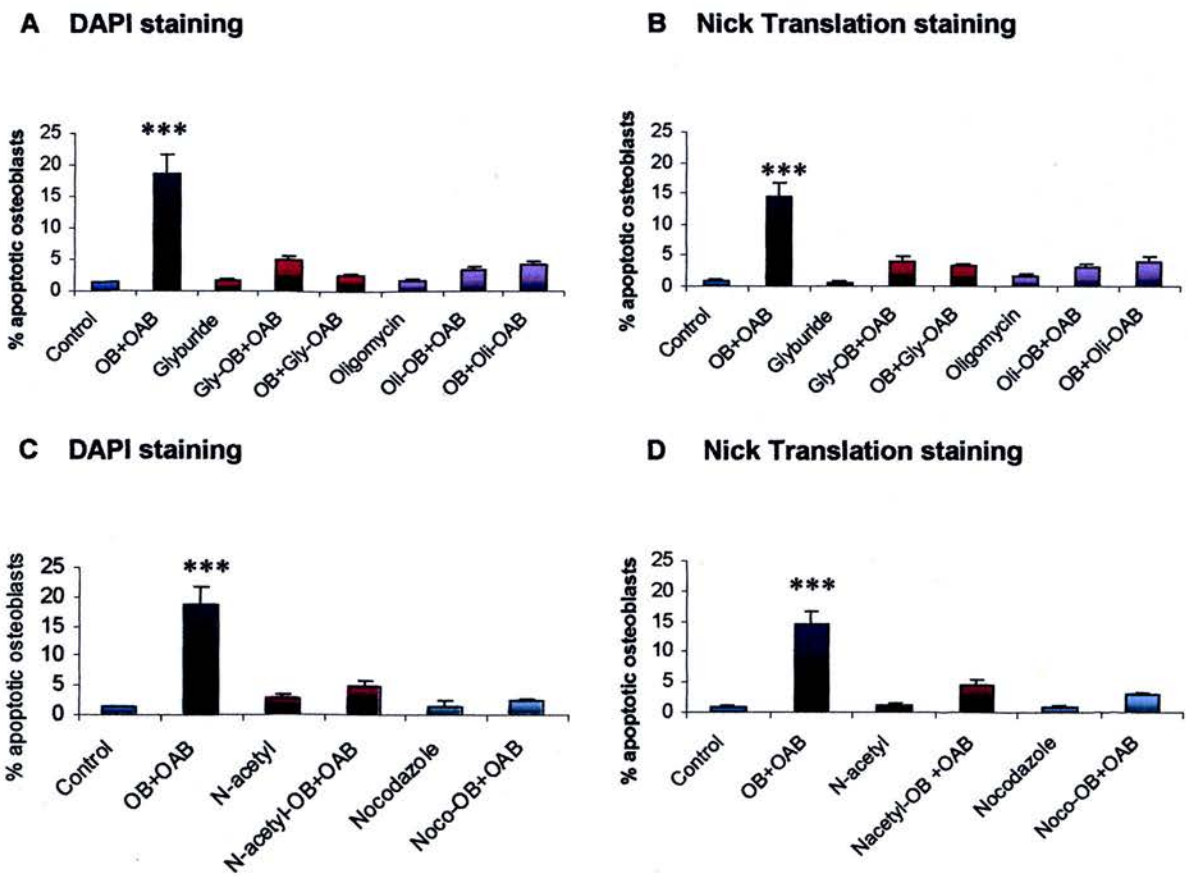

Figure 29. Inhibition of osteoblast apoptosis. Osteoblasts were incubated with OAB for 24 hours and apoptosis was estimated with DAPI and Nick Translation nuclear staining, using fluorescent microscopy. Graphs represent reduced percentages of osteoblast apoptosis in cultures in which **A** and **B.** both the phagocyte and the prey were incubated with Glyburide (Gly) and Oligomycin (Oli) and **C** and **D.** osteoblast cultures were pre-treated with N-acetylglucosamine (Nacetyl) and Nocodazole (Noco). Control treatments represent vehicle treatments for the medium in which OAB were prepared (αMEM) and percentages of apoptotic osteoblasts are statistically indifferent from untreated cultures (1.3 ± 0.21 S.D., $p > 0.05$). Error bars represent ± SD. *** = $p < 0.0001$, compared to control cultures (Dunnetts test).

A % Phagocytosis in osteoblast cultures

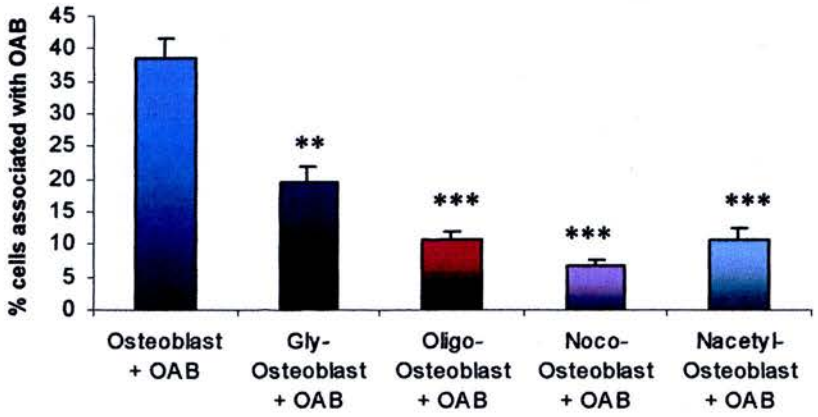

B % Phagocytosis in macrophage cultures

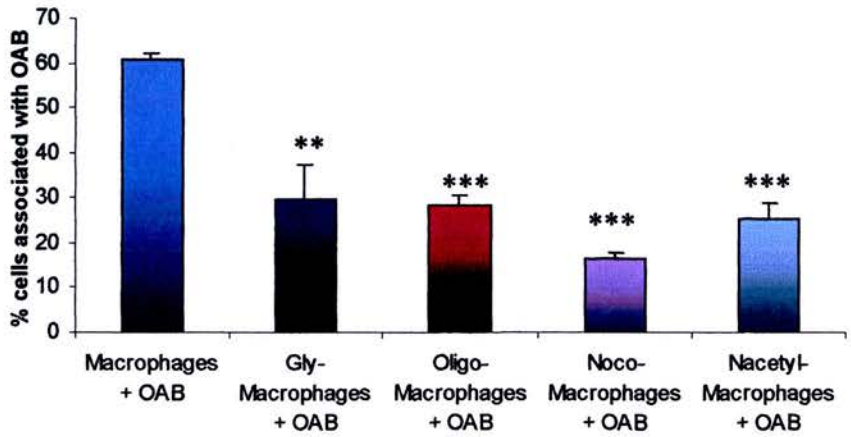

Figure 30. Glyburide, Oligomycin, N-acetylglucosamine and Nocodazole impair the interaction of OAB with phagocytes. Reduced percentages of **A.** osteoblasts and **B.** macrophages associated with OAB following the pre-treatment of cultures with Glyburide, Oligomycin, Nocodazole and N-acetylglucosamine. Association between OAB and osteoblasts was estimated using combined images of fluorescence staining of both the phagocyte and the prey. Error bars represent ± S.D. *** = $p < 0.0001$, ** = $p < 0.001$, compared to cultures incubated with OAB (Dunnetts test).

4.4.5 Apoptotic osteocytes increase production of nitric oxide (NO) in osteoblasts.

NO plays a central role that has biphasic effects on bone formation and resorption activity and is a potential inducer and inhibitor of apoptosis (Van't Hof et al. 1997). To establish any role of NO in the induction of osteoblast apoptosis by apoptotic osteocytes, we exposed the osteoblast and osteocyte cultures to L-NAME, an inhibitor of NO production, prior to preparation of phagocytic meals. Inhibition of NO production by osteocytes did not reduce apoptosis of osteoblasts. However, apoptosis (**Figure 31A**) as well as association of osteoblasts with OAB (**Figure 31B**) were reduced in osteoblast cultures in which NO production was inhibited by L-NAME treatment. To determine whether osteocyte apoptotic bodies affect NO production by osteoblasts, media were collected and analysed from phagocytic meals by Griess assay. This finding confirmed firstly that OAB induced production of NO by osteoblasts and that the increase in NO production induced by apoptotic osteocytes was partially inhibited by L-NAME (**Figure 32**). Necrotic debris did not induce NO production, pointing again to differences in the response of osteoblasts to products of the two different types of cell death, as discussed in chapter 3.

In addition, in macrophage cultures, the presence of apoptotic osteocytes was also associated with increased production of NO by macrophages, indicating that phagocytosis of apoptotic osteocytes could be mediated or associated with NO production by the target cells and that production of NO alone is not necessarily responsible for induction of death in the phagocyte (**Figure 31C**).

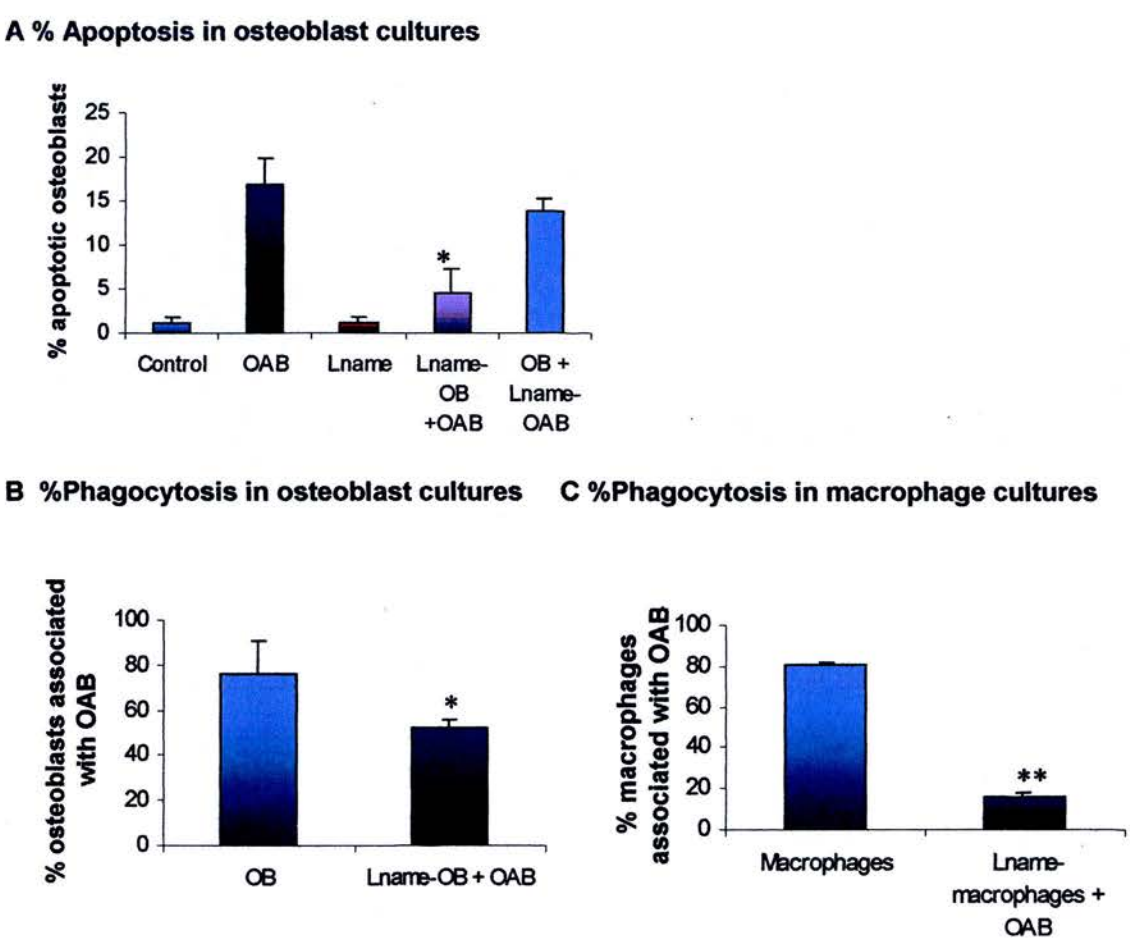

Figure 31. NO mediated induction of osteoblast apoptosis and interaction of OAB with target cells. **A**. Pre-treatment of osteoblast cultures with L-NAME reduced mean percentages of osteoblast apoptosis as estimated by DAPI staining. Control treatment represents vehicle treatments for the medium in which OAB were prepared (αMEM) and percentages of apoptotic osteoblasts are statistically non-significant from untreated cultures (1.01 ± 0.11 S.D., $p > 0.05$). Pre-treatment of **B**. osteoblast and **C**. macrophage cultures with L-NAME reduced mean percentages of cells associated with OAB. Association between OAB and osteoblasts was estimated using combined images of fluorescence staining of both the phagocyte and the prey. Error bars represent ± SD. ** = $p < 0.001$, * = $p < 0.05$, compared to cultures incubated with OAB.

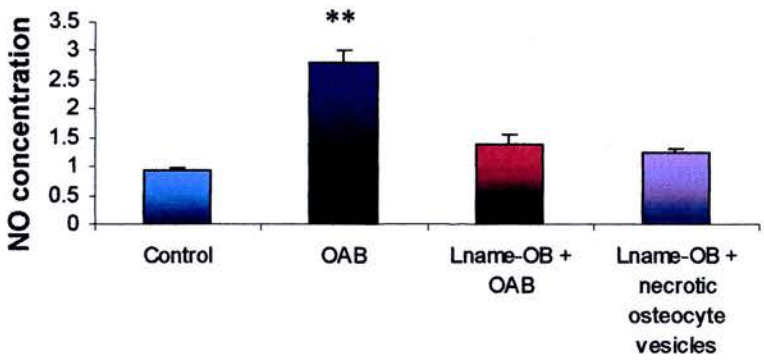

Figure 32. OAB increase production of NO by osteoblasts. Osteoblast cultures were incubated with L-NAME prior to OAB. Griess assay showed reduced NO concentration in the presence of OAB in cultures pre-treated with L-NAME. Control treatment represents vehicle treatments for the medium in which OAB were prepared (αMEM) and NO concentration is statistically indifferent from blank cultures (0.68 ± 0.452 S.D., $p > 0.05$). Error bars represent ± S.D. ** = $p < 0.001$, compared to control cultures (Dunnetts test).

4.4.6 Scavenger receptor A mediates interaction between OAB and osteoblasts

The involvement of scavenger receptor A (SRA) in the recognition of apoptotic bodies has been demonstrated in several studies (Platt et al. 1998, Yamamoto et al. 1999). Osteoblasts were isolated from mice that were transgenically modified to not express the scavenger receptor A gene and were incubated with OAB and the medium in which they were produced (CM). Physical interaction of osteoblasts with OAB was significantly reduced by about 50% in SRA null mice (**Figure 33**) ($p = 0.001$), compared to wild type mice. However the absence of the scavenger receptor A did not reduce mean percentages of apoptotic osteoblasts in response to OAB ($p > 0.05$), as shown by DAPI (**Figure 34A**) and Nick Translation staining of cultures (**Figure 34B**). In addition, there was no reduction in the percentage of osteoblasts (**Figure 34D**) and apoptotic osteoblasts (**Figure 34D**) associated with OAB either engulfed or bound to their surface, indicating that osteoblasts isolated either from wild-type or SRA null mice appeared equally likely to be apoptotic the more OAB were associated with them, as shown by regression analysis. In both wild-type and SRA null osteoblast cultures, the proportion of apoptotic osteoblasts appeared to depend on the number of OAB engulfed (**Figure 34D**) ($p = 0.045$ in both cultures).

4.4.7 Absence of CD14 reduces osteoblast apoptosis *in vitro* and *ex vivo.*

CD14 has been shown to interact with LPS on bacteria, but also to mediate tethering and uptake of apoptotic cells, in a noninflammatory manner (Devitt et al. 1998). RT-PCR studies and subsequent gene sequencing confirmed the presence of CD14 mRNA in osteoblasts (**Figure 35A**). In this study CD14 null mice were used to determine the effect of CD14 in mediating recognition of OAB by osteoblasts. In a similar way to SRA knockout cells, engulfment of osteocyte apoptotic bodies by osteoblasts was reduced by 50% compared to wild-type cultures ($p = 0.002$), indicating that the absence of CD14 might affect interaction of OAB with osteoblasts (**Figure 35B**). In addition, a significant reduction was observed in apoptosis of osteoblasts isolated from CD14 null mice ($p = 0.0001$ compared to wild type cultures) (**Figure 36A and 36B and 37**), indicating that CD14 might mediate

pathways that involve initiation of apoptotic osteoblast death in response to OAB. Furthermore, there was a reduction in the percentage both of total osteoblasts (**Figure 36C**) and apoptotic osteoblasts (**Figure 36D**) associated with OAB either engulfed or bound to their surface, isolated from CD14 null mice compared to wild-type osteoblast cultures. Regression analysis showed that the absence of CD14 from osteoblasts reduced the dependence of the proportion of apoptotic osteoblasts on the number of OAB engulfed (**Figure 36D**) ($p = 0.039$ in wild-type osteoblast cultures and $p = 0.08$ in CD14 knockout osteoblast cultures).

Ex vivo studies using calvaria derived from CD14 null mice, which were incubated with OAB for 24 hours, confirmed the reduction in OAB-engendered osteoblast apoptosis in the absence of CD14, compared to mean percentages of osteoblast apoptosis estimated from wild-type calvarial sections ($p = 0.0001$) (**Figure 38A**). In addition, estimation of osteocyte apoptosis indicated that the presence of OAB induced bone resident osteocytes to undergo apoptosis, which was however reduced in the absence of CD14 ($p = 0.001$) (**Figure 38B**).

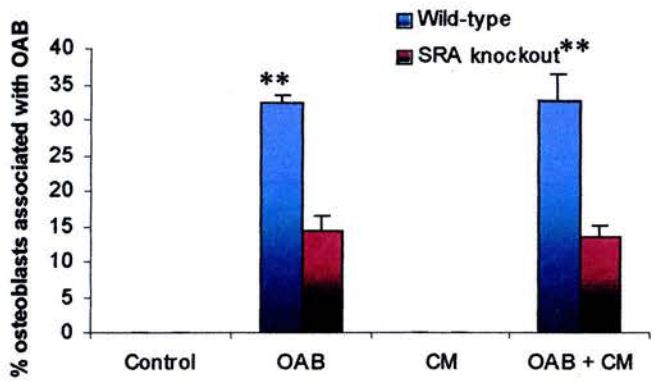

Figure 33. Scavenger receptor A-dependent uptake of OAB. Osteoblasts were isolated from wild-type and SRA null mice and incubated with OAB for 24 hours in the presence and absence of their conditioned media (CM). Graph shows the mean percentages of osteoblasts associated with OAB. Error bars represent ± SD. ** = $p < 0.001$, compared to knockout cultures (Tukey test).

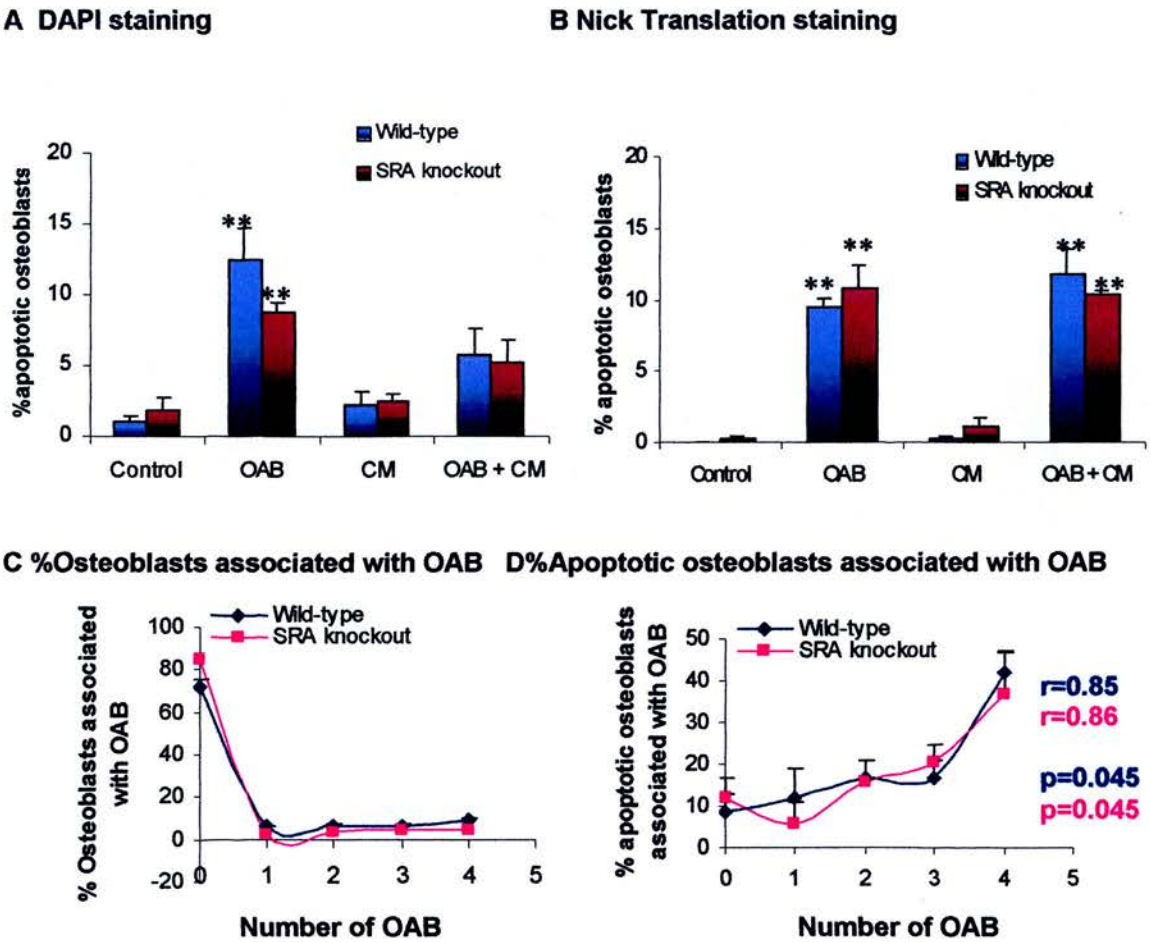

Figure 34. Absence of Scavenger Receptor A does not affect osteoblast apoptosis in response to OAB. Osteoblasts were isolated from SRA null mice and incubated with OAB for 24 hours in the presence and absence of their conditioned media (CM). Mean percentages of apoptotic osteoblasts were estimated using **A**. DAPI staining and epifluorescence. Control treatment represents vehicle for the medium in which OAB were prepared (αMEM) and percentages of apoptotic osteoblasts are statistically indifferent from untreated cultures (1.26 ± 0.7 S.D., and 1.76 ± 0.91 S.D., $p > 0.05$, for wild-type and knockout cultures respectively). **B**. Nick Translation staining. Control treatment represents vehicle treatment for the medium in which OAB were prepared (αMEM) and percentages of apoptotic osteoblasts are statistically indifferent from untreated cultures (0.00 ± 0.00 S.D. and 0.25 ± 0.25 S.D. $p > 0.05$, for wild-type and knockout cultures respectively). Osteoblasts were incubated with OAB and the percentage of **C**. osteoblasts and **D**. apoptotic osteoblasts that carried none, 1, 2, 3 or ≥ 4 OAB was determined. Error bars represent ± SD. **=$p<0.001$, compared to control cultures. r= correlation coefficient.

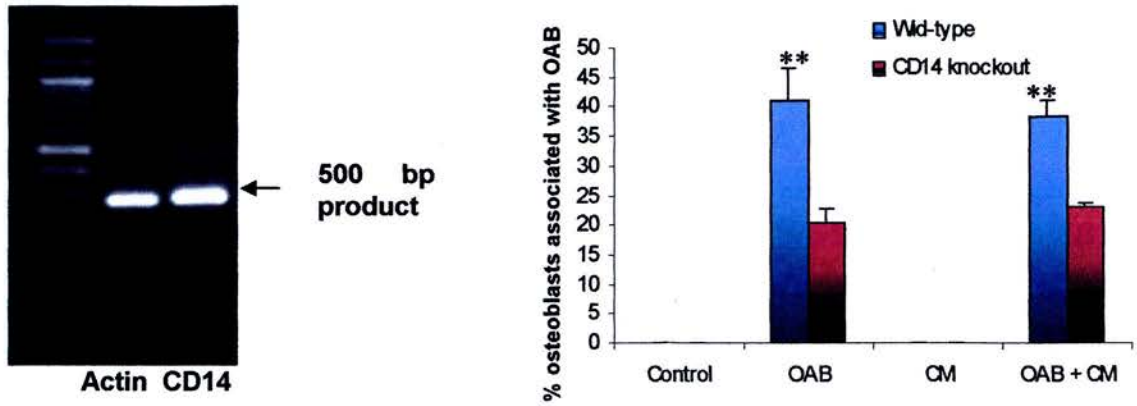

Figure 35. CD14-dependent uptake of OAB. Osteoblasts were isolated from CD14 null mice and incubated with OAB for 24 hours in the presence and absence of their conditioned media (CM). **A**. RT-PCR studies showed expression of CD14 mRNA in wild-type murine osteoblasts. **B**. Estimation of mean percentages of osteoblasts associated with OAB. Error bars represent ± S.D. ** = $p < 0.001$ compared to control cultures (Tukey test)

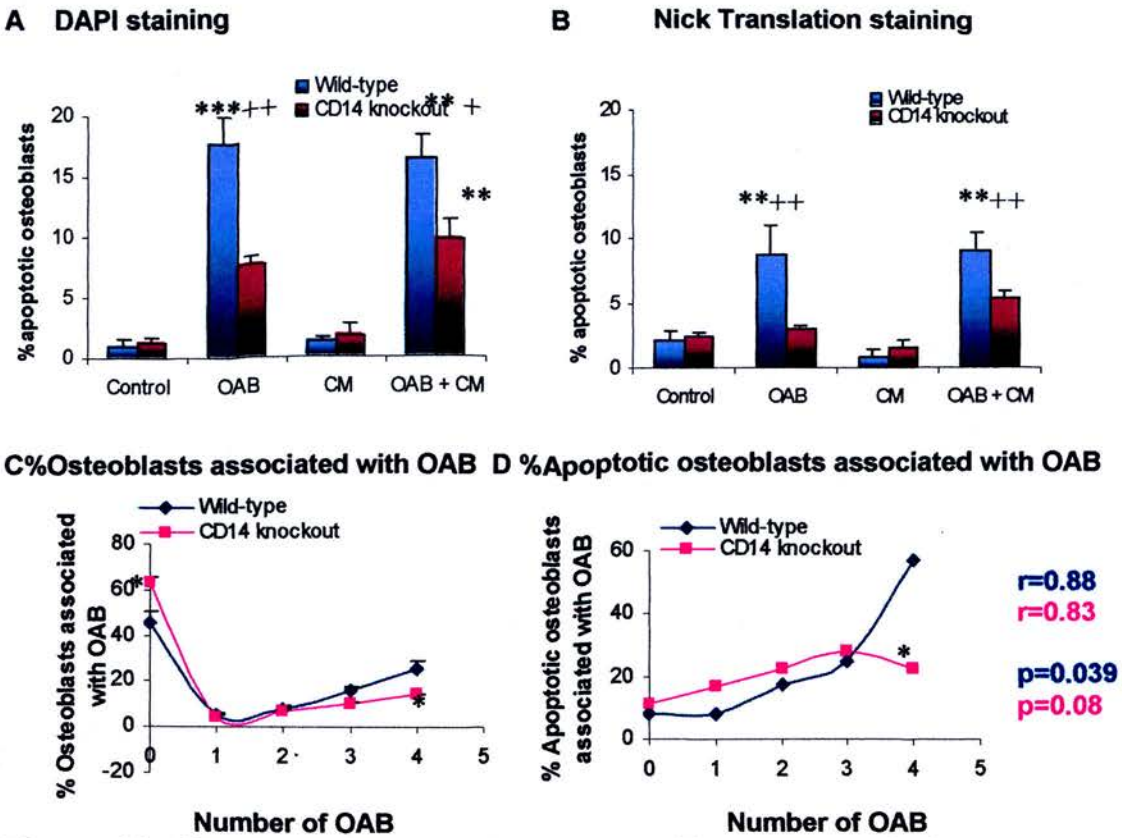

Figure 36. Absence of CD14 reduces osteoblast apoptosis in response to OAB. Osteoblasts were isolated from CD14 null mice and incubated with OAB for 24 hours in the presence and absence of their conditioned media (CM). Mean percentages of apoptotic osteoblasts were estimated using **A**. DAPI staining and fluorescence microscopy. Control treatment represents vehicle for the medium in which OAB were prepared (αMEM) and percentages of apoptotic osteoblasts are statistically indifferent from untreated cultures (1.16 ± 0.5 S.D. for wild-type and 1.34 ± 0.81 S.D. for knockout osteoblast cultures) **B**. Nick Translation staining of cultures. Control treatment represents vehicle treatment for the medium in which OAB were prepared (αMEM) and percentages of apoptotic osteoblasts are statistically indifferent from untreated cultures (2.01 ± 0.7 S.D. for wild-type and 2.21 ± 0.3 S.D. for knockout osteoblast cultures). Osteoblasts were incubated with OAB and the percentage of **C**. osteoblasts **D.** apoptotic osteoblasts that carried none, 1, 2, 3 or ≥ 4 OAB was determined. Error bars represent ± S.D. *** = $p < 0.0001$, ** = $p < 0.001$ and * = $p < 0.05$ compared to control cultures (Dunnetts test). +=$p<0.05$ and ++=$p<0.001$ compared to knockout cultures (Tukey test). r = correlation coefficient

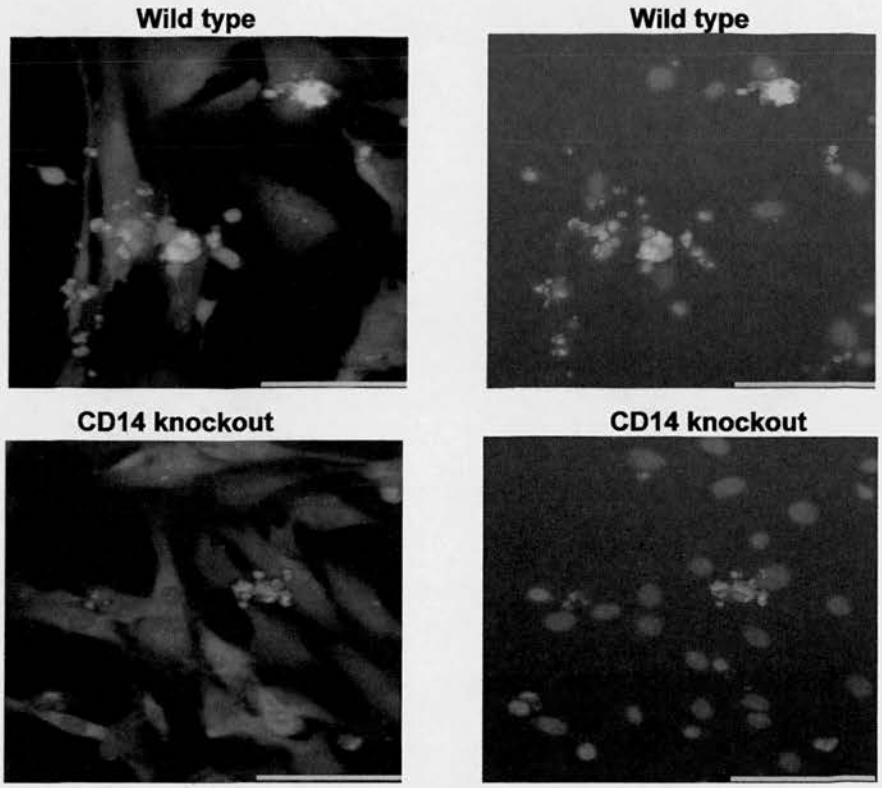

Figure 37. CD14 null osteoblasts do not undergo apoptosis in the presence of OAB. Demonstration of representative images of WT (upper panel) and CD14 null (lower panel) cultures. Osteoblasts (green Cell tracker) were fed with OAV (Orange Cell tracker). Images show increased number of cells in CD14 null cultures and reduced DNA fragmentation identified by DAPI nuclear staining of osteoblasts. Bar = 10 μm.

A Nick Translation staining of osteoblast population

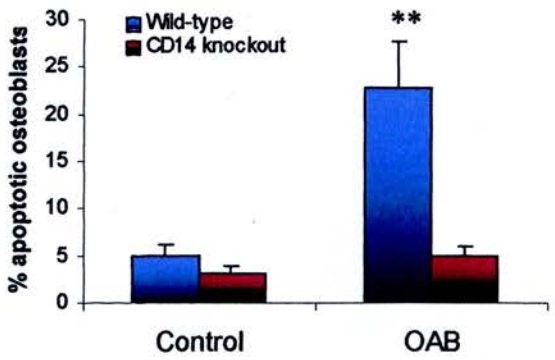

B Nick Translation staining of osteocyte population

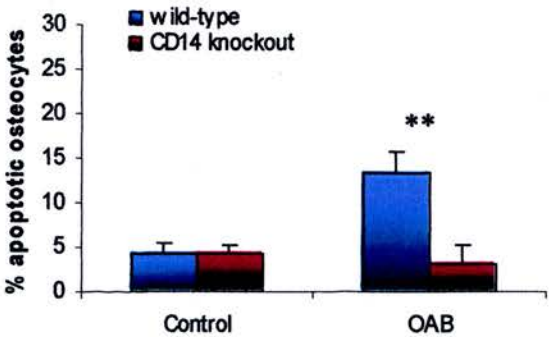

Figure 38. CD14-dependent induction of osteoblast and osteocyte apoptosis. Murine calvariae were incubated for 24 hours in the presence and absence of OAB. Graphs represent mean percentages of **A**. osteoblast and **B**. osteocyte apoptosis. Control treatments represent vehicle treatments for the medium in which OAB were prepared (αMEM). Error bars represent ± S.D. ** = $p < 0.001$, compared to knockout cultures (Tukey test).

4.4.8 Caspase-8 dependent induction of apoptosis

Osteocyte apoptotic bodies were shown in chapter 3 to induce apoptosis in osteoblast cultures, in a caspase 3 and/or 7 dependent manner. In order to determine whether OAB-engendered osteoblast apoptosis involved activation of death receptor pathways, a caspase 8 inhibitor II (Martin et al. 1998) was administered and shown to block osteoblast apoptosis as evidenced by nick Translation (**Figure 39A**) and DAPI staining (**Figure 39B**) of cultures ($p = 0.001$ and $p = 0.002$ respectively, compared to treatment with OAB alone), indicating the possible involvement of a death receptor-mediated pathway in the response to OAB.

4.4.9 Upregulation of membrane-bound Fas receptor expression

Seeking a link between inhibition of osteoblast apoptosis by inhibition of caspase 8 and activation of death receptor pathways, the expression of Fas receptor on osteoblast membrane was investigated using a FITC-labelled anti-Fas antibody. Results indicated that the presence of OAB increased the mean percentages of osteoblasts that were positive for Fas ($p = 0.003$) (**Figure 40A**).

Similar results were obtained for macrophage cultures (**Figure 40B**) in the presence of osteocyte apoptotic bodies indicating that Fas expression on the target cells is influenced by the interaction with apoptotic osteocytes. However in macrophage cultures the in increase in Fas presence was not associated with induction of death.

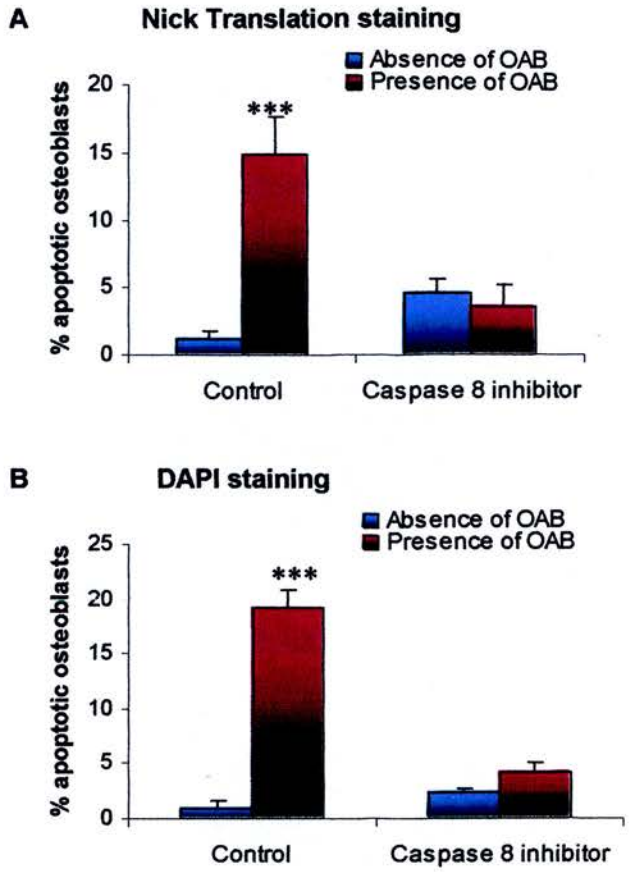

Figure 39. Caspase-8 dependent induction of osteoblast apoptosis. Incubation of osteoblast cultures with caspases-8 inhibitor II reduced mean percentages of apoptosis in the presence of OAB as estimated by **A**. Nick Translation staining and **B**. DAPI staining of cultures. Control treatments represent vehicle treatments for the medium in which OAB were prepared (αMEM) and percentages of apoptotic osteoblasts are statistically indifferent from untreated cultures (0.97 ± 0.1 S.D., $p > 0.05$) and vehicle cultures (DMSO) for caspase inhibitors (0.97 ± 0.65 S.D.). Error bars represent ± S.D. *** = $p < 0.0001$, compared to control cultures (Dunnetts test)

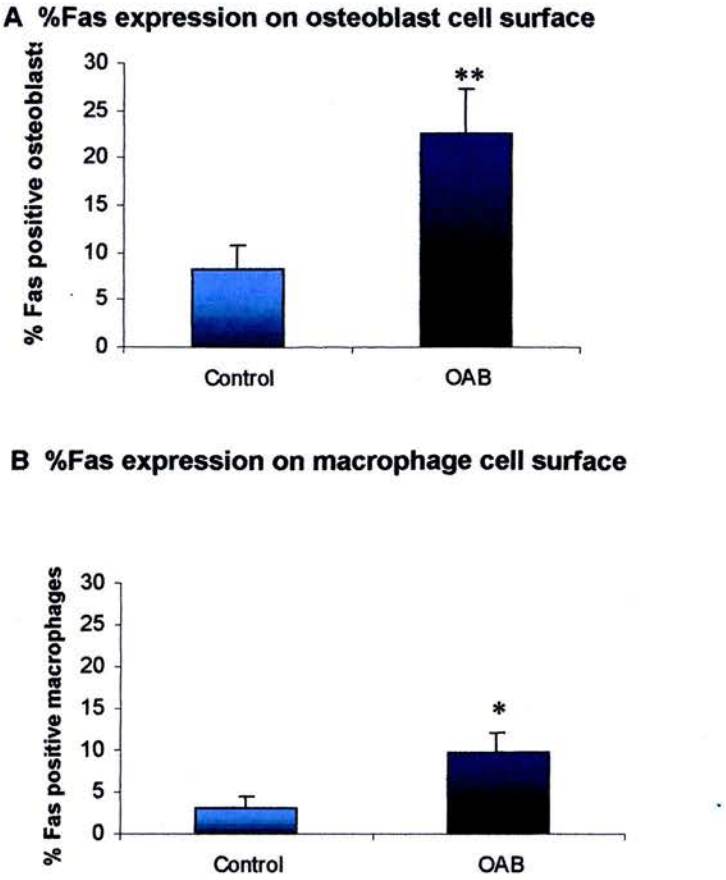

Figure 40. Upregulation of Fas in the presence of OAB. Mean percentages of **A**. Osteoblasts and **B**. Macrophages that are positive for Fas following incubation with OAB. Control treatments represent vehicle treatments for the medium in which OAB were prepared (αMEM). Error bars represent ± S.D. ** = $p < 0.001$ and * = $p < 0.05$ compared to control cultures.

4.5 Discussion

As discussed in chapter 3, osteocyte apoptotic bodies deliver a specific death inducing signal recognised only by osteoblastic cells in cultures. The aim of the experiments outlined in this chapter was to identify the existence of phagocytic mechanisms commonly involved in the recognition between apoptotic bodies and phagocytes, as well as molecules that might be associated with the specific recognition of OAB by osteoblasts, and the induction of osteoblast apoptosis. Phagocytosis is a complex process that requires specific changes to occur on the apoptotic cell membrane, in order to allow recognition and engulfment by phagocytes, without disturbing neighboring living cells (Savill 1997). Several molecules expressed on the apoptotic and/or the phagocyte cell surface have been implicated in the recognition mechanism and the engulfment of the apoptotic cells, which are summarized in §2.7 and are investigated in this chapter.

Having shown in the previous chapter that osteoblasts readily bind and engulf OAB and that osteoblasts are more likely to be apoptotic if they have phagocytosed OAB, I first undertook studies to determine the role of membrane associated changes/activities in the phagocytosis of OAB by phagocytes, by using a range of compounds that are known to affect, through different mechanisms, the binding, recognition and/or internalisation of apoptotic bodies by phagocytes. Estimation of the phagocytic index, which is the proportion of osteoblasts having phagocytosed (bound or internalised) OAB, was followed by estimation of osteoblast apoptosis, following treatment with these compounds, in order to identify the implication or requirement of binding, recognition and engulfment in the death inducing response. Glyburide is a long-acting sulfonylurea compound that has been used in the treatment of non-insulin dependent diabetes melitus and acts as a potent inhibitor of ATP-dependent K^+ channels (Quast and Cook 1989) leading to membrane depolarisation and insulin secretion (Luzi and Pozza 1997). Glyburide has also been shown to block the anion flux induced by the ATP-binding cassette A-1 (ABCA-1) transporter in Xenopus oocytes at 100 μM (Becq et al. 1997). Inhibition of ABCA-1 by Glyburide at concentrations up to 100 μM has also been shown to affect endosomal membrane trafficking by enhancing endocytosis of LDL and transferrin

(Zha et al. 2001) and to prevent secretion of IL-1b, which is required in inflammation and engulfment by mouse macrophages and monocytes (Hamon et al. 1997). ABCA-1 transporter has been implicated by other studies in the ingestion of apoptotic cells by macrophages (Luciani and Chimini 1996) and the movement of anionic phospholipids across the plasma membrane in apoptotic cells (Hamon et al 2000). Treatment of apoptotic thymocytes with glyburide at 50 μM was shown to decrease their recognition by macrophages, while similar treatment of the macrophages reduced the efficient engulfment of the apoptotic thymocytes (Marguet et al 1999), possibly by inhibiting ABCA-1 induced phospholipid efflux and PS externalisation in both the phagocytes and the prey. Since OAB were shown to express phosphatidyl serine on the outer leaflet of the plasma membrane by binding to fluorescently labelled Annexin V, while their purification was also enabled by biotinylated Annexin V-streptavidin magnetic bead-conjugatesIn the current study, glyburide was used to determine the effect of phospholipid efflux in the recognition mechanisms between OAB and both osteoblasts and macrophages. Treatment of phagocytes with glyburide at 50 μM led to reduced interaction by almost 50% of OAB both with osteoblasts and macrophages. Furthermore, reduction in the uptake of OAB by osteoblasts was accompanied by reduced osteoblast apoptosis by more than 70% following treatment of either OAB or osteoblasts with glyburide, indicating that glyburide treatment affected both the recognition of the apoptotic bodies and the phagocytic mechanisms employed by osteoblasts. Although I have not directly blocked PS binding, these findings indicated that changes in phospholipids inducing exposure of PS on the outer leaflet membrane of both the phagocyte and the prey is possibly one of the mechanisms by which OAB are recognised by phagocytes. In addition, these data pointed to a requirement for physical association between the phagocyte and the prey in order for osteoblasts to become apoptotic or it could be due to the loss of delivery of a signal to the inside of the cell.

Phagocyte cultures were also treated with the FoF"-ATPase inhibitor Oligomycin, which has also been shown to inhibit Ca^{2+}-influx by interacting directly with store-operated channels independently of its effects on ATP production (Cho et al. 1997). Oligomycin has been shown to impair Ca^{2+}-induced transmembrane movement of

phospholipids at 6 μM (Marguet et al. 1999), and to block recognition of apoptotic THP-1 cells by phagocytes, by inhibiting externalization of phosphatidylserine at concentrations of 0.1-6 μM without however affecting other apoptotic features such as caspase-3 activation or DNA fragmentation in the apoptotic cells (Zhuang et al. 1998). In these studies Oligomycin was used in accordance to Marguet et al. and Zhuang et al. in order to prevent the Ca^{2+} -dependent phospholipid exposure on the outer leaflet of the plasma membrane of both the phagocytes and osteocyte apoptotic bodies. Data obtained following treatment of osteoblast cultures with Oligomycin at 6 μM, indicated a significant reduction of almost 70% in osteoblast apoptosis induced by OAB, while Oligomycin treatment of OAB also effectively reduced osteoblast apoptosis by 70%. In addition, both in macrophage and osteoblast cultures, phagocytosis was decreased by almost 3.7- and 2.1-fold respectively, suggesting possibly that Oligomycin affected recognition of OAB by the phagocytes. These data indicated that membrane phospholipid asymmetry or Ca^{2+} fluxes might be important in the recognition between OAB and phagocytes and that the subsequent induction of osteoblast apoptosis depends upon binding and /or engulfment of OAB. Alternatively, it might be possible that Oligomycin prevented apoptosis by acting through inhibition of ATP levels as shown at 1.3 μM in rat thymocytes against Dexamethasone induced apoptosis (Stefanelli et al 1997) or release of cytochrome c at 1.2×10^{-2} M as shown in gastric epithelial cells induced in response to nitric oxide-induced apoptosis (Dairaku et al. 2004).

Impairment of phagocytosis has also been demonstrated by reducing the availability of Ca^{2+} by EDTA treatment by several studies in the past. For example, binding and uptake of myelin derived from the central nervous system by macrophages (van der Laan et al. 1996), phagocytosis of malaria pigment particles by monocytes and neutrophils (Pichyangkul et al. 1997) and engulfment of apoptotic bodies by dendritic cells (Rubartelli et al. 1997) were all inhibited following treatment with EDTA. In addition, phagocytosis of yeast particles by Dictyostelium discoideum cells was also reduced following treatment with EDTA at concentrations between 0.01-10 mM, which was however fully restored following addition of Ca^{2+} (Yuan et al. 2001), indicating the dependence of phagocytosis on the availability of Ca^{2+}. In

the present study, engulfment of OAB by macrophages and osteoblasts was reduced by 1.5 and 4.5-fold respectively, following treatment with EDTA at 5 mM, indicating that phagocytosis of OAB might depend on the availability of Ca^{2+}, also possibly suggested by the phagocytic studies using Oligomycin mentioned above. In addition, impairment of phagocytosis was accompanied by a significant reduction in osteoblast apoptosis by more than 60%, pointing again to a requirement for physical association between OAB and osteoblasts in order for the latter to become apoptotic.

Carbohydrate and glycoprotein moieties have also been implicated in the recognition of the apoptotic cells by phagocytes as it has been shown that apoptotic cells loose sialic acid moieties leading to exposure of mannose, fucose and N-acetylglucosamine which allows their recognition by the mannose-binding lectin receptor on phagocytes (for review see Savill 1997 and Saevarsdottir et al 2004). Duvall et al. indicated that the binding of apoptotic mouse thymocytes involved the recognition of N-acetylglucosamine, N-acetylgalactosamine and galactose residues by a macrophage lectin receptor, as shown by inhibition studies using the monosaccharides at concentrations of 10 or 20 mM. Later studies also showed that cells undergoing apoptosis appeared to express modified glycoprotein residues which might have enabled their engulfment by endothelial cells expressing mannose and galactose specific receptors on their surface, as suggested by treatment of the phagocytes with Nacetylglucosamine, galacose and mannose at a concentration of 80 mM (Dini et al 1995). In addition, N-acetylglucosamine at 20 mM was shown to reduce phagocytosis of apoptotic lymphocytes by activated mouse peritoneal macrophages but not J774 macrophages (Pradhan et al. 1997). Based on these studies indicating the involvement of sugar moieties in the recognition of apoptotic bodies by phagocytes, N-acetylglucosamine was used to determine whether osteocytes underwent modifications on the glycoprotein residues on their surface following induction of apoptosis and to clarify the importance of these residues in their recognition by the phagocytic osteoblasts and macrophages. Incubation of phagocytes with N-acetylglucosamine reduced uptake of OAB both by macrophages and osteoblasts by 2.4- and 3-fold respectively, indicating that recognition involved asialoglycoprotein-like lectins on osteoblast and macrophage cell membranes. These

molecules are likely to interact with exposed monosaccharide residues such as N-acetylglucosamine on OAB, although further studies are required to determine the presence of such a galactose specific receptor on osteoblast cell membranes and the possible interaction of this receptor with monosaccharride residues on apoptotic osteocytes. In addition, treatment with N-acetylglucosamine reduced induction of osteoblast apoptosis by almost 70%, further indicating that apoptosis of osteoblasts in response to OAB was dependent on interaction and possibly uptake of OAB by osteoblasts or the implication of carbohydrate residues in the death response.

Treatment of OAB with the proteolytic enzyme trypsin also reduced the percentage of macrophages and osteoblasts physically interacting with OAB by 2.5- and 1.5-fold respectively. Furthermore, treatment with trypsin led to almost 70% reduction in the proportion of osteoblasts that appeared apoptotic following incubation with OAB, indicating that protein residues are implicated in recognition and binding mechanisms of OAB with phagocytes, which are required for induction of osteoblast apoptosis. Studies by others have shown that alteration of surface glycoporteins by treatment with trypsin, affected recognition and uptake of microsporidians by splenic macrophages (Leiro et al. 1997) and binding of porphyromonas gingivalis to epithelial cells (Agnani et al. 2003). These findings have also further supported the involvement of glycoprotein residues in the recognition and uptake of osteocyte apoptotic bodies both by professional phagocytes such as macrophages and by osteoblasts, although the phagocytic receptors that mediate binding to these has not been identified in these studies.

Having investigated the effect of physical binding/recognition between osteocyte apoptotic bodies and the phagocytes, by using compounds that possibly affect the availability of Ca^{2+}, externalisation of PS and modification of cell surface glycoproteins, I then examined the effect of Nocodazole in the phagocytic response, since phagocytosis requires the rearrangement of the actin cytoskeleton in the phagocytes in order for engulfment to occur (for review see May and Mackesky 2001). Nocodazole is a widely used anti-neoplastic agent that disrupts microtubules by binding to b-tubulin (Chen et al. 2002), inhibits formation of microtubules and

subsequent binding to centromere (Burakov et al. 2003) and has been reported to arrest the cell cycle to G2/M phase (Blajeski et al. 2002). Nocodazole has also been used in a number of studies to affect phagocytosis due to its effects on microtubules (Cannon and Swanson 1992). For example, Nocodazole inhibited the engulfment of hepatocyte apoptotic bodies by primary and immortalised stellate cells and prevented expression of the profibrogenic cytokine TGF-β and collagen-α1 mRNA (Canbay et al. 2003a). Phagocytosis of L.monocytogenes by P388D1 macrophages was inhibited by treatment with Nocodazole (Kuhn 1998) which also reduced internalization of the pathogen Candida Albicans and mannose-rich particles by macrophages at 10 μM (Kaposzta et al. 1999) and the uptake of the pathogen Yersinia pseudotuberculosis by affecting the organization of microtubules in HeLa cells at doses up to 10 μM (McGee et al. 2002). Incubation of osteoblast and macrophage cultures in the present study with 7 μM Nocodazole reduced engulfment of OAB by the phagocytes by 6- and 4-fold respectively, compared to control cultures. In addition, Nocodazole treatment also managed to effectively decrease the proportion of osteoblasts that appeared apoptotic by almost 80% following incubation with OAB. Although I have not directly investigated the effect of Nocodazole on the arrangement of microtubules by using epifluorescence and antibodies against tubulin or the phagocyte cell cycle progression and the influence that it might have on the engulfment of OAB, these studies suggested that Nocodazole inhibits uptake of OAB by osteoblasts and macrophages, and that internalisation of OAB is possibly required for the induction of osteoblast apoptosis.

Having shown both a close physical association of OAB with apoptotic osteoblasts and the involvement of peptide-containing molecules in the response, I went on to study the possible role of phagocytic recognition receptors using knockout animal models. Several receptors have been identified so far on the phagocytes that enable binding and engulfment of apoptotic cells, including the phosphatidylserine receptor (Fadok et al. 2000), the scavenger receptors A (Platt et al. 1996) and CD36 (Savill et al. 1992), ABCA-1 (Luciani and Chimini 1996) and CD14 (Devitt et al. 1998), as reviewed in more detail in §2.7. Here I have used animal models that are deficient in scavenger receptor A (SRA) (Suzuki et al. 1997) in order to study the possible

involvement of this receptor in the uptake of OAB by osteoblasts, since osteoblasts have been shown to express a variety of scavenger receptors (Roman-Roman et al. 2003). The scavenger receptor A is a membrane glycoprotein that has a high affinity for interacting with acetylated LDL and has been suggested to contribute in the pathologic accumulation of cholesterol during vascular diseases (Goldstein et al. 1979). More recently, SRA was shown to mediate the uptake of apoptotic thymocytes by macrophages by using a monoclonal antibody against SRA which managed to reduce phagocytosis by 50% compared to control (Platt et al. 1996). Suzuki et al. developed in 1997 mice that were deficient in SRA and were shown to develop smaller atherosclerotic lesions. In addition, macrophages isolated from these animal models displayed a 50% reduced ability to phagocytose apoptotic thymocytes, while the remaining phagocytic capacity was attributed to the possible involvement of other scavenger receptors as shown by treatment with ligands, which could interact with more than one class of SR (Terpsra et al. 1997).

Using SRA knockout models for the purpose of this study, I observed a reduction by almost 50% in the uptake of OAB by osteoblasts, compared to cells derived from wild-type models, indicating a significant role for SRA in the uptake of OAB, but also the involvement of other phagocytic mechanisms compensating for the residual phagocytosis. Alhtough the absence of SRA reduced the proportion of osteoblasts physically interacting with OAB, there was no reduction in the percentage of apoptotic osteoblasts in the presence of OAB in cells from scavenger receptor-null mice, pointing to the possible requirement for a threshold amount of reduction in phagocytosis in order to reduce osteoblast apoptosis. In addition, there appeared to be no difference between the wild-type and knockout cultures in the average number of OAB interacting with osteoblasts and the likelihood of these cells to be apoptotic, which as discussed in chapter 3 indicated that it was more likely for osteoblasts to be apoptotic having interacted with more than four apoptotic bodies. These findings suggested that induction of osteoblast apoptosis also dependent on the amount of apoptotic bodies interacting with osteoblasts and pointed to the possible existence of another mechanism that is associated with recognition of OAB and induction of the specific response in the osteoblast.

During phagocytosis, multiple mechanisms may co-operate in order for engulfment to occur (Savill 2002), indicating that inhibition of a single phagocytic receptor will not achieve complete inhibition of phagocytosis. It has been suggested that professional phagocytes usually enable different receptors to become implicated at different phases of the apoptotic program by employing a variety of first-line molecules involved in the initial tethering followed by tight binding receptors to ensure rapid clearance of apoptotic cells (Gregory 2000). In order to determine the possible existence of such additional mechanisms that might be employed by osteoblasts in order to phagocytose OAB I used animal models that are deficient in CD14. CD14 is a glycosylphosphatidylinositol-linked plasma membrane glycoprotein that acts as a bacterial pattern recognition receptor (Pugin et al. 1994) and comprises part of the lipopolysaccharide (LPS) receptor complex along with Toll-like receptors (TLR) and MD2 (da Silva et al. 2001). Following interaction with LPS, CD14 needs to interact with TLR-4 in order to initiate inflammatory responses as part of the innate immune response, since CD14 lacks a cytoplasmic domain and cannot transmit a signal on its own (for review see Miyake 2003). In addition, CD14 has been shown to mediate uptake of apoptotic cells (Devitt et al. 1998, Fadok et al. 1998) and has been proposed to interact with apoptotic-cell associated molecular patterns (ACAMPs) displayed by apoptotic cells (Gregory 2000). Devitt et al. suggested that CD14 interacts with apoptotic cells through a region that is very similar to the LPS-binding site, and that CD14 co-operates with additional molecules in order to achieve the binding and phagocytosis of apoptotic cells (Devitt et al. 1998). Generation of CD14 knockout animal models (Haziot et al 1996) led to increased resistance to shock induced by LPS; however there is no evidence available to date regarding the efficient clearance of apoptotic cells from CD14 deficient animal models.

Initially I went on to examine the presence of CD14 mRNA on primary mouse osteoblasts, since there are contradictory reports concerning the ability of osteoblasts to express CD14 (Kondo et al. 2001, Reyes-Bottela et al. 2000). RT-PCR studies clearly indicated the existence of CD14 on primary mouse osteoblasts, while the demonstration of TLR4 mRNA on osteoblasts (Kikuchi et al. 2001) recently

suggested that these cells are capable of interacting with LPS and initiate a cellular response. Knock out studies for CD14 showed that uptake of OAB by osteoblasts was reduced by almost 50% compared to osteoblasts derived from wild-type mice, indicating that the residual phagocytosis might be attributed to other phagocytic mechanisms, as yet unidentified. More interestingly however, was that reduction in phagocytosis in CD14 null osteoblasts was associated with more than 60% reduction in apoptosis of osteoblasts in response to OAB. The absence of CD14 also prevented the pro-apoptotic signals induced by OAB in ex vivo experimental conditions, using calvaria obtained from CD14 null mice, compared to osteoblast apoptosis estimated from wild-type calvarial sections. Findings by others have shown that CD14 might suppress LPS-induced monocyte apoptosis (Heidenreich et al. 1997) or negatively regulate cell survival by mediating LPS-induced endothelial cell apoptosis (Frey et al 1998), demonstrating that CD14 could act both as a phagocytic receptor enabling interaction with apoptotic cells and as surface molecule regulating survival, although no association has been established so far between the presence of apoptotic cells and CD14-mediated induction of apoptosis.

Here, absence of CD14 reduced the proportion of osteoblasts, within the total population of cells in culture, interacting with more than 4 OAB as well as the proportion of apoptotic osteoblasts interacting with more than 4 OAB, reducing therefore the likelihood of osteoblasts being apoptotic in response to increased uptake of OAB. These findings indicated that the CD14 glycoprotein might be implicated in the osteoblast death response, supporting the reduction both in osteoblast apoptosis and phagocytosis obtained by proteolytic treatment, which pointed to the involvement of peptide-containing molecules in the ensuing response. Furthermore, these data suggested that CD14 might be somehow, specifically associated with induction of osteoblast death, since SRA which is also a glycoprotein did not appear to contribute to the death process as discussed above. Findings in this chapter do not mean however that the presence of CD14 alone on phagocytes is sufficient for the induction of apoptosis in the phagocyte in the presence of OAB, since as described in chapter 3, other phagocytes, such as macrophages that are expressing CD14 (Lee et al. 1988), did not undergo apoptosis having ingested OAB.

These data suggest that the presence of CD14 and some other factor specifically associated with the osteoblastic lineage are both required for the induction of osteoblast apoptosis.

Seeking to identify potential molecules that might be implicated in the induction of osteoblast apoptosis in response to OAB, I studied the effects of nitric oxide (NO) that is physiologically produced by all three bone cell types and participates in the regulation of bone turnover (for review see van't Hof and Ralston 2001). Production of NO at low concentrations by osteoblasts has been shown to positively regulate osteoblast proliferation and differentiation (Hikiji et al. 1997, Buttery et al. 1999). Others have shown that high concentrations of NO might be associated with the induction of osteoblast apoptosis (Chen et al. 2002) in response to pro-inflammatory cytokines (Damoulis and Hauschka 1997) and might be associated with increased production of Bax protein (Chen et al. 2002). Several studies have also shown that NO is produced in response to mechanical stress both by osteoblasts and osteocytes (Klein-Nulend et al 1995, Zaman et al. 1999), while NO production by osteocytes has also been suggested to regulate osteoclastic activity by directing depth and orientation of the resorption process (Burger et al. 2003), indicating that NO is an important regulator of bone remodelling.

In this study, both osteoblast cultures and osteocytes, prior to production of OAB, were incubated with the nitric oxide synthase inhibitor L-NAME. Inhibition of NO production by osteocytes had no effect in the engulfment of OAB by osteoblasts or in the induction of osteoblast apoptosis in response to OAB. However, inhibition of NO production by osteoblasts reduced both the phagocytosis of OAB by 1.6-fold and the apoptotic death of osteoblasts by almost 70%. In addition, Griess assay showed a 3.5-fold increased production of nitrate and nitrite in osteoblast cultures in the presence of OAB, which was decreased to control levels following pre-treatment of osteoblasts with L-NAME. These findings suggested that the presence of OAB induced production of NO by osteoblasts, which was associated with increased induction of osteoblast apoptosis, however, without necessarily indicating a direct role for NO in the apoptotic response. Reduced phagocytosis of OAB both by osteoblasts and macrophages following treatment with L-NAME could possibly be

attributed to altered recognition mechanisms on the phagocyte, since it has been shown that anti-oxidant enzymes reduce phagocytosis by blocking oxidative stress and PS oxidation (Kagan et al. 2003), although I have not further investigated this phenomenon.

Further experiments involved the blockade of osteoblast apoptosis in response to OAB by using an inhibitor of caspase 8 in order to identify the dependency of the apoptotic response on death receptor pathways, since caspase 8 is mainly recruited by death receptors (Muzio et al. 1996, Medema et al. 1997) (for review see Thornberry et al. 1998). Inhibition of caspase 8 in osteoblast cultures efficiently managed to reduce the apoptotic response, indicating that osteoblast apoptosis induced by OAB is mediated both by upstream caspases such as caspase 8 and downstream effector caspases such as caspases 3 and 7, as shown in chapter 3. Activation of caspase 8 in osteoblasts in response to OAB could lead to activation of caspases 3 and 7 through two distinct pathways involving direct activation (Hirata et al. 1998), or it could activate the Bcl-2 family member Bid which then translocates into the mitochondria, inducing cytochrome c release and eventually leads to caspase 3 activation (Li et al. 1998), although the involvement of the mitochondria in the apoptotic response has not been investigated in this study.

Furthermore, the presence of OAB in osteoblast cultures increased the percentage of cells that were positive for the Fas death receptor on their membranes, which were in most cases associated with OAB. In fact, expression of Fas on the surface of osteoblasts was found to be associated with induction of apoptosis as demonstrated by dual labelling of osteoblasts in order to reveal both the Fas positive cells and the cells undergoing apoptosis in response to OAB, indicating possibly that Fas could be mediating the apoptotic response in osteoblasts (Kawakami et al. 1997, Ozeki et al. 2002) leading to activation of caspases 8, -3 and -7 although no direct association has been shown in this study between Fas recruitment and activation of caspase 8. Further work is required however to identify the signals that could be mediating activation of the Fas death receptor, since MLO-Y4 osteocytes have been shown not to express Fas Ligand (Kogianni et al. 2004, Ahuja et al. 2003) and to determine

whether Fas activation is indeed responsible for induction of osteoblast apoptosis. Similar increase in Fas expression on the cell surface was observed in macrophage cultures indicating that the presence of OAB is inducing Fas receptor aggregation that results possibly in the cytotoxicity mediated by macrophages (Nissen-Meyer et al. 1988), and might support the observation that macrophages appeared morphologically activated, as discussed in chapter 3, indicating that OAB induce a pro-inflammatory response that could possibly be targeting the activity of macrophages at particular sites on bones.

In conclusion, osteoblast apoptosis was shown to depend upon interaction with or internalisation of OAB, and was reduced by interfering with the production or presentation of molecules associated with changes that occurred in the apoptotic osteocytes and/or the phagocytes, such as phospholipid, carbohydrate and cytoskeletal changes. However, binding and phagocytosis alone did not produce an apoptotic response since other cell types that had phagocytosed OAB did not die. Recognition and tight binding of OAB to osteoblasts was also shown to depend on phagocyte receptors such as SRA and CD14. The finding that CD14 was also shown to be associated with induction of osteoblast apoptosis could possibly provide very useful information in identifying the nature of the specific signals delivered by apoptotic osteocytes that only induce apoptosis in osteoblasts and not in other phagocytes investigated in this study. Identification of this specific signal implicated in the induction of osteoblast apoptosis could be of extreme importance in the bone microenvironment, since it might be modulating the removal of osteoblasts from a particular site in order to signal the initiation of bone resorption by osteoclasts, regulating therefore the bone turnover process. In addition, it was shown that apoptosis of osteoblasts was associated with the Fas death receptor pathway, involving possibly the caspases 8 and 3 or 7 in the execution of apoptosis, while both osteoblast apoptosis and phagocytosis of OAB were impaired by inhibition of NO production in osteoblasts. Furthermore, it might be interesting to identify possible links between activation of NO and Fas (Fukuo et al. 1996) or CD14 in the osteoblast death response, in order to determine whether these molecules form part of a common signaling pathway or different pathways all leading to the induction of

osteoblast apoptosis in response to OAB. In addition, since deficiency in CD14 prevented osteoblast apoptotic death both *in vitro* and *ex vivo* systems, it would be very important to identify potential implication of CD14 in the development of pathologic bone diseases, characterised by excess osteoblast and/or osteocyte apoptosis, such as in postmenopausal or glucocorticoid induced osteoporosis.

SECTION 3

Blockade of osteocyte apoptosis

Introduction to Section 3

As discussed in section 2, osteocytes are thought to regulate bone remodelling, while osteocyte apoptosis might target resorption to particular areas, indicating that the incidence of osteocyte apoptosis is in line with the description of apoptosis as an essential homeostatic mechanism for the healthy maintenance of tissues and that deregulation of apoptosis could give rise to several pathological conditions. Increased osteocyte apoptosis in relation to age has been described in the femoral head and might account for hip fractures in the elderly (Dunstan et al. 1993), while increased osteocyte death also appears following treatment with agents such as glucocorticoids (Weinstein et al. 1998). Glucocorticoid therapy induces an imbalance in bone formation and resorption processes, leading initially to osteopetrosis, osteocyte death and osteonecrosis, followed by rapid bone loss and osteoporosis (Glade and Krook 1982). These observations indicate that it is likely to be beneficial to develop therapeutic approaches that might prevent excess osteocyte apoptosis, which might lead to pathologic bone conditions. This section investigates potential molecules implicated in pathways that might lead to osteocyte death, such as Dexamethasone or survival such as inhibitors of intracellular signalling pathways and Bisphosphonates, in order to maintain a balance between osteocyte viability and death, which ultimately leads to better bone quality.

CHAPTER 5

Fas/CD95 is associated with glucocorticoid-induced osteocyte apoptosis.

5.1 Abstract

This work is the subject of a published manuscript (**Appendix**). Prolonged use of glucocorticoids is associated with decreased bone formation, increased resorption and osteonecrosis, through direct and indirect effects on the activity and viability of bone effector cells, osteoblasts and osteoclasts, and osteocytes. This study has investigated molecular pathways implicated in Dexamethasone-induced apoptosis of osteocytes, using a cell line and primary chicken cells. MLO-Y4 osteocytes were pre-treated with several bisphosphonates representing a range of anti-resorptive activities and conformation/structure relationships, and were subsequently challenged with Dexamethasone. Apoptotic cells were detected at various times after treatment using morphological and biochemical criteria. Dex was shown to induce apoptosis associated with the Fas/CD95 death receptor in a caspase 8 dependent manner. The apoptotic response was inhibited by all variants of the BP molecules, indicating that Dex-induced apoptosis is independent of anti-osteoclastic activity. Dex-induced apoptosis was associated with a transient increase in phosphorylated ERK 1/2 and was blocked by the ERK inhibitor UO126. In addition, both UO126 and BPs decreased localization of Fas to the cell membrane. ERK activation by PMA did not induce death or Fas upregulation, suggesting that Fas may be important for the induction of apoptosis and the existence of an additional factor activated by Dex which enables the cooperation between the Dex-activated ERK and Fas pathways, during apoptosis of osteocytes. Furthermore, upregulation of death and Fas was not accompanied by upregulation of FasL, pointing to the possible existence of FasL-independent Fas-associated death in these cells.

5.2 Introduction

Glucocorticoids (GCs) have been extensively used as anti-inflammatory agents due to their ability to modulate immune responses (Ashwell et al. 2000), by repression of many inflammatory cytokines and chemokines that perpetuate inflammation (Tao et al. 2001). Glucocorticoids offer an effective treatment available for the control of allergic diseases such as asthma and allergic rhinitis, as well as rheumatoid arthritis, hepatitis, organ transplant and premature birth (Bijlsma 1997, Epstein 1997, Compston 1997, Dekhuijzen and Bootsma 1997). GCs exert their effects commonly through activation of the Fas pathway, one of the best-characterised apoptotic pathways (Schmidt et al. 2001). Binding of FasL to FasR causes receptor oligomerisation and recruitment of an adapter protein, FADD, which interacts with caspase-8, initiating a caspase cascade leading to apoptosis (**Figure 5**). (Ashkenazi et al. 1998).

As a side effect to their clinical applications, GCs are responsible for rapid and profound bone loss and osteonecrosis, which increase with dose and duration of treatment (Epstein 1997). GCs have been shown to exert anti-mitotic effects on osteoblast precursor cells, induce apoptosis of mature osteoblasts and increase the resorptive activity of osteoclasts (Hamdy 1997). Studies by Weinstein et al. identified the presence of a high proportion of apoptotic osteocytes in mice, compared to healthy controls, following chronic administration of prednisolone (Weinstein et al. 1998). It would be of benefit clinically to develop a concurrent prescription capable of reducing the unwanted side effects associated with GC-treatment.

BPs are non-hydrolysable analogs of pyrophosphate in which the oxygen linking the phosphates has been replaced by a carbon atom, with two side chains R1 and R2 (Rodan 1998). BPs inhibit the precipitation of calcium phosphate and were initially used in industry as anticorrosive and antiscaling agents (Menschutkin 1865). In later studies, they were found to strongly bind to hydroxyapatite crystals and to affect bone mineralization (for review see Fleisch 2000). In addition, BPs have been shown to act as potent competitive inhibitors of the soluble mammalian, yeast and bacterial

and the membrane-bound plant inorganic pyrophosphatases (Smirnova et al 1988, Zhen et al 1994). The beneficial effects of Bisphosphonates (BPs) on bone have long been demonstrated against Paget's disease, post-menopausal osteoporosis and GC-induced osteoporosis, by decreasing the resorptive activity of osteoclasts (Rodan 1998). BPs are classed as nitrogen-containing (such as PAM and ALN) and non N-BPs (such as CLO). In osteoclasts, N-BPs inhibit farnesyl diphosphate (FPP) synthase and prevent prenylation of small GTPases, such as Ras and Rho that are required for osteoclast polarization, resorption and cell survival, whereas non N-BPs are metabolized into cytotoxic analogues of ATP, that probably act as inhibitors of various ATP-dependent enzymes (Rodan 1998, Rogers et al. 1999). Changes in structure and conformation have allowed the development of various N-BPs, which differ in their anti-resorptive activity since they differ in their ability to inhibit FPP synthase (Dunford et al. 2001).

In contrast to osteoclasts, the effect of BPs on osteocytes, which are considered the mechanosensors and transducers in bone, has not been well characterised. BPs have variously been shown to both decrease and increase ERK (Nishida et al. 2003, Plotkin et al. 1999). Studies by Plotkin et al. have implicated the ERK 1/2 pathway in the ability of BPs to prevent pro-apoptotic effects of Dex on MLO-Y4 osteocyte-like cells (Plotkin et al. 1999).

This study attempts to identify pro-apoptotic pathways employed by Dex as well as compounds that could potentially protect osteocytes from glucocorticoid-induced apoptosis. BPs and the MEK inhibitor UO126 were shown to protect against Dex–induced apoptosis, while upregulation of the Fas receptor appeared to be important in the induction of apoptosis.

5.3 Materials and Methods

All chemicals were purchased from Sigma, UK, all tissue culture reagents were purchased from Invitrogen, UK and tissue culture well plates and petri dishes were purchased from Corning, UK unless otherwise stated. Tissue culture procedures were performed in a laminar flow hood (class 2) receiving HEPA-filtered air, using sterile equipment.

5.3.1 Cell culture

5.3.1.1 Culture of MLO-Y4 osteocytes

The murine osteocyte-like MLO-Y4 cell line was cultured as described in §3.3.1. Briefly, cells were maintained in α-Modified Essential Medium (αMEM) supplemented with 5% fetal bovine serum (FBS), 5% newborn calf serum (NCS), 1% Penicillin/Streptomycin (P/S) and 1% L-glutamine. Subculturing was performed twice weekly upon reaching 90% of confluency, maintaining the cells in the log phase of proliferation.

5.3.1.2 Isolation and culture of primary chicken osteocytes

Primary osteocytes were isolated by P. Nijweide as previously described (Nijweide and Mulder, 1986) and were subjected to immunomagnetic isolation by use of the chicken osteocyte-specific monoclonal antibody (MAb) OB7.3 bound to magnetic beads (DYNAL, Norway), which reacts specifically with osteocytes.

5.3.2 Cell treatment

Cells were plated in growth medium at a density of $1x10^4$ cells/ml in 24 multi-well plates or $1x10^5$ cells/ml in 60 mm petri dishes for 24 hours, prior to experimentation. Following appropriate treatment, cells were returned to the incubator at 37 °C for the time points indicated in the figure legends. Experiments were carried out a minimum of 3 times, and each treatment group was represented by 3 wells in each independent experiment. Cells were observed in 3 fields per well resulting in 9 fields per treatment group. Identical magnifications were used for all apoptosis estimates allowing similar numbers of cells to be counted per field in all experiments. Control treatments represent vehicle treatments for the different agents, which were subjected

to identical dilutions to the agents. Vehicle treatments were carried out on a routinely basis and were identical in terms of cell number and percentages of apoptotic osteocytes with untreated control cultures.

5.3.3 Induction of Cell Death

Cells were incubated in growth medium supplemented with 10^{-7} to 10^{-5} M Dex (Calbiochem, UK) and 0.4 μM to 0.4 mM H_2O_2 for 1-24 hours.

5.3.4 Prevention of Cell Death

5.3.4.1 Bisphosphonates

Cells were pre-treated for 1 hour with pamidronate (PAM), alendronate (ALN), clodronate (CLO) (kind gift from Prof. M. Rogers) diluted in phosphate buffer saline (PBS) at concentrations of 10^{-8} to 10^{-6} M, followed by Dex treatment or H_2O_2.

5.3.4.2 Inhibitors of intracellular signalling proteins.

Caspase inhibitors

Osteocytes were incubated with caspase 3/7-selective inhibitors (GlaxoSmithKline, USA) and caspase 8 substrate II inhibitor Z-IETD-FMK (Calbiochem, UK), described in §3.3.11 and 4.3.15, respectively at 10^{-6} M in DMSO for 1 hour, prior to Dex treatment to evaluate the role of the Fas pathway in Dex-induced apoptosis.

MAPK inhibitors

Cells were incubated for 30 minutes with the MEK 1/2 inhibitor, UO126 (Calbiochem, UK), at concentrations of 10 to 30 μM in DMSO (Favata et al. 1998), the p38 inhibitor SB203580 (Calbiochem, UK) at concentrations of 5 to 15 μM in DMSO (Cuenda et al. 1995) and PMA (phorbol 12-myristate 13-acetate) at 2 ng/ml-200 μg/ml for 1 to 5 hours. All pre-treatment agents were maintained in cultures in the presence of Dex or H_2O_2.

5.3.5 Determination of Apoptotic State

A range of techniques were used to assess the apoptotic state, for all the independent experimental culture setups, as described in §3.3.10. Cells were observed in 3 fields per well resulting in 9 fields per treatment group.

5.3.5.1 DAPI staining for healthy and apoptotic cell morphology

Cells were incubated with DAPI (4',6-Diamidino-2-phenylindole) at 2.5 ng/ml in water for 10 minutes and examined by fluorescence microscopy as described in §3.3.10.3.

5.3.5.2 Acridine orange (AO) staining for healthy and apoptotic cell morphology.

Acridine orange (3,6-bis(dimethylamino)acridinium chloride) is a cell permeable dye that stains DNA and RNA having excitation approximately at 280 nm and emission at 530 nm. When it intercalates into double-stranded DNA, it fluoresces green, while binding to the phosphate groups of denatured single-stranded DNA or to RNA, produces orange fluorescence (Abrams et al. 1993). Following treatment, cells were immediately incubated in Walpole's acetate buffer pH 4.2 (10:7, 1 M NaAc: 1 M HCl) for 5 min. Cells were stained with AO for 25 minutes, washed twice and examined under fluorescence microscopy. Healthy cells were characterised by intact nucleus and normal cytoplasmic appearance, while apoptotic cells were characterised by nuclear or cytoplasmic condensation, DNA fragmentation or blebbing. Large multinuclear cells occasionally present in MLO-Y4 cultures were ignored.

5.3.5.3 DNA fragmentation using *in situ* Nick Translation

The percentage of target cells demonstrating DNA breaks was investigated using *in situ* nick translation staining (Noble et al. 1997), which allows the determination of DNA breaks following the incorporation of DIG-labelled dUTP as described in §3.3.10.2. The ratio of total cells (PI positive) to apoptotic (FITC positive) was determined using fluorescence microscopy and digital image capture.

5.3.5.4 Annexin-V-FITC Assay

Cells were incubated with Annexin-V-FITC to detect exposure of phosphatidyl serine on the outer leaflet of the membrane bilayer followed by propidium iodide (PI) as described in §3.3.10.1 in order to distinguish between viable (FITC negative, PI negative), early apoptotic (FITC positive, PI negative) and late apoptotic or necrotic cells (FITC negative, PI positive).

5.3.6 Determination of Fas expression by immunocytochemical staining.

The Fas/CD95 death receptor was detected on the surface of MLO-Y4 osteocytes as described in §4.3.16. Briefly, cells were incubated with anti-Fas monoclonal antibody (BD Transduction labs, UK) followed by secondary anti-mouse FITC antibody and were counterstained with PI. Cells were visualised by fluorescence microscopy and digital image capture. The ratio of total (PI positive) to Fas positive (FITC positive) was detected based on 3 fields from a total of 3 wells.

5.3.7 Reverse Transcription-polymerase chain reaction

Total RNA was isolated from cultures of MLO-Y4 cells using RNA-B™ (Biogenesis) according to the manufacturers instruction, as described in §4.3.17. Briefly, cDNA was synthesised from total RNA using oligo dT primers, and RNA was converted into cDNA by SuperScript II RNaseH$^-$ reverse transcriptase first strand synthesis system for RT-PCR (Invitrogen). The PCR reaction was performed using Qiagen Taq PCR core kit. Mouse Fas specific primers were designed against sequence accession number M83649, Fas Ligand primers against sequence accession number U10984 and mouse β-Actin specific primers against sequence accession number X03765 from HGMP database as shown below. The resulting PCR products for Fas and Actin were 220 bp and 290 bp respectively. The PCR reaction was carried out for 33 cycles with PTC-200 Peltier thermal cycler (MJ Research). PCR conditions were denaturation at 94 °C for 50 seconds, annealing at 50.5 °C for 1 minute and extension at 72 °C for 1 minute 30 seconds. The PCR products were analysed in 1.5% agarose gel containing ethidium bromide.

Fas forward 5'- CATGCTGTGGATCTGGGCTGT-3'
Fas reverse 5' -GTGTACCCCCATTCATTTTGC-3'
FasL forward 5'-ATGCAGCAGCCCGTGAATTAC-3'
FasL reverse 5'-CCATATCTGGCCAGTAGTGC-3'
Actin forward 5'- CAAGGTGTGATGGTGGGAATG-3'
Actin reverse 5'-GCTACGTACATGGCTGGGGTG-3'

5.3.8 Preparation of cell lysates

Following appropriate treatment, the medium was removed and the cells were washed twice in ice-cold PBS. Cells were left to lyse on ice (**Figure 41**) for 45 minutes by addition of 500 µl of lysis buffer (50 µM Tris-HCl, pH 7.4, 1% (v/v)

Novidet P-40, 6 mM sodium deoxycholate, 150 mM NaCl, 1 mM EGTA, 1 mM PMSF, 1 mM Na_3VO_4 and 1 mM NaF and a protease cocktail tablet (Roche, UK)). The cells were then scraped into chilled microcentrifuge tubes and the lysate cleared by centrifugation at 4 °C (13,000 g for 10 minutes). The cell pellets were thrown away and the supernatants were transferred to fresh tubes and either used immediately or stored at –20 °C.

5.3.9 Determination of protein concentration

Protein concentrations were estimated based on the method described by Bradford (Bradford 1976). Samples and standards were diluted in water to give a final volume of 200 µl. Protein standards were bovine serum albumin (BSA) within a range of 0-20 µg/ml. Bio-Rad protein acid reagent (50 µl) (Bio-Rad, UK) was added and samples were mixed thoroughly. Sample and standards were prepared in triplicate by addition of 200 µl into a well on a 96 multi-well plate. The protein concentration was then determined using an Athos 2001 automated plate reader (Athos Labtec Instruments) which measured the absorbance of the dye:protein complex at 570 nm and calculated the protein concentration relative to the BSA standards. The results were modified to compensate for dilutions incurred during the procedure.

5.3.10 Protein gel electrophoresis

Protein extracts were separated by electrophoresis through a polyacrylamide gel containing sodium dodecyl sulphate (SDS) (**Figure 41**). Proteins were denatured to form random coils and given a net negative charge by heating them in a reducing buffer containing SDS. Proteins were then separated on the basis of molecular weight with small proteins migrating more quickly than large proteins due to lower steric hindrance imposed by the gel crosslinks. SDS PAGE was performed on denaturing stacking/resolving gels with a gel thickness of 0.1 mm.

5.3.10.1 Electrophoresis reagents.

Tris resolving buffer: 1.5 M Tris base, pH 8.9 and 13.9 mM SDS.

Tris stacking buffer: 0.5 M Tris-HCl, pH 6.8 and 13.9 mM SDS.

Acrylamide/bisacrylamide (Protogel) solution: 30% (w/v) acrylamide and 0.8% (w/v) bisacrylamide.

Ammonium persulphate (APS) solution: 10% (w/v) APS in dH_2O.

Blue loading buffer (2x): 10% (v/v) glycerol, 10% (v/v) β-mercaptoethanol, 0.1 M SDS, 6% (w/v) urea, 0.125 M Tris and 0.02% bromophenol blue.

Tris running buffer: 190 mM glycine, 25 mM Tris base and 17 mM SDS.

5.3.10.2 Preparation of resolving gel.

Gel plates were washed sequentially with detergent, distilled water and methanol.

Composition of resolving gel (ml)

	Percentage polyacrylamide gel		
	8%	10%	12%
Tris resolving buffer	1.5	1.5	1.5
dH_2O	2.69	2.6	2.24
Protogel	1.44	1.8	2.16

Polymerisation of the gel mixture was initiated by addition of 90µl freshly prepared 10% ammonium persulphate and 6 µl of N,N,N',N'-tetramethylethylenediamine (TEMED). The gel mixture was pippeted into the gel cast, layered with water and allowed to polymerise for 30 minutes at room temperature.

5.3.10.3 Preparation of stacking gel

Composition of stacking gel (for 2 gels)

Tris stacking gel	1.25 ml
dH_2O	3 ml
Protogel	0.75 ml

Polymerisation was initiated by addition of 75 µl ammonium persulphate and 5 µl of TEMED. The stacking gel was poured onto the surface of the polymerised resolving gel. A spacer comb was inserted into the gel cast and the gel was allowed to polymerise for 30 minutes at room temperature. The gel cast was then placed into a gel tank containing running buffer in both upper and lower chambers to submerge the gel and the spacer comb was removed.

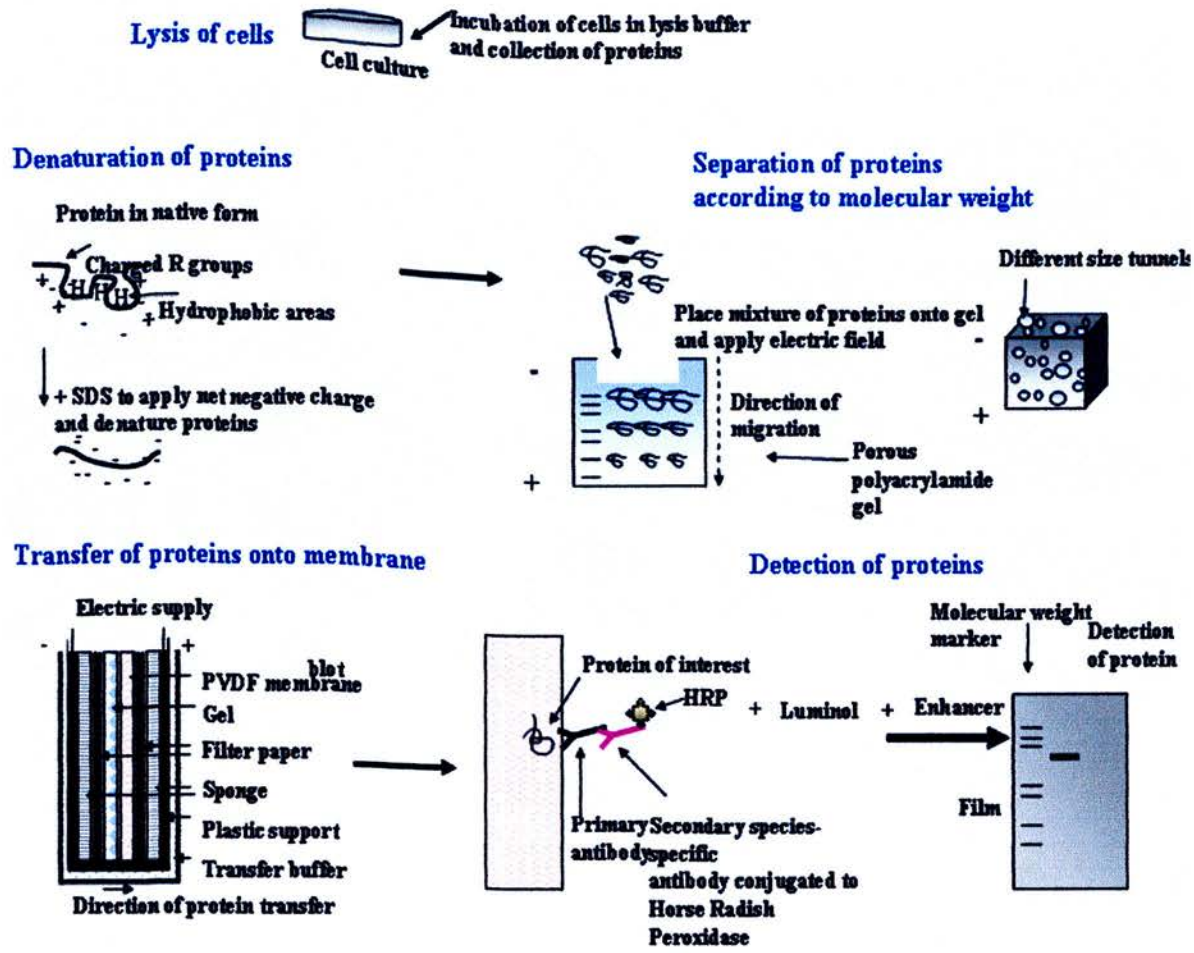

Figure 41. SDS PAGE electrophoresis and Western blot analysis. Cells in culture were incubated in lysis buffer and proteins were collected, which were denatured with SDS to acquire their primary structure and a net negative charge. Proteins were then separated on a polyacrylamide gel based on SDS, according to their molecular weight, and were transferred onto a membrane blot. Finally the blot was hybridised with primary and secondary antibodies and exposed on a film enabling the detection of the protein of interest.

5.3.10.4 Electrophoresis.

Protein samples and coloured molecular weight rainbow markers (Bio-Rad, UK) were mixed with an equal volume of reducing buffer and were denatured by boiling for 5 minutes prior to loading into the sample wells. The gel was then subjected to electrophoresis at a constant current of 20 mAmps (**Figure 41**) (Power Pac 3000, Bio-Rad, UK). Fractionation was terminated when the bromophenol blue in the reducing buffer reached the bottom of the gel.

5.3.11 Western Blot analysis.

5.3.11.1 Transfer of proteins to polyvinylidene difluoride (PVDF) membrane.

After electrophoresis, proteins were transferred from the gel onto a PVDF membrane (**Figure 41**). The membrane (cut to the dimensions of the gel) was soaked in methanol and then in transfer buffer (48 mM Tris-base, 38 mM glycine, 1.3 mM SDS and 20% (v/v) methanol, pH 9.0-9.4) for 15 minutes, along with the gel and layers of filter paper and fibre pads. A fibre pad was placed on the gel holder cassette, followed by filter paper, gel, PVDF membrane and by another filter paper and a fibre pad. The cassette was placed in the Mini trans-Blot Cell Assembly, which has the capacity to hold two cassettes between parallel electrodes only 4cm apart, along with a bio-ice cooling unit, which was kept frozen at –20 ^{o}C (Trans-blot SD, Bio-Rad, UK). Proteins were transferred onto the membrane at 30 V for 1 hour.

5.3.11.2 Detection of proteins on PVDF.

The membrane was incubated in Tris-buffered saline/Tween (25 mM Tris-base pH 8.0, 150 mM NaCl and 0.1% (v/v) Tween 20, (TBS-T) containing 3% (w/v) BSA) for 24hrs at room temperature to block non-specific binding sites. The proteins were then probed with the appropriate primary antibody (rabbit polyclonal antibodies against phosphorylated p44/42 MAPK, p90rsk, MEK 1/2 and c-Raf kinases, New England Biolabs, UK) in TBS-T containing 0.3% BSA overnight at 4 ^{o}C. The membrane was washed for 45 minutes in TBS-T and was incubated with a species-specific secondary antibody, at room temperature for 1 hour. The membrane was washed again in TBS-T for 45 minutes and the bound-antibody complexes were visualised using the Enhanced Chemiluminscence (ECL) (Amersham, UK) system,

according to the manufacturer's instructions. The membrane was exposed to autoradiograph film and developed (**Figure 41**).

5.3.11.3 Stripping and reprobing membranes

Once developed, the membrane could be stripped and reprobed for other proteins. The membrane was incubated in stripping buffer (100 mM β-mercaptoethanol, 69 mM SDS and 62.5 mM Tris-HCl, pH 6.7) at 56 °C for 30 minutes and washed extensively in TBS-T for 45 minutes at room temperature. The membrane was then blocked in TBS-T containing 3% BSA overnight and immunological detection of proteins performed as described in 5.3.11.2.

5.3.12 Immunoprecipitation

Protein extracts (1 mg) from cell lysates were diluted to 1mg/ml and added to microcentrifuge tubes containing 15 µl of protein A/G agarose conjugate bead slurry (50% conjugate/ 50% PBS) and 4 µl of Jo2 hamster monoclonal antibody against murine Fas (Pharmigen, USA). The reaction mixture was rotated overnight at 4 °C. The agarose beads were collected by centrifugation at 4 °C (13,000 g for 20 minutes), washed four times with 1ml of ice-cold lysis buffer and were then subjected to electrophoresis as described above.

5.3.13 Statistical analysis

Statistical analysis was performed using quantitative data analysis with SPSS release 11.5 for Windows, as described in §3.3.12, using Analysis of Variance (ANOVA), Tukey test and Dunnett test for comparison between the treatment groups. Results are expressed as means ± S.D. $p < 0.05$ was considered to be statistically significant.

5.4 Results

5.4.1 Dexamethasone induces MLO-Y4 cell apoptosis in a time- and dose-dependent manner.

MLO-Y4 osteocytes were cultured with Dex at 10^{-7} to 10^{-5} M for various times between 1 and 24 hours (**Figure 42A and 42B**). Apoptotic osteocytes appeared irregularly shaped and smaller in size, as shown by AO staining, while DAPI staining (**Figure 43**) revealed chromatin condensation, shrinkage of nuclei and the fragmentation of the nuclear material into smaller blebs. Estimation of apoptotic osteocytes revealed that maximal levels of death accompanied by cell loss, were reached at 5 hours of incubation with concentrations of 10^{-5} M and 10^{-6} M ($p = 0.0001$ and $p = 0.001$ compared to control respectively). At 24 hours numbers of osteocytes in culture recovered somewhat, while apoptotic levels decreased, suggesting that Dex-induced death of osteocytes is transient (**Figure 42A and 42B**). At concentrations of 10^{-7} M, Dex did not induce apoptosis in these cells. At 10^{-5} M a small proportion of cells were noted to have expanded and burst characteristics of necrosis. Based on the apoptotic criteria in response to the different concentrations and time points investigated, the dose of 10^{-6} M, which did not induce necrosis, was selected for future experiments, reaching a peak at 5 hours incubation.

5.4.2 Assessment of Dex-induced apoptosis by Annexin-V-FITC and Nick Translation assays.

AO and DAPI staining allowed the observation of plasma membrane blebbing, cytoplasmic condensation and nuclear blebbing, respectively, which are considered to occur during final stages of apoptosis, following the proteolytic cleavage of cytoplasmic and nuclear cytoskeletal factors (Thornberry et al. 1998). In order to characterise further the osteocytes following incubation with Dex at 10^{-6} M for 5 hours, externalisation of PS and fragmentation of DNA were examined, which occur at earlier apoptotic stages than nuclear and cytoplasmic blebbing, by Annexin-V-FITC binding **(Figure 44A)** (<1% necrotic cells identified by PI counter-staining), and by Nick Translation assay **(Figure 44B),** respectively. This indicated that osteocytes underwent apoptosis with plasma membrane changes and fragmentation of DNA in the presence of Dex.

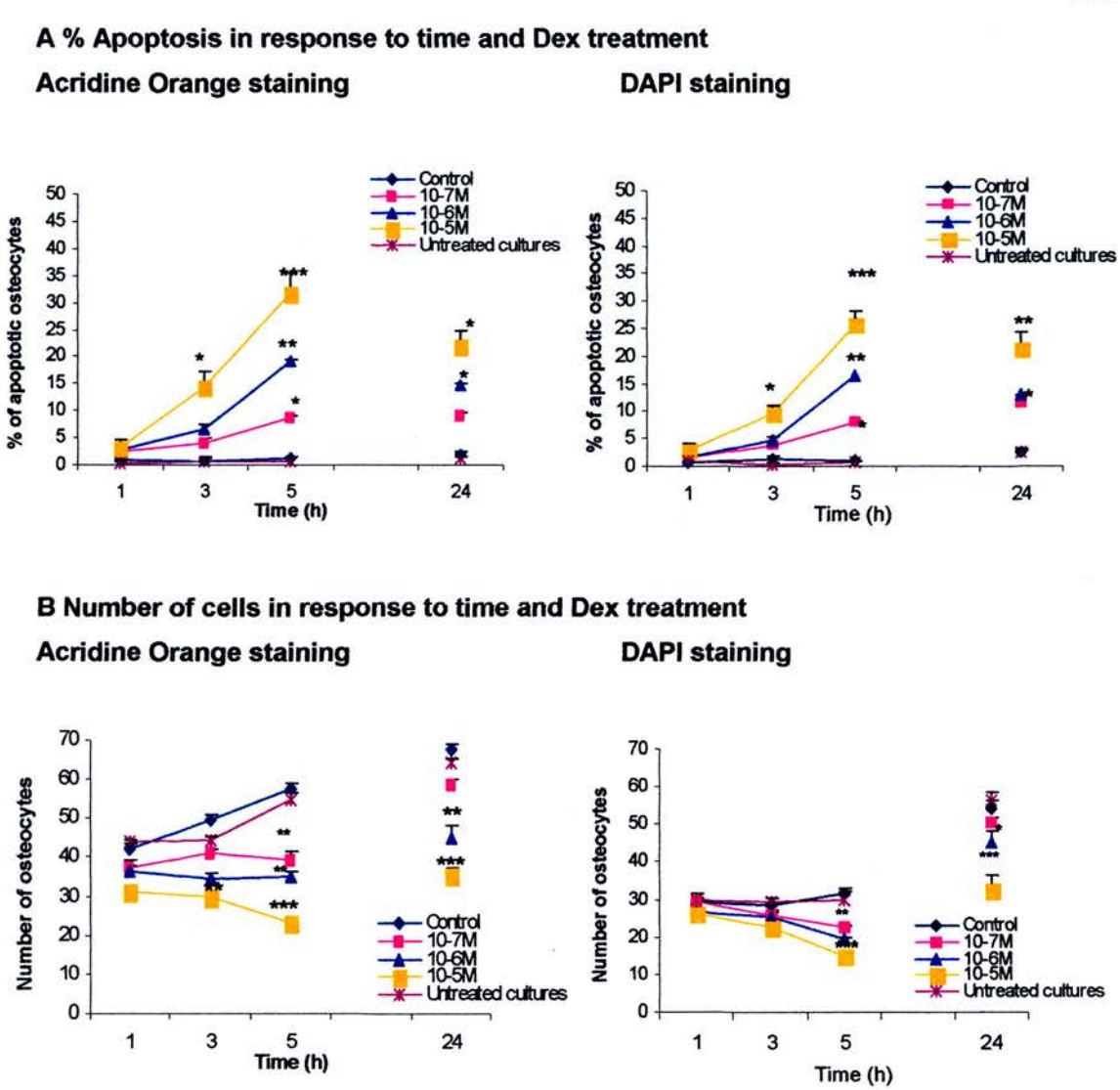

Figure 42. Dexamethasone induces apoptosis in MLO-Y4 osteocytes in a concentration-dependent manner. MLO-Y4 osteocytes were incubated in the presence of Dex at 10^{-7} to 10^{-5} M for 1-24 hours and apoptosis was determined by Acridine Orange and DAPI staining and fluorescence microscopy, by examining 3 fields per well and 3 wells per treatment group. **A**. Mean percentages of apoptotic osteocytes and **B**. Mean number of osteocytes in culture. Control cultures represent vehicle (ethanol) cultures and are similar to untreated cultures in percentages of apoptotic osteocytes and number of cells in cultures. Graphs represent means ± S.D.

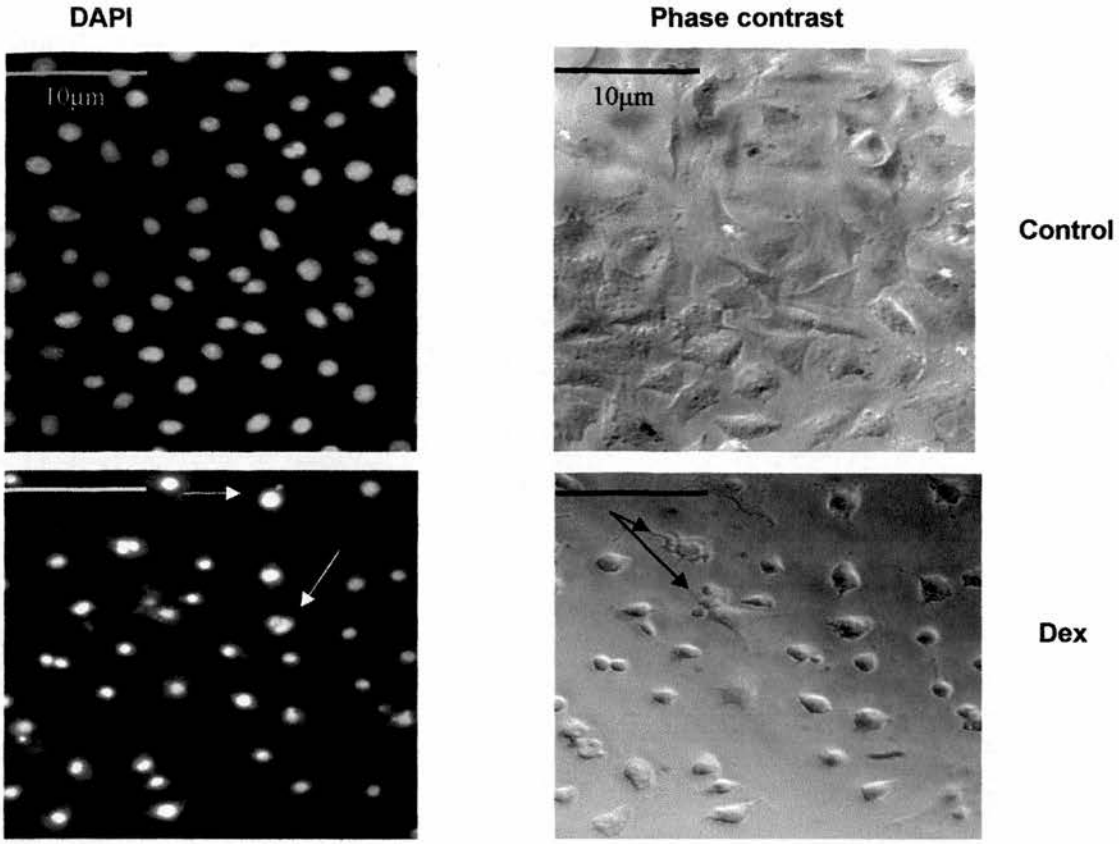

Figure 43. Dexamethasone induces cytoplasmic and nuclear condensation, DNA fragmentation and formation of osteocyte apoptotic bodies. Representative images of untreated (top panel) and Dex-treated MLO-Y4 osteocytes (bottom panel) at 10^{-6} M for 5 hours stained with DAPI. White arrows indicate nuclear condensation and fragmentation. Black arrows indicate cytoplacmic condensation and formation of apoptotic bodies. Bar = 10 μm, 20x magnification.

A

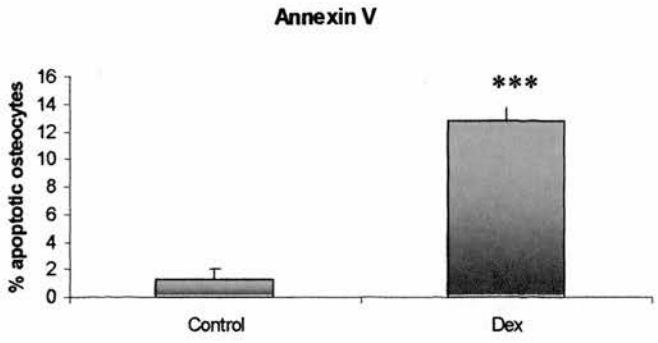

B

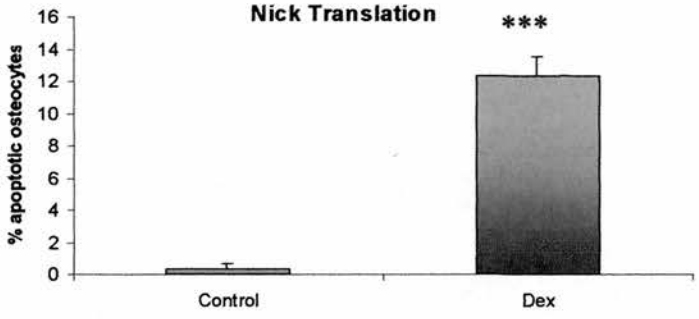

Figure 44. Dexamethasone induces apoptotic changes in MLO-Y4 osteocytes. MLO-Y4 osteocytes were incubated with Dex at 10^{-6} M for 5 hours. Mean percentages of apoptotic osteocytes were characterised by **A**. Annexin V FITC binding and **B**. DNA fragmentation. Results are expressed as means ± S.D.

5.4.3 Dexamethasone upregulates the Fas pathway

RT-PCR studies revealed that MLO-Y4 osteocytes express Fas receptor both in basal state and following treatment with Dex (**Figure 45A**). However, FasL expression was not detected in both treated and untreated samples. Quantification of osteocytes that exhibited binding with an anti-Fas receptor antibody showed that Dex increased the percentage of cells staining positive for Fas (**Figure 45B**) as early as 3 hours by 7-fold (**Figure 45C**). In addition, western blot analysis demonstrated a time-dependent increase in Fas protein upon treatment with Dex (**Figure 45D**).

The involvement of Caspase 8, which lies downstream of Fas, was then investigated in Dex-induced apoptosis. Pre-treatment with the caspase 8 inhibitor Z-IETD-FMK reduced the induction of death at 5 hours, up to 5-fold, compared to cultures treated with Dex, as shown by Annexin-V-FITC assay and DAPI nuclear staining, suggesting that caspase 8 is involved in the apoptotic machinery activated by Dex in MLO-Y4 osteocytes (**Figure 46**). In addition, pre-treatment with a selective inhibitor against caspases 3 and 7 reduced the percentage of apoptotic osteocytes up to 6-fold (**Figure 46**).

5.4.4 Bisphosphonates prevent Dex-induced apoptosis in MLO-Y4 osteocytes. Dose response studies were used to identify concentrations of the non N-containing CLO and the N-BPs PAM and ALN (Figure 47) that did not increase apoptosis above control levels (Figure 48). Mean percentages of osteocytes displaying apoptotic morphology were statistically different compared to control following treatment with all BPs at 10^{-6} M, after 6 hours of treatment ($p = 0.03$), whereas the lowest concentration of 10^{-8} M did not increase apoptosis above control levels for all BPs ($p > 0.05$). BPs were then used to treat osteocytes prior to addition of Dex in cultures. Estimation of apoptosis showed that BPs at the lowest effective dose of 10^{-8} M significantly decreased the pro-apoptotic effect of the corticosteroid in osteocytes (Figure 49). The apparent lack of saving from death using doses higher than 10^{-8}M might be due to the fact that at those doses BPs appear themselves to be causing apoptosis.

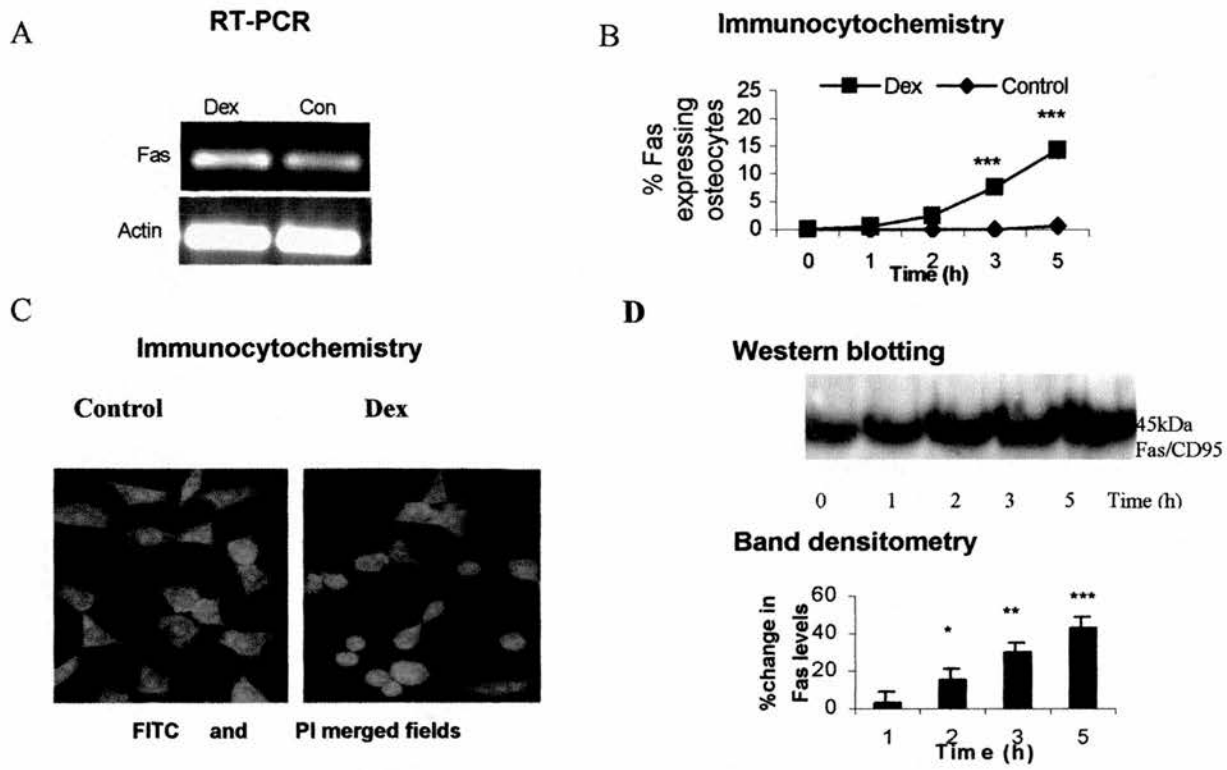

Figure 45. Dex upregulates Fas expression in MLO-Y4 osteocytes. MLO-Y4 osteocytes were incubated with Dex at 10^{-6} M for 5 hours and Fas expression was confirmed using **A.** RT-PCR analysis **B.** Immunocytochemistry using anti-Fas mAb for 1 to 5 hours. The graph represents the percentage of osteocytes, expressing Fas per number of cells ± S.D., determined by fluorescence microscopy. Control cultures represent vehicle (ethanol) cultures for Dex and are similar to untreated cultures in percentages of apoptotic osteocytes. **C.** Representative images of Fas positive cells identified by Fas mAb conjugated to FITC-labelled secondary antibody (green) and counter-stained with PI (red) using fluorescence microscopy (20x magn.) Untreated osteocytes (left panel) and Dex-treated osteocytes (right panel). **D.** Detection of Fas protein levels following Dex treatment for 1 to 5 hours using western blot analysis. Changes in band densitometry were quantified using NHI image analysis system and expressed as percentage change relative to zero time control ± S.D. (Graphs represent means ± S.D. *** = $p < 0.0001$, ** = $p < 0.001$, * = $p < 0.05$).

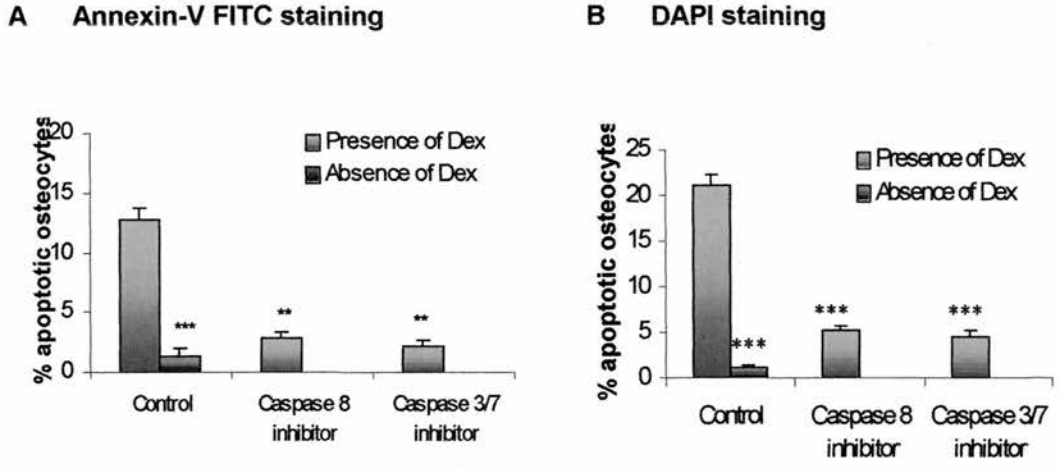

Figure 46. Inhibitors of caspases 8 and 3,7 reduce pro-apoptotic stimuli induced by Dex. MLO-Y4 osteocytes were incubated with inhibitors of caspase-8 (Z-IETD-FMK) and a caspase 3/7 selective inhibitor for 1 hour, followed by Dex treatment at 10^{-6} M for 5 hours. Cells were stained with **A**. Annexin-V FITC and **B**. DAPI and examined by fluorescence microscopy for phosphatidylserine detection and chromatin condensation, respectively. Graphs represent percentage means of apoptotic osteocytes ± S.D. (*** = $p < 0.0001$, ** = $p < 0.001$, * = $p < 0.05$). Control cultures represent vehicle (ethanol) cultures for Dex and are similar to untreated cultures (0.98 ± 0.58 S.D., $p > 0.05$ estimated by Annexin-V FITC and 1.27 ± 0.33 S.D., $p > 0.05$ estimated by DAPI) in percentages of apoptotic osteocytes.

CLO

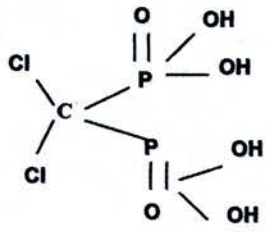

PAM

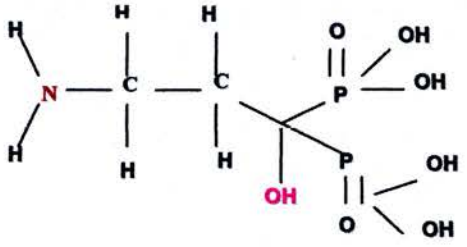

ALN

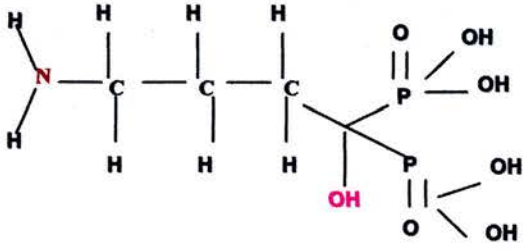

Figure 47. Chemical structures of CLO, PAM and ALN. All BPs are characterised by two phosphonate groups attached to a central carbon atom. The R2 side chain in CLO, which is a first generation BP, is a Cl- atom, while PAM and ALN are second generation BPs and both contain a N-group but different lengths in the R2 side chain. The presence or absence of a N-group accounts for differences in anti-osteoclastic activity and anti-resorptive potency. Image adapted from Dunford et al. *J.Pharm.Exper.Therap* 2001, page 238.

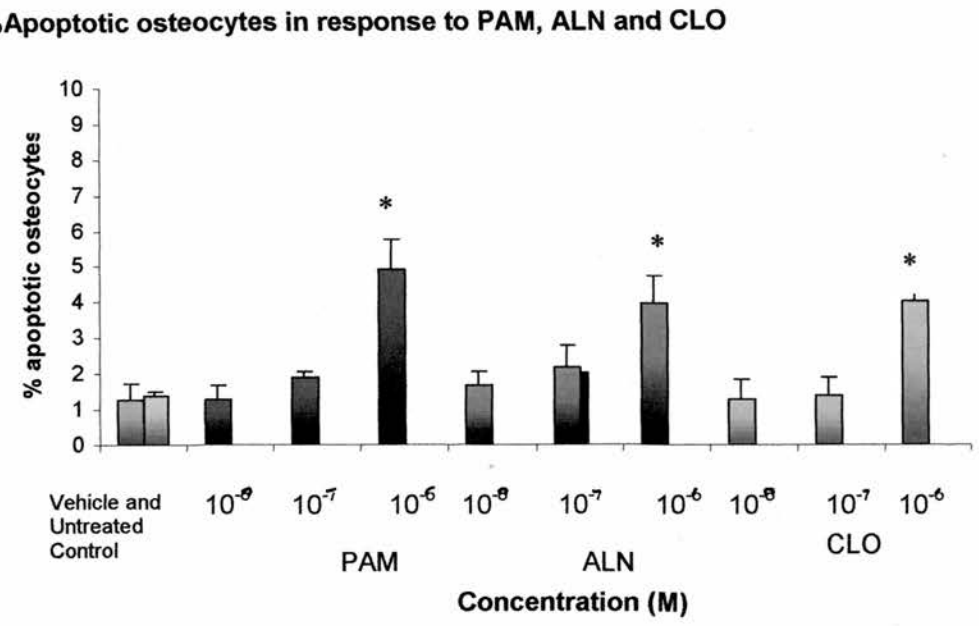

Figure 48. Dose-response studies of PAM, ALN and CLO. MLO-Y4 osteocytes were incubated with PAM, ALN and CLO to identify concentration that did not induce osteocyte apoptosis over a period of 6 hours. Cells were stained with AO and examined by fluorescence microscopy. Graphs represent percentage means of apoptotic osteocytes, per number of cells ± S.D (*** = $p < 0.0001$, ** = $p < 0.001$, * = $p < 0.05$). ■=control cultures, ■ =untreated control. Control cultures represent vehicle (PBS) cultures and are similar to untreated cultures in percentages of apoptotic osteocytes.

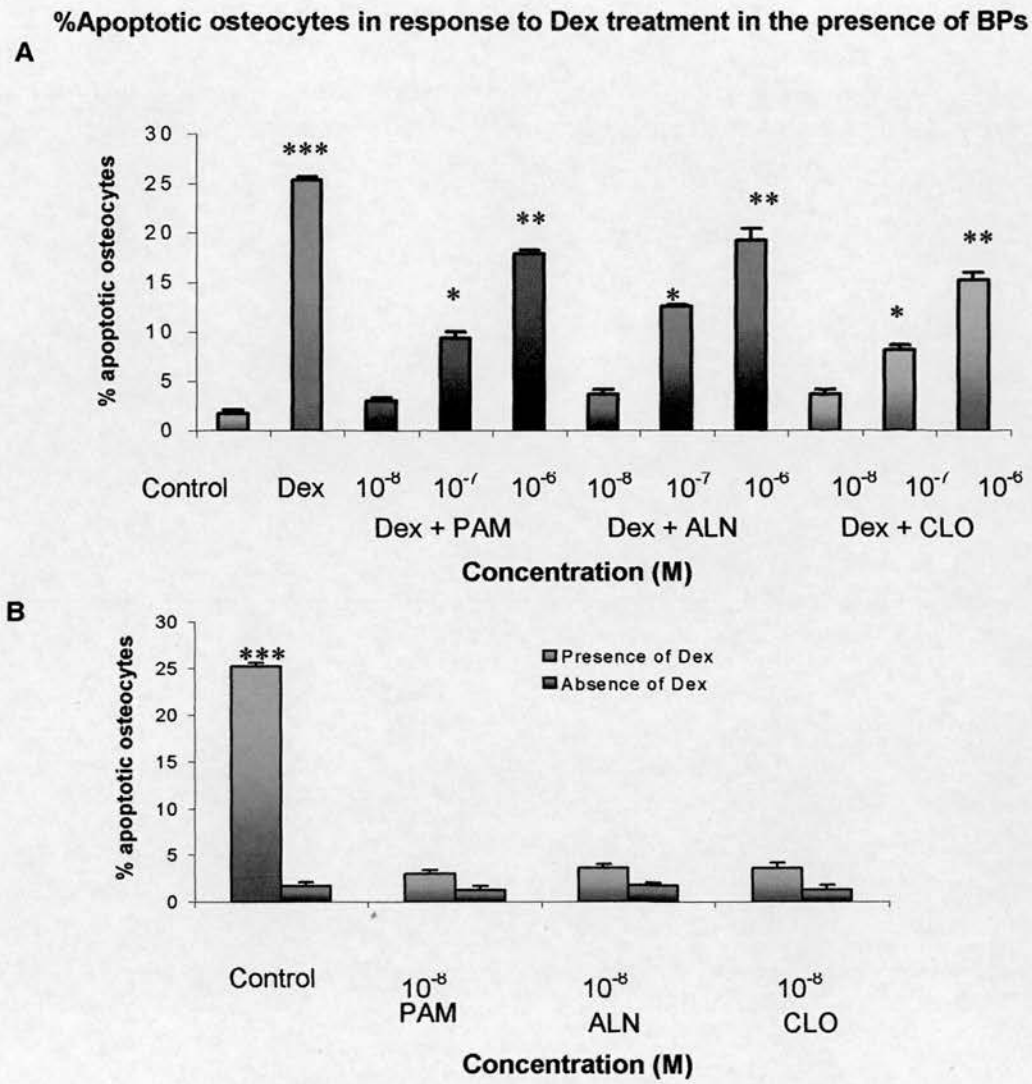

Figure 49. Bisphosphonates prevent MLO-Y4 osteocyte apoptosis induced by Dexamethasone in a concentration-dependent manner. Osteocytes were incubated with BPs at 10^{-8} to 10^{-6} M for 1 hour prior to Dex treatment, for 5 hours. **A.** Mean percentages of apoptotic osteocytes were statistically different compared to control following treatment with all BPs at 10^{-6} M, in the presence of Dex. **B.** The lowest concentration of 10^{-8} M for all BP molecules reduced percentages of apoptotic osteocytes to levels similar to control. Cells were stained with AO and examined by fluorescence microscopy (*** = $p < 0.0001$, ** = $p < 0.001$, * = $p < 0.05$) Control cultures represent vehicle (ethanol) cultures for Dex and are similar to untreated cultures in percentages of apoptotic osteocytes (1.42 ± 0.11 S.D., $p > 0.05$).

5.4.5 Inhibitors of MAP kinase signalling molecules prevent Dex-induced apoptosis in MLO-Y4 osteocytes.

The effect of Dex on MLO-Y4 osteocytes was further characterised in the presence of protein inhibitors such as the MEK 1/2 inhibitor UO126 and the p38 inhibitor SB203580. Dose response studies identified optimal concentrations of UO126, which did not significantly increase apoptosis above control levels either for the compound alone, or the vehicle in which it was delivered, within the range of concentrations known to inhibit ERK 1/2 (Favata et al. 1998) (**Figure 50A**). Quantification of apoptosis showed that concentrations of UO126 at 10 and 20 μM exerted protective effects on osteocytes following 5-hour incubation period with Dex (**Figure 50B**). In contrast, SB203580 at concentrations of 5 to 15 μM known to inhibit p38 (Cuenda et al. 1995), did not prevent GC-induced apoptosis, while doses above 10 μM induced significant apoptosis when added alone to osteocyte cultures (**Figure 51**).

5.4.6 BPs and protein kinase inhibitors do not protect osteocytes from oxidant-induced death.

To evaluate the role of the BP and ERK pathways in the induction of osteocyte apoptosis by other agents, MLO-Y4 cells were pre-treated with PAM and UO126 prior to their exposure to H_2O_2. MLO-Y4 osteocytes were cultured with H_2O_2 at concentrations shown to induce apoptosis (0.08 mM to 0.4 mM), for various times between 1 and 24 hours (**Figure 52A**). Maximal levels of death accompanied by cell loss were reached at 24 hours of incubation by all different concentrations (**Figure 52B**). At 0.8 mM a small proportion of cells were noted to have expanded and burst characteristics of necrosis. Based on the apoptotic criteria, the dose of 0.4 mM, which did not induce necrosis, at 5 hours incubation, was selected to induce apoptosis in cultures pre-treated with BPs and the ERK 1/2 inhibitor (**Figure 53**). Mean percentages of apoptotic osteocytes revealed that H_2O_2-induced osteocyte death was not reduced in the presence of either UO126 or PAM.

A %Apoptotic osteocytes in response to UO126 treatment

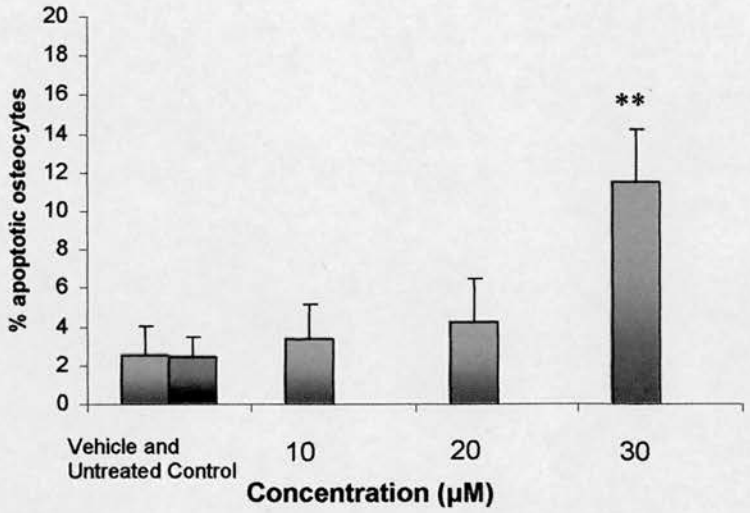

B %Apoptotic osteocytes in response to Dex and UO126 treatment

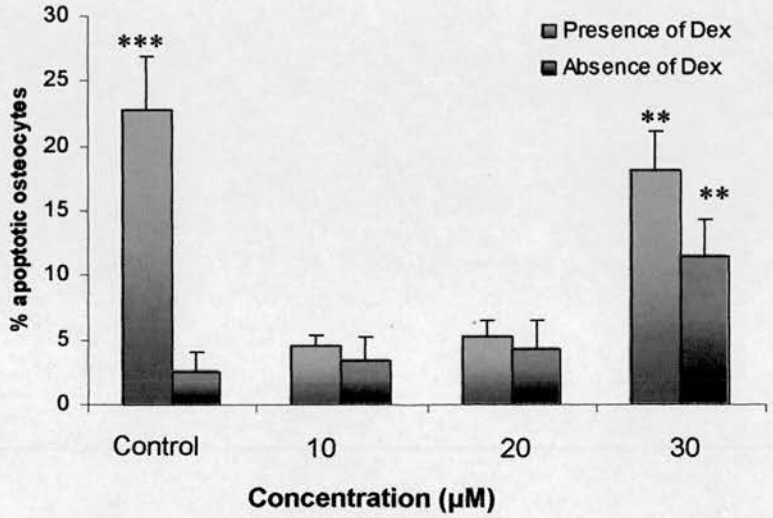

Figure 50. The MEK 1/2 inhibitor UO126 prevents Dex-induced apoptosis. MLO-Y4 osteocytes were incubated with UO126 for 30 minutes at 10-30 μM in the presence and absence of Dex at 10^{-6} M for 5 hours. **A**. Dose-response studies of UO126 at 10-30 μM. and **B**. UO126 prevents MLO-Y4 osteocyte apoptosis induced by Dex, at 10 and 20 μM at 5 hours. Cells were stained with AO and examined by fluorescence microscopy. Graphs represent the mean percentages of apoptotic osteocytes ± SD (*** = $p < 0.0001$, ** = $p < 0.001$, * = $p < 0.05$) Control cultures represent vehicle (DMSO) cultures and are similar to untreated cultures in percentages of apoptotic osteocytes.

A %Apoptotic osteocytes in response to SB203580 treatment

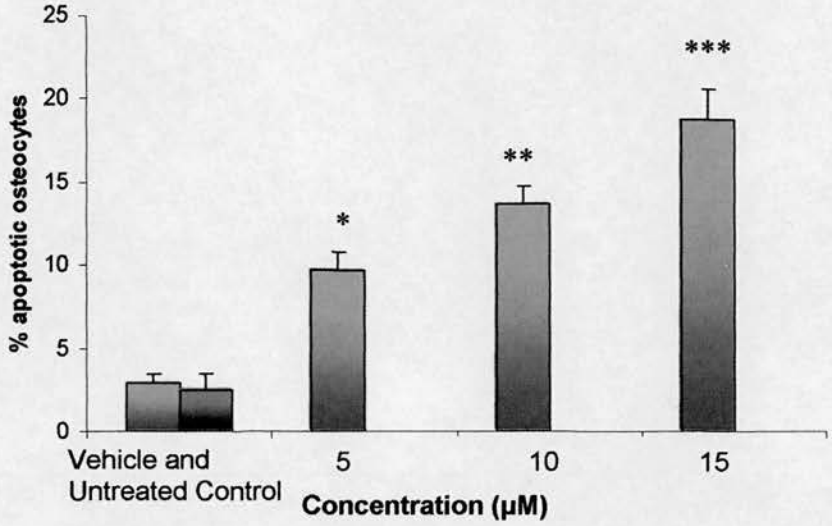

B%Apoptotic osteocytes in response to Dex and SB203580 treatment

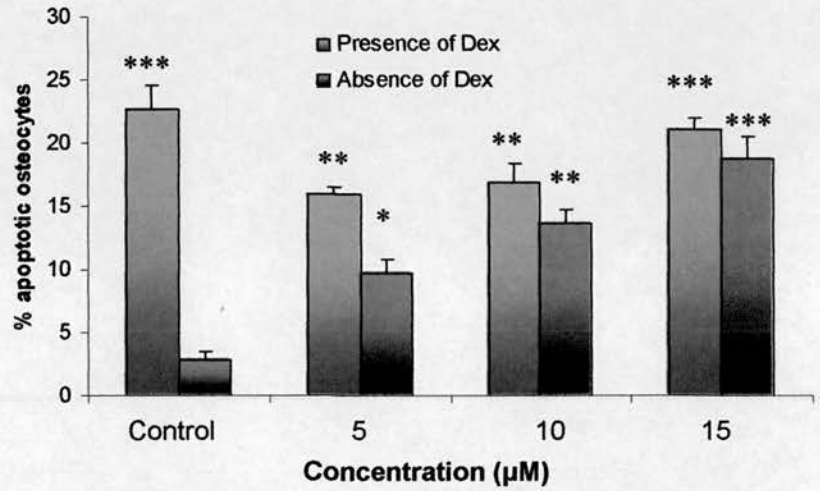

Figure 51. The p38 inhibitor SB203580 induces apoptosis in the presence or absence of Dex. MLO-Y4 osteocytes were incubated with SB203580 at 5-15 μM for 30 minutes in the presence and absence of Dex at 10^{-6} M, for 5 hours. **A**. Dose-response studies of SB203580 at 5-15 μM. **B**. SB203580 at 5-15 μM does not prevent Dex-induced osteocyte apoptosis at 5 hours. Cells were stained with AO and examined by fluorescence microscopy. Graphs represent mean percentages of apoptotic osteocytes ± S.D. (*** = $p < 0.0001$, ** = $p < 0.001$, * = $p < 0.05$). Control cultures represent vehicle (DMSO) cultures and are similar to untreated cultures in percentages of apoptotic osteocytes.

A %Apoptotic osteocytes in response to time and H_2O_2 treatment

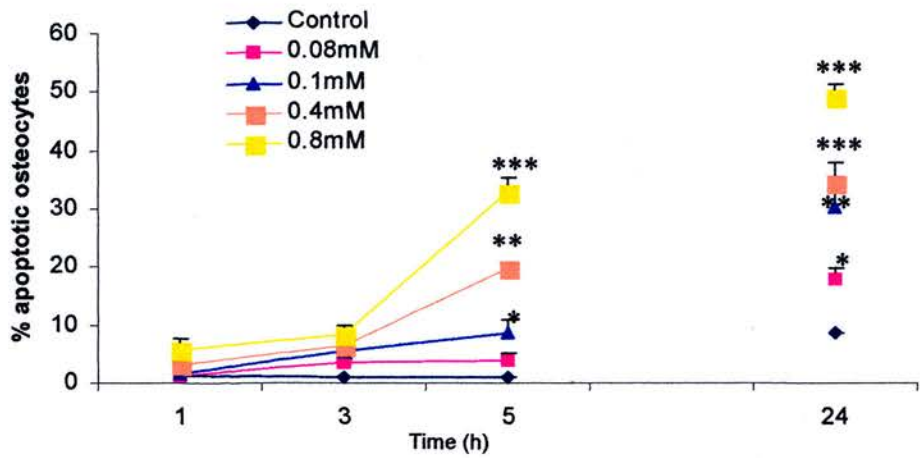

B Number of cells in response to time and H_2O_2 treatment

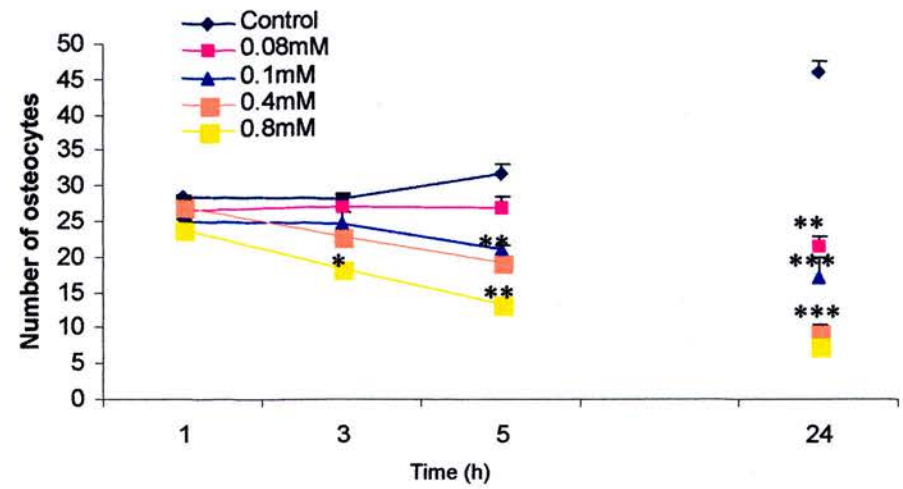

Figure 52. H_2O_2 induces apoptosis in MLO-Y4 osteocytes in a concentration-dependent manner. MLO-Y4 osteocytes were incubated with H_2O_2 at 0.08-0.8 mM for 1-24 hours. Cells were stained with AO and examined by fluorescence microscopy. **A**. Mean percentages of apoptotic osteocytes and **B**. Mean number of osteocytes in culture. Graphs represent mean percentages of apoptotic osteocytes ± SD (*** = $p < 0.0001$, ** = $p < 0.001$, * = $p < 0.05$).

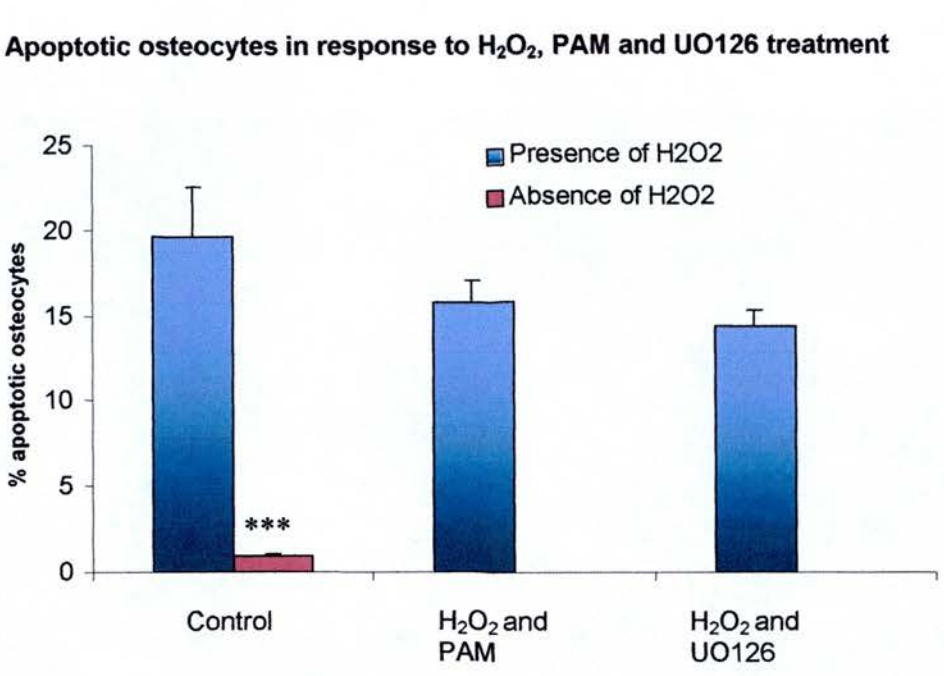

Figure 53. BPs and UO126 do not protect osteocytes from oxidant-induced death. MLO-Y4 osteocytes were incubated with PAM at 10^{-8} M and UO126 at 20 μM prior to H_2O_2 treatment, for 5 hours. Cells were stained with AO and examined by fluorescence microscopy. Graphs represent percentage of apoptotic osteocytes, per number of cells ± S.D. (*** = $p < 0.0001$)

5.4.7 Primary osteocytes are protected from Dex-induced death by BPs and the MEK1/2 inhibitor.

Primary cultures of chicken osteocytes were also used to observe responses to inducers of osteocyte death. AO staining revealed that in a similar way to that seen in the MLO-Y4 cell line, both BPs and the MEK inhibitor UO126 were capable of blocking Dex-induced death in these primary cells (**Figure 54**).

5.4.8 Dexamethasone activates the MEK/ERK kinase signaling pathway.

Incubation with Dex, increased the amount of activated ERK 1/2 protein in osteocytes, compared to vehicle, in a time dependent manner, as evidenced by western blot analysis, using an anti-phospho ERK 1/2 antibody (**Figure 55A**). Activation of ERK 1/2 protein by Dex was acute, since it was detected as soon as 1 minute following treatment and was decreased to basal control levels, after 1 hour of treatment. BPs transiently increased ERK 1/2 phosphorylation within 1 minute of treatment, returning to baseline by 5 minutes, as shown previously by Plotkin et al. (Plotkin et al. 1999). In this treatment group baseline levels were maintained for all subsequent time points investigated, up to 5 hours (**Figure 55B**). Addition of Dex to cells pre-treated for 1 hour with BPs resulted in a reduced activation of ERK 1/2 relative to samples treated with Dex alone (**Figure 56**). The MEK 1/2 protein inhibitor, UO126 blocked Dex and/or BP-induced ERK 1/2 activation in all cases.

In order to characterize further the role of ERK 1/2 pathway in Dex-induced apoptosis, the presence of proteins lying both upstream (MEK 1/2 and c-Raf) and downstream (p90rsk) of ERK 1/2 protein, was investigated. Western blot analysis showed that MEK (**Figure 57A**) and p90rsk (**Figure 57B**) activation by Dex coincided with ERK 1/2 activation, while pre-treatment with ALN slightly reduced phosphorylated levels of both proteins. In addition, UO126 prevented activation of p90rsk by Dex, but did not affect phosphorylated MEK 1/2 protein, in accordance with previous reports (Favata et al., 1998). Levels of c-Raf remained constant and similar to vehicle levels, during all different treatments and time points investigated (**Figure 57C**).

% Apoptotic primary osteocytes in response to UO126, PAM and Dex treatment

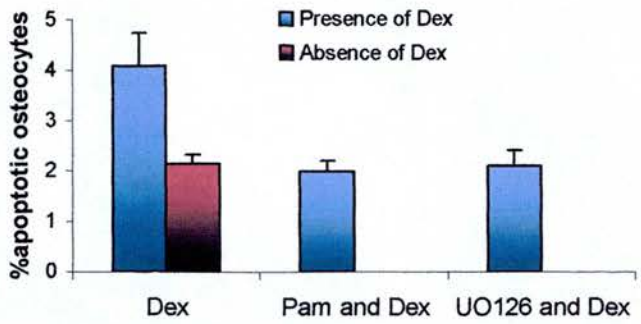

Figure 54. BPs and MEK 1/2 inhibitor reduce apoptotic stimuli induced by Dex, in primary chicken osteocytes. Primary osteocytes were incubated with PAM at 10^{-8} M for 1 hour and UO126 at 20 μM for 30 minutes prior to addition of Dex at 10^{-6} M for 5 hours. Cells were stained with AO and examined by fluorescence microscopy. Graph represents percentage of apoptotic osteocytes per total number of cells ± S.D.

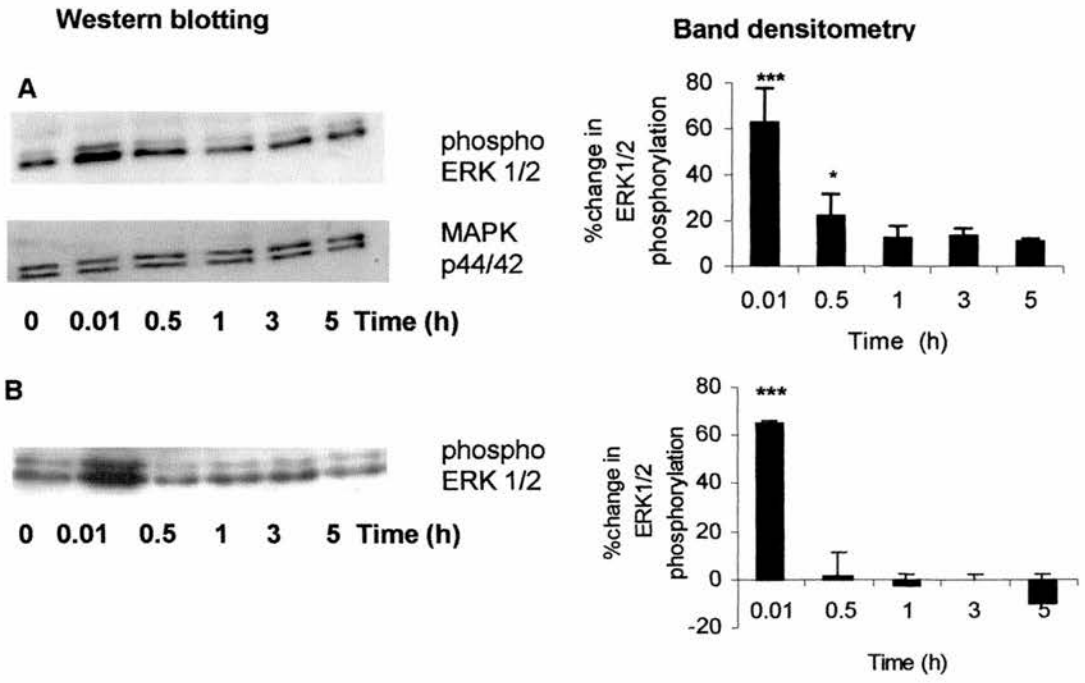

Figure 55. Dex activates the ERK 1/2 protein kinase. A. Dex activates the ERK 1/2 protein kinase, in a time dependent manner. **B**. ALN activates the ERK 1/2 protein kinase, only during the first five minutes of addition to the cultures. MLO-Y4 cell lysates were subjected to Western blot analysis using an anti-phospho MAPK p44/42 antibody. The blots were stripped and reprobed with a total anti-MAPK p44/p42 antibody, to verify equal loading of samples. Changes in band densitometry were quantified using NHI image analysis system from 3 independent experiments and expressed as percentage change relative to control samples, representing either vehicle control or zero time control ± S.D. (*** = $p < 0.0001$, * = $p < 0.05$ compared to control)

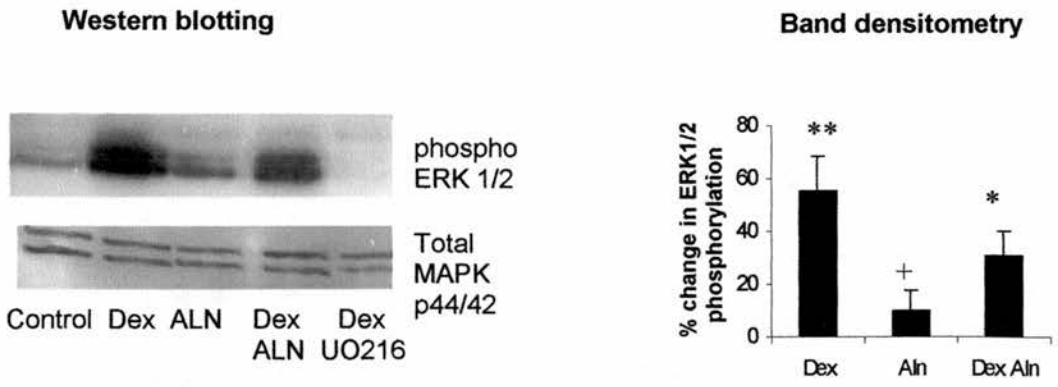

Figure 56. ALN reduces the Dex-induced ERK 1/2 activation. ALN was shown to reduce Dex-induced activation of ERK 1/2, at 5 minutes, whereas UO126 blocked Dex-induced ERK 1/2 activation. Lysates were subjected to Western Blot analysis, using an anti-phospho MAPK p44/p42 antibody. The blots were stripped and reprobed with a total anti-MAPK p44/p42 antibody, to verify equal loading of samples. Changes in band densitometry were quantified using NHI image analysis system from 3 independent experiments and expressed as percentage change relative to control samples, representing either vehicle control or zero time control ± S.D. ** = $p < 0.001$, * = $p < 0.05$ compared to control, + = $p < 0.05$ compared to Dex treatment

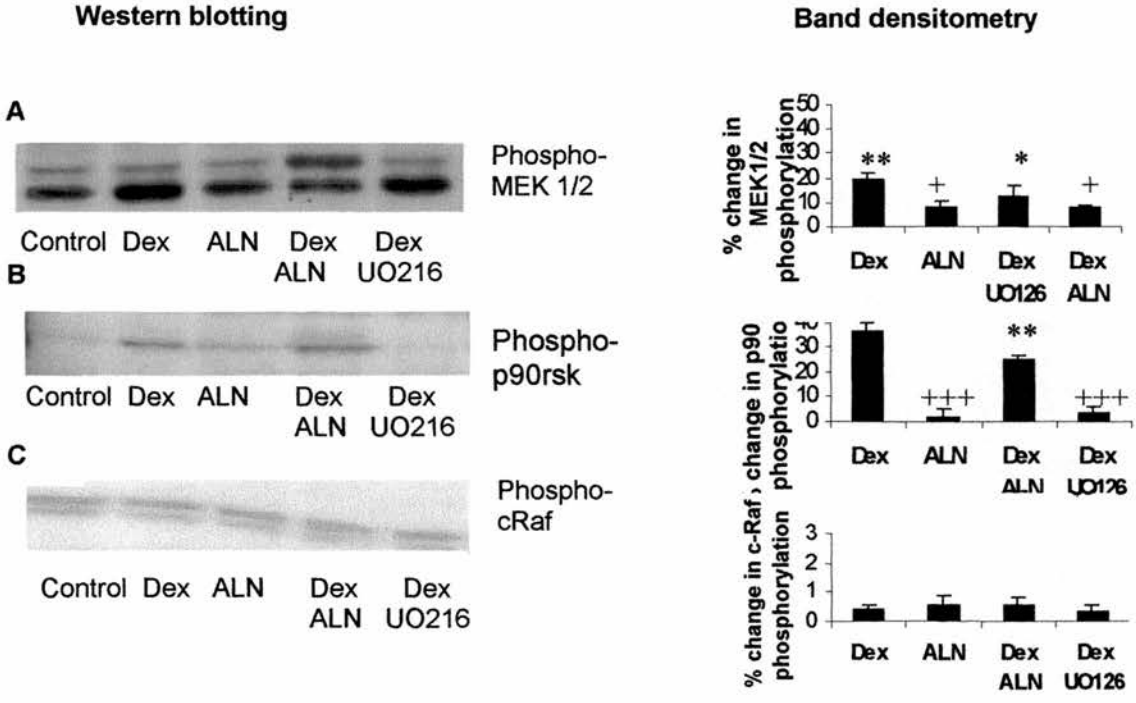

Figure 57. Dexamethasone activates the ERK 1/2 pathway. Lysates prepared from MLO-Y4 cells treated with Dex, ALN and UO126, were subjected to Western Blot analysis, using **A.** anti-phospho MEK 1/2 antibody, **B**. anti-phospho p90rsk and **C**. anti-phospho c-Raf antibody. Changes in band densitometry were quantified using NHI image analysis system from 3 independent experiments and expressed as percentage change relative to vehicle sample ± S.D. ** = $p < 0.001$, * = $p < 0.05$ compared to control, + = $p < 0.05$ compared to Dex treatment

5.4.9 Suppression of Dex-induced Fas activation by MEK 1/2 inhibitor and BPs.

The role of BPs and ERK1/2 protein kinase in Dex-induced activation of Fas was investigated by immunocytochemistry studies (**Figure 58A**). Previous studies have shown interaction between ERK and Fas protein pathways in the induction of apoptosis (Goillot et al. 1997). Pre-treatment of osteocytes with UO126 at 20 μM, prevented activation of Fas by Dex ($p = 0.0001$, compared to Dex-treated samples). In a similar manner to UO126, pre-treatment of MLO-Y4 cells with both N- and non N-BPs at 10^{-8} M, reduced activation of Fas by Dex ($p = 0.0001$).

5.4.10 PMA-induced ERK1/2 activation is not associated with osteocyte apoptosis

PMA when administered alone at concentrations of 2 ng/ml to 200 μg/ml for 1 to 5 hours (**Figure 58B**) did not increase Fas, while prior to Dex treatment PMA did not enhance Dex-induced Fas upregulation, in contrast to Dex treated cultures (**Figure 58B**). In addition, PMA did not induce osteocyte apoptosis (**Figure 59B**), despite demonstrating a clear increase in phosphorylated ERK in MLO-Y4 osteocytes as determined by western blotting (**Figure 59A**).

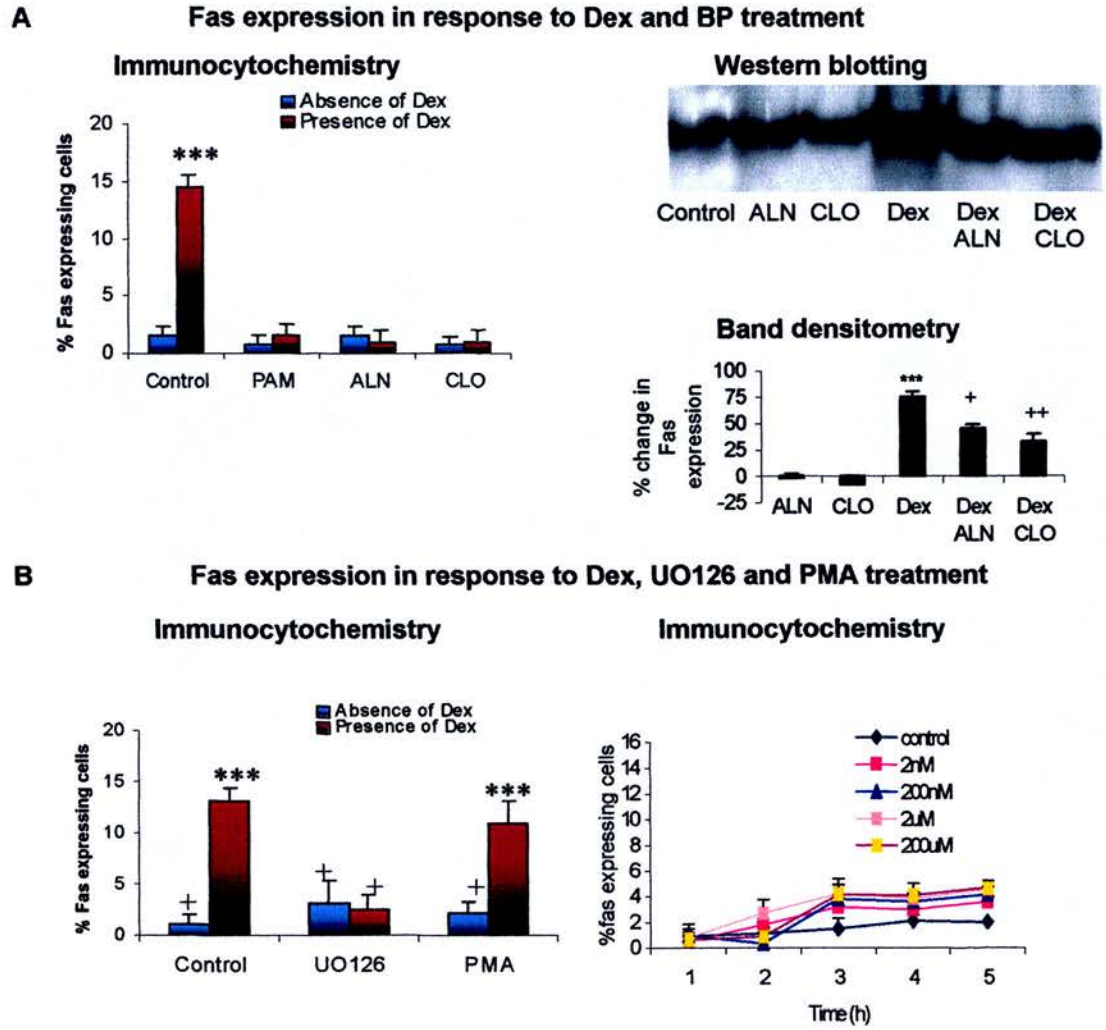

Figure 58. BPs and UO126 suppress Dex-induced Fas activation. Cells were probed with an anti-Fas antibody and examined by fluorescence microscopy. **A.** N- and non N-BPs reduce Dex-induced Fas expression as shown by immunocytochemistry and western blot analysis. Changes in band densitometry were quantified using NHI image analysis system and expressed as percentage change relative to vehicle sample ± S.D. from 3 independent blots. **B.** UO126 suppressed Dex-induced Fas expression while PMA did not increase Fas expression, compared to control, when administered at a range of concentrations and time points. Graphs represent mean percentages of osteocytes, expressing Fas per number of cells ± S.D. (*** = $p < 0.0001$, ** = $p < 0.001$, * = $p < 0.05$ compared to control, + = $p < 0.05$ compared to Dex treatment)

A ERK activation in response to PMA treatment

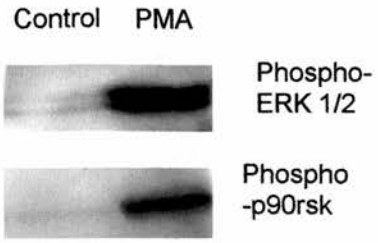

B %Apoptotic osteocytes in response to Dex and PMA treatment

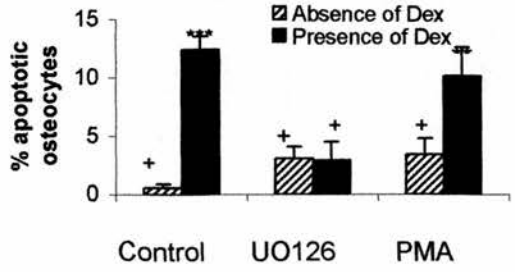

Figure 59. PMA-induced ERK1/2 activation is not associated with osteocyte apoptosis. Cells treated with PMA followed by Dex were **A**. subjected to western blot analysis to reveal pERK 1/2 and p90rsk activation and **B**. treated to reveal DNA breaks using the Nick Translation assay. PMA did not affect osteocyte apoptosis, compared to control. Graphs represent percentage of apoptotic osteocytes, per number of cells ± S.D. (*** = $p < 0.0001$, compared to control, + = $p < 0.05$ compared to Dex treatment)

5.5 Discussion

Death of the osteocytes, and therefore interruption of the sophisticated network that they form within the bone, could account for the increased bone fragility and osteonecrosis associated with patients affected by glucocorticoid-induced osteoporosis (Glade and Krook 1982, Weinstein et al. 1998).

Data in this chapter investigate molecular pathways implicated in Dex-induced death of osteocytes, the mechanosensors and transducers in bone, and on molecules that might provide therapeutic approaches to combat this death. Induction of osteocyte apoptosis by Dex was characterised by several classical apoptotic features, including chromatin and cytoplasmic condensation, DNA fragmentation, exposure of phosphatidylserine and formation of apoptotic bodies, and was concentration- and time-dependent. In addition, apoptosis was caspase-dependent since inhibition of caspases -3 and –7 (Lee et al. 2000), which are responsible for chromatin condensation, DNA fragmentation and membrane blebbing, suppressed Dex-induced death.

Dex-induced apoptosis has been associated with the Fas/FasL apoptotic pathway in several different cell types, in relation to its action as an immunosuppressive agent (Schmidt et al. 2001). Fas receptor mRNA was detected in MLO-Y4 osteocytes both in response to Dex treatment and in untreated cultures. However, Dex treatment upregulated localisation of Fas protein on the osteocyte plasma membranes, in a time-dependent manner compared to untreated controls, indicating a possible association between Fas recruitment and the incidence of osteocyte apoptosis in the presence of Dex. Indeed, inhibition of caspase 8, the upstream caspase participating in the Fas pathway, using a peptide inhibitor (Martin et al. 1998), blocked Dex-induced apoptosis, further supporting a possible association between Dex and the Fas pathway in osteocyte apoptosis. However, expression of Fas Ligand in both Dex-treated and untreated cultures was not detected, suggesting that if indeed there is activation of the Fas-related pathway in the presence of Dex it is FasL independent. Similar phenomenon has been observed in tumour cell studies, showing that anticancer agents directly promote Fas receptor trimerisation and activation of the

FADD/caspase 8 pathway, independently of FasL (Misceau et al. 1999). Other studies by Ahuja et al, have also reported expression of Fas receptor on MLO-Y4 osteocytes, while the authors also failed to detect FasL expression (Ahuja et al 2003).

BPs suppressed Dex-induced apoptosis in MLO-Y4 osteocytes after 5 hours treatment with Dex, in accordance to previous reports (Plotkin et al. 1999). Although the half-life of BPs *in vitro* experimental conditions is not known, the pharmacokinetics of these molecules *in vivo,* might allow them to suppress GC-induced apoptosis of osteocytes for longer periods of time, since they can be retained active in the skeleton until their release, following resorption of the multiple sites in which they were deposited (Fleisch 2000).

Dex-induced apoptosis was prevented by both non N-BPs (CLO), which are metabolized into cytotoxic analogues of ATP and N-BPs (PAM and ALN), which inhibit prenylation through inhibition of FPP synthase (Rogers et al. 1999). Both groups of BPs were equally effective inhibitors of death, indicating that prevention of Dex-induced osteocyte apoptosis by BPs does not depend on the presence of a N-group (**Figure 47**) and hence on inhibition of FPP synthase.

Activation of the ERK pathway is generally associated with the induction of proliferative and survival signals. In osteoblasts, activation of the ERK cascade has been shown to regulate growth, differentiation, function and integrin expression, whereas in T cells it protects from GC-induced apoptosis and exerts negative effects on the pro-apoptotic signals induced by death receptors such as Fas and TNF (Lai et al. 2001, Jamieson and Yamamoto 2000, Tran et al. 2001). However, in contrast to the known pro-survival effects, the ERK pathway has also been associated with the induction of pro-apoptotic signals. Activation of ERK appears to be important for the induction of cisplatin-induced apoptosis in HeLa cells and activation-induced cell death of T cells, whereas other evidence suggest that increased levels of ERK contribute to brain injury during focal cerebral ischemia. (Wang et al. 2000, van den Brink et al. 1999, Alessandrini et al. 1999).

Recently, Nishida et al. have reported that YM529, a new bisphosphonate, decreases phosphorylation of ERK1/2 during apoptosis of HL60 cells (Nishida et al. 2003). Nevertheless, Plotkin et al. observed an acute activation of ERK by BPs, which was sustained for 5 minutes during the pre-treatment period (Plotkin et al. 1999), and suggested that activated ERK is involved in the protective effects of BPs on Dex-induced apoptosis. Data in this study have shown activation of ERK by BPs, which peaked at 5 minutes of addition of BPs to osteocyte cultures. However, this study did not measure possible ERK production in response to Dex, as has been noted in other cell types (Jamieson and Yamamoto 2000). Following on from both studies, this work has investigated the course of ERK activation in order to characterize the effect of Dex on the ERK pathway, during osteocyte apoptosis. In contrast to activation of ERK by BPs during the pre-treatment period, Dex transiently increased the amount of activated ERK1/2 in osteocytes, which remained elevated for the first hour of incubation, and was suggestive of a specific non-genomic effect, involving membrane-bound GC receptors, since activation of cytosolic receptors requires at least 30 minutes (Patschan et al. 2001). Inhibition of ERK by UO126 suppressed Dex-induced osteocyte apoptosis, both in the presence and absence of BPs, indicating that induction of death signals by Dex-activated ERK compared to non-damaging BP-activated ERK is due to either differences in the timing and duration of activation or to the generation of secondary factors by Dex, which render ERK pro- rather than anti-apoptotic. Furthermore, in the presence of BPs, ERK phosphorylation in response to Dex was significantly reduced.

Variance between the findings of Plotkin et al. in which ERK appears as an anti-apoptotic signal and the current conclusion in this chapter regarding its positive role in apoptotic death, may be due to differences in experimental conditions between the two studies. Plotkin et al. studied apoptosis in serum-replete conditions and ERK under serum free conditions, while in this study both apoptosis (the phenomenon) and ERK phosphorylation in these cells were investigated under identical serum-replete conditions. On the other hand, PMA treatment failed to increase the proportion of apoptotic osteocytes when added alone, and did not prevent or enhance

the pro-apoptotic stimuli in the presence of Dex, indicating that activation of ERK through other pathways is not sufficient to induce osteocyte apoptosis.

Dex treatment also increased MEK and p90rsk activation at identical times to the activation of ERK, which was however reduced in cultures pre-treated with BPs, whereas levels of c-Raf were not altered, compared to control levels, suggesting that Dex is acting downstream of c-Raf or through another isoform of Raf in the signalling pathway involving Raf, MEK and ERK. In contrast to ERK, p38 inhibition did not reduce osteocyte apoptosis, indicating specificity in the pro-apoptotic effects of MAPK family members. In neuroblastoma cells transfection with activated MEK1 upregulated Fas activity (Goillot et al. 1997), while in T cells, during activation-induced cell death, transfection of a dominant negative MEK1 inhibited FasL expression (van den Brink et al. 1999). In this study, inhibition of ERK in experiments using the Fas/CD95 antibody reduced the Dex-induced Fas activation, whereas upregulation of ERK by PMA did not affect Fas levels, indicating that production of Fas is closely associated to the pro-apoptotic signals induced by Dex. In addition, prevention of Dex-induced apoptosis by non N-BPs and N-BPs also decreased Fas expression, supporting the importance of Fas in the death response and pointing to the existence of an additional factor associated with Dex-treatment that might enable the co-operation between ERK and Fas pathways during the induction of osteocyte apoptosis.

In conclusion, this study has shown that Dex-induced apoptosis in osteocytes is associated with activation of the ERK and Fas pathways and could be prevented by BP molecules in a manner that is independent of their chemical structure and the ability to inhibit FPP synthase. These findings might have important applications for the management of patients affected by glucocorticoid-induced osteoporosis, since death of osteocytes, which are considered to be the mechanosensors and transducers in bone, might lead to impairment of the adaptive response to mechanical loading and to increased bone fragility.

CHAPTER 6

NE11808 and NE11809 inhibit Dex-induced apoptosis in osteocytes

6.1 Abstract

This work is the subject of a published manuscript (**Appendix**). Bisphosphonates like PAM, ALN and CLO prevent osteocyte apoptosis following treatment with Dexamethasone, as shown in chapter 5. This study has used additional BP molecules that have minor structural and conformational changes compared to CLO, PAM and ALN, in order to determine whether the anti-apoptotic effects of BPs on osteocytes correlate with their anti-resorptive potency.

NE11808 and NE11809 are structurally similar N-containing BPs, which differ in the presence of a methyl group in NE11809. However NE11809 is associated with decreased anti-resorptive activity and reduced ability to inhibit FPP synthase, compared to NE11808, indicating an association between the activity of BPs to inhibit osteoclast resorption and the three-dimensional structure of the molecules.

Osteocyte cultures were incubated with Dexamethasone in the absence or presence of NE11808 and NE11809. Estimation of apoptotic osteocytes showed that both BPs were equally effective inhibitors of death. In addition both BPs reduced the Dex-induced ERK 1/2 activation, in a manner similar to the BPs described in chapter 5. Results in this chapter have indicated that the protective effects of BP on osteocytes against Dex-induced apoptosis are independent of their structure and activity against osteoclasts. These findings suggest that alterations in the three-dimensional structure might provide BP molecules that could be independently applied to affect osteoclast activity or osteocyte survival, in patients affected by glucocorticoid-induced osteoporosis.

6.2 Introduction

BPs are non-hydrolysable pyrophosphate analogs, in which the oxygen linking the phosphates (P-O-P) has been replaced by carbon (P-C-P), which has two side chains, R1 and R2 (Rodan 1998). BPs, such as etidronate were initially used as early as 1897 as anticorrosive and antiscaling agents in industrial procedures (Menschutkin 1865). BPs were subsequently found to have a high affinity for hydroxyapatite crystals and to affect calcium phosphate formation and were designed to prevent calcification of bone mineral, which depends both on the presence of a hydroxyl group in the R1 chain and on the dose of the bisphosphonate (Papapoulos 1997). Finally, BPs were shown to be very effective anti-resorptive agents *in vivo* and to exert direct effects on osteoclasts and were used in the treatment of glucocorticoid-induced osteoporosis, post-menopausal osteoporosis, Paget's disease, hypercalcemia, osteogenesis imperfecta, and tumor-associated bone diseases (Adami and Zamberlan 1996).

The anti-resorptive property of BPs depends mostly on the structure and conformation of the R2 side chain, whereas the R1 side chain participates mainly in the binding to mineralised matrix (Rogers et al.1999) (**Figure 60**). First generation of BPs have a short R2 side chain, and are characterised by an alkyl or halide side chains, such as etidronate and clodronate respectively. Second generation BPs contain a primary amino group in the R2 chain and they are 10- to 1,000-fold more potent than first generation. Third generation BPs were developed in the 1980s and contain a tertiary amino group or a nitrogen atom within a heterocyclic ring and are 10,000-fold more potent than first generation BPs (Sietsema et al. 1989, Rogers et al. 1999). The presence of two phosphonate groups is also important, although the structure and conformation of the R2 side chain is the major determinant of the antiresorptive activity (Dunford et al. 2001).

In the previous chapter, Bisphosphonates were shown to prevent osteocyte apoptosis following treatment with Dexamethasone. The BPs that were administered included the first generation non N- containing CLO and the second generation N-BPs PAM and ALN (**Figure 61**), indicating that the absence or presence of the nitrogen group

in the R2 side chain did not affect the anti-apoptotic activity of BPs against Dexamethasone-induced osteocyte death.

NE11808 and NE11809 are both N-containing third generation BPs characterised by the presence of a heterocyclic ring. NE11808 and NE11809 have a similar chemical composition (**Figure 62**); however they have minor conformational changes and also differ in the presence of a methyl group in NE11809 in the R2 side chain, which accounts for differences in their potency against bone resoprtion (Dunford et al. 2001). This study has investigated the effect of NE11808 and NE11809 on osteocytes against Dexamethasone-induced apoptosis, in order to identify a correlation between structure/conformation of BPs and anti-apoptotic activity on osteocytes.

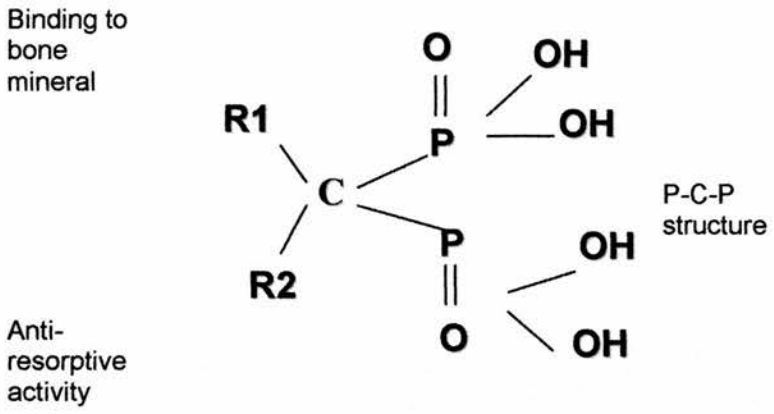

Figure 60. Basic chemical structure of BP molecules. BPs consist of two phosphonate groups attached to a central carbon atom and two side chains, R1 and R2, responsible for attachment to bone mineral and anti-resorptive activity respectively. Image adapted from van Beek et al. *Bone* 1998, page 438.

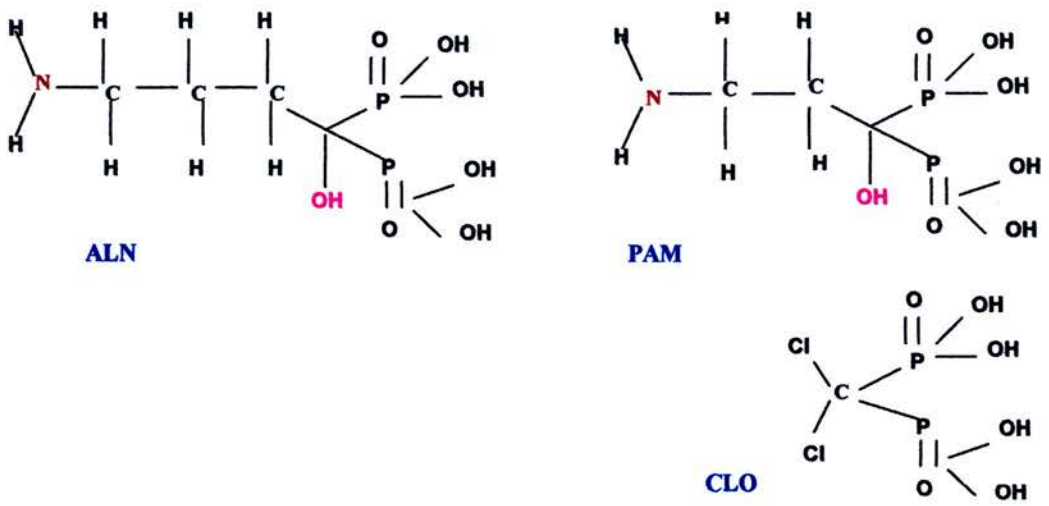

Figure 61. Chemical structures of BPs belonging to first (CLO) and second (PAM and ALN) generation of BPs. All molecules are characterised by two phosphonate groups attached to a central carbon atom which has a R1 side chain (-H or –OH) and different R2, which account for differences in anti-resorptive activity. Image adapted from Dunford et al. *J.Pharm.Exper.Therap* 2001, page 238.

NE11808

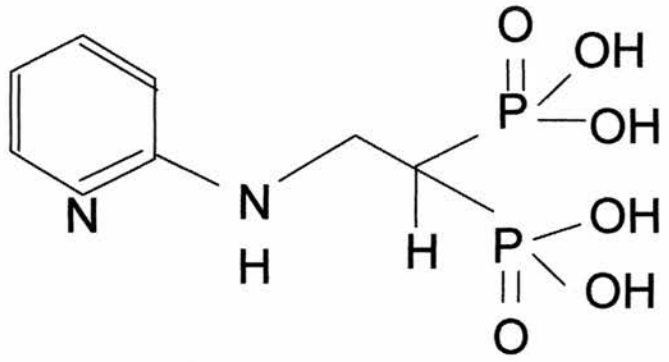

NE11809

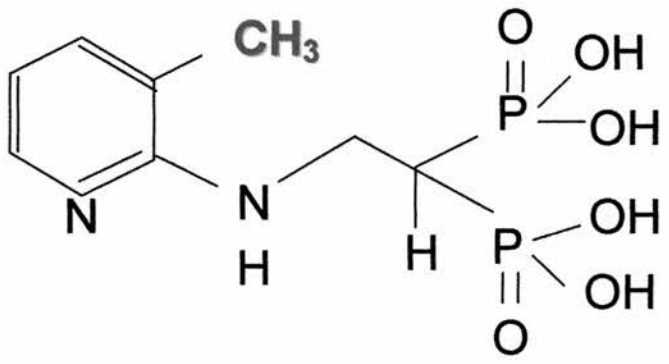

Figure 62. Chemical structures of third generation bisphosphonates NE11808 and NE11809. NE11808 and NE11809 are N-BPs that contain a heterocyclic-group in the R2 side chain; however they differ in the presence of a methyl group in NE11809, which dramatically reduces the anti-resorptive potency and ability to inhibit FPP synthase of NE11809, compared to NE11808. Image adapted from Dunford et al. *J.Pharm.Exper.Therap.* 2001, page 238.

6.3 Materials and Methods

All chemicals were purchased from Sigma, UK; all tissue culture reagents were purchased from Invitrogen, UK and tissue culture well plates and petri dishes were purchased from Corning, UK unless otherwise stated. Tissue culture procedures were performed in a laminar flow hood (class 2) receiving HEPA-filtered air, using sterile equipment.

6.3.1 MLO-Y4 cell culture

The MLO-Y4 osteocyte cell line was cultured as described in §3.3.1. Briefly, cells were maintained in α-Modified Essential Medium (αMEM) supplemented with 5% FBS, 5% newborn calf serum (NCS), 1% Penicillin/Streptomycin and 1% L-glutamine. Subculturing was performed twice weekly upon reaching 90% of confluency, maintaining the cells in the log phase of proliferation.

6.3.2 Cell treatment

Cells were plated in growth medium at a density of $1x10^4$ cells/ml in 24 multi-well plates or $1x10^5$ cells/ml in 60 mm petri dishes for 24 hours, prior to experimentation, as described in §5.3.2. Experiments were carried out a minimum of 3 times, and each treatment group was represented by 3 wells in each independent experiment. Control treatments represent vehicle treatments for the different agents, which were subjected to identical dilutions to the agents.

6.3.3 Induction of Cell Death

Cells were incubated in growth medium supplemented with 10^{-8} to 10^{-6} M Dex in DMSO (Calbiochem, UK)

6.3.4 Prevention of Cell Death

6.3.4.1 Bisphosphonates

Cells were treated for 1 hour with the heterocyclic-containing N-BPs, NEII808 and NEII809 (Procter & Gamble) at concentrations of 10^{-8} to 10^{-6} M in PBS, followed by Dex treatment.

6.3.4.2 Inhibitors of intracellular signalling proteins.

MAPK inhibitors

Cells were incubated for 30 minutes with UO126 (Promega, UK), at concentrations of 20 μM in DMSO (Favata et al. 1998) in order to inhibit MEK 1/2 protein kinase.

6.3.5 Determination of Apoptotic State

6.3.5.1 DAPI staining for healthy and apoptotic cell morphology

Cells were fixed in 4% paraformaldehyde and incubated with DAPI at 2.5 ng/ml in water for 10 minutes, as described in §3.3.10.3.

6.3.5.2 Acridine orange (AO) staining for healthy and apoptotic cell morphology.

Acridine Orange staining was performed as described in §5.3.5.2. Briefly, cells were incubated in Walpole's acetate buffer, stained with AO and examined on an inverted fluorescence microscope.

6.3.5.3 DNA fragmentation using *in situ* Nick Translation

The percentage of target cells demonstrating DNA breaks was investigated using *in situ* nick translation staining (Noble et al. 1997), which allows the determination of DNA breaks following the incorporation of DIG-labelled dUTP as described in §3.3.10.2. The ratio of total cells (PI positive) to apoptotic (FITC positive) was determined using fluorescence microscopy and digital image capture.

6.3.6 Preparation of cell lysates

Cell lysates were prepared as described in §5.3.8 (**Figure 41**). Briefly, cells were lysed on ice and the lysates were either used immediately or stored at –20 °C.

6.3.7 Determination of protein concentration

Protein concentrations in samples were estimated as described in §5.3.9, against standards of BSA within a range of 0-20 μg/ml using an automated plate reader, which measured the absorbance at 570 nm.

6.3.8 Protein gel electrophoresis

Protein extracts were separated by electrophoresis through a polyacrylamide gel containing sodium dodecyl sulphate (SDS), on the basis of molecular weight, as described in § 5.3.10 (**Figure 41**).

6.3.8.1 Electrophoresis reagents.

Tris resolving buffer: 1.5 M Tris base, pH 8.9 and 13.9 mM SDS.

Tris stacking buffer: 0.5 M Tris-HCl, pH 6.8 and 13.9 mM SDS.

Acrylamide/bisacrylamide (Protogel) solution: 30% (w/v) acrylamide and 0.8% (w/v) bisacrylamide.

Ammonium persulphate (APS) solution: 10% (w/v) APS in dH_2O.

Blue loading buffer (2x): 10% (v/v) glycerol, 10% (v/v) β-mercaptoethanol, 0.1M SDS, 6% (w/v) urea, 0.125 M Tris and 0.02% bromophenol blue.

Tris running buffer: 190 mM glycine, 25 mM Tris base and 17 mM SDS.

Resolving and stacking buffers were prepared and allowed to polymerise on gel plates as described in § 5.3.10.2-3.

6.3.8.2 Electrophoresis.

Electrophoresis was carried out as described in §5.3.10.4 at a constant current of 20 mAmps (Power Pac 3000, Bio-Rad, UK).

6.3.9 Western Blot analysis.

6.3.9.1 Transfer of proteins to a polyvinylidene difluoride (PVDF) membrane.

Proteins were transferred onto a PVDF membrane (**Figure 41**) as described in §5.3.11.1 using a Mini trans-Blot Cell Assembly, (Bio-Rad, UK) at 30 V for 1 hour.

6.3.9.2 Detection of proteins on PVDF.

Proteins were detected on PVDF as described in §5.3.11.2. Briefly, proteins were probed with the appropriate primary antibody (rabbit polyclonal antibodies against phosphorylated p44/42 MAPK, p90rsk and c-Raf kinases) followed by a species-specific secondary antibody, and were detected using the Enhanced

Chemiluminscence (ECL) system and autoradiograph film, according to the manufacturer's instructions. (**Figure 41**).

6.3.10 Statistical analysis

Statistical analysis was performed using quantitative data analysis with SPSS release 11.5 for Windows, as described in §3.3.12, using Analysis of Variance (ANOVA), Tukey test and Dunnett test for comparison between the treatment groups. Results are expressed as means ± S.D. $p < 0.05$ was considered to be statistically significant.

6.4 Results

6.4.1 NE11808 and NE11809 prevent Dex-induced apoptosis in MLO-Y4 osteocytes.

Dose response studies were used to identify concentrations of NE11808 and NE11809 that did not increase apoptosis above control levels. (**Figure 63**). Mean percentages of apoptotic osteocytes were statistically different compared to control following treatment with NE11808 at 10^{-6} M, after 5 hours of treatment ($p = 0.03$). The lowest concentration of 10^{-8} M, which did not increase osteocyte apoptosis above control levels for both NE11808 and NE11809 ($p > 0.05$), was chosen to treat osteocytes prior to addition of Dex in cultures. The optimum concentration and incubation period for induction of apoptosis by Dex was identified through concentration- and time-dependent studies, as described in chapter 5 (**Figure 42 and 43**).

Estimation of apoptotic osteocytes based on morphological criteria showed that both NE11808 and NE11809 at 10^{-8} M significantly decreased the pro-apoptotic effect of the corticosteroid at 10^{-6} M, following 5 hours incubation in osteocyte cultures (**Figure 64 and 65**).

6.4.2 NE11808 and NE11809 reduce the Dex-induced activation of ERK1/2 protein kinase.

As described in chapter 5, Dex increased the amount of phosphorylated ERK 1/2 in osteocytes, compared to vehicle, in a time dependent manner, as evidenced by western blot analysis, using an anti-phospho ERK1/2 antibody (**Figure 55**). Activation of ERK 1/2 protein by Dex was detected as soon as 1 minute following treatment and was decreased to basal control levels after 1 hour of treatment. Addition of Dex to cells pre-treated for 1 hour with NE11808 and NE11809 resulted in a reduced activation of ERK 1/2 relative to samples treated with Dex alone (**Figure 66**). The MEK 1/2 protein inhibitor, UO126, blocked Dex-induced ERK 1/2 activation in all cases.

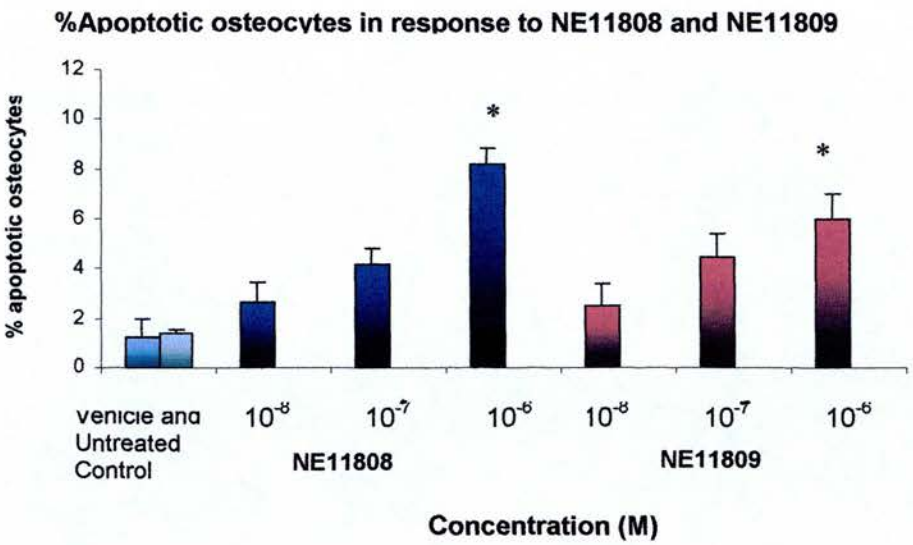

Figure 63. Dose-response studies of NE11808 and NE11809. Osteocytes were incubated with NE11808 and NE11809 at 10^{-8} M to10^{-6} M in order identify concentrations that did not induce osteocyte apoptosis over a period of 6 hours. Graph represents mean percentage of apoptotic osteocytes ± SD, estimated by AO nuclear staining and fluorescence microscopy. ■= control cultures, ■ =untreated cultures. Control cultures represent vehicle (PBS) cultures and are similar to untreated cultures in percentages of apoptotic osteocytes.

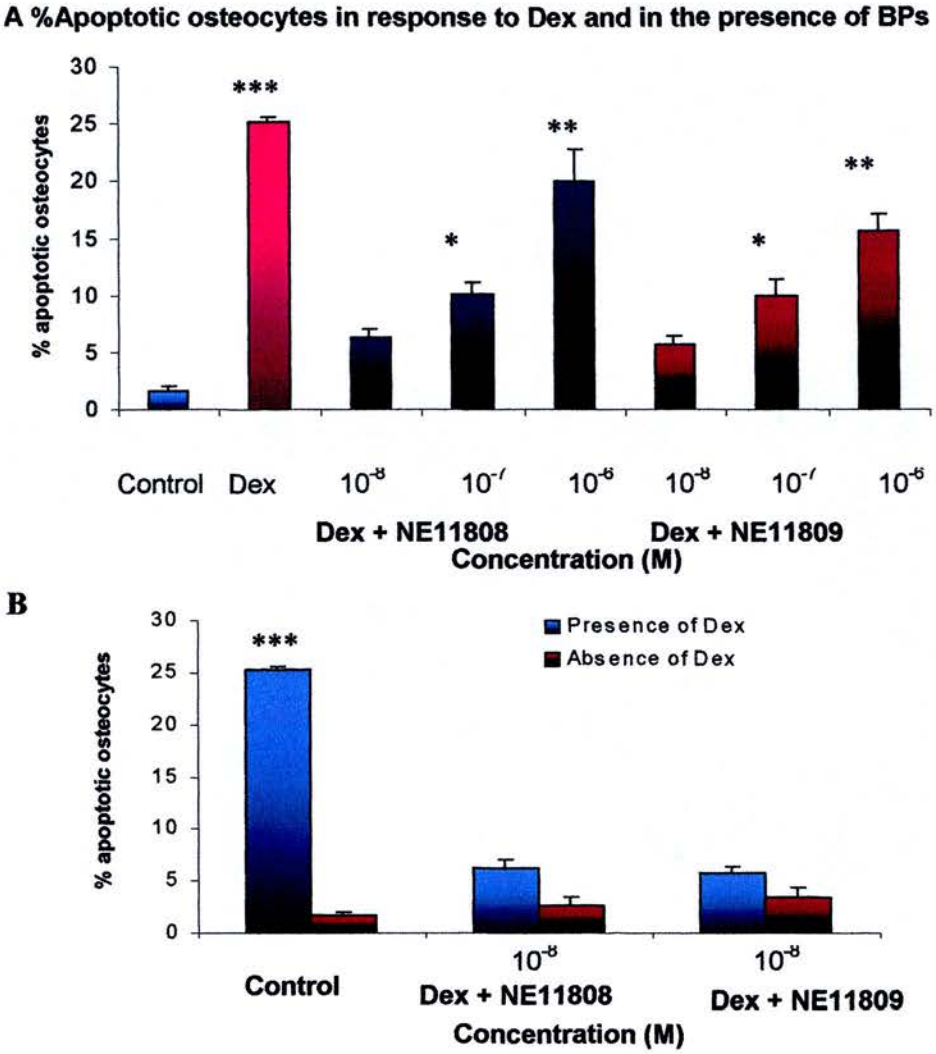

Figure 64. NE11808 and NE11809 prevent MLO-Y4 osteocyte apoptosis induced by Dexamethasone in a concentration-dependent manner. Osteocytes were incubated with BPs at 10^{-8} to 10^{-6} M for 1 hour prior to Dex treatment, for 5 hours. **A.** Percentages of apoptotic osteocytes were statistically different compared to control following treatment with all BPs at 10^{-6} M, in the presence of Dex. **B.** The lowest concentration of 10^{-8} M for both BPs reduced percentages of apoptotic osteocytes to levels similar to control. Graphs represent mean percentages of apoptotic osteocytes ± SE, estimated by AO staining and fluorescence microscopy. ■ =control cultures, ■ =Dexamethasone treated cultures in absence or presence of NE11808 and NE11809. Control cultures represent vehicle (ethanol) cultures for Dex and are similar to untreated cultures in percentages of apoptotic osteocytes (1.42 ± 0.11 % S.D., $p > 0.05$).

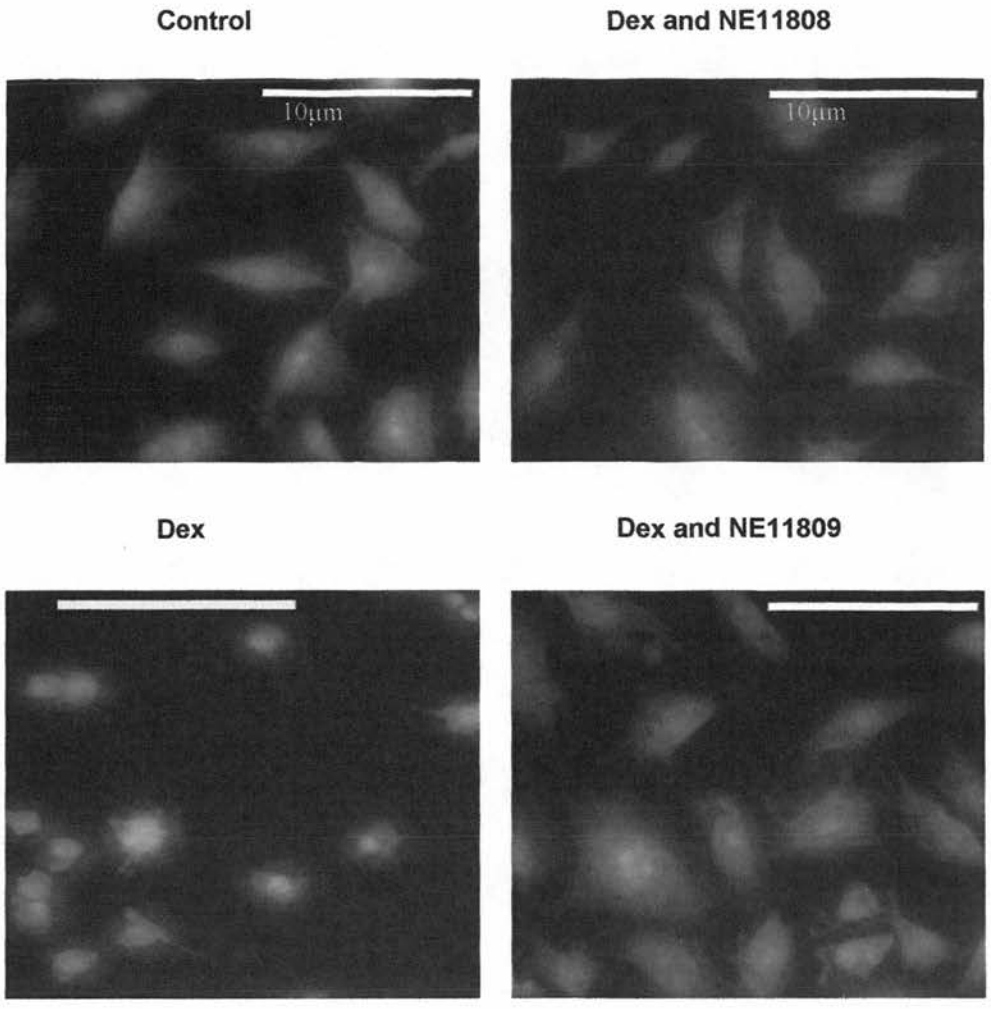

Figure 65. NE11808 and NE11809 prevent Dex-induced apoptosis in MLO-Y4 osteocyte cultures. Representative images of osteocyte cultures treated with NE11808 and NE11809 for 1 hour followed by Dex treatment for 5 hours and stained with Acridine Orange. NE11808 (top right panel) and NE11809 (lower right panel) reduce Dex-induced apoptosis in osteocytes (lower left panel). Bar =10 μm.

A Western Blotting

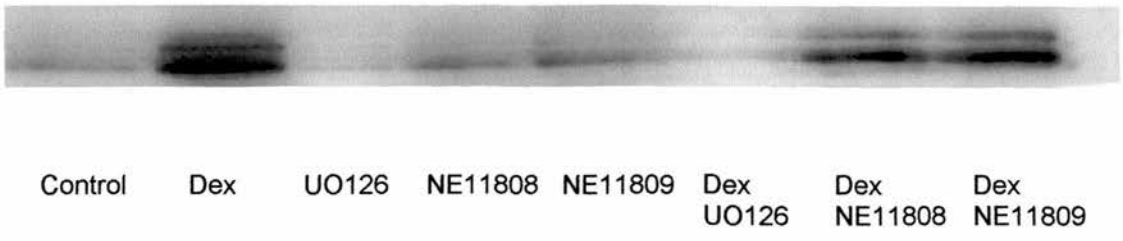

B Band Densitometry

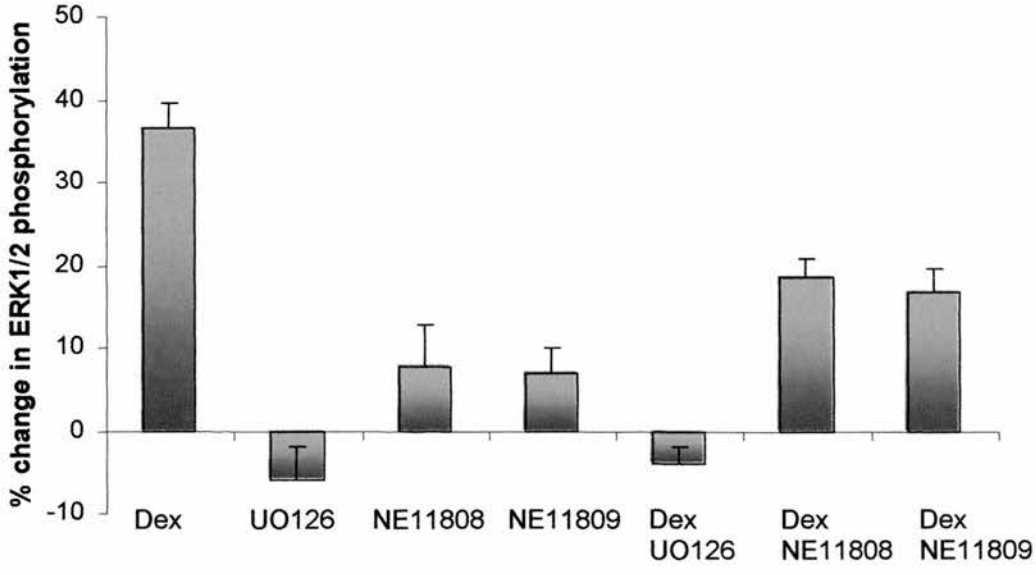

Figure 66. NE11808 and NE11809 reduce Dex-induced ERK 1/2 activation. **A**. Western blot of phosphorylated ERK 1/2 activity in response to Dex, UO126, NE11808 and NE11809. **B**. Mean percentages of changes in ERK 1/2 phosphorylation in response to the different treatments, compared to control. Changes in band densitometry were quantified using NHI image analysis system from 3 independent experiments and expressed as percentage change relative to control samples ± S.D.

6.4.3 NE11808 and NE11809 reduce the Dex-induced activation of p90rsk protein kinase.

In order to characterize further the role of ERK 1/2 pathway in Dex-induced apoptosis, the presence of proteins lying both upstream (c-Raf) and downstream (p90rsk) of ERK 1/2 protein, was investigated. Western blot analysis showed that p90rsk (**Figure 67**) activation by Dex coincided with ERK 1/2 activation, while pre-treatment with NE11808 and NE11809 slightly reduced phosphorylated levels of p90rsk. In addition, UO126 prevented activation of p90rsk by Dex. Levels of c-Raf remained constant and similar to vehicle levels, during all different treatments investigated (**Figure 68**).

6.4.4 Suppression of Dex-induced Fas activation by NE11808 and NE11809.

The role of NE11808 and NE11809 in Dex-induced activation of Fas was investigated by immunocytochemistry studies using an anti-Fas monoclonal antibody (**Figure 69**). Pre-treatment of MLO-Y4 cells with both NE11808 and NE11809 at 10^{-8} M, reduced activation of Fas by Dex ($p = 0.0001$).

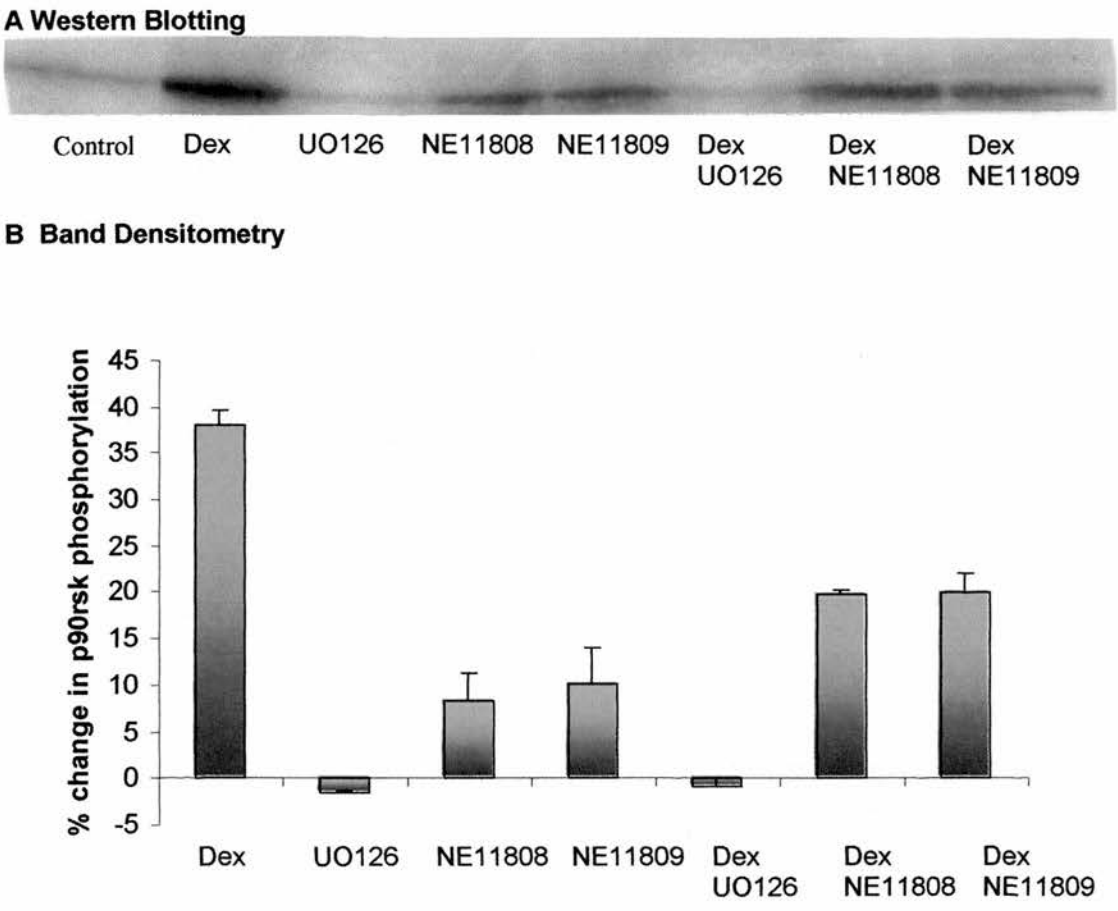

Figure 67. NE11808 and NE11809 reduce Dex-induced p90rsk activation. **A**. Western blot of phosphorylated ERK 1/2 activity in response to Dex, UO126, NE11808 and NE11809. **B**. Mean percentages of changes in p90rsk phosphorylation in response to the different treatments, compared to control. Changes in band densitometry were quantified using NHI image analysis system from 3 independent experiments and expressed as percentage change relative to control samples ± S.D.

A Western blotting

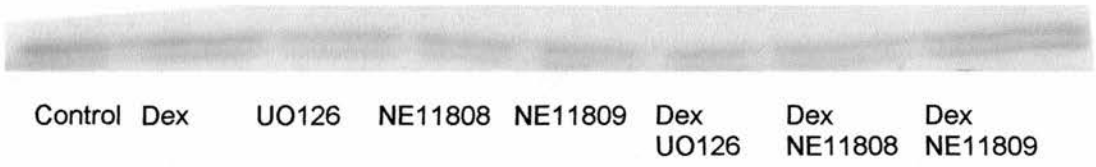

B Band Densitometry

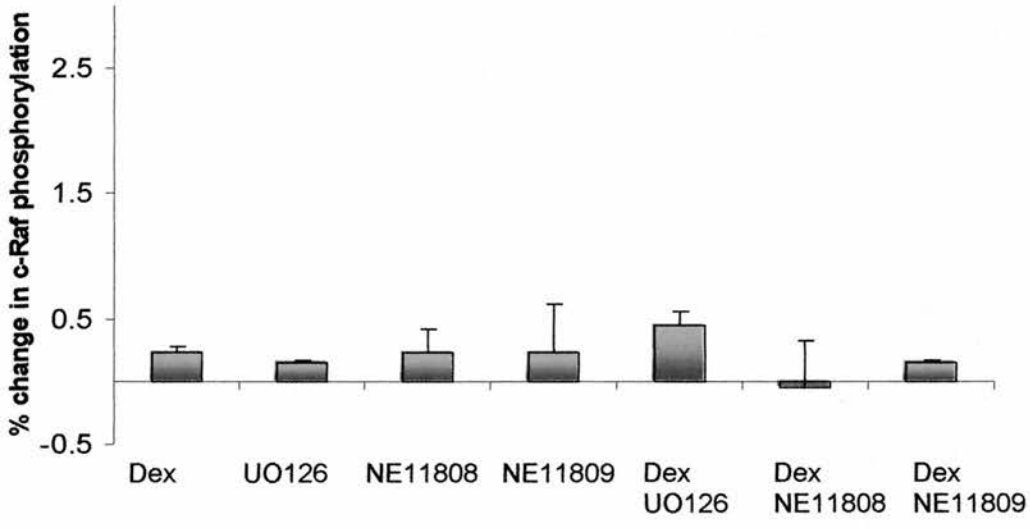

Figure 68. c-Raf activity is not altered in the presence of NE11808, NE11809, Dex and UO126. **A**. Western blot of phosphorylated ERK 1/2 activity in response to Dex, UO126, NE11808 and NE11809. **B**. Mean percentages of changes in c-raf phosphorylation in response to the different treatments, compared to control. Changes in band densitometry were quantified using NHI image analysis system from 3 independent experiments and expressed as percentage change relative to control samples ± S.D.

Fas expression in response to Dex and BP treatment

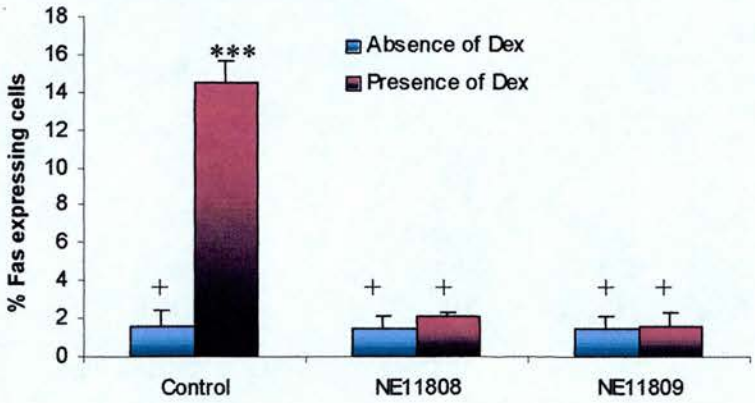

Figure 69. NE11808 and NE11809 suppress Dex-induced Fas expression. NE11808 and NE11809 reduce Dex-induced Fas expression as shown by immunocytochemistry. Cells were probed with an anti-Fas antibody and examined by fluorescence microscopy. Graph represents mean percentages of osteocytes, expressing Fas per number of cells ± S.D (*** = $p < 0.0001$, + = $p < 0.05$ compared to Dex treatment)

6.5 Discussion

This study has shown that NE11808 and NE11809 prevented the pro-apoptotic effects of Dexamethasone in a manner that implicated the ERK 1/2 pathway in osteocyte cultures. Pre-treatment of osteocyte cultures with NE11808 and NE11809 reduced the proportion of osteocytes that displayed chromatin and cytoplasmic condensation and membrane blebbing induced by Dex treatment.

Investigation of the ERK 1/2 pathway revealed that NE11808 and NE11809 reduced the amount of phosphorylated ERK 1/2 and p90rsk protein kinases in osteocytes treated with Dex, pointing to a pro-apoptotic role for the ERK pathway in osteocytes in the presence of Dexamethasone. These findings are in agreement with results from chapter 5, which demonstrated that PAM, ALN and CLO were equally effective inhibitors of Dex-induced apoptosis in osteocytes and reduced activation of ERK and p90rsk proteins, as described in detail in chapter 5.

Bisphosphonates are stable analogues of naturally occurring pyrophosphate compounds, characterised by two C-P bonds located on the same carbon atom which also has two side chains, R1 and R2 (Rodan 1998) (**Figure 60 and Table 1**). All the BP molecules adhere to hydroxyapatite crystals and display anti-resorptive actions. Binding to bone mineral is dependent on the R1 side chain, which acts as a bone hook, while the presence of a –OH group increases the affinity possibly due to tridentate configuration (van Beek et al. 1998). In addition it has been shown that R1 with the phosphonate groups might contribute to the anti-resorptive activity as well, which is however determined mainly by the R2 side chain (Ibbotson et al. 1989) (**Figure 61**).

At the cellular level, the action of BPs is primarily dependent on the presence or absence of a nitrogen group in the R2 side chain. (Fleisch 2000). BPs that do not contain a nitrogen group, like CLO and ETI become metabolised into non-hydrolysable analogues of ATP, initially demonstrated in the cellular slime mould Dictyostelium discoideum (Rogers et al. 1992), which accumulate in the cytoplasm and inhibit numerous intracellular metabolic enzymes (Rodan and Fleisch 1996).

Bisphosphonate molecules	R1 side chain	R2 side chain
Etidronate	OH	CH_3
Clodronate	Cl	Cl
Pamidronate	OH	$CH_2CH_2NH_2$
Alendronate	OH	$(CH_2)_3NH_2$
Risedronate	OH	CH_2-3-pyridine
Ibandronate	OH	$CH_2CH_2N(CH_3)$(pentyl)
Zoledronate	OH	CH_2-imidazole
Incadronate	H	N-(cyclo-heptyl)
Olpadronate	OH	$CH_2CH_2N(CH_3)_2$
Neridronate	OH	$(CH_2)_5NH_2$
EB-1053	OH	CH_2-1-pyrrolidinyl
Tiludronate	H	CH_2-S-phenyl-Cl

Table 1. R1 and R2 side chains of commonly used Bisphosphonates.

In particular it has been shown that CLO becomes metabolised into AppCCl2p, which inhibits the mitochondrial electrogenic ATP/ADP translocase, inducing membrane depolymerisation, cytochrome c release, caspase activation (Benford et al. 2001) and finally apoptosis (Lehenkari et al. 2002).

N-containing BPs appear to inhibit farnesyl diphosphate (FPP) synthase, an enzyme in the mevalonate pathway, leading to a decrease in the synthesis of geranylgeranyl diphosphate (GPP) (Benford et al. 1999). This enzyme is responsible for the production of cholesterol and isoprenoid lipids, which are required for the post-translational modification and hence function of small GTPases, such as Ras, Rho and Rac, which regulate several functions including membrane ruffling, morphology and survival in osteoclasts and macrophages (Coxon et al. 1998, Rogers et al.1999). Similar action by N-BPs which results in apoptotic cell death through inhibition of the mevalonate pathway has been shown both in vitro (Shipman et al.1998) and in vivo (Gordon et al. 2002) in myeloma cells, demonstrating an important anti-tumour activity by BPs (Croucher et al. 2003), while induction of apoptosis in Caco-2 human epithelial cells, might account for the gastrointestinal toxicity observed by N-BPs (Suri et al. 2001). Interestingly, however, it has been demonstrated that unlike the non N-BPs, induction of apoptosis by N-BPs is not necessary to prevent osteoclastic resorption, since at lower doses they have been shown to potently inhibit bone resorption without inducing osteoclast apoptosis (Halasy-Nagy et al. 2001).

Recently N-BPs have been developed that are more potent inhibitors of bone resorption and in addition to inhibiting FPP synthase, they also prevent isopentenyl diphosphate isomerase (Thompson et al. 2002), indicating that small modifications in the structure and conformation of the R2 side chain can dramatically affect the anti-resorptive activity of N-BPs and suggest that the nitrogen group and the R2 side chain have an important role in the interaction between BPs and the pharmacological target (Ebetino et al. 1996). These observations have allowed the conclusion that there is a clear correlation between the activity of BPs to inhibit osteoclast resorption and the three-dimensional structure of the molecules.

This study has used the third generation N-BPs NE11808 and NE11809 for which clear structure/activity relationships have been observed in the past (Rogers et al. 1995). NE11808 and NE11809 contain a heterocyclic-group in the R2 side chain, while they lack a –OH group in the R1 side chain (**Figure 62**) which confers increased binding affinity to bone minerals, possibly due to tridentate configuration (van Beek et al. 1998). This might indicate that these two BPs do not adhere strongly to hydroxyapatite crystals; however no relationship has been reported between anti-resorptive activity and decreased binding to bone mineral. NE11808 and NE11809 have similar chemical structures (**Figure 62**); however they differ in the presence of a methyl group in NE11809, which dramatically reduces the anti-resorptive potency of NE11809, compared to NE11808, in rodents *in vivo* (Rogers et al. 1995). In addition, recent studies by Dunford et al. have shown that NE11809 has a reduced ability, compared to NE11808 to inhibit farnesyl diphosphate (FPP) synthase, which correlates with the reduced anti-resorptive activity of the molecule (Dunford et al. 2001). Furthermore, it has been observed for strong anti-resorptive BPs, such as RIS and NE11808, that there is a close overlap between the nitrogen group in their three-dimensional structures, in contrast to NE11809, which has a weak anti-osteoclastic activity, indicating that location of the nitrogen group at a fixed position provides strong anti-resorptive potency to BPs (Ebetino et al. 1995).

Both NE11808 and NE11809 were equally effective inhibitors of death at doses of 10^{-8} M, in this study, indicating that prevention of Dex-induced osteocyte apoptosis by BPs does not depend on inhibition of FPP synthase or on structure/activity relations of BP molecules. Although it has not been investigated in this thesis, it might be possible that both BPs reduce the availability of Ca^{2+} by acting as Ca^{2+} chelators or the protective effects might be due to an as yet unidentified mechanism of bisphosphonate action. These findings confirm the protective role of BPs on osteocytes as demonstrated in chapter 5 and open up new areas of research in the field of glucocorticoid-induced osteoporosis as minor modifications in the structure or conformation of the R2 side chain might enable BP molecules to be independently applied to affect osteoclast activity or osteocyte survival.

SECTION 4

Conclusions and Future work

Conclusions and Future work

Bone adapts to changes in its form and function by inducing alterations in its structure and shape, through the targeted activity of the bone remodelling process. Since the osteocyte is located within the bone matrix and forms an extensive network of canalicular processes, it has been proposed to act as the cell that senses mechanical strains and accordingly transmits signals to osteoblasts and osteoclasts that direct the remodeling process.

Co-localization has been established between apoptosis of the osteocytes and the targeted activity of specific bone resorbing cell types. (Noble et al. 1997, Noble et al. 2003). However, previously no specific behavior of osteoclasts or osteoblasts had been linked with the process of osteocyte apoptotic death. This thesis has provided evidence that demonstrate for the first time a direct effect on osteoblasts following interaction with products derived from apoptotic osteocytes. Osteocyte apoptotic bodies induced the apoptotic death of osteoblasts, while ingestion of apoptotic bodies derived from a range of other cell types did not affect osteoblast viability. In addition, osteocyte apoptotic bodies did not induce an apoptotic response to cells other than osteoblasts.

These findings provide a functional role for osteocyte apoptosis in bone and imply that osteocyte apoptosis occurs in order to target a specific area that requires remodelling, according to mechanical stimuli, by inducing the apoptotic death of osteoblasts lining the bone surface, which possibly provides the signals that attract osteoclasts to that area and initiate bone resorption. Although these data point to a biological significance for osteocyte apoptosis in bone, certain questions remain to be answered as to the events that occur downstream of interaction of apoptotic osteocytes with osteoblasts. Further studies are required to identify factors released during osteoblast apoptosis, including cytokines and growth factors, which possibly attract osteoclasts into that specific area, targeting the resorption process. In addition, it appears very important to understand the identity of osteocyte apoptotic bodies, that is the molecular signature that enables them to induce specific responses to some cells but not others. Evidence provided in this

thesis point to the existence of a specific osteocytic marker, since vesicles from cells of osteoblastic and other lineages did not induce similar phenomena, indicating that this marker is responsible for the functional identity of osteocytes. Characterisation of this factor could be possible through the use of 2-D gel electrophoresis and proteomics analysis, which will enable the production of extensive protein maps unique to osteocytes. This approach will involve comparison of the membrane-associated and cytoplasmic protein composition between OAB and apoptotic products derived from different cell types. Based on data provided in this thesis, it appeared that a membrane associated protein on OAB might be mediating the OAB-induced osteoblast apoptotic response. Therefore, the proteomics analysis in combination with appropriate treatment of the samples, will allow the identification of this factor, whether it is unique to OAB, or whether it contains different glycosylation patterns for example, compared to apoptotic bodies from different cell types. Based on the results obtained using this approach it might be possible to raise functional antibodies against this factor or to silence target genes in osteocyte cultures, in order to determine their role in physiological and pathological conditions.

Having identified biological significance I also looked at ways to control the apoptosis of osteocytes. Data in this thesis have provided evidence on some of the pathways that Dexamethasone possibly engages to induce apoptosis in osteocytes. In addition it has been demonstrated that Bisphosphonates protect osteocytes from the adverse effects of glucocorticoid use in a manner that is independent of their activity and potency against osteoclasts and bone resorption. Further studies are required to determine whether all bisphosphonates use a common signalling pathway in osteocytes that also interacts at some point with pathways used by Dexamethasone during induction of osteocyte apoptosis. This information could allow manipulation of the apoptotic and survival pathways engaged by BPs and Dex in order to maintain the osteocyte population and/or control osteocyte apoptosis.

Most bone-related diseases arise due to imbalances between the processes of bone formation and bone resorption. Previous findings which have shown that osteocyte apoptosis might be directing the activity of osteoclasts to particular sites in bone requiring remodeling, along with the findings provided in this thesis that osteocyte apoptosis directly influences the behaviour of osteoblasts by inducing their apoptotic death, might provide the basis for the development of novel therapeutic interventions in bone pathology. Such novel approaches could involve the targeting of pathways that mediate apoptosis in osteocytes in order to induce or prevent apoptosis by using functional apoptosis-related antibodies or by applying mechanical loading as it has been shown previously. It might also be possible having characterised the unique osteocytic factor that is responsible for inducing osteoblast apoptosis to directly influence the behaviour of osteoblasts at particular sites in order to initiate the turnover process. In addition, further work is required to understand the functional significance of apoptosis itself and how it relates to the physiological function of tissues.

References

Aarden, E., Burger, E., Nijweide, P. Function of osteocytes in bone. *J.Cell Biochem* 1994, 55:287-299.

Aarden, E., Wasenaar, A., Alblas, M., Nijweide, P. Immunocytochemical demonstration of extracellular matrix proteins in isolated osteocytes. *Histochem.Cell Biol* 1996, 106:495-501.

Abrams, J., White, K., Fessler, L. Steller, H. Programmed cell death during Drosophila embryogenesis. *Development* 1993, 117:29-43.

Adami, S. and Zamberlan, N. Adverse effects of bisphosphonates: A comparative review. *Drug.Saf* 1996, 14 (3):158-170.

Adams, C., Mansfield, K., Perlot, R., Sharipo, I. Matrix regulation of skeletal cell apoptosis. Role of calcium and phosphate ions. *J.Biol.Chem* 2001, 276(23):20316-20322.

Adams, J. and Cory, S. The Bcl-2 protein family: arbiters of cell survival. *Science* 1998, 281:1322-1326.

Agnani, G., Tricot-Doleux, S., Houalet, S., Bonnaure-Mallet, M. Epithelial cell surface sites involved in the polyvalent adherence of porphyromonas gingivalis: a convincing role for neuraminic acid and glucuronic acid. *Infection Immun.* 2003, 71(2):991-996.

Ahuja, S., Zhao, S., Bellido, T., Plotkin, L., Jimenez, F., Bonewald, L. CD40 ligand blocks apoptosis induced by tumour necrosis factor a, glucocorticoids, and etoposide in osteoblasts and the osteocyte-like cell line murine long bone osteocyte Y4. *Endocrinology* 2003, 144(5):1761-1769.

Ajubi, N., Klein-Nulend, J., Alblas, M., Burger, E., Nijweide, P. Signal transduction pathways involved in fluid flow-induced PGE_2 production by cultured osteocytes. *Am.J Physiol* 1999, 276:E171-178.

Albert, M., Jegathesan, M., Darnell, R. Dendritic cell maturation is required for the cross-tolerization of CD8+ T cells. *Nat.Immunol.* 2001, 2(11):1010-7.

Albert, M., Pearce, S., Francisco, L., Sauter, B., Roy, P., Silverstein, R., Bhardwaj, N. Immature dendritic cells phagocytose apoptotic cells via alphavbeta5 and CD36, and cross-present antigens to cytotoxic T lymphocytes. *J.Exp.Med.* 1998, 188(7):1359-68.

Alessandrini, A., Namura, S., Moskowitz, M., Bonventre, J. MEK1 protein kinase inhibition protects against damage resulting from focal cerebral ischemia. *PNAS* 1999, 96:12866-12869.

Allen, R., Cluck, M., Agrawal, D. Mechanism controlling cellular suicide: role of Bcl-2 and caspases. *Cell Mol.Life Sci.* 1998, 54(5): 427-445.

Amano, T., Tanabe, K., Eto, T., Narumiya, S., Mizuno, K. LIM-kinase 2 induces formation of stress fibres, focal adhesions and membrane blebs, dependent on its activation by Rho-associated kinase-catalysed phosphorylation at threonine-505. *Biochem.J.* 2001, 354: 149-159.

Ashkenazi, A. and Dixit, V. Death Receptors: signalling and modulation. *Science* 1998, 281:1305-1308.

Ashwell, J., Lu, F., Vacchio, M. Glucocorticoids in T cell development and function. *Annu.Rev.Immunol.* 2000, 18:309-345.

Aupeix, K., Hugel, B., Martin, T., Bishoff, P., Lill, H., Pasquali, J., Freussinet, J. The significance of shed membrane particles during programmed cell death in vitro and in vivo, in HIV-1 infection. *J.Clin.Invest* 1997, 99(7):1546-1554.

Balemans, W., Ebeling, M., Patel N, Van Hul, E., Olson, P., Dioszegi, M., Lacza, C., Wuyts, W., Van Den Ende, J., Willems, P., Paes-Alves, A., Hill S, Bueno M, Ramos, F., Tacconi. P, Dikkers, F., Stratakis, C., Lindpaintner, K, Vickery, B., Foernzler, D., Van Hul, W. Increased bone density in sclerosteosis is due to the deficiency of a novel secreted protein (SOST). *Hum.Mol.Genet.* 2001, 10:537–543.

Baron, R. Anatomy and ultrastructure of bone. Primer on the metabolic bone diseases and disorders of mineral metabolism, Lippincott-Raven, New York, 1996, 3-10.

Beavan, S., Horner, A., Bord, S., Ireland, D., Compston, J. Colocalization of glucocorticoid and mineralocorticoid receptors in human bone. *Bone.Miner.Res* 2001, 16(8): 1496-504.

Becq, F., Hamon, Y., Bajetto, A., Gola, M., Verrier, B., Chimini, G. ABC1, and ATP binding cassette transporter required for phagocytosis of apoptotic cells, generates a regulated anion flux after expression in Xenopus laevis oocytes. *J.Biol.Chem* 1997, 272:2695-2699.

Belanger, L., Robichon, J., Migicovsky, B., Copp, D., Vincent, J. Resorption without osteoclasts (osteolysis). Mechanisms of hard tissue destruction. American Association for the advancement of Science, R. Sognnaes, ed., Washington DC, 1963, 531-556.

Bellone, M., Iezzi, G., Rovere, P., Galati, G., Ronchetti, A., Protti, M., Davoust, J. Rugarli, C., Manfredi, A. Processing of engulfed apoptotic bodies yields T cell epitopes. *J.Immunol* 1997, 59(11):5391-9.

Benford, H., Frith, C., Auriola, S., Monkkonen, J., Rogers, M. Farnesol and geranylgeraniol prevent activation of caspases by aminobisphosphonates: biochemical evidence for two distinct pharmacological classes of bisphosphonate drugs. *Mol. Pharmacol* 1999, 56:131-140.

Benford, H., McGowan, N., Helfrich, M., Nuttall, M., Rogers, M. Visualization of bisphosphonate-induced caspase-3 activity in apoptotic osteoclasts in vitro. *Bone* 2001, 28(5):465-73.

Bengtsson, T., Jaconi, M., Gufstafson, M., Magnusson, K., Theler, J., Lew, D., Stendahl, O. Actin dynamics in human neutrophils during adhesion and phagocytosis is controlled by changes in intracellular free calcium. *Eur.J. Cell Biol* 1993, 62: 49-58.

Bijlsma, J. Glucocorticoids and rheumatoid arthritis. Glucocorticoids and bone: the clinical problem. Boerhaave Committee for Postgraduate Education of medicine, Leiden University, The Netherlands, 1997, 29-36.

Bills, C., Eisenberg, H., Pallante, S. Complexes of organic acids with calcium phosphate: the Von Kossa stain as a clue to the composition of bone mineral. *Johns Hopkins Med.J.* 1974, 128(4):194-207.

Blair, H. How the osteoclast degrades bone. *BioEssays* 1998, 29: 837-846.

Blajeski, A, Phan, V, Kettke, T, Kaufmann, S. G(1) and G(2) cell-cycle arrest following microtubule depolymerisation in human breast cancer cells. *JClin.Invest* 2002, 110(1):91-9.

Boabaid, F, Cerri, P, Katchburian, E. Apoptotic bone cells may be engulfed by osteoclasts during alveolar bone resorption in young rats. *TissueCell* 2001,33(4):318-325.

Boivin, G., Mesguich, P., Pike, J., Bouillon, R., Meunier, P., Haussler, M., Dubois, P., Morel, G. Ultrastructural immunocytochemical localization of endogenous 1,25-dihydroxyvitamin D3 and its receptors in osteoblasts and osteocytes from neonatal mouse and rat calvaria. *Bone.Miner* 1987, 3(2): 125-36.

Bonewald, L., Zhao, Y, Harris, S. Expression of the osteocytic-specific antigen, E11, in MLO-Y4 cells and mineralising osteoblasts. *JBMR* 2000, 15 (Suppl):S502.

Boot-Handford, R., Michaelidis, T., Hillarby, M., Zambelli, A., Denton, J., Hoyland, J., Freemont, A., Grant, M., Wallis, G. The bcl-2 knockout mouse exhibits marked changes

in osteoblast phenotype and collagen deposition in bone as well as a mild growth plate phenotype. *Int.J.Exp.Pathol.* 1998, 79(5):329-35.

Boyde, A. Evidence against 'osteocyte osteolysis'. *Metab.Bone.Dis.Rel.Res* 1980, S239-255.

Boyden, L., Mao, J., Belsky, J., Mitzner, L., Farhi, A., Mitnick, M., Wu, D., Insogna, K., Lifton, R. High bone density due to a mutation in LDL-receptor-related protein 5. *N. Engl.J.Med* 2002, 346:1513–1521.

Bradford M. A rapid and sensitive method for the quantitation of microgram quantities of protein utilizing the principle of protein-dye binding. *Anal.Biochem* 1976, 72:248-54.

Breiteneder-Geleff, S., Matsui, K., Soleiman, A., Meraner, P., Poczewski, H., Kalt, R., Schaffner, G., Kerjaschski, D. Podoplanin, novel 43-kDa membrane protein of glomelular epithelial cells, is down-regulated in puromycin nephrosis. *Am.J.Path* 1997, 151:1141-1152.

Bronckers, A., Goei, W., van Heerde, W., Dumont, E., Reytelingsperger, C., van den Eijnde, S. Phagocytosis of dying chondrocytes by osteoclasts in the mouse growth plate as demonstrated by annexin-V labeling. *Cell Tiss.Res* 2000, 301 (2): 267-272.

Brown, S., Heinisch, I., Ross, E., Kate, S., Buckley, C., Savill, J. Apoptosis disables CD31-mediated cell detachment from phagocytes promoting bonding and engulfment. *Nature* 2002, 418, 200-203.

Brown, S. and Savill, J. Phagocytosis triggers macrophage release of fas ligand and induces apoptosis of bystander leucocytes. *J.Immunol.* 1999, 162:480-485.

Brunkow, M, Gardner, J, Van Ness, J, Paeper, B, Kovacevich, B, Proll, S, Skonier, J, Zhao, L, Sabo, P, Fu, Y, Alisch, R., Gillett, L, Colbert, T, Tacconi, P, Galas, D, Hamersma, H, Beighton, P, Mulligan, J. Bone dysplasia sclerosteosis results from loss of the SOST gene product, a novel cysteine knot-containing protein. *Am.J.Hum.Genet* 2001, 68:577–589.

Burakov, A., Nadezhdina, E., Slepchenko, B., Rodionov, V. Centrosome positioning in interphase cells. *J.Cell Biol.* 2003, 162(2):963-9.

Burger, E., Klein-Nulend, J., Smit, T. Strain-derived canalicular fluid flow regulates osteoclast activity in a remodelling osteon-a proposal. *J.Biomech.* 2003, 36:1453-1459.

Burr, D. Targeted and nontargeted Remodeling. *Bone* 2002, 30 (1): 2-4.

Burr, D. and Martin, R. Calculating the probability that microcracks initiate resorption spaces. *J.Biomech.* 1993, 26(4-5):613-6.

Buttery, L., Aguirre, I., Hukkanen, M., Mancini, L., Moradi-Bidhendi, N., Huang, P., MacIntyre, I., Polak, J. Nitric oxide stimulates osteoblast replication and development. *JBMR* 1999, 14:1154.

Canbay, A, Feldstein, A., Higuchi, H., Werneburg, N., Grambihler, A., Bronk, S., Gores, G. Kupffer cell engulfment of apoptotic bodies stimulates death ligand and cytokine expression. *Hepatology*. 2003b, 38(5):1188-98.

Canbay, A., Taimr, P., Torok, N., Higuchi, H., Friedman, S., Gores, G. Apoptotic body engulfment by a human stellate cell line is profibrogenic. *Lab.Invest*. 2003a, 83(5):655-63.

Cannon, G. and Swanson, J. The macrophage capacity for phagocytosis. *J.Cell Sci.* 1992, 101:907-13.

Carter, D., and Orr, T. Skeletal development and bone functional adaptation. *JBMR* 1992, 7(2): S389-395.

Carter, D., van der Meulen, M., Beaupre, G. Mechanical factors in bone growth and development. *Bone* 1996, 18(1), 5S-10S.

Casciola-Rosen, L., Rosen, A., Petri, M., Schlissel, M. Surface blebs on apoptotic cells are sites of enhanced procoagulant activity: Implications for coagulation events and antigenic spread in systemic lupus erythematosus. *PNAS* 1996, 93:1624-1629.

Catz, S., Speziale, E., Sterin-Speziale, N. Polyphosphoinositide synthesis in human neutrophils. Effects of a low metabolic energy state. *Prostaglandins Other Lipid Mediat.* 1998, 55(4):245-64.

Cerri, P., Boabaid, F., Katchburian, E. Combined TUNEL and TRAP methods suggest that apoptotic bone cells are inside vacuoles of alveolar bone osteoclasts in young rats. *J.Periodontal Res*. 2003, 28:223-6.

Chen, J. and Horwitz, S. Differential mitotic responses to microtubule-stabilizing and destabilizing drugs. *Cancer Res*. 2002, 62:1935-1938.

Chen, R., Liu, H., Lin, Y., Jean, W., Chen, J., Wang, J. Nitric oxide induces osteoblast apoptosis through the de novo synthesis of Bax protein. *J.Orthop.Res* 2002, 20:295-302.

Chen, W., Frank, M.E., Jin, W., Wahl, S. TGF-beta released by apoptotic T cells contributes to an immunosuppressive milieu. *Immunity* 2001, 14(6):715-25.

Cheng, B., Kato, Y., Shujie, Z., Luo, J., Sprague, E., Bonewald, L., Jiang, J. PGE_2 is essential for gap junction-mediated intercellular communication between osteocytes-like MLO-Y4 cells in response to mechanical strain. *Endocrinology* 2001,142(8):3464-3473.

Cherian, P., Cheng, B., Gu, S., Sprague, E., Bonewald, L., Jiang, J. Effects of mechanical strain on the function of gap junctions in osteocytes is mediated through the prostaglandin EP2 receptor. *J.Biol.Chem.* 2003, 278(44):43146-56.

Cho, J., Balasubramanyam, M., Chernaya, G., Gardner, J., Aviv, A., Reeves, J. Dargis, P., Christian, E. Oligomycin inhibits store-operated channels by a mechanism independent of its effects on mitochondrial ATP. *Biochem.J* 1997, 324: 971-980.

Coleman, M., Olson, M. Rho GTPase signalling pathways in the morphological changes associated with apoptosis. *Cell Death Diff.* 2002, 9: 493-504.

Coleman, M., Sahai, E., Yeo, M., Bosch, M., Dewar, A., Olson, M. Membrane blebbibg during apoptosis results from caspase-mediated activation of ROCKI. *Nat.Cell Biol.* 2001, 3: 339-345.

Compston, J. Glucocorticoids, bone loss and inflammatory bowel disease. Glucocorticoids and bone: the clinical oroblem, Boerhaave Committee for Postgraduate Education of medicine, Leiden University, The Netherlands, 1997, 47-56.

Conaway, H, Grigorie, D, Lerner, U. Stimulation of neonatal mouse calvarial bone resorption by the glucocorticoids hydrocortisone and Dexamethasone. *JBMR*1996, 10:1419-29.

Corradin, S., Buchmuller-Rouiller, Y., Mauel, J. Phagocytosis enhances murine macrophage activation by interferon-gamma and tumor necrosis factor-alpha. *Eur.J. Immunol* 1991, 21(10):2553-8.

Corral, D., Amling, M., Priemel, M., Loyer, E., Fuchs, S., Ducy, P., Baron, R., Karsenty, G. Dissociation between bone resorption and bone formation in osteopenic transgenic mice. *PNAS* 1998, 95(23):13835-40.

Cotman, C. and Anderson, A. A potential role for apoptosis in neurodegeneration and Alzheimer's disease. *Mol.Neurobiol.* 1995, 10:19.

Cowden, R. and Curtis, S. Microfluorometric investigations of chromatin structure. I. Evaluation of nine DNA-specific fluorochromes as probes of chromatin organization. *Histochemistry* 1981, 72(1):11-23.

Cox, D., Tseng, C., Bjekic, G., Grenberg, G. A requirement for phosphatidylinositol-3 Kinase in pseudopod extension. *J.Biol.Chem* 1999, 274(3):1240-1247.

Coxon, F., Benford, H., Russell, R., Rogers, M. Protein synthesis is required for caspase activation and induction of apoptosis by bisphosphonate drugs. *Mol.Pharmacol.* 1998 ,54(4):631-8.

Croucher, P, De Hendrik, R, Perry, M, Hijzen, A., Shipman, C, Lippitt, J, Green, J., Van Marck, E, Van Camp, B, Vanderkerken, K. Zoledronic acid treatment of 5T2MM-bearing mice inhibits the development of myeloma bone disease: evidence for decreased osteolysis, tumor burden and angiogenesis and increased survival. *JBMR*2003, 18(3):482-92.

Cuenda, A., Rouse, J., Dosa, Y.N., Meier, R., Cohen, P., Gallagher, T., Young, P., Lee, J. SB 203580 is a specific inhibitor of a MAP kinase homologue which is stimulated by cellular stresses and interleukin-1. *FEBS Letters* 1995, 364: 229-233.

da Silva Correia, J., Soldau, K., Christen, U., Tobias, P., Ulevitch, R. Lipopolysaccharide is in close proximity to each of the proteins in its membrane receptor complex. Transfer from CD14 to TLR4 and MD-2. *J.Biol.Chem* 2001, 276(24): 21129-35.

Dairaku, N., Kato, K., Honda, K., Koike, T., Iijima, K., Imatani, A., Sekine, H., Ohara, S., Matsui, H., Shimosegawa, T. Oligomycin and antimycin A prevent nitric oxide-induced apoptosis by blocking cytochrome C leakage. *J.Lab.Clin.Med.* 2004, 143(3):143-51.

Damoulis, P., Hauschka, P. Nitric oxide acts in conjunction with pro-inflammatory cytokines to promote cell death in osteoblasts. *JBMR* 1997, 12:412-23.

Decaudin, D., Marzp, I., Brenner, C., Kroemer, G. Mitochondria in chemotherapy-induced apoptosis: A prospective novel target of cancer therapy (Review). *Int.J.Oncol* 1998, 12: 141-152.

Dekhuijzen, P. and Bootsma, G. Glucocorticoids and airways disease. Glucocorticoids and bone: the clinical problem, Boerhaave Committee for Postgraduate Education of medicine, Leiden University, The Netherlands, 1997, 37-45.

Dempster, D., Moonga, B., Stein, L., Horbert, W., Antakly, T. Glucocorticoids inhibit bone resorption by isolated rat osteoclasts by enhancing apoptosis. *J.Endocrinol.* 1997, 3:397-406.

Devitt, A., Moffatt, O, Raykundalia, C, Capra, J, Simmons, D, Gregory, C.Human CD14 mediates recognition and phagocytosis of apoptotic cells. *Nature* 1998, 392:505-509.

Dini, L., Lentini, L., Diez, G., Rocha, M., Falasca, L., Serafino, L., Vidal-Vanaclocha, F Phagocytosis of apoptotic bodies by liver endothelial cells. *J.Cell Sci* 1995,108:967-973

Divieti, P., Inomata, N. Chapin, K., Singh, R., Juppner, H., and Bringhurst, F. Receptors for the carboxyl-terminal region of PTH (1-84) are highly expressed in osteocytic cells. *Endocrinology* 2001,142 (2):916-925.

Doty, S. Morphological evidence of gap junctions between bone cells. *Calci.Tissue Int.* 1981, 33:509-512.

Dragovich, T., Rudin, C., Thompson, C. Signal transduction pathways that regulate cell survival and cell death. *Oncogene* 1998, 17:3207-3213.

Ducy, P., Schinke, T., Karsenty, G. The Osteoblast: A sophisticated fibroblast under central surveillance. *Science* 2000, 289:1501-1504.

Duffield, J., Ware, C., Ryffel, B., Savill, J. Suppression by apoptotic cells defines tumor necrosis factor-mediated induction of glomerular mesangial cell apoptosis by activated macrophages. *Am.J.Pathol.* 2001, 159(4):1397-404

Dunford, J., Thomsom, K., Coxon, F., Luckman, S., Hahn, F., Poulter, C., Ebetino, F., Rogers, M. Structure-activity relationships for inhibition of farnesyl diphosphate synthase in vitro and inhibition of bone resorption in vivo by nitrogen-containing bisphopshonates. *J.Pharm.Exper.Therap.* 2001, 297(2): 235-242).

Dunstan, C., Somers, N., Evans, R. Osteocyte death and hip fractures. *Calc.Tissue.Int* 1993, 53:S113-S117.

Duvall, E, Wyllie, A, Morris, R. macrophage recognition of cells undergoing programmed cell death (apoptosis). *Immunology* 1985, 56(2):351-8

Eagar, T., Tang, Q., Wolfe, M., He, Y., Pear, W., Bluestone, J. Notch 1 signaling regulates peripheral T cell activation. *Immunity* 2004, 20(4):407-15.

Ebetino, F., Bayless, A., Amburgey, J., Ibbotson, K., Dansereau, S., Ebrahimpour, A. Elucidation of a pharmacophore for the bisphosphonate mechanism of bone resorptive activity. *Phosphorus Sulfur Silicon* 1996, 109–110:217–220.

Ebetino, F. and Dansereau, S. Bisphosphonate antiresorptive structure activity relationships, in Bisphosphonate on Bones. (Bijvoet OLM, Fleisch HA, Canfield RE and Russell RGG eds), 1995, pp 139–153, Elsevier Publishing Co., Amsterdam.

Einhorn, T. The bone organ system: Form and function. Osteoporosis, 1996, R. Marcus, D. Feldman and J. Kelsey, eds., Academic Press, California, 3-21.

Ellis, H. and Horvitz, H. Genetic control of programmed cell death in the nematode C. elegans. *Cell* 1986, 44817-44829.

Epstein, S. Post-transplantation bone disease: the role of immunosuppressive agents and the skeleton. Glucocorticoids and Bone: the Clinical Problem, Boerhaave Committee for Postgraduate Education of medicine, Leiden University, The Netherlands, 1997, 59-73.

Fadok, V., Bratton, D., Henson, P. Phagocyte receptors for apoptotic cells: recognition, uptake, and consequences. *J.Clin.Invest* 2001, 108:957-962.
Fadok, V., Bratton, D., Rose, D., Pearson, A., Ezekewitz, R., Henson, P. A receptor for phosphatidylserine-specific clearance of apoptotic cells. *Nature* 2000, 405:28-9

Fadok, V., Warner, M., Bratton, D., Henson, P. CD36 is required for phagocytosis of apoptotic cells by human macrophages that use either a phosphatidylserine receptor or the vitronectin receptor (alpha v beta 3). *J.Immunol.* 1998, 161(11):6250-7

Favata, M., Horiuchi, K., Manos, E., Daulerio, A., Stradley, D., Feezer, W., Van Dyk, D., Pitts, W., Earl, R., Hobbs, F., Copeland, R., Magolda, R., Scherle, P., Trzaskos, J. Identification of a Novel Inhibitor of Mitogen-activated Protein Kinase Kinase. *J.Biol Chem* 1998, 273(29): 18623-18632.

Fedier, A and Keeller, H. Suppression of bleb formation, locomotion and polarity of Walker carcinosarcoma cells by hypertonic media correlates with cell volume reduction but not with changes in the F-actin content. *Cell Motil. Cytosk.* 1997, 37:326-337.

Felix, R., Hofstetter, W., Wetterwald, A., Cecchini, M., Fleisch, H. Role of Colony-Stimulating Facto-1 in Bone Metabolism. *J.Cell.Biochem.* 1994, 55(3): 340-349.

Felsenfeld, A. Bone, parathyroid hormone and the response to the rapid induction of hypocalcaemia. *Eur.J.Clin.Invest* 1999, 29:274-277.

Fermor, B, and Skerry, T. PTH/PTHrP receptor expression on osteoblasts and osteocytes but not resorbing bone surfaces in growing rats. *JBMR* 1995, 10(12):1935-43

Fleisch, H. Bisphosphonates in Bone disease: From the laboratory to the patient. Academic press, USA, 2000, Fourth edition.

Flora, P. and Gregory, C. Recognition of apoptotic cells by human macrophages: inhibition by a monocyte/macrophage-specific monoclonal antibody. *Eur.J.Immunol* 1994, 24(11):2625-32.

Frey, E. and Finlay, B. Lipopolysaccharide induces apoptosis in a bovine endothelial cell line via a soluble CD14 dependent pathway. *Microb.Pathog.* 1998, 24(2):101-9.

Frost, H. In vivo osteocytes death. *J.Bone Joint Surg* 1960, 42 (1):138-143.

Frost, H. Tetracycline-based histological analysis of bone remodeling. *Calc.Tiss.Res* 1969, 3:211-237.

Fukuo, K., Hata, S., Suhara, T., Nakahashi, T., Shinto, Y., Tsujimoto, Y., Morimoto, S., Ogihara, T. Nitric oxide induces upregulation of Fas and apoptosis in vascular smooth muscle. *Hypertension* 1996, 27(3):823-6.

Gao, Y., Herndon, J., Zhang, H., Griffith, T., Ferguson, T.A. Anti-inflammatory effects of CD95 ligand (FasL)-induced apoptosis. *J. Exp.Med.* 1998, 188:887-896.

Glade, M. and Krook, L. Glucocorticoid-induced inhibition of osteolysis and the development of osteopetrosis, osteonecrosis and osteoporosis. *Cornell Vet.* 1982, 72(1):76-91.

Glantschnig, H., Rodan, G., Reszka, A. Mapping of MST1 kinase sites of phosphorylation. Activation and autophosphorylation. *J.Biol.Chem* 2002, 277(45):42987-96.

Gluhak-Heinrich, J., Ye, L., Bonewald, L., Feng, J., MacDougall, M., Harris, S., Pavlin, D. Mechanical loading stimulates dentin matrix protein 1 (DMP1) expression in osteocytes in vivo. *JBMR.* 2003, 18(5):807-17.

Goillot, E., Raingeaud, J., Ranger, A., Tepper, R., Davis, R., Harlow, E., Sanchez, I. Mitogen activated protein kinase-mediated Fas apoptotic signalling pathway. *PNAS* 1997, 94 (7):3302-3307.

Goldstein, J., Ho, Y., Basu, S., Brown, M. Binding site on macrophages that mediates uptake and degradation of acetylated low density lipoprotein, producing massive cholesterol deposition. *PNAS* 1979, 76:333-337.

Gordon S, Helfrich, M., Sati, H., Greaves, M., Ralston, S., Culligan, D., Soutar, R., Rogers, M. Pamidronate causes apoptosis of plasma cells in vivo in patients with multiple myeloma. *Br.J.Haematol.* 2002, 119(2):475-83.

Goto, T., Yamaza, T., Kido, M., Tanaka, T. Light- and electron-microscopic study of the distribution of axons containing substance P and the localization of neurokinin-1 receptor in bone. *Cell Tissue Res* 1998, 293:287-93.

Gowen, L., Petersen, D., Mansolf, A., Qi, H., Stock, J., Tkalcevic, G., Immons, H., Crawfors, D., Chidsey-Frink, K., McNeish, J., Brown, T. Targeted disruption of the osteoblast/osteocyte factor 45 gene (OF45) results in increased bone formation and bone mass. *J.Biol.Chem* 2003, 278(3):1998-2007.

Green, D. and Kroemer, G. The central executioners of apoptosis: caspases or mitochondria? *Trends in Cell Biol.* 1998, 8:267-271.

Green, L., Wagner, D., Glogowski, J., Skipper, P., Wishnock, J., Tannenbaum, S. Analysis of nitrate, nitrite and (15N) nitrate in biological fluids. *Anal.Biochem.* 1982, 126:131–138.

Gregory, C. CD14-dependent clearance of apoptotic cells: relevance to the immune system. *Curr.Op.Immunol.* 2000, 12:27-34.

Guchelaar, H., Vermes, A., Haanen, C. Apoptosis: molecular mechanisms and implications for cancer chemotherapy. *Pharm. World Sci.* 1997, 19:119-125.

Hadjiargyrou, M., Rightmire, E., Ando, T., Lombardo, F. The E11 osteoblastic lineage marker is differentially expressed during fracture healing. *Bone* 2001, 29(2):149-154.

Hakeda, Y., Arakawa, T., Ogasagara, A., Kumegawa, M. Recent progress in studies on osteocytes-osteocytes and mechanical stress. *Kaibogaku Zasshi J.Anatomy* 2000,75 (5):451-456.

Halasy-Nagy, J., Rodan, G., Reszka, A. Inhibition of bone resorption by alendronate and risedronate does not require osteoclast apoptosis. *Bone*. 2001,29(6):553-9.

Hamaya, M., Mizogushi, I., Sakakura, Y., Yajima, T. Abiko, Y. Cell death of osteocytes occurs in rat alveolar bone during experimental tooth movement. *Calc.Tiss.Inter* 2002, 70: 117-126.

Hamdy, N. Pathophysiology of glucocorticoid-induced osteoporosis. Glucocorticoids and Bone: the Clinical Problem, Boerhaave Committee for Postgraduate Education of medicine, Leiden University, The Netherlands, 1997,11-17.

Hamon, Y., Broccardo, C., Chambenoit, O., Luciani, M., Toti, F., Chaslin, S., Freyssinet, J., Devaux, P., McNeish, J., Marguet, D., Chimini, G. ABC1 promotes engulfment of apoptotic cells and transbilayer redistribution of phosphatidylserine. *Nat.Cell Biol.* 2000, 2:399-406.

Hamon, Y., Luciani, M., Becq, F., Verrier, B., Rubartelli, A., Chimini, G. Interleukin-1beta secretion is impaired by inhibitors of the Atp binding cassette transporter, ABC1. *Blood* 1997, 90(8):2911-5.

Hanayama, R., Tanaka, M., Miwa, K., Shinohara, A., Iwamatsu, A., Nagata, S. Identification of a factor that links apoptotic cells to phagocytes. *Nature* 2002, 417(6885):182-7.

Harada, H., Tagashira, S., Fujiwara, M., Ogawa, S., Katsumata, T., Yamaguchi, A., Komori, T., Nakatsuka, M. Cbfa1 isoforms exert functional differences in osteoblast differentiation. *J.Biol.Chem*. 1999, 274(11):6972-6978.

Harada, S. and Rodan, G. Control of osteoblast function and regulation of bone mass. *Nature* 2003, 423:349-355.

Haziot, A., Ferrero, E., Kontgen, F., Hijiya, N., Yamamoto, S., Silver, J., Stewart, C., Goyert, S. Resistance to endotoxin shock and reduced dissemination of gram-negative bacteria in CD14-deficient mice. *Immunity* 1996, 4(4):407-14.

Heidenreich, S., Schmidt, M., August, C., Cullen, P., Rademaekers, A., Pauels, H. Regulation of human monocyte apoptosis by the CD14 molecule. *J.Immunol.* 1997, 159(7):3178-88.

Heinemann, D., Lohmann, C., Siggelkow, H., Alves, A., Engel, I., Koster, G. Human osteoblast-like cells phagocytose metal particles and express the macrophage marker CD68 in vitro. *J.Bone Joint Surg (Br)* 2000 (82):283-289.

Heino, T., Hentunen, T., Vaananen, H. Osteocytes inhibit osteoclastic bone resorption through transforming growth factor-β: Enhancement by estrogen. *J.Cell.Biochem* 2002, 85:185-197.

Helfrich, M. Osteoclast diseases. *Microsc Res Tech* 2003, 61(6): 514-32.

Henson, P, Bratton, D, Fadok, V. Apoptotic cell removal. *CurrentBiol.* 2001,11:795-805

Hikiji, H., Shin, W., Oida, S., Takato, T., Koizumi, T., Toyo-oka, T. Direct action of nitric oxide on osteoblastic differentiation. *FEBS Lett.* 1997, 410(2-3):238-42.

Hirata, H, Takahashi, A, Kobayashi, S, Yonehara, S, Sawai, H, Okazaki, T, Yamamoto, K, Sasada, M. Caspases are activated in a branched protease cascade and control distinct downstream processes in Fas-induced apoptosis. *J.Exp.Med.* 1999, 187(4):587-600.

Hong, C., Lin, S., Kok, S., Cheng, S., Lee, M., Wang, T., Chen, C., Lin, L., Wang, J. The role of lipopolysaccharide in infectious bone resorption of periapical lesion. *J.Oral Pathol.Med.* 2004, 33(3):162-9.

Hughes, D., Dai, A., Tiffee, J., Li H., Mundy, G., Boyce, B. Estrogen promotes apoptosis of murine osteoclasts mediated by TGF-beta. *Nat.Med.* 1996 10:1132-6.

Huynh, M.-L., Fadok, V., Henson, P. Phosphatidylsserine ingestion fo apoptotic cells promoted TGF-b1 secretion and the resolution of inflammation. *J.Clin.Invest* 2002, 109:41-50.

Ibbotson, K., D'Souza, S., Bayless, A., Ebrahimpour, A., Ebetino, F., Woodiel, F., Fall, P., Raisz, L. The phosphonate moieties of bisphosphonates are more than just a targeting function: Evidence from the study of bisphosphonate analogues in vitro. *Bone Miner.* 1994, 25 (Suppl. 1):S66.

Igarashi, M., Kamiya, N., Ito, K., Takagi, M. In situ localization and in vitro expression of osteoblast/osteocyte factor 45 mRNA during bone cell differentiation. *Histochem.J* 2002, 34(5):255-63.

Ikeda, T., Yamagushi, A., Yokose, S., Nagai, Y., Yamato, H., Nakamura, T., Tsurukami, H., Tanizawa, T., Yoshiki, S. Changes in biological activity of bone cells in ovariectomised rats revealed by in situ hybridization. *JBMR* 1996, 11:780-788.

Inaba, K., Turley, S., Yamaide, F., Iyoda, T., Mahnke, K., Inaba, M., Pack, M., Subklewe, M., Sauter, B., Sheff, D., Albert, M., Bhardwaj, N., Mellman, I., Steinman, R. Efficient presentation of phagocytosed cellular fragments on the major histocompatibility complex class II products of dendritic cells. *J.Exp.Med* 1998, 188:2163-73.

Jamieson, C., Yamamoto, K.Crosstalk pathway for inhibition of glucocorticoid-induced apoptosis by T cell receptor signaling. *PNAS* 2000, 97(13):7319-7324.

Jilka, R., Weinstein, R., Bellido, T., Parfitt, A., Manolagas, S. Osteoblast programmed cell death (apoptosis): modulation by growth factors and cytokines. *JBMR* 1998, 13:793-802.

Kagan, V., Borisenko, G., Serinkan, B., Tyurina, Y., Tyrin, A., Jiang, J., Liu, S., Shvedova, A., Fabisiak, J., Uthaisang, W., Fadeel, B. Appetising rancidity of apoptotic cells for macrophages: oxidation, externalisation and recognition of phosphatidylserine. *Am.J.Physiol.Lung Cell Mol.Physiol* 2003, 285:L1-L17.

Kameda, T., Mano, H., Yuasa, T., Mori, Y., Miyazawa, K., Shiokawa, M., Nakamaru, Y., Hiroi, E., Hiura, K., Kameda, A., Yang, N., Hakeda, Y., Kumegawa, M. Estrogen inhibits bone resorption by directly inducing apoptosis of the bone-resorbing osteoclasts. *J.Exp.Med.* 1997, 186(4):489

Kameda, T., Miyazawa, K., Mori, Y., Yuasa, T., Shiokawa, M., Nakamaru, Y., Mano, H., Hakeda, Y., Kameda, A., Kumegawa, M. Vitamin K2 inhibits osteoclastic bone resorption by inducing osteoclast apoptosis. *Biochem.Biophys.Res.Commun.* 1996, 220(3):515-9.

Kamioka, H., Honjo, T., Takano-Yamamoto, T. A three-dimensional distribution of osteocyte processes revealed by the combination of confocal laser scanning microscopy and differential interference contrast microscopy. *Bone* 2001, 28:145-149.

Kamp, D., Sieberg, T., Haest, C. Inhibition and stimulation of phospholipid scrambling activity. Consequences for lipid asymmetry, echinocytosis, and microvesiculation of erythrocytes. *Biochemistry* 2001, 40:9438-9446.

Kaposzta, R., Marodi, L., Hollinshead, M., Gordon, S., da Silva, R. Rapid recruitment of late endosomes and lysosomes in mouse macrophages ingesting Candida albicans. *J.Cell Sci.* 1999, 112:3237-3248.

Karsdal, M, Larsen, L., Engsig, M., Lou, H., Ferreras, M., Lochter, A., Delaisse, J., Foged, N. Matrix metalloproteinase-dependent activation of latent transforming growth factor-beta controls the conversion of osteoblasts into osteocytes by blocking osteoblast apoptosis. *J.Biol.Chem.* 2002, 277(46):44061-7.

Kato, Y., Windle, J., Koop, B., Mundy, G., Bonewald, L. Establishment of an osteocyte-like cell line, MLO-Y4. *JBMR* 1997, 12: 2014-2023.

Kawakami, A., Eguchi, K., Matsuoka, N., Tsuboi, N., Koji, T., Urayama, S., Fujiyama, K., Kiriyama, T., Nakashima, T., Nakane, P., Nagataki, S. Fas and fas ligand interaction is necessary for human osteoblast apoptosis. *JBMR* 1997, 12(10):1637-1646.

Kenzora, J., Steele, R, Yosipovitch, Z., Glimcher, M. Experimental osteonecrosis of the femoral head in adult rabbits. *Clin.Orthop.* 1978, (130):8-46.

Kerr, J., Wylie, A., Currie, A. Apoptosis: a basic biological phenomenon with wide-ranging implications in tissue kinetics. *Br.J.Cancer* 1972, 26:239-257.

Kikuchi, T., Matsuguchi, T. Tsuboi, N. Mitani, A. Tanaka, S., Matsuoka, M., Yamamoto, G., Hishikawa, T., Noguchi, T., Yoshikai, Y.Gene expression of osteoclast differentiation factor is induced by lipopolysaccharide in mouse osteoblasts via Toll-like receptors. *J. Immunol.* 2001, 166:3574-3579.

Kitson, J., Raven, T., Jiang Y., Goeddel, D., Giles, K., Pun, K., Grinham, C., Brown, R Farrow, S. A death domain containing receptor that mediates apoptosis. *Nature* 1996, 384:372-375.

Klein-Nulend, J., Helfrich, M., Sterck, J., MacPherson, H., Joldersma, M., Ralston, S., Semeins, C., Burger, E. Nitric oxide response to shear stress by human bone cell cultures is endothelial nitric oxide synthase dependent. *Biochem.Biophys.Res.Commun.* 1998, 250(1):108-14.

Klein-Nulend, J., Van der Plas, A, Semeins, C., Ajubi, N., Frangos, J., Nijweibe, P., Burger, E. Sensitivity of osteocytes to biomechanical stress in vitro. *FASEB* 1995, 9: 441-445.

Kogianni, G., Mann, V., Ebetino, F., Nuttal, M., Nijweide, P., Simpson, H., Noble, B. Fas/CD95 is associated with glucocorticoid-induced osteocyte apoptosis. *Lif.Sci* 2004, In Press.

Kondo, A., Koshihara, Y. Togari. A. Signal transduction system for interleukin-6 synthesis stimulated by lipopolysaccharide in human osteoblasts. *J. Interferon Cytokine Res.* 2001, 21:943-950

Kong, Y., Yoshida, H., Sarosi, I., Bolon, B., Tafuri, A., Morony, S., Capparelli, C., Li, J., Elliott, R., McCabe, S., Wong, T., Campagnuolo, G., Moran, E., Bogoch, E., Van, G., Nguyen, L., Ohashi, P., Lacey, D., Fish, E., Boyle, W., Penninger, J. OPGL is a key regulator of osteoclastogenesis, lymphocyte development and lymph-node organogenesis. *Nature* 1999, 397:315-323.

Kroemer, G. The proto-oncogene Bcl-2 and its role I regulating apoptosis. *Nat.Med.* 1997, 3:614-620.

Kuhn, M. The microtubule depolymerising drugs nocodazole and colchicines inhibit the uptake of Listeria monocytogenes by P388D1 macrophages. *FEMS Microbiol Lett.* 1998, 160(1):87-90.

Kurosaka, K., Watanabe, N., Kobayashi, Y. Production of proinflammatory cytokines by phorbol myristate acetate-treated THP-1 cells and monocyte-derived macrophages after phagocytosis of apoptotic CTLL-2 cells. *J.Immunol.* 1998, 161:6245-6249.

Kwon, S., Takei, H., Pioletti, D. Lin, T., Ma, Q. Akeson, W., Wood, D., Sung, K. Titanium particles inhibit osteoblast adhesion to fibronectin-coated substrates. *J.Orthop. Res.* 2000, 18(2):203–211.

Lacey, D., Tan, H., Lu, J., Kaufman, S., Van, G., Qiu, W., Rattan, A., Scully, S., Fletcher, F., Juan, T., Kelley, M., Burgess, T., Boyle, W., Polverino, A. Osteoprotegerin ligand modulates murine osteoclast survival in vitro and in vivo. *Am.J.Path. 2000,* 157(2):435-448.

Lai, C.F., Chaudhary, L., Fausto, A., Halstead, L., Ory, D., Avioli, L., Cheng, S.L. Erk is essential for growth, differentiation, integrin expression, and cell function in human osteoblastic cells. *J.Biol.Chem* 2001, 276(17):14443-50.

Landry, P., Sadasivan, K., Marino, A., Albright, J. Apoptosis is co-ordinately regulated with osteoblast formation during bone healing. *Tiss.Cell* 1997, 29(4):413-419.

Lanyon, L. Osteocytes, strain detection, bone modelling and remodeling. *Calcif.Tissue Int.* 1993, 53: S102-S107.

Lee, D., Long, S., Adams, J., Chan, G., Vaidya, K., Francis, T., Kikly, K., Winkler, J., Sung, C., Debouck, C., Richardson, S., Levy, M., DeWolf, W., Keller, P., Tomaszek, T., Head, M., Ryan, M., Haltiwanger, R., Liang, P., Janson, C., McDevitt, P., Johanson, K, Concha, N., Chan, W., Abdel-Meguid, S., Badger, A., Lark, M., Nadeau, D., Suva, L., Gowen, M., Nuttall, M. Potent and selective nonpeptide inhibitors of caspases 3 and 7 inhibit apoptosis and maintain cell functionality. *J.Biol.Chem* 2000, 275 (21):16007-16014.

Lee, F., Choi, Y., Behrens, F., DeFouw, D., Einhorn, E. Programmed removal of chondrocytes during endochondral fracture healing. *J.Orth.Res.* 1998, 16:144-150.

Lee, S., Crocker, P., Westaby, S., Key, N., Mason, D., Gordon, S., Weatherall, D. Isolation and immunocytochemical characterization of human bone marrow stromal macrophages in hemopoietic clusters. *J.Exp.Med.* 1988, 168(3):1193-8.

Lehenkari, P., Kellinsalmi, M., Napankangas, J., Ylitalo, K., Monkkonen, J., Rogers, M., Azhayev, A., Vaananen, H., Hassinen, I. Further insight into mechanism of action of clodronate: inhibition of mitochondrial ADP/ATP translocase by a nonhydrolyzable, adenine-containing metabolite. *Mol.Pharmacol* 2002, 61(5):1255-62.

Leiro, J., Ortega, M., Siso, M., Sanmartin, M., Ubeira, F. Effects of chitinolytic and proteolytic enzymes on in vitro phagocytosis of microsporidians by spleen macrophages of turbot, Scophthalmus maximus L. *Vet Immunol.Immunopathol* 1997, 59(1-2):171-80

Leverrier, Y. and Ridley, A. Requirement for Rho GTPases and PI3-Kinases during apoptotic cell phagocytosis by macrophages. *Curr.Biol* 2001, 11:195-199.

Levine, A., Pery, M., Chung, A., Silver, A., Dittmer, D., Wu, M., Welsh D. The 1993 Walter Hubert lecture: The role of the p53 tumour-suppressor gene in toumorigenesis. *Br.J.Cancer* 1994, 69:409-416.

Li, H., Zhu, H., Xu, C., Yuan, J. Cleavage of BID by caspase 8 mediates the mitochondrial damage in the Fas pathway of apoptosis. *Cell* 1998, 94, 491–501.

Lian, J., Sten. G., Canalis, E., Robey Gehron, P., Boskey, A. Bone formation: Osteoblast lineage cells, growth factors, matrix proteins and the mineralization process. In: Favus, J., Ed. Primer on the Metabolic Bone Diseases and Disorders of Mineral Metabolism, Philadelphia: Lippincott-Williams & Wilkins; 1999:14-29.

Little, R., Carulli, J., Del Mastro, R., Dupuis, J. Osborne, M., Folz, C., Manning, S., Swain, P., Zhao, S., Eustace, B., Lappe, M., Spitzer, L., Zweier, S., Braunschweiger, K., Benchekroun, Y., Hu, X., Adair, R., Chee, L., FitzGerald, M., Tulig, C., Caruso, A., Tzellas, N., Bawa, A., Franklin, B., McGuire, S., Nogues, X., Gong, G., Allen, K., Anisowicz, A., Morales, A., Lomedico, P., Recker, S., Van Eerdewegh, P., Recker, R., Lohmann, C., Dean, D., Koster, G., Casasola, D., Buchhorn, G., Fink, U., Schwartz, Z., Boyan, B. Ceramic and PMMA particles differentially affect osteoblast phenotype. *Biomaterials* 2002 (23):1855-1863.

Lohmann, C., Schwartz, Z., Koster, G., Jahn, U., Buchhorn, G., MacDougall, M., Casasola, D., Liu, Y., Sylvia, V., Dean, D., Boyan, B. Phagocytosis of wear debris by osteoblasts affects differentiation and local factor production in a manner dependent on particle composition. *Biomaterials* 2000 (21):551-561.

Lomri, A., Marie, P., Tran, P., Hott, M. Characterization of endosteal osteoblastic cells isolated from mouse caudal vertebrae. *Bone*. 1988, 9(3):165-75.

Lorget, F., Kamel, S., Mentaverri, R., Wattel, A., Naassila, M., Maamer, M., Brazier, M. High extracellular calcium concentrations directly stimulate osteoclast apoptosis. *Biochem.Biophys.Res.Commun* 2000, 268:899-903.

Lorimore, S., Coates, P., Scobie, G.E., Milne, G., Wright, E. Inflammatory-type responses after exposure to ionizing radiation in vivo: a mechanism for radiation-induced bystander effects? *Oncogene* 2001, 20: 7085-7095.

Loveridge, N., Fletcher, S., Power, J., Caballero, A., Das-GUPTA, V., Rushton, N., Parker, M., Reeve, J., Pitsillides, A. Patterns of osteocytic endothelial nitrous oxide synthase expression in the femoral neck cortex: Differences between cases of intracapsular hip fracture and controls. *Bone* 2002, 30(6):866-71

Luciani, M. and Chimini, G. The ATP binding cassette transporter ABC1 is required for the engulfment of corpses generated by apoptotic cells death. *EMBO* 1996, 15:226-35.

Luzi, L. and Pozza, G. Glibenclamide: an old drug with a novel mechanism of action? *Acta Diabetol.* 1997, 34(4):239-44.

MacDougall, M., Simmons, D., Gu, T., Dong, J. MEPE/OF45, a new dentin/bone matrix protein and candidate gene for dentin diseases mapping to chromosome 4q21. *Connect.Tissue.Res* 2002, 43(2-3):320-30.

Mantell, L., Kazzaz, J., Xu, J., Palaia, T., Piedboeuf, B., Hall, S., Rhodes, G., Niu, G., Fein, A., Horowitz, S. Unscheduled apoptosis during acute inflammatory lung injury. *Cell Death Differ.* 1997, 4(7):600-7.

Marguet, D., Luciani, M, Moynault, A., Williamson, P., Chimini, G. Engulfment of apoptotic cells involves the redistribution of membrane phosphatidylserine on phagocyte and prey. *Nat.Cell Biol.* 1999, 1:454-456.

Marotti, G. The structure of bone tissues and the cellular control of their deposition. *Ital.J.Anat.Embryol.* 1996, 101(4):25-79.

Marotti, G., Cane, V., Palazzini, S., Palumbo, C. Structure-function relationships in the osteocytes. *Ital.J.Min.Electrolyte Metab.* 1990, 4:93-106.

Martin, D., Siegel, R., Zheng, L., Lenardo, M. Membrane oligomerisation and cleavage activates the caspase-8 (FLICE/MACHa1) death signal. *J.Biol.Chem*1998, 273 (8):4345-4349.

Martin, R. Towards a unifying theory of bone remodeling. *Bone* 2000, 26:1-6.

Martin, S., Reutelingsperger, C., McGahon, A., Rader, J., van Schie, R., LaFace, D., Green, D. Early redistribution of plasma membrane phosphatidylserine is a general feature of apoptosis regardless of the initiating stimulus: inhibition by overexpression of Bcl-2 and Abl. *J.Exp.Med.* 1995, 182(5):1545-56.

Mason, D. Suva, L. Genever, P., Patton, A. Steuckle, S. Hillam, R., Skerry, T Mechanically regulated expression of a neural glutamate transporter in bone: A role for excitatory amino acids as osteotropic agents? *Bone* 1997, 20: 199-205.

Matsui, K., Breitender-Geleff, S., Soleiman, A., Kowalski, H., Kerjaschki, D. Podoplanin, a novel 43-kDa membrane protein, controls the shape of podocytes. *Nephrol.Dial.Transplant* 1999, 14:9-11.

Mauel, J. and Defendi, V. Infection and transformation of mouse peritoneal macrophages by simian virus 40. *Exp. Med.* 1971, 134:335.

May, R., Machesky, L. Phagocytosis and the actin cytoskeleton. *J.Cell Sci.* 2001, 114(6):1061-67.

McAllister, R. Gardner, M., Greene, A., Bradt, C., Nichols, W., Landing, B. Cultivation in vitro of cells derived form a human osteosarcoma. *Cancer* 1971, 27:397-402.

McGee, K., Holmfeldt, P., Fallman, M. Microtubule-dependent regulation of Rho GTPases during internalisation of Yersinia pseudotuberculosis. *FEBS lett.* 2002, 553:35-41.

McGill, G., Horstmann, M., Widlund, H., Du, J., Motyckova, G., Nishimura, E., Lin, Y., Ramaswamy, S., Avery, W., Ding, H., Jordan, S., Jackson, I., Korsmeyer, S., Golub, T., Fisher, D. Bcl2 regulation by the melanocyte master regulator Mitf modulates lineage survival and melanoma cell viability. *Cell* 2002, 109(6):707-18.

Medema, J., Scaffidi, C., Kischkel, F., Shevchenko, A., Mann, M., Krammer, P., Peter, M. FLICE is activated by association with the CD95 death-inducing signaling complex (DISC). *EMBO J.* 1997, 16(10):2794-804.

Meschutkin, N. Uber die Einwirkung des Chloracetyls auf phosphorige Saure. *Ann. Chem.Pharm.* 1865, 133: 317-320.

Mikuni-Takagaki, Y., Kakai, Y., Satoyoshi, M., Kawano, E., Suzuki, Y., Kawase. T, Saito, S. Matrix mineralization and the differentiation of osteocyte-like cells in culture. *JBMR.* 1995, 10(2):231-42.

Mills, J., Stone, N., Pittman, R. Extranuclear apoptosis. The role of the cytoplasm in the execution phase. *J.Cell Biol.* 1999, 146: 703-708.

Misceau, O., Solary, E., Hammann, A., Dimanche-Boitrel, M. Fas ligand-independent, FADD-mediated activation of the fas death pathway by anticancer drugs. *J.Biol.Chem* 1999, 274:7987-7992.

Miyake K. Innate recognition of lipopolysaccharide by CD14 and toll-like receptor 4-MD-2: unique roles for MD-2. *Int.Immunopharmacol.* 2003, 3(1):119-28.

Miyamoto, T., Arai, F., Ohneda, O., Takagi, K., Anderson, D., Suda, T. An adherent condition is required for formation of multinuclear osteoclasts in the presence of macrophage colony-stimulating factor and receptor activator of nuclear factor kB ligand. *Blood* 2000, 96:4335-4343.

Miyashita, T., Harigai, M., Hanada, M., Reed, J. Identification of a p53-dependent negative response element in the Bcl-2 gene. *Cancer Res.* 1994, 54: 3131-3135.

Moodley, Y., Rigby, P., Bundell, C., Bunt, S., Hayashi, H., Misso, N., McAnulty, R., Laurent, G., Scaffidi, A., Thompson, P., Knight, D. Macrophage recognition and phagocytosis of apoptotic fibroblasts is critically dependent on fibroblast-derived thrombospondin 1 and CD36. *Am J Pathol.* 2003, 162(3):771-9.

Morimoto, Y., Ohba, T., Kobayashi, S., Haneji, T. The protein phosphatase inhibitors okadaic acid and calyculin A induce apoptosis in human osteoblastic cells. *Exp.Cell Res.* 1997, 230(2):181-6.

Mostov, K., Werb, Z. Journey ccross the osteoclast. *Science* 1997, 276:5310.

Mundy, G. Bone-resorbing cells. Primer on the metabolic bone diseases and disorders of mineral metabolism, Lippincott-Raven, New York, 1996, 16-24.

Mundy, G. Factors regulating bone resorbing and bone forming cells. Bone remodeling and its disorders 1995, Martin Dunitz Publishers, 39-65.

Muzio, M., Chinnaiyan, A., Kischkel, F., O'Rourke, K., Shevchenko, A., Ni, J., Scaffidi, C., Bretz, J., Zhang, M., Gentz, R., Mann, M., Krammer, P., Peter, M., Dixit, V. FLICE, a novel FADD-homologous ICE/CED-3-like protease, is recruited to the CD95 (Fas/APO-1) death--inducing signaling complex. *Cell* 1996, 85(6):817-27.

Newman, S., Henson, J., Henson, P. Phagocytosis of senescent neutrophils by human monocyte-derived macrophages and rabbit inflammatory macrophages. *J.Exp.Med.* 1982, 156(2):430-442.

Nijweide, P. and Mulder, R. Identification of osteocytes in osteoblast-like cell cultures using a monoclonal antibody specifically directed against osteocytes. *Histochemistry* 1986, 84(4-6):342-7.

Nishida, S., Fujii, Y., Yoshioka, S., Kikuichi, S., Tsubaki, M., Irimajiri, K. A new bisphosphonate, YM529 induces apoptosis in HL60 cells by decreasing phosphorylation of single survival signal ERL. *Lif. Sci* 2003, 73(21):2655-64.

Nissen-Meyer, J, Hofsli, E., Espevik, T., Austgulen, R. Involvement of tumor necrosis factor in cytotoxicity mediated by human monocytes. *NatImmun Cell Growth Regul.* 1988, 7(5-6):266-79.

Noble, B., Dean, V., Loveridge, N., Thomson, B. Dextran sulphate promotes the rapid aggregation of porcine bone-marrow stromal cells. *Bone* 1995, 17 (4):375-382.

Noble, B., Peet, N., Stevens, H., Brabbs, A., Mosley, J., Reilly, G, Reeve, J., Skerry, T., Lanyon, L. Mechanical loading: biphasic osteocyte survival and targeting of osteoclasts for bone destruction in rat cortical bone. *Am.J.Physiol.Cell Physiol* 2003, 284(4):934-43.

Noble, B. and Reeve, J. Osteocytes function, osteocytes death and bone fracture resistance. *Moll. and Cell. Endocrinology* 2000, 159:7-13.

Noble, B., Stevens, H., Reeve, J., Loveridge, N. Identification of apoptotic changes in osteocytes in normal and pathological human bone. *Bone* 1997, 20(3): 273-282.

Noda, M., Yoon, K., Rodan, G., Koppel, D. High lateral mobility of endogenous and transfected alkaline phosphatase: a phosphatidylinositol- anchored membrane protein. *J. Cell Biol.*1987, 105: 1671-1677.

Nose, K., Saito, H., Kuroki, T. Isolation of a gene sequence induced later by tumour-promoting 12-Otetradecanoylphorbol-13-acetate in mouse osteoblastic cells (MC3T3-E1) and expressed constitutively in ras-transformed cells. *CellGrowth Differ* 1990, 1:511-518.

O'Connor, D., Choi, M., Kwon, S., Paul Sung K.L. New insight into the mechanism of hip prosthesis loosening: effect of titanium debris size on osteoblast function. *J.Orth. Res.* 2004, 22(2):229-236

Ohizumi, I., Harrada, N., Taniguchi, K., Tsutsumi, Y., Nakagawa, S., Kaiho, S., Mayumi, T. Association of CD44 with OTS-8 in tumour vascular endothelial cells. *Biochim.Biophys.Acta* 2000, 1497:197-203.

Ozeki, N., Mogi, M., nakamura, H., Togari, A. Differential expression of the Fas-Fas ligand system on cytokine-induced apoptotic cell death in mouse osteoblastic cells *Arch.Oral Biol.* 2002, 47:511-517.

Palazzini, S., Palumbo, C., Ferretti, M., Marotti, G. Stromal cell structure and relationships in perimedullary spaces of chick embryo shaft bones. *Anat Embryol (Berl).* 1998, 197(5):349-57.

Palumbo, C., Palazzini, S., Marotti, G. Morphological study of intercellular junctions during osteocyte differentiation. *Bone* 1990a, 11(6): 401-6.

Palumbo, C., Palazzini, S., Zaffe, D., Marotti, G. Osteocyte differentiation in the tibia of newborn rabbit: an ultrastructural study of the formation of cytoplasmic processes. *Acta Anat (Basel).* 1990b, 137(4): 350-8.

Papapoulos, S. Bisphosphonates: Pharmacology and rationale for their use in the prevention and treatment of glucocorticoid-induced osteoporosis. Glucocorticoids and Bone: the Clinical Problem, Boerhaave Committee for Postgraduate Education of medicine, Leiden University, The Netherlands, 1997, 83-92.

Parfitt, A. Osteonal and hemiosteonal remodelling: the spatial and temporal framework for signal traffic in adult human bone. *J.Cell.Biochem.* 1994, 55:273-286.

Parfitt, A. Targeted and non targeted bone remodeling: Relationship to basic multicellular unit origination and progression. *Bone* 2003, 30(1):5-7.

Parfitt, A. The actions of parathyroid hormone on bone: relation to bone remodeling and turnover, calcium homeostasis, and metabolic bone disease. Part III of IV parts; PTH and osteoblasts, the relationship between bone turnover and bone loss, and the state of the bones in primary hyperparathyroidism. *Metabolism.* 1976, 25(9):1033-69.

Patschan, D., Loddenkemper, K., Buttgereit, F. Molecular mechanisms of glucocorticoid-induced osteoporosis. *Bone* 2001, 29 (6):498-505.

Petersen, D., Tkalcevic, G., Manslof, A., Rivera-Gonzalez, R. Brown, T. Identification of osteoblast/osteocyte factor 45 (OF45), a bone-specific cDNA encoding an RGD-containing protein that is highly expressed in osteoblasts and osteocytes. *J.Biol.Chem* 2000, 275 (46): 35172-36180.

Pichyangkul, S., Saengkrai, P., Yongvanitchit, K., Heppner, D., Kyle, D., Webster, H. Regulation of leucocyte adhesion molecules CD11b/CD18 and leukocyte adhesion molecule-1 on phagocytic cells activated by malaria pigment. *Am.J.Trp.MedHyg.* 1997, 57:383-388.

Pioletti, D. Takei, H., Kwon, S., Wood, D., Paul Sung K-L. The cytotoxic effect of titanium particles phagocytosed by osteoblasts. *J.Biomed.Mat.Res.* 1999, 46(3):399-407.

Platt, N., da Silva, R., Gordon, S. Recognizing death: the phagocytosis of apoptotic cells. *Trends Cell Biol.* 1998, 8(9):365-72.

Platt, N., Suzuki, H, Kurihara, Y., Kodama, T., Gordon, S. Role for the class A macrophage scavenger receptor in the phagocytosis of apoptotic thymocytes in vitro. *PNAS* 1996, 93:12456-12460.

Plotkin, L., Weintein, R., Parfitt, A., Roberson, P., Manolagas, S., Bellido, T. Prevention of osteocytes and osteoblast apoptosis by bisphosphonates and calcitonin. *J. Clin.Invest* 1999, 104:1363-1374.

Power, J., Loveridge, N., Rushton, N., Parker, M. ,Reeve, J. Osteocyte density in aging subjects is enhanced in bone adjacent to remodeling harvesian systems. *Bone* 2002, 30:859-865.

Pradhan, D. Krahling, S., Williamson, P., Schlegel, R.Multiple systems for recognition of apoptotic lymphocytes by macrophages.*Mol Biol Cell.* 1997, 8(5):767–778

Prockop, D. Marrow stromal cells as stem cells for nonhematopoietic tissues. *Science* 1997, 276(4): 71-74.

Pugin, J. Heumann, I., Tomasz, A., Kravchenko, V., Akamatsu, Y., Nishijima, M., Glauser, M., Tobias, P., Ulevitch, R. CD14 is a pattern recognition receptor. *Immunity* 1994, 1(6):509-16.

Puzas, J. Osteoblast cell biology-lineage and functions. Primer on the metabolic bone diseases and disorders of mineral metabolism, Lippincott-Raven, New York1996, 11-16.

Quast, U., Cook, N. Moving together: K+ channel openers and ATP-sensitive K+ channels. *Trends Pharmacol Sci.* 1989, 10(11):431-5.

Rahimi, P., Wang, C., Stashenko, P., Lee, S., Lorenzo, J., Graves, D. Monocyte chemoattractant protein-1 expression and monocyte recruitment in osseous inflammation in the mouse. *Endocrinology* 1995, 136(6):2752-9.

Rao, L., Murray, T., Heersche, J. Immunohistochemical demonstration of parathyroid hormone binding to specific cell types in fixed rat bone tissue. *Endocrinology* 1983, 113(2):805-10

Rasmussen, H. Ionic and hormonal control of calcium homeostasis. *AmJ.Med* 1971, 50(5): 567-88.

Reyes-Botella, C., Montes, M., Vallecillo-Capilla, M., Olivares, E., Ruiz, C. Expression of molecules involved in antigen presentation and T cell activation (HLA-DR, CD80, CD86, CD44 and CD54) by cultured human osteoblasts. *J.Periodontol* 2000,71:614-617

Riggs, B., Wahner, H., Seeman, E., Offord, K., Dunn, W., Mazess, R., Johnson, K., Melton, L. Changes in bone mineral density of the proximal femur and spine with aging. Differences between the postmenopausal and senile osteoporosis syndromes. *J. Clin.Invest* 1982, 70(4):716-23.

Rodan, G, Martin, J. Therapeutic approaches to bone diseases. *Science* 2000, 289:5484.
Rodan, G. Introduction to bone biology. *Bone* 1992, 13 (Suppl 1):S3-6.

Rodan, G. Mechanism of action of Bisphosphonates. *Annu.Rev.Pharm.Toxicol* 1998, 38:375-88.

Rodan, G. and Fleisch, H. Bisphosphonates: Mechanism of action. *J.Clin.Inv* 1996, 97(12): 2692-2696.

Rogers, M., Frith, C., Luckman, P., Coxon, F., Benford, H., Monkkonen, J, Auriola, S., Chilton, K., Russel, R. Molecular mechanisms of action of bisphosphonates. *Bone* 1999, 24(5):73S-79S.

Rogers, M., Russell, R., Blackburn, G., Williamson, M., Watts, D. Metabolism of halogenated bisphosphonates by the cellular slime mould Dictyostelium discoideum. *Biochem.Biophys.Res.Commun* 1992, 189(1):414-23.

Rogers, M., Xiong, X., Brown, R., Watts, D., Russell, R., Bayless, A., Ebetino, F., Structure-activity relationships of new heterocycle-containing bisphosphonates as inhibitors of bone resorption and as inhibitors of growth of Dictyostelium discoideum amoebae. *Mol.Pharmacol.* 1995, 47(2):398-402.

Roman-Roman, S. Garcia, T., Jackson, A., Theilhaber, J., Rawadi, G. Connolly, T., Spinella-Jaegle, S., Kawai, S., Courtois, B., Bushnell, S., Auberval, M., Call, K., Barona R. Identification of genes regulated during osteoblastic differentiation by genome-wide expression analysis of mouse calvaria primary osteoblasts in vitro. *Bone* 32, 2003:474–482

Roodman G. Advances in bone biology: the osteoclast. *Endocr.Rev.* 1996, 4:308-32.

Rothe, M., Sarma, V., Dixit, V., Goeddel, D. TRAF-2 –mediated activation of NF-kB by TNF receptor 2 and CD40. *Science* 1995, 269:1424-1426.

Rubartelli, A., Poggi, A., Zocchi, M. The selective engulfment of apoptotic bodies by denndritic cells is mediated bu the alpha(v)beta3 integrin and requires intracellular and extracellular calcium. *Eur.J.Immunol* 1997, 27(8):1893-900.

Russell, G., Mueller, G., Shipman, C., Croucher, P. Clinical disorders of bone resorption. Novartis Found. Symp. 2001, 232:251-67; discussion 267-71.

Sabbagh, Y., Boileau, G., Campos, M., Carmona, A., Tenenhouse, H. Structure and function of disease-causing missense mutations in the PHEX gene. *J.Clin.Endocrinol Metab*. 2003, 88(5):2213-22.

Saevarsdottir, S., Vikingsdottir, T., Valdimarsson, H. The potential role of mannan-binbing lectin in the clearance of self-components including immune complexes. Scandin. *J. Immunol* 2004, 60(1-2):23-29.

Samoto, H., Shimizu, E., Matsuda-Honjyo, Y., Saito, R., Nakao, S., Yamazaki, M., Furuyama, S., Sugiya, H., Sodek, J., Ogata, Y. Prostaglandin E2 stimulates bone sialoprotein (BSP) expression through cAMP and fibroblast growth factor 2 response

elements in the proximal promoter of the rat BSP gene. *J.Biol.Chem* 2003, 278(31):28659-67

Savill J. Recognition and phagocytosis of cells undergoing apoptosis. *Br.Med.Bull.* 1997, 53(3):491-508.

Savill, J., Dransfield, I., Gregory, C., Haslett, C. A blast from the past: Clearance of apoptotic cells regulates immune responses. *Nat.Rev.Immunol* 2002, 2:965-975.

Savill, J. and Fadok, V. Corpse clearance defines the meaning of cell death. *Nature* 2000, 407:784-788.

Savill, J., Hogg, N., Ren, Y., Hasslet, C. Thrombospondin cooperates with CD36 and the vitronectin receptor in macrophage recognition of neutrophils undergoing apoptosis. *J.Clin.Invest* 1992, 90: 1513-1522.

Schiller, P., D'Ippolito, G., Bramdilla, R., Roos, B., Howard, G. Inhibition of gap-junctional communication induces the trans-differentiation of osteoblasts to an adipocytic phenotype in vitro. *J.Biol.Chem* 2000, 276(17): 14133-14138.

Schmidt, M., Lugering, N., Lugering, A., Pauels, H., Schulze-Osthoff, K., Domschke, W., Kucharzik, T. Role of the CD95/CD95 ligand system in glucocorticoid-induced monocyte apoptosis. *J.Immunol* 2001, 166:1344-1351.

Schulze, E., Witt, M., Kasper, M., Lowik, C.W., and Funk, R. Immunohistochemical investigations on the differentiation marker protein E11 in rat calvaria, calvaria cell culture and the osteoblastic cell line ROS 17/2.8. *Histochem.Cell Biol* 1999, 111:61-69.

Sexton, D., Blaylock, M., Walsh, G. Human alveolar epithelial cells engulf apoptotic eosinophils by means of integrin- and phosphatidylserine receptor-dependent mechanisms: a process upregulated by dexamethasone. *J.Allergy Clin.Immunol.* 2001, 108(6):962-9.

Shapiro, F. Variable conformation of GAP junctions linking bone cells: A transmission electron microscopic study of linear, stacked linear, curvilinear, oval, and annular junctions. *Calcif.Tissue Int.* 1997, 61:285-293.

Shipman, C., Croucher, P., Russell, R., Helfrich, M., Rogers, M. The bisphosphonate incadronate (YM175) causes apoptosis of human myeloma cells in vitro by inhibiting the mevalonate pathway. *Cancer Res.* 1998, 58(23):5294-7.

Shouman, Y., Feng, X., O'Connell, P. Apoptosis detection by annexin V binding: a novel method for the quantification of cell-mediated cytotoxicity. *J.Immunol.Meth* 1998, 217:61-70.

Siddhanti, S. and Quarles, L. Molecular to pharmacologic control of osteoblast proliferation and differentiation. *J.Cell Biochem.* 1994, 55(3): 310-320.

Sietsema, W., Ebetino, F., Salvagno, A., Bevan, J. Antiresorptive dose-response relationships across three generations of bisphosphonates. *Drugs Exp.Clin.Res* 1989, 15(9): 389-96.

Sikavitsas, V., Temenoff, J., Mikos, A. Biomaterials and bone mechanotransduction. *Biomaterials* 2001, 22(19): 2581-2593.

Smirnova, I., Kudryavtseva, N., Komissarenko, S., Tarusova, N., Baykov, A. Diphosphonates are potent inhibitors of mammalian inorganic pyrophosphatase. *Arch. Biochem. Biophys.* 1988, 267: 280–284

Stefanelli, C., Bonavita, F., Stanic, I., Farruggia, G., Falcieri, E., Robuffo, I., Pignatti, C., Muscari, C., Rossoni, C., Guarnieri, C., Caldarera, C. ATP depletion inhibits glucocorticoid-induced thymocyte apoptosis. *Biochem.J.* 1997, 322(3): 909-917

Stevens, H, Reeve, J, Noble, B. Bcl-2 tissue transglutaminase and p53 protein expression in the apoptotic cascade in ribs of premature infants. *J.Anat* 2000,196:181-191

Strewler, G. Local and systemic control of the osteoblast. *J.Clin.Invest* 2001, 107(3): 271-272.

Stuart, L., Lucas, M., Simpson, C., Lamb, J., Savill, J., Lacy-Hulbert, A. Inhibitory effects of apoptotic cell ingestion upon endotoxin-driven myeloid dendritic cell maturation. *J.Immunol.* 2002, 168(4):1627-35.

Suda, T., Udagawa, N., Nakamura, I., Miyaura, C., Takahashi, N. Modulation of osteoclast differentiation by local factors. *Bone* 1995, 17(2 Suppl):87S-91S.

Sugimoto, M., Takahashi, S., Kotoura, Y., Shibamoto, Y., Takahashi, M., Abe, M., Ishizaki, K., Yamamuro, T. Osteocyte viability after high-dose irradiation in the rabbit. *Clin.Orth.Related Res* 1993, 297:247-252.

Suri, S., Monkkonen, J., Taskinen, M., Pesonen, J., Blank, M., Phipps, R., Rogers, M. Nitrogen-containing bisphosphonates induce apoptosis of Caco-2 cells in vitro by inhibiting the mevalonate pathway: a model of bisphosphonate-induced gastrointestinal toxicity. *Bone* 2001, 29(4):336-43.

Suzuki, H., Kurihara, Y., Takeya, M., Kamada, N., Kataoka, M., Jishage, K., Ueda, O., Sakaguchi, H., Higashi, T., Suzuki, T., Takashima, Y., Kawabe, Y., Cynshi, O., Wada, Y, Honda, M., Kurihara, H., Aburatani, H., Doi, T., Matsumoto, A, Azuma, S., Noda, T.,

Toyoda, Y., Itakura, H., Yazaki, Y., Kodama, T. A role for macrophage scavenger receptors in atherosclerosis and susceptibility to infection. *Nature* 1997, 386:292-6.

Tao, Y., Williams-Skipp, C., Scheinman, R. Mapping of glucocorticoid receptor DNA binding domain surfaces contributing to transrepression of NF-kB and induction of apoptosis. *J.Biol.Chem* 2001, 276(4): 2329-2332.

Tarnowski, B. and McLaughlin, B. Phagocytic interactions of sialated glycoprotein, sugar, and lectin coated beads with rat retinal pigment epithelium. *Curr.Eye.Res* 1987,6(9):1079-89.

Teitelbaum, S.L. Bone Resorption by Osteoclasts. *Science* 2000, 289: 1504-1508.

Terai, K., Takano-Yamamoto, T., Ohba, Y., Hiura, K; Sugimoto, M., Sato, M., Kawahata, H., Inaguma, N., Kitamura, Y., Nomura, S Role of osteopontin in bone remodeling caused by mechanical stress. *JBMR* 1999, 14:839-849.

Terpstra, V., Kondratenko, N., Steinberg, D. Macrophages lacking scavenger receptor A show a decrease in binding and uptake of acetylated low-density lipoprotein and of apoptotic thymocytes, but not of oxidatively damaged red blood cells. *PNAS* 1997, 94: 8127–8131.

Thi, M., Kojima, T., Cowin, SC., Weinbaum, S., and Spray, D. Fluid shear stress remodels expression and function of junctional proteins in cultured bone cells. *Am.J Physiol Cell Physiol* 2003, 284(2):C389-C403.

Thompson, G. Apoptosis in the pathogenesis and treatment of disease. *Science* 1995, 267:1456-1460.

Thompson, K., Dunford, J., Ebetino, F., Rogers, M. Identification of a bisphosphonate that inhibits isopentenyl diphosphate isomerase and farnesyl diphosphate synthase. *Biochem.Biophys.Res.Commun* 2002, 18;290(2):869-73.

Thomson, B., Deav, V., Farquharson, C., Noble B. Visualisation and selective elimination of a subpopulation of mitogen-responsive bone marrow stromal cells using bromodeoxyuridine and photo-induced cell killing. *Bone* 1993, 14:779-986.

Thornberry, N. and Lazebnik Y. Caspases: Enemies within. *Science* 1998, 281: 1312-1322.

Tobias, J., Chambers, T. Glucocorticoids impair bone resorptive activity and viability of osteoclasts disaggregated from neonatal rat long bones. *Endocrinology* 1989 3:1290-5.
Tomkinson, A., Gevers, E., Wit, J., Reeve, J., Noble, B. The role of estrogen in the conrtol of rat osteocyte apoptosis. *JBMR* 1998, 13(8):1243-1250.

Tomkinson, A., Reeve, J., Shaw, R., Noble, B. The death of osteocytes via apoptosis accompanies estrogen withdrawal in human bone. *J.Clin.Endocrinol.Metab* 1997, 82: 3128-3135.

Tosello-Trampont, A., Brugnera, E, Ravichandran, K. Evidence for a conserved role for CrkII and Rac in engulfment of apoptotic cells. *J.Biol.Chem* 2001,276(17):13797-13802.

Tran, S., Holstrom, T., Ahonen, M., Kahari, V., Eriksson, J. MAPK/ERK overrides the apoptotic signalling from Fas, TNF, and TRAIL receptors. *J.Biol.Chem* 2001, 276(19): 16484-16490.

Turner, C. Editorial: Functional determinants of bone structure: Beyond Wolff's law of bone transformation. *Bone* 1992, 13: 403-409.

Underhill, D., Bassetti, M., Rudensky, A., Aderem, A. Dynamic interactions of macrophages with T cells during antigen presentation.*J.Exp.Med* 1999,190(12):1909-1914.

van Beek, E, Lowik, C., Ebetino, F., Papapoulos, S. Binding and antiresorptive properties of heterocycle-containing bisphosphonate analogs: Structure-activity relationships. *Bone* 1998, 23:437–442.

van den Brink, M., Kapeller R., Pratt, J., Chang, J., Burakoff, S. The extracellular signal-regulated kinase pathway is required for activation-induced cell death of T cells. *J.Biol.Chem* 1999, 274 (16), 11178-11185.

van der Laan, L., Ruuls, S., Weber, K., Lodder, I., Dopp, E., Dijksta, C. Macrophage phagocytosis of myelin in vitro determined by flow cytometry: phagoctysosis is mediated by CR3 and induced production of tumor necrosis factor-a and nitric oxide. *J. Neuroimmunol.* 1996, 70(2):145-152.

van der Plas, A., Nijweide, P. Isolation and purification of osteocytes. *JBMR* 1992, 7:389-39

Vanderbilt, J., Dobbs, L. Characterisation of the gene and promoter for RT140, a differentiation marker of type I alveolar epithelial cells. *Am.J.Resp.Cell Mol.Biol.* 1998, 19:662-671.

van't Hoff, R., Ralston, S. Cytokine-induced nitric oxide inhibits bone resorption by inducing apoptosis of osteoclast progenitors and suppressing osteoclast activity. *Bone* Miner.Res 1997, 12(11):1797-804.

van't Hof, R., Ralston S. Nitric oxide and bone. *Immunology*. 2001,103(3):255-61.

Vashishth, D., Verborgt, O., Divine, G., Schaffler, M., Fyhrie, D. Decline in osteocyte lacunar density in human cortical bone is associated with accumulation of microcracks with age. *Bone* 2000, 26(4): 375-80.

Verborgt, O., Gibson, G., Schaffler, M. Loss of osteocyte integrity in association with microdamage and bone remodeling after fatigue in vivo. *JBMR* 2000, 15(1): 60-67.

Verborgt, O., Tatton, N., Majeska, R., Schaffler, M. Spatial distribution of Bax and Bcl-2 in osteocytes after bone fatigue: Complementary roles in bone remodeling regulation? *JBMR* 2002, 17(5):907-914.

Verheij, M., Bose, R., Lin, X., Yao, B., Jarvis, W. Requirement for ceramide-initiated SAPK/JNK signalling in stress induced apoptosis. *Nature* 1996, 380: 75-79.

Vermes, C, Glant, T., Hallab, N., Fritz, E., Roebuck, K., Jacobs, J. The potential role of the osteoblast in the development of periprosthetic osteolysis: review of in vitro osteoblast responses to wear debris, corrosion products, and cytokines and growth factors. *J Arthroplasty*. 2001, 16(8 Suppl 1):95-100.

Voll, R., Herrmann, M. Roth, E., Stach, C., Kalden, J. Immunosuppressive effects of apoptotic cells *Nature* 1997, 390: 350-351.

Wang, L., Ciani, C., Stephen, B., Doty, S., Fritton, S. Delineating bone's interstitial fluid pathway in vivo. *Bone* 2004, 34(3):499-509

Wang, L.. Cowin, S Weinbaum, S., Fritton, S. Modeling tracer transport in an osteon under cyclic loading. *Ann. Biomed. Eng.* 2000, 28:1200–1209

Wang, W., Ferguson, D., Quinn, J., Simpson, A., Athanasou, N. Osteoclasts are capable of particle phagocytosis and bone resorption. *J.Path* 1997, 182: 92-98.

Wang, X., Martindale, J., Holbrook, N. Requirement for ERK activation in cisplatin-induced apoptosis. *J.Biol.Chem* 2000, 275(50): 39435-39443.

Waymire, K., Mahuren, J., Jaje, J., Guilarte, T., Coburn, S., Macgreyor, G. Mice lacking tissue non-specific alkaline phosphatase die from seizure due to defective metabolism of vitamin B-6 Nature Genet. *Nat.Genet* 1995, 11:45-51.

Wehrli, P., Viard, I., Bullani, R., Tschopp, J., French, L. Death receptors in cutaneous biology and disease. *J.Invest.Dermatol* 2000, 115:141-148.

Weiner, S., Traub, W., Wagner, H. Lamellar bone: Structure-function relations. *J. Struct.Biol* 1999, 126:241-255.
Weiner, S. and Wagner, H. The material bone: Structure–mechanical function relations. *Annu.Rev.Mater.Sci.* 1998, 28: 271–298.

Weinstein, R. Apoptosis and osteoporosis. *Am.J.Med* 2000, 108(2): 153-164.

Weinstein, R., Jilka, R., Parfitt, A., Manolagas, S. Inhibition of osteoblastogenesis and promotion of apoptosis of osteoblasts and osteocytes by glucocorticoids. *J.Clin.Invest* 1998, 102(2): 274-282.

Wenisch, S., Stahl, J., Horas, U., Heiss, C., Kilian, O., Trinkhaus, K., Hild, A., Schnettler, R. In vivo mechanisms of hydroxyapatite ceramic degradation by osteoclasts: fine structural microscopy. *JBMR* 2003, 67A(3): 713-8.

Westbroek, I., de Rooij, K., Nijweibe, P. Osteocyte-specific monoclonal antibody mAb OB7.3 is directed against Phex protein. *JBMR* 2002, 17 (5): 845-853.

Westbroek, I., van der Plas, A., de Rooij, K., Klein-Nulend, J., Nijweibe, P. Expression of serotonin receptors in bone. *J.Biol.Chem* 2001, 276 (31): 28961-28969.

Wetterwald, A., Hoffstetter, W., Cecchini, M., Lanske, B., Wagner, C., Fleisch, H. Atkinson, M. Characterization and cloning of the E11 antigen, a marker expressed by rat osteoblasts and osteocyte. *Bone* 1996, 18:125-132.

Wiegand, U., Corbach, S., Prescott, A., Savill, J., Spruce, B. The trigger to cell death determines the efficiency with which dying cells are cleared by neighbours. *Cell Death Diff* 2001, 8(7):734-746.

Wolff J. Das gasetz der transformation der knochen. Berlin, 1892, In: Hirchwald A, editor (An English translation of this monograph has been published by Springer-Verlag in 1986)

Wong, G. and Kocour, B. Differential serum dependence of cultured osteoclastic and osteoblastic bone cells. *Calcif.Tissue Int* 1983, 35(6):778-82.

Wong, S., Evans, R., Needs, C., Dunstan, R., Hills, E., Garvan, J. The pathogenesis of Osteoarthritis of the hip. *Clin.Orth.Related Res* 1987, 214: 305-312.

Wylie, A., Kerr, J., Currie, A. Cell death: The significance of apoptosis. *Int.Rev.Cyt* 1980, 68:251-306.

Yamaguchi, A., Komori, T., Suda, T. Regulation of osteoblast differentiation mediated by bone morphogenetic proteins, hedgehogs and cbfa1. *Endocr.Rev* 2000, 21(4):393-411.

Yamamoto, T., Ebe, Y., Hasegawa, G., Kataoka, M., Yamamoto, S., Naito, M Expression of scavenger receptor class A and CD14 in lipopolysaccharide-induced lung injury. *Pathol.Int* 1999, 49(11):983-92.

Yamazaki, M., Nakajima, F., Ogasawara, A., Moriya, H., Majeska, R., Einhorn, T. Spatial and temporal distribution of CD44 and osteopontin in fracture callus. *J.Bone.Jt Surg (Br)* 1999, 81: 508-515.

Yasuda, H., Shima, N., Nakagawa, N., Yamaguchi, K., Kinosaki, M., Goto, M., Mochizuki, S., Tsuda, E., Morinaga, T., Udagawa, N., Takahashi, N., Suda, T., Higashio, K. A novel molecular mechanism modulating osteoclast differentiation and function. *Bone.* 1999, 25(1):109-13.

Yellowley, C., Li, Z., Zhou, Z., Jacobs, C., Donahue, H. Functional gap junctions between osteocytic and osteoblastic cells. *JBMR* 2000, 15(2): 209-217.

Yuan, A., Siu, C. Chia, C. Calcium requirement for efficient phagocytosis by Dictyostelium discoideum. *Cell Calcium* 2001, 29(4), 229–238

Zaman, G., Pitsillides, A., Rawlinson, S., Suswillo, R., Mosley, J., Cheng, M., Platts, L., Hukkanen, M., Polak, J., Lanyon, L. Mechanical strain stimulates nitric oxide production by rapid activation of endothelial nitric oxide synthase in osteocytes. *J Bone Miner Res.* 1999, 14(7):1123-31.

Zar, J. Biostatistical Analysis. Prentice-Hall Int. Editions, Second Edition, 1984.

Zha, X., Genest, J., McPherson. R. Endocytosis is enhanced in Tangier fibroblasts: possible role of ATP-binding cassette protein A1 in endosomal vesicular transport. *J. Biol.Chem* 2001, 276(42):39476-83.

Zhang, D., Cowin, S., Weinbaum, S. Electrical signal transmission and gap junction regulation in a bone cell network: a cable model for an osteon. *Ann.Biomed.Eng.* 1997, 25(2):357-74.

Zhao, S., Kato, Y., Zhang, Y., Harris, S., Ahuja, S., Bonewald, L. MLO-Y4 osteocyte-like cells support osteoclast formation and activation. *JBMR* 2002, 17 (11):2068-2079.

Zhen, R-G., Baykov, A., Bakuleva, N., Rea, P. Aminomethylenediphosphonate: A Potent Type-Specific Inhibitor of Both Plant and Phototrophic Bacterial H+-Pyrophosphatases. *Plant Physiol.* 1994, 104: 153–159

Zhuang, J, Ren, Y., Snowden, R., Zhu, H., Gogvadze, V., Savill, J., Cohen, G. Dissociation of phagocyte recognition of cells undergoing apoptosis from other features of the apoptotic program. *J.Biol.Chem.* 1998, 273(25):15628-32.

Appendix-Publications

Available online at www.sciencedirect.com

SCIENCE DIRECT

Life Sciences 75 (2004) 2879–2895

Life Sciences

www.elsevier.com/locate/lifescie

Fas/CD95 is associated with glucocorticoid-induced osteocyte apoptosis

G. Kogianni[a], V. Mann[a], F. Ebetino[b], M. Nuttall[c], P. Nijweide[d], H. Simpson[a], B. Noble[a,*]

[a]*University of Edinburgh, Musculoskeletal Research Unit, Edinburgh, UK*
[b]*P&G Pharmaceuticals, Health Care Research Center, 8700 Mason-Montgomery Road, USA*
[c]*Department of Musculoskeletal Diseases, GlaxoSmithKline, King of Prussia, USA*
[d]*Leiden University, Netherlands*

Received 29 September 2003; accepted 7 April 2004

Abstract

Prolonged use of glucocorticoids is associated with decreased bone formation, increased resorption and osteonecrosis, through direct and indirect effects on the activity and viability of bone effector cells, osteoblasts and osteoclasts, and osteocytes. This study has investigated molecular pathways implicated in Dexamethasone-induced apoptosis of osteocytes, using a cell line and primary chicken cells. MLO-Y4 osteocytes were pre-treated with several bisphosphonates representing a range of anti-resorptive activities and conformation/structure relationships, and were subsequently challenged with Dexamethasone. Apoptotic cells were detected at various times after treatment using morphological and biochemical criteria. Dex was shown to induce apoptosis associated with the Fas/CD95 death receptor and in a caspase 8 dependent manner. The apoptotic response was inhibited by all variants of the BP molecules, including those with reduced anti-resorptive activity, indicating that Dex-induced apoptosis is independent of anti-osteoclastic activity. Dex-induced apoptosis was associated with a transient increase in phosphorylated ERK 1/2 and was blocked by the ERK inhibitor UO126. In addition, both UO126 and BPs decreased localization of Fas to the cell membrane. ERK activation by PMA did not induce death or Fas upregulation, suggesting that Fas may be important for the induction of apoptosis and the existence of an additional factor activated by Dex which enables the cooperation between the Dex-activated

* Corresponding author. Tel.: +44 131 6502964; fax: +44 131 6513077.
E-mail address: Brendon.Noble@ed.ac.uk (B. Noble).

0024-3205/$ - see front matter
doi:10.1016/j.lfs.2004.04.048

ERK and Fas pathways, during apoptosis of osteocytes. Furthermore, upregulation of death and Fas was not accompanied by upregulation of FasL, pointing to the possible existence of FasL-independent Fas-associated death in these cells.

Keywords: Dexamethasone; Fas; ERK; Bisphosphonates; Osteocyte; Apoptosis

Introduction

Glucocorticoids (GCs) have been extensively used as anti-inflammatory agents due to their ability to modulate immune responses (Ashwell et al., 2000), commonly through activation of the Fas pathway, one of the best-characterised apoptotic pathways (Schmidt et al., 2001). Binding of FasL to FasR causes receptor oligomerisation and recruitment of an adapter protein, FADD, which interacts with caspase-8, initiating a caspase cascade leading to apoptosis. (Ashkenazi and Dixit, 1998).

As a side effect to their clinical applications, GCs are responsible for rapid and profound bone loss since they exert anti-mitotic effects on osteoblast precursor cells, induce apoptosis of mature osteoblasts and increase the resorptive activity of osteoclasts (Hamdy, 1997). Studies by Weinstein et al. identified the presence of a high proportion of apoptotic osteocytes in mice, compared to healthy controls, following chronic administration of prednisolone (Weinstein et al., 1998). It would be of benefit clinically to develop a concurrent prescription capable of reducing the unwanted side effects associated with GC-treatment.

The beneficial effects of Bisphosphonates (BPs) on bone have long been demonstrated against Paget's disease, post-menopausal osteoporosis and GC-induced osteoporosis, by decreasing the resorptive activity of osteoclasts (Rodan, 1998). BPs are classed as nitrogen-containing (such as PAM and ALN) and non N- BPs (such as CLO). In osteoclasts, N-BPs inhibit farnesyl diphosphate (FPP) synthase and prevent prenylation of small GTPases, such as Ras and Rho that are required for osteoclast polarization, resorption and cell survival, whereas non N-BPs are metabolized into cytotoxic analogues of ATP, that probably act as inhibitors of various ATP-dependent enzymes (Rodan, 1998; Rogers et al., 1999). Changes in structure and conformation have allowed the development of various N-BPs, which differ in their anti-resorptive activity since they differ in their ability to inhibit FPP synthase (Dunford et al., 2001).

In contrast to osteoclasts, the effect of BPs on osteocytes, which are considered the mechanosensors and transducers in bone, has not been well characterised. BPs have variously been shown to both decrease and increase ERK (Nishida et al., 2003; Plotkin et al., 1999). Studies by Plotkin et al have implicated the ERK1/2 pathway in the ability of BPs to prevent pro-apoptotic effects of Dex on MLO-Y4 osteocyte-like cells (Plotkin et al., 1999).

This study attempts to identify pro-apoptotic pathways employed by Dex as well as compounds that could potentially protect osteocytes from glucocorticoid-induced apoptosis. BPs and the MEK inhibitor UO126 were shown to protect against Dex-induced apoptosis, while upregulation of the Fas receptor appeared to be important in the induction of apoptosis.

Materials and methods

Cell culture

MLO-Y4 cell line

Unless otherwise stated, chemicals were purchased from Sigma, UK. MLO-Y4 murine osteocyte cell line was obtained from L. F. Bonewald (San Antonio, USA) and grown in collagen coated flasks in áMEM (Invitrogen, UK) supplemented with 5% fetal bovine serum, 5% newborn calf serum, 1% L-glutamine and 1% antibiotics, according to previously described methods (Kato et al., 1997). Cells were cultured until 90% confluence, before passage for experimental use.

Primary chicken osteocytes

Primary osteocytes were obtained and characterised as previously described (Nijweide and Mulder, 1986; Van der Plas and Nijweide, 1992; Aarden et al., 1996). Briefly, a mixture of osteoblasts and osteocytes was isolated by sequential collagenase-EDTA digestion from calvariae of 18-day-old chicken fetuses. Cell fractions were pooled and cultured for 1 day in MEM containing 2% chicken serum, 1.4 mM L-glutamine, 0.3 mM L-ascorbic acid (Merck, UK), 5.6 mM glucose (Invitrogen, UK), and 0.5 μg/ml gentamycin (Invitrogen, UK). Cell fractions were harvested by trypsin-EDTA, subjected to immunomagnetic isolation of osteocytes (OCY) by use of the chicken OCY-specific monoclonal antibody (MAb) OB 7.3, bound to magnetic beads (DYNAL, Oslo, Norway), which reacts specifically with OCY. A magnetic field was used to separate cells bound to beads, (1–8 beads/cell), used as isolated OCY. More than 95% of the cell population were OCY, as shown by staining with MAb OB 7.3. Then 2.5×10^4 OCY with beads were seeded onto glass slides and used for experiments the next day.

Cell treatment

For experimental manipulations, cells were plated in growth medium at a density of 1×10^4, in 24 multiwell plates for 24 hours, prior to experimentation. Experiments were carried out a minimum of 3 times, and each treatment group was represented by 3 wells in each independent experiment. Cells were observed in 3 fields per well (×20 magnification lens, approximately 40–100 cells per field) resulting in 9 fields per treatment group. Identical magnifications were used for all apoptosis estimates allowing similar numbers of cells to be counted per field in all experiments. For western blot analysis, cells were plated at a density of 1×10^5 in 60 mm petri dishes.

Induction of cell death

Cells were incubated in growth medium supplemented with 10^{-8} to 10^{-6} M Dex (Calbiochem, UK) and 0.4 μM to 0.4 mM H_2O_2 for 1–24 hours.

Prevention of cell death using BPs and inhibitors of intracellular signaling proteins

Osteocytes were pre-incubated with caspase 8 substrate II inhibitor Z-IETD-FMK (Calbiochem, UK) and caspase 3/7-selective inhibitors (GlaxoSmithKline, USA) at 10^{-6} M for 1 and 24 hours, to evaluate the

role of the Fas pathway in Dex-induced apoptosis. Cells were also pre-treated for 1 hour with PAM, ALN, CLO (kind gift form Prof. Mike Rogers, University of Aberdeen, UK) and the heterocyclic-containing N-BPs, NEII808 and NEII809 (Procter and Gamble, USA), at concentrations of 10^{-8} to 10^{-6} M, followed by Dex treatment. In addition, cells were pre-incubated for 30 minutes with UO126, a MEK 1/2 inhibitor (Promega, UK) at concentrations of 10 to 30 μM (Favata et al., 1998), SB203580 (Calbiochem, UK), a p38 inhibitor at concentrations of 5 to 15 μM (Cucnda et al., 1995) and with PMA at 2 ng/ml-200 μg/ml for 1 to 5 hours. All pre-treatment agents were maintained in cultures in the presence of Dex or H_2O_2.

Determination of apoptotic state

A range of techniques were used to determine the presence of apoptotic cells, for all the independent experimental culture setups, but only representative examples of each technique are shown throughout the manuscript:

1) DAPI staining for healthy and apoptotic cell morphology

Following treatment, cells were fixed in 4% paraformaldehyde, washed in PBS and air dried. Cells were then incubated with DAPI at 2.5 ng/ml for 10 minutes, washed in PBS and examined by fluorescence microscopy and digital image capture.

2) Acridine orange (AO) staining for healthy and apoptotic cell morphology.

Following treatment, cells were immediately incubated in Walpole's acetate buffer pH 4.2 (10:7, 1 M NaAc: 1 M HCl) for 5 minutes, followed by AO staining for 25 minutes. Cells scored as apoptotic were characterised by nuclear or cytoplasmic condensation, two or more nuclear fragments, single crescent-shaped nucleus or blebbing.

3) DNA fragmentation using in situ Nick Translation (NT)

Cells demonstrating DNA breaks were investigated in samples fixed in 4% paraformaldehyde, using a previously described DNA nick translation technique (Noble et al., 1995, 1997). Positive controls were established through pre-treatment with DNaseI at 0.2 mg/ml for 30 minutes. Cells were exposed to NT mixture which consisted of 3 μM Digoxigenin (DIG) labelled dUTP (DIG-11-dUTP), 3 μM each of dATP, dGTP, dCTP, 50 mM Tris HCl, pH 7.5, 5 mM $MgCl_2$ and 0.1 mM dithiotreitol and 0.5 μl/100 μl DNA polymerase for 1 hour at 37 °C, in a humidified chamber (Roche, UK). Wells were incubated for 1 hour at RT with fluorescein isothiocyanate (FITC)-labelled anti-DIG antibody and 5% normal sheep serum. Wells were then washed in PBS and counter stained with propidium iodide (PI). Cells containing fragmented DNA stained positive for FITC label and PI, as determined using fluorescence microscopy and digital image capture, based on 3 fields from a total of 3 wells per treatment.

4) Annexin-V-FITC Assay

During apoptosis, PS exposure on the outer leaflet of the membrane bilayer can be detected with fluorescently labelled Annexin V. Cells were incubated with Annexin-V-FITC at 1 μg/ml for 15 minutes at RT, followed by PI to identify necrotic cells in the culture. Fluorescence microscopy, allowed discrimination between viable (FITC negative, PI negative), apoptotic (FITC positive) or necrotic cells (FITC negative, PI positive).

Determination of Fas expression by immunocytochemical staining

Following incubation with various agents, cells were fixed in 4% paraformaldehyde and subsequently washed in PBS. Cells were incubated for 5 minutes with 0.1% SDS, and were washed

in PBS thoroughly. Cells were then blocked for 20 minutes in goat serum followed by 1 hour incubation with anti-Fas mAb at RT. After washing in PBS, cells were incubated with secondary anti-mouse FITC antibody for 1 hour and were counterstained with PI. Cells staining positive for FITC label and PI, were considered as cells expressing Fas on the plasma membrane, as determined using fluorescence microscopy and digital image capture, based on 3 fields from a total of 3 wells per treatment.

Reverse transcription-polymerase chain reaction

Total RNA was isolated from cultures of MLO-Y4 cells using RNA-B™ (Biogenesis) according to the manufacturers instruction. cDNA was synthesized from 3 μg of total RNA using oligo dT primers, and RNA was converted into cDNA by SuperScript II RNaseH$^-$ reverse transcriptase first strand synthesis system for RT-PCR (Invitrogen). The PCR reaction was performed using Qiagen Taq PCR core kit (10X reaction buffer, Taq 5 u/μl, Q buffer and dNTP 10 mM each) in a total of 25 μl reaction containing 5 μM each forward and reverse primers. Mouse Fas specific primers were designed against sequence accession number M83649 and mouse β-Actin specific primers against sequence accession number X03765 from HGMP database as shown below. The resulting PCR products for Fas and Actin were 220 bp and 290 bp respectively. The PCR reaction was carried out for 33 cycles with PTC-200 Peltier thermal cycler (MJ Research). PCR conditions were denaturation at 94 °C for 50 seconds, annealing at 50.5 °C for 1 minute and extension at 72° for 1 minute 30 seconds. The PCR products were analysed in 1.5% agarose gel containing ethidium bromide.

Primer Sequences:

Fas forward 5′ -CATGCTGTGGATCTGGGCTGT-3′
Fas reverse 5′ -GTGTACCCCCATTCATTTTGC-3′
Actin forward 5′ -CAAGGTGTGATGGTGGGAATG-3′
Actin reverse 5′ -GCTACGTACATGGCTGGGGTG-3′

The Accession number for the primers used for FAS ligand PCR is U10984. The identity of all PCR products was confirmed on DNA sequencing.

Western blot analysis of intracellular signalling proteins

Cells were maintained in identical culture conditions (presence of serum) to those used to study effects on apoptosis. Lysates were prepared (lysis buffer: 20 mM Tris-HCl, pH 7.5, 0.1% (v/v) Igepal, 6 mM sodium deoxycholate, 150 mM NaCl, 2 mM EGTA, 2 mM EDTA, 0.1 mM Na_3VO_4 and 20 mM NaF and a protease inhibitor cocktail tablet (Roche, UK)), and protein concentrations were estimated using a commercially available kit (Bio-Rad, UK). Lysates (30 μg/lane) were resolved on SDS-PAGE gels, transferred onto PVDF membranes and blocked with TBST solution (10 mM Tris-HCl, pH 7.4, 150 mM NaCl, 0.1% Tween 20) supplemented with 3% BSA, and then hybridized with rabbit polyclonal antibodies against phospho-p44/42MAPK, phospho-MEK 1/2, phospho-cRaf, phospho-p90rsk and total MAPK p44/42 (New England Biolabs, UK). Proteins were detected using ECL reagents according to the manufacturers instructions. Blots were stripped (100 mM β-mercaptoethanol, 69 mM SDS and 62.5 mM

Tris-HCl, pH 6.7) and rehybridised with an antibody that recognises total p44/42 MAPK, to verify equal loading of samples.

Immunoprecipitation and western blot analysis of Fas

Protein extracts (1 mg) from cell lysates were diluted to 1 mg/ml and incubated with 15 μl of protein A agarose conjugate bead slurry (50% conjugate/ 50% PBS) and 4 μl of Jo2 hamster anti-Fas monoclonal antibody (BD Transduction Laboratories, USA) overnight at 4 °C. The agarose beads were collected by centrifugation at 4 °C, washed four times in lysis buffer and were then subjected to electrophoresis as described above. Proteins on PVDF membranes were hybridized with Jo2 antibody followed by secondary anti-hamster antibody (Abcam, USA) and were detected using ECL reagents.

Statistical analysis

All statistical analyses were performed using quantitative data analysis with SPSS release 11.5 for Windows. Analysis of Variance (ANOVA), Tukey test and Dunnett test were performed for comparison between the treatment groups. The Tukey test allows comparison of more than two means at once since this reduces the error associated with multiple t-tests (Zar, 1984). The Dunnett test allows comparison between the control mean and every other mean in the group (Zar, 1984). Results are expressed as means ± S.D. $p<0.05$ was considered to be statistically significant.

Results

Dexamethasone induces MLO-Y4 cell apoptosis in a time- and dose-dependent manner

MLO-Y4 osteocytes were cultured with Dex at 10^{-7}–10^{-5} M for various times between 1 and 24 hours (Fig. 1A and B). Apoptotic osteocytes appeared irregularly shaped and smaller in size, as shown by AO staining, while DAPI staining revealed chromatin condensation, shrinkage of nuclei and the fragmentation of the nuclear material into smaller blebs (Fig. 1C). Maximal levels of death accompanied by cell loss were reached at 5 hours of incubation with concentrations of 10^{-5} M and 10^{-6} M, whereas, at 24 hours, numbers of osteocytes in culture recovered somewhat, while apoptotic levels decreased, suggesting that Dex-induced death of osteocytes is transient (Fig. 1A and B). At concentrations of 10^{-7} M, Dex did not induce apoptosis in these cells. At 10^{-5} M a small proportion of cells were noted to have expanded and burst characteristics of necrosis. Based on the apoptotic criteria in response to the different concentrations and time points investigated, the dose of 10^{-6} M, which did not induce necrosis, was selected for future experiments, reaching a peak at 5 hours incubation.

Assessment of Dex-induced apoptosis by Annexin-V-FITC and nick translation assays

Early apoptotic features induced by Dex at 5 hours, were detected by both Annexin-V-FITC, which resulted in 12.35% ±1.14 osteocytes expressing PS (<1% necrotic cells identified by PI counter-

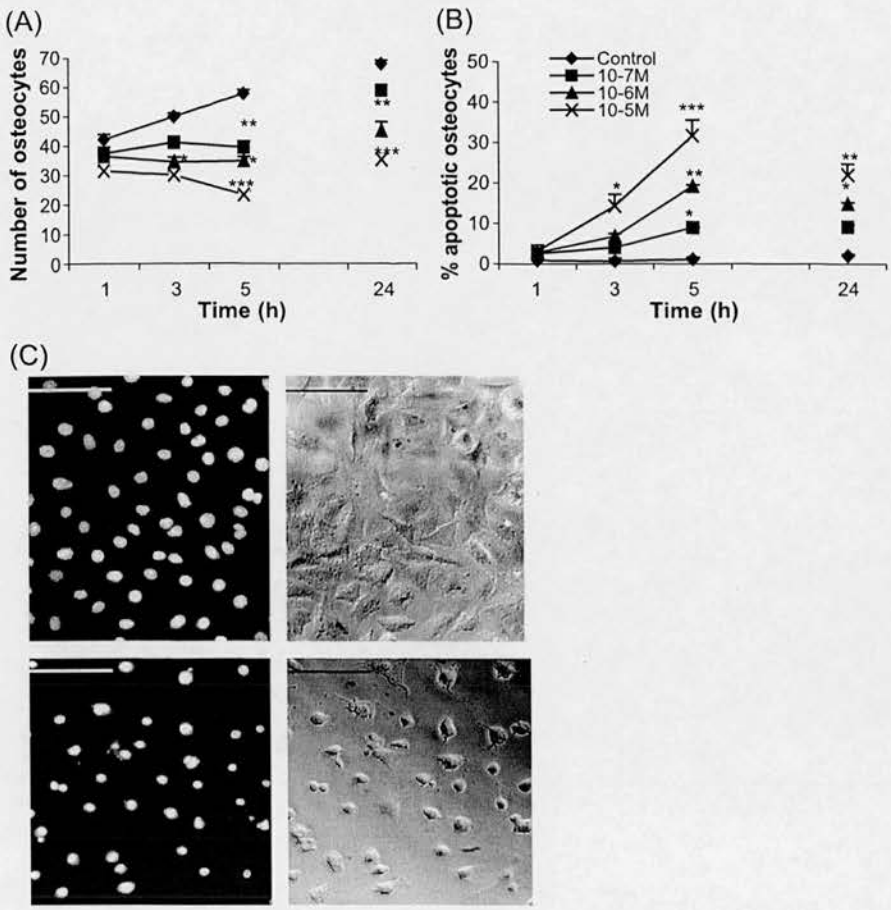

Fig. 1. Dexamethasone induces apoptosis in MLO-Y4 osteocytes in a time- and dose-dependent manner. MLO-Y4 cells were then stained with A.O. and examined by fluorescence microscopy to determine (A) Number of cellsand (B) Percentage of apoptotic osteocytes per number of cells ± S.D., in response to different doses of Dex and time. (C) Representative images of untreated (top panel) and Dex-treated MLO-Y4 osteocytes (bottom panel) at 10^{-6} M for 5 hours stained with DAPI. Bar = 5 μm. (*** = $p < 0.0001$, ** = $p < 0.001$, * = $p < 0.05$).

staining), and by Nick Translation assay, which resulted in 12.83% ±1.00 osteocytes positive for DNA breaks, compared to 1.33 ± 0.67 and 1.85 ± 1.38 in control cultures, respectively (data not shown).

Dexamethasone upregulates the Fas pathway

RT-PCR studies revealed that MLO-Y4 osteocytes express Fas receptor either in basal state or following treatment with Dex (Fig. 2A). However, FasL expression was not detected in both treated or untreated samples (data not shown). Immunocytochemistry showed that Dex increased the percentage of cells staining positive for Fas as early as 3 hours by 7-fold and at 5 hours by 22-fold compared to control (Fig. 2B and D). In addition, western blot analysis demonstrated time-dependent increase in Fas protein upon treatment with Dex (Fig. 2D).

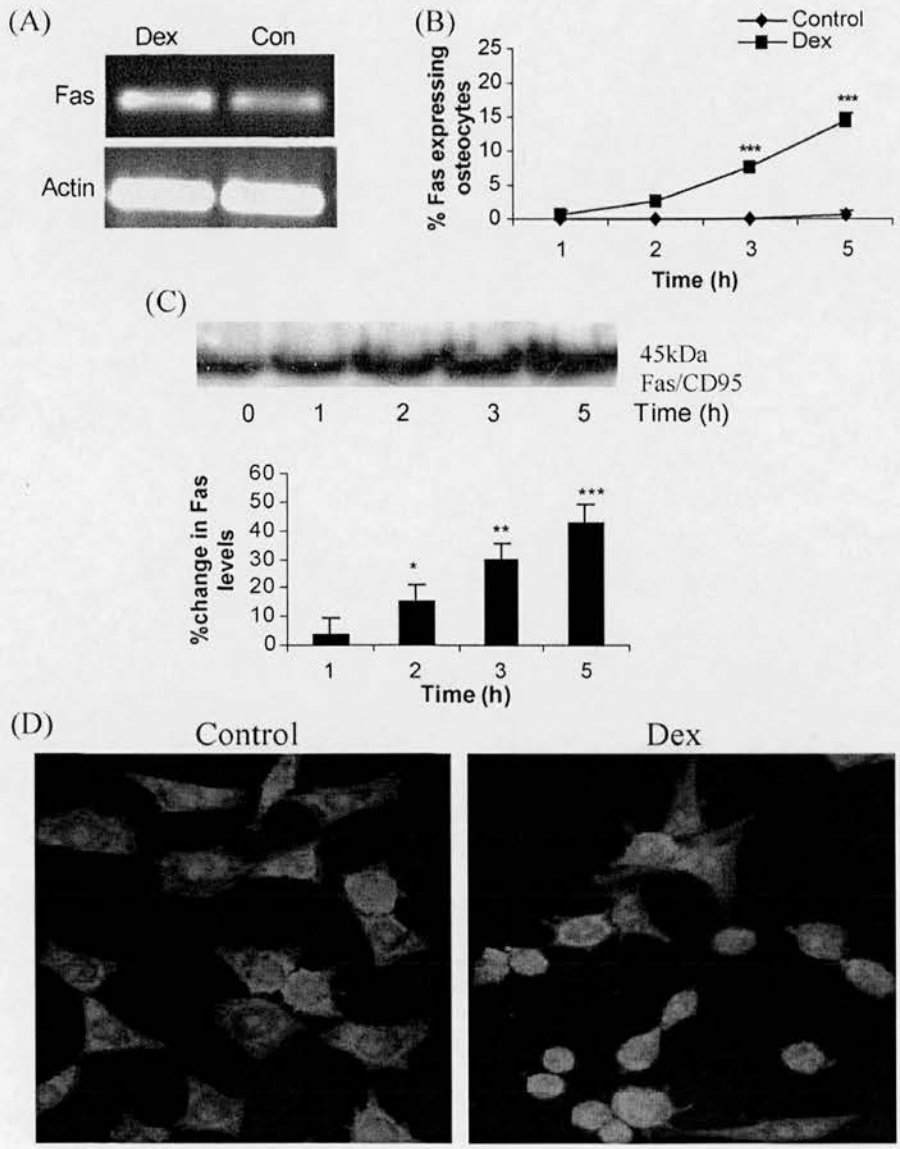

Fig. 2. Dex upregulates Fas expression in MLO-Y4 osteocytes. (A) Fas expression was confirmed using RT-PCR with RNA extracted from MLO-Y4 cultures treated with Dex. (B) Fas protein was detected following Dex treatment for 1 to 5 hours using a Fas mAb and fluorescence microscopy. Graph shows percentage of cells expressing Fas ± S.D. (C) Detection of Fas protein levels following Dex treatment for 1 to 5 hours using western blot analysis. Changes in band densitometry were quantified using NHI image analysis system and expressed as percentage change relative to zero time control ± S.D. (D) Representative images of fluorescence microscopy (20x magn.). Untreated osteocytes (left panel) and Dex-treated osteocytes (right panel). (*** = $p < 0.0001$, ** = $p < 0.001$, * = $p < 0.05$ compared to control).

The involvement of Caspase 8/FLICE, which lies downstream of Fas, was then investigated, in Dex-induced apoptosis. Pre-treatment with the caspase 8 inhibitor Z-IETD-FMK reduced the induction of death at 5 hours, up to 5-fold, compared to cultures treated with Dex, as shown by Annexin-V-FITC assay, suggesting that caspase 8 is involved in the apoptotic machinery

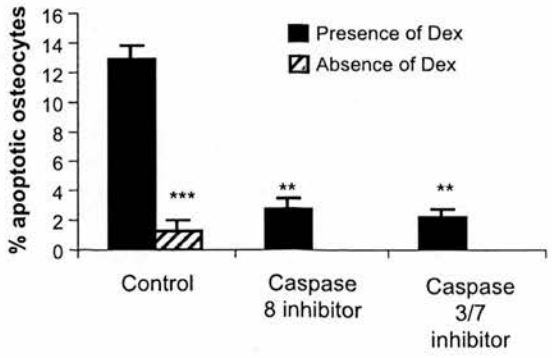

Fig. 3. Inhibitors of caspases 8 and 3,7 reduce pro-apoptotic stimuli induced by Dex. MLO-Y4 osteocytes were incubated with inhibitors of caspase-8 (Z-IETD-FMK) and a caspase 3/7 selective inhibitor for 1 hour, followed by Dex treatment for 5 hours. Cells were incubated with Annexin-V FITC and examined by fluorescence microscopy for PS detection. Graphs represent percentage of apoptotic osteocytes per number of cells ± S.D. (*** = $p < 0.0001$, ** = $p < 0.001$, * = $p < 0.05$).

activated by Dex in MLO-Y4 osteocytes (Fig. 3). In addition, pre-treatment with caspase 3/7 - selective inhibitors for identical times reduced the percentage of apoptotic osteocytes up to 6-fold (Fig. 3).

Bisphosphonates prevent Dex-induced apoptosis in MLO-Y4 osteocytes

BPs were used at concentrations that did not increase apoptosis above control levels (data not shown), to treat osteocytes prior to addition of Dex in cultures. Estimation of apoptosis showed that N-BPs (PAM, ALN and the heterocyclic-containing NEII808 and NEII809) and non N- BPs (CLO) at 10^{-8} M significantly decreased the pro-apoptotic effect of the corticosteroid at 5 hours incubation on osteocytes (Fig. 4).

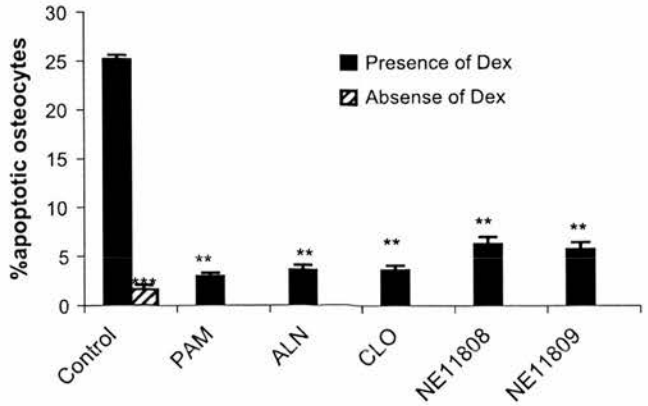

Fig. 4. BPs prevent MLO-Y4 osteocyte apoptosis induced by Dex. MLO-Y4 osteocytes were incubated with BPs at 10^{-8}M prior to Dex treatment, for 5 hours. Cells were stained with AO and examined by fluorescence microscopy. Graphs represent percentage of apoptotic osteocytes, per number of cells ± S.D. (*** = $p < 0.0001$, ** = $p < 0.001$, * = $p < 0.05$).

Inhibitors of MAP kinase signalling molecules prevent Dex-induced apoptosis in MLO-Y4 osteocytes

The effect of Dex on MLO-Y4 osteocytes was further characterised in the presence of protein inhibitors such as the MEK1/2 inhibitor UO126 and the p38 inhibitor SB203580. Dose response studies identified optimal concentrations of UO126, which did not significantly increase apoptosis above control levels either for the compound alone, or the vehicle in which it was delivered, within the range of concentrations known to inhibit ERK 1/2 (Favata et al., 1998) (Fig. 5). Quantification of apoptosis showed that concentrations of UO126 at 10 and 20 μM exerted protective effects on osteocytes following 5-hour incubation period with Dex (Fig. 5). In contrast, SB203580 at concentrations of 5 to 15 μM known to inhibit p38 (Cuenda et al., 1995), did not prevent GC-induced apoptosis, while doses above 10 μM induced significant apoptosis when added alone to osteocyte cultures (data not shown).

Primary cultures of chicken osteocytes were also used to observe the Dex induced death response in primary cells. Evaluation of apoptosis after a 5 hour-culture period, revealed that in a similar way to that seen in the MLO-Y4 cell line, both BPs and the MEK inhibitor UO126 were capable of blocking Dex-induced death in these primary cells (data not shown).

BPs and protein kinase inhibitors do not protect osteocytes from oxidant-induced death

To evaluate the role of the BP and ERK pathways in the induction of osteocyte apoptosis by other agents, MLO-Y4 cells were pre-treated with PAM and UO126 prior to their exposure to H_2O_2, at concentrations shown to induce apoptosis (0.08 mM to 0.4 mM). Examination of apoptotic morphology by AO staining revealed that PAM and UO126 did not protect MLO-Y4 osteocytes against H_2O_2 induced death stimuli (data not shown).

Dexamethasone activates the MEK/ERK protein signaling pathway

Incubation with Dex, increased the amount of activated ERK 1/2 protein in osteocytes, compared to vehicle, in a time dependent manner, as evidenced by western blot analysis, using an anti-

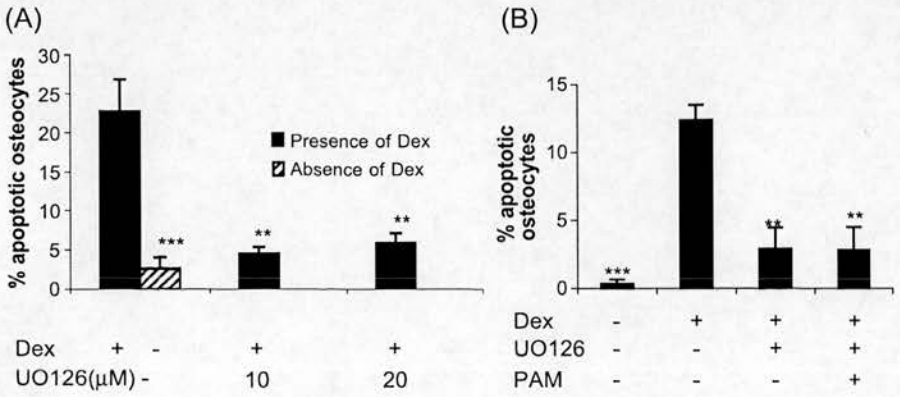

Fig. 5. The MEK 1/2 inhibitor UO126 prevents Dex-induced apoptosis. (A) UO126 prevents MLO-Y4 osteocyte apoptosis induced by Dex, in a dose dependent manner, and (B) in the presence of PAM. Cells were stained with AO and examined by fluorescence microscopy. Graphs represent the percentage of apoptotic osteocytes per number of cells ± S.D. (*** = $p < 0.0001$, ** = $p < 0.001$, * = $p < 0.05$).

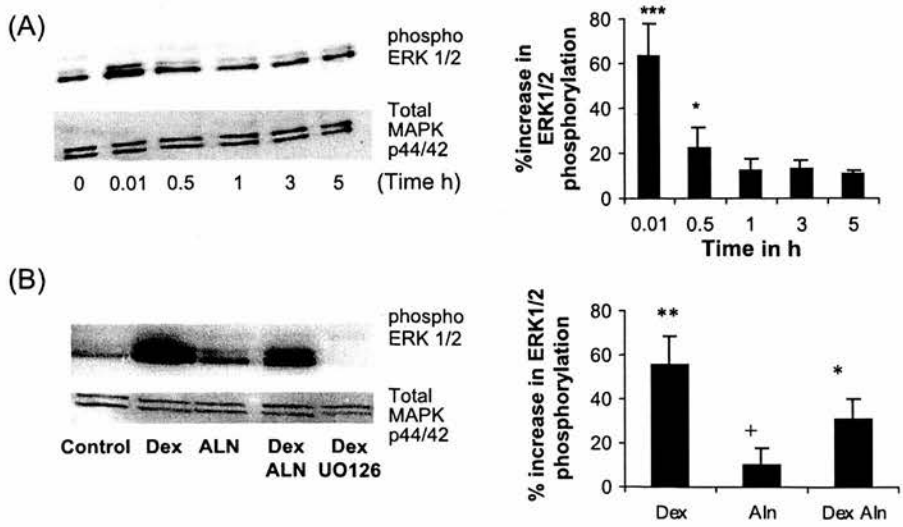

Fig. 6. (A) Dex activates the ERK 1/2 protein kinase, in a time dependent manner. ERK phosphorylation induced by Dex was statistically different from control during all time points investigated. (B) ALN reduces the Dex-induced ERK1/2 activation, at 5 minutes, whereas UO126 blocks Dex-induced ERK 1/2 activation. MLO-Y4 cell lysates were subjected to Western Blot analysis, using an anti-phospho MAPK p44/p42 antibody. The blots were stripped and reprobed with a total anti-MAPK p44/p42 antibody, to verify equal loading of samples. Changes in band densitometry were quantified using NHI image analysis system and expressed as percentage change relative to control samples, representing either vehicle control or zero time control ± S.D., from 3 independent blots. ** = $p < 0.001$, * = $p < 0.05$ compared to control, + = $p < 0.05$ compared to Dex treatment.

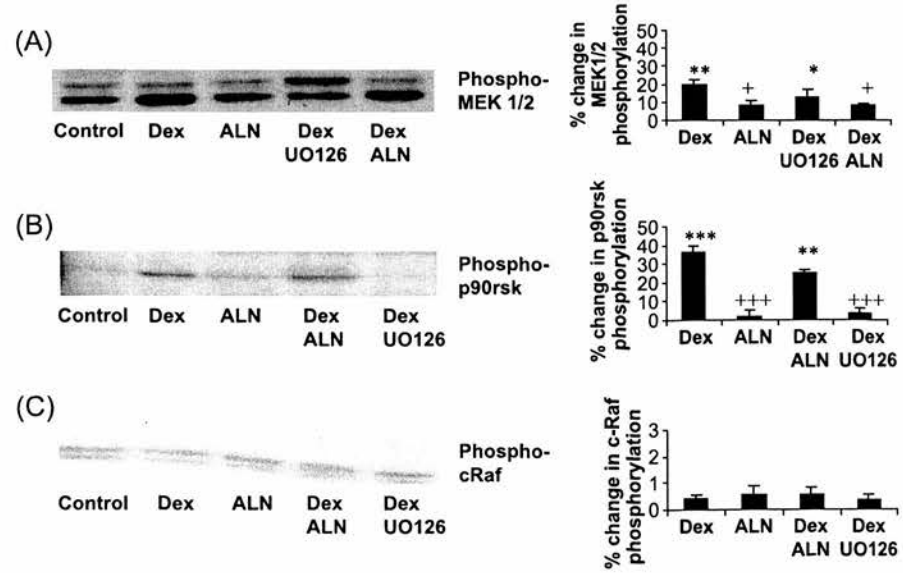

Fig. 7. Dexamethasone activates the ERK 1/2 pathway. Lysates prepared from MLO-Y4 cells treated with Dex, ALN and UO126, were subjected to Western Blot analysis, using (A) anti-phospho MEK 1/2 antibody, (B) anti-phospho p90rsk and (C) anti-phospho c-Raf antibody. Changes in band densitometry were quantified using NHI image analysis system and expressed as percentage change relative to vehicle sample ± S.D., from 3 independent blots. ***=$p < 0.0001$, **=$p < 0.001$, * = $p < 0.05$, compared to control +++ = $p < 0.0001$, + = $p < 0.05$ compared to Dex treatment.

phospho ERK 1/2 antibody (Fig. 6A). Activation of ERK 1/2 protein by Dex was acute, since it was detected as soon as 1 minute following treatment and was decreased to basal control levels, after 1 hour of treatment.

BPs transiently increased ERK 1/2 phosphorylation within 1 minute of treatment, returning to baseline by 5 minutes, as shown previously by Plotkin et al. (Plotkin et al., 1999). In this treatment group baseline levels were maintained for all subsequent time points investigated, up to 5 hours (data not shown). Addition of Dex to cells pre-treated for 1 hour with BPs resulted in a reduced activation of ERK 1/2 relative to samples treated with Dex alone (Fig. 6B). The MEK 1/2 protein inhibitor, UO126, blocked Dex and/or BP-induced ERK 1/2 activation in all cases.

In order to further characterize the role of ERK1/2 pathway in Dex-induced apoptosis, the presence of proteins lying both upstream (MEK1/2 and C-Raf) and downstream (p90rsk) of ERK1/2 protein, was investigated. Western blot analysis showed that MEK (Fig. 7A) and p90rsk (Fig. 7B) activation by Dex coincided with ERK1/2 activation, while pre-treatment with ALN slightly reduced phosphorylated levels of both proteins. In addition, UO126 prevented activation of p90rsk by Dex, but did not affect phosphorylated MEK1/2 protein, in accordance with previous reports (Favata et al., 1998). Levels of c-Raf remained constant and similar to vehicle levels, during all different treatments and time points investigated (Fig. 7C).

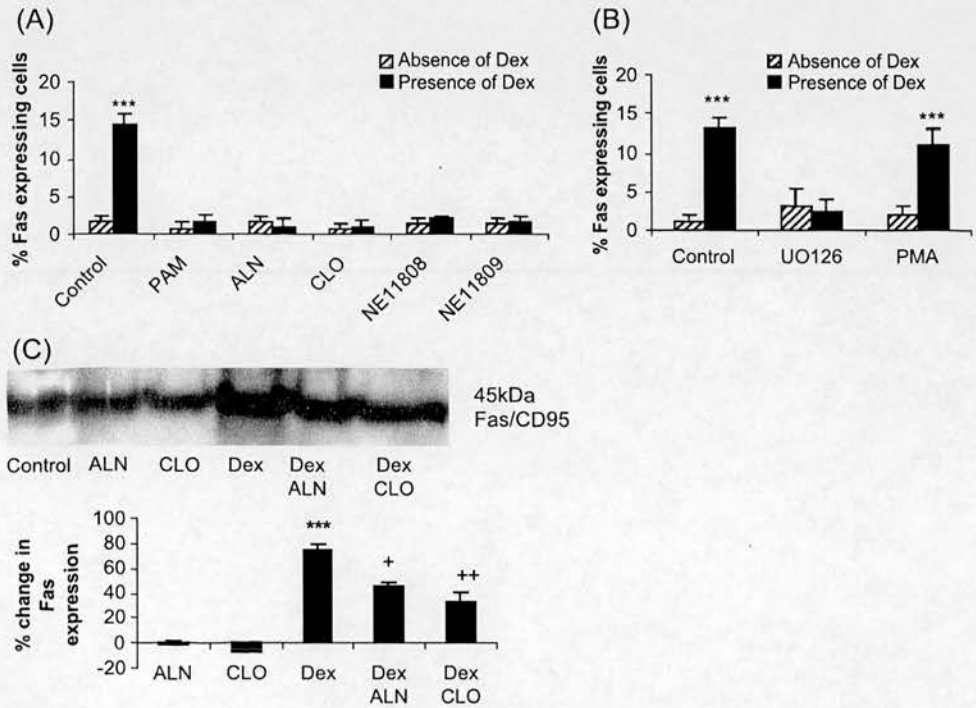

Fig. 8. BPs and UO126 suppress Dex-induced Fas expression. Cells were probed with an anti-Fas antibody and examined by fluorescence microscopy. (A) N- and non N-BPs reduce Dex-induced Fas expression as shown by immunocytochemistry and western blot analysis. Changes in band densitometry were quantified using NHI image analysis system and expressed as percentage change relative to vehicle sample ± S.D. from 3 independent blots (B) PMA alone did not increase Fas expression, compared to control. Graphs represent percentage of osteocytes, expressing Fas per number of cells ± S.D. (*** = $p < 0.0001$, compared to control, ++ = $p < 0.001$, + = $p < 0.05$ compared to Dex treatment).

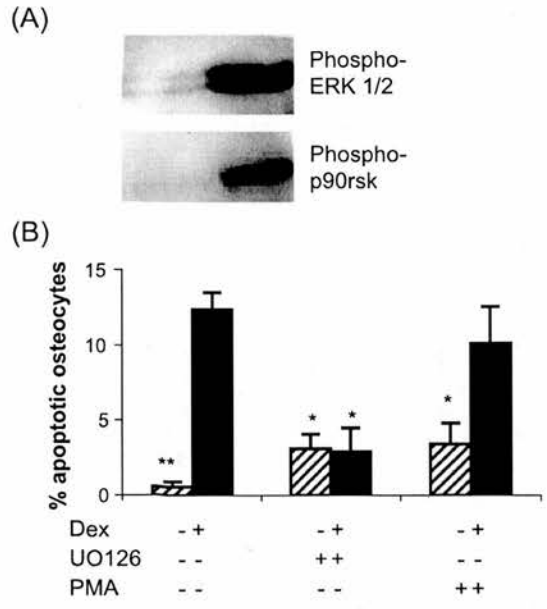

Fig. 9. PMA-induced ERK1/2 activation is not associated with osteocyte apoptosis. Cells treated with PMA followed by Dex were (A) subjected to western blot analysis to reveal pERK1/2 and p90rsk activation and (B) treated to reveal DNA breaks using the Nick Translation assay. PMA did not affect osteocyte apoptosis, compared to control. Graphs represent percentage of apoptotic osteocytes, per number of cells ± S.D. (*** = $p < 0.0001$, ** = $p < 0.001$, * = $p < 0.05$).

Suppression of Dex-induced Fas activation by MEK 1/2 inhibitor and BPs

The role of BPs and ERK 1/2 protein kinase in Dex-induced activation of Fas was investigated by immunocytochemistry studies and western blot analysis (Fig. 8). Previous studies have shown interaction between ERK and Fas protein pathways in the induction of apoptosis (Goillot et al., 1997). Pre-treatment of osteocytes with UO126 at 20 μM, prevented activation of Fas by Dex ($p=0.0001$, compared to Dex-treated samples). In a similar manner to UO126, pre-treatment of MLO-Y4 cells with both N- and non N-BPs at 10^{-8} M, reduced activation of Fas by Dex ($p=0.0001$).

PMA-induced ERK1/2 activation is not associated with osteocyte apoptosis

PMA did not induce osteocyte apoptosis (Fig. 8), despite demonstrating a clear increase in phosphorylated ERK in MLO-Y4 osteocytes as determined by western blotting (Fig. 9A). Furthermore, PMA when administered alone at concentrations of 2 ng/ml to 200 μg/ml for 1 to 5 hours did not increase Fas, while prior to Dex treatment PMA did not enhance Dex-induced Fas upregulation, in contrast to Dex treated cultures (Fig. 9B).

Discussion

Prolonged administration of glucocorticoids leads to bone loss and osteoporosis, through stimulation of resorption and induction of osteoblast and osteocyte apoptosis (Weinstein et al., 1998). This study has

attempted to investigate molecular pathways implicated in Dex-induced death of osteocytes, the mechanosensors and transducers in bone, and on molecules that might provide therapeutic approaches to combat this death. Dex induction of osteocyte apoptosis characterised by several classical apoptotic features, including chromatin and cytoplasmic condensation, DNA fragmentation, exposure of phosphatidylserine and formation of apoptotic bodies, was concentration- and time-dependent. In addition, apoptosis was caspase-dependent since inhibition of caspases −3 and −7 (Lee et al., 2000), which are responsible for chromatin condensation, DNA fragmentation and membrane blebbing, suppressed Dex-induced death.

Dex-induced apoptosis has been associated with the Fas/FasL apoptotic pathway in several different cell types, in relation to its action as an immunosuppressive agent (Schmidt et al., 2001). Fas receptor mRNA was detected in MLO-Y4 osteocytes both in response to Dex treatment and in untreated cultures. However, Dex treatment upregulated localisation of Fas protein on the osteocyte plasma membranes, in a time-dependent manner compared to untreated controls, indicating a possible association between Fas recruitment and the incidence of osteocyte apoptosis in the presence of Dex. Indeed, inhibition of caspase 8 using a peptide inhibitor (Martin et al., 1998), the upstream caspase participating in the Fas pathway, blocked Dex-induced apoptosis, further supporting a possible association between Dex and the Fas pathway in osteocyte apoptosis. However, we failed to detect expression of Fas Ligand in both Dex-treated and untreated cultures, suggesting that if indeed there is activation of the Fas-related pathway in the presence of Dex it is FasL independent. Similar phenomenon has been observed in tumour cell studies, showing that anticancer agents directly promote Fas receptor trimerisation and activation of the FADD/caspase 8 pathway, independently of FasL (Misceau et al., 1999).

BPs suppressed Dex-induced apoptosis in MLO-Y4 osteocytes after 5 hours treatment with Dex, in accordance to previous reports by Plotkin, et al. (Plotkin et al., 1999). Although we do not know the half-life of BPs in in vitro experimental conditions, the pharmacokinetics of these molecules in vivo, might allow them to suppress GC-induced apoptosis of osteocytes for longer periods of time, since they can be retained active in the skeleton until their release, following resorption of the multiple sites in which they were deposited.

Dex-induced apoptosis was prevented by both non N-BPs (CLO), which are metabolized into cytotoxic analogues of ATP and N-BPs (PAM and ALN), which inhibit prenylation through inhibition of FPP synthase (Rogers et al., 1999). The third generation heterocyclic-containing NE11808 was used as well as the structurally similar NE11809 which differs in terms of having a methyl group, which confers reduced inhibition of FPP synthase (Dunford et al., 2001). Both BPs were equally effective inhibitors of death, indicating that prevention of Dex-induced osteocyte apoptosis by BPs does not depend on inhibition of FPP synthase or on structure/activity relations of BP molecules.

ERK 1/2 is associated variously with the induction of proliferative and survival signals (Robinson and Cobb, 1997; Lai et al., 2001; Jamieson and Yamamoto, 2000; Tran et al., 2001). However, in contrast to the known pro-survival effects, ERK is also implicated in cisplatin-induced apoptosis in HeLa cells, brain injury during focal cerebral ischemia and activation-induced cell death of T cells (Wang et al., 2000; Alessandrini et al., 1999; Van den Brink et al., 1999).

Recently, Nishida, et al have reported that YM529, a new bisphosphonate, decreases phosphorylation of ERK1/2 during apoptosis of HL60 cells (Nishida et al., 2003). Nevertheless, Plotkin, et al observed an acute activation of ERK by BPs, which was sustained for 5 minutes during

the pre-treatment period (Plotkin et al., 1999), and suggested that activated ERK is involved in the protective effects of BPs on Dex-induced apoptosis. Our study has also shown activation of ERK by BPs, which peaked at 5 minutes of addition of BPs to osteocyte cultures. However, Plotkin, et al did not measure possible ERK production in response to Dex, as has been noted in other cell types (Jamieson and Yamamoto, 2000). Following on from both studies, our work has investigated the course of ERK activation in order to characterize the effect of Dex on the ERK pathway, during osteocyte apoptosis. In contrast to activation of ERK by BPs during the pre-treatment period, Dex transiently increased the amount of activated ERK1/2 in osteocytes, which remained elevated for the first hour of incubation, and was suggestive of a specific non-genomic effect, involving membrane-bound GC receptors, since activation of cytosolic receptors requires at least 30 minutes (Patschan et al., 2001). Inhibition of ERK by UO126 suppressed Dex-induced osteocyte apoptosis, both in the presence and absence of BPs, indicating that induction of death signals by Dex-activated ERK compared to non-damaging BP-activated ERK is due to either differences in the timing and duration of activation or to the generation of secondary factors by Dex, which render ERK pro- rather than anti-apoptotic. Furthermore, our data indicated a significant reduction in ERK phosphorylation induced by Dex, in the presence of BPs. Variance between the findings of Plotkin et al., in which ERK appears as an anti-apoptotic signal and our current conclusion regarding its positive role in apoptotic death, may be due to differences in experimental conditions between the two studies. Plotkin et al studied apoptosis in serum-replete conditions and ERK under serum free conditions, while we studied both apoptosis (the phenomenon) and ERK phosphorylation in these cells under identical serum-replete conditions. On the other hand, PMA treatment failed to increase the proportion of apoptotic osteocytes when added alone, and did not prevent or enhance the pro-apoptotic stimuli in the presence of Dex, indicating that activation of ERK through other pathways is not sufficient to induce osteocyte apoptosis.

Dex treatment also increased MEK and p90rsk activation at identical times to the activation of ERK, which was however reduced in cultures pre-treated with BPs, whereas levels of c-Raf were not altered compared to control levels, suggesting that Dex is acting downstream of c-Raf or through another isoform of Raf in the signalling pathway involving Raf, MEK and ERK. In contrast to ERK, p38 inhibition did not reduce osteocyte apoptosis, indicating specificity in the pro-apoptotic effects of MAPK family members.

In neuroblastoma cells transfection with activated MEK1 upregulated Fas activity (Goillot et al., 1997), while in T cells, during activation-induced cell death, transfection of a dominant negative MEK1 inhibited FasL expression (Van den Brink et al., 1999). In our study, inhibition of ERK in experiments using the Fas/CD95 antibody reduced the Dex-induced Fas activation, whereas upregulation of ERK by PMA did not affect Fas levels, indicating that production of Fas is closely associated to the pro-apoptotic signals induced by Dex. In addition, prevention of Dex-induced apoptosis by non N-BPs and N-BPs also decreased Fas expression, supporting the importance of Fas in the death response and pointing to the existence of an additional factor associated with Dex-treatment that might enable the co-operation between ERK and Fas pathways during the induction of osteocyte apoptosis. In conclusion, inhibition of Dex-induced osteocyte apoptosis by BPs was independent of the FPP synthase pathway associated with strongly anti-resorptive molecules, suggesting that BPs might in principal by modifying the structure or conformation of the R2 side chain, be independently applied to affect osteoclast activity or osteocyte survival, providing therapeutic approaches for various bone diseases induced by glucocorticoids.

Acknowledgements

We are grateful to Prof. Mike Rogers for supplying the BPs PAM, ALN and CLO and for his valuable comments on the manuscript and to Prof. Lynda Bonewald for supplying the murine osteocyte-like cell line MLO-Y4. This study was supported by SHEFC grant number R36230.

References

Aarden, E.M., Wassenaar, A.M., Alblas, M.J., Nijweide, P.J., 1996. Immunocytochemical demonstration of extracellular matrix proteins in isolated osteocytes. Histochemistry and Cell Biology 106, 495–501.

Alessandrini, A., Namura, S., Moskowitz, M., Bonventre, J., 1999. MEK1 protein kinase inhibition protects against damage resulting from focal cerebral ischemia. Proceedings of the National Academy of Sciences 96, 12866–12869.

Ashkenazi, A., Dixit, V.M., 1998. Death Receptors: signalling and modulation. Science 281, 1303–1308.

Ashwell, J.D., Lu, F.W.M., Vacchio, M.S., 2000. Glucocorticoids in T cell development and function. Annual. Review of Immunology 18, 309–345.

Cuenda, A., Rouse, J., Doza, Y., Meier, R., Cohen, P., Gallagher, T., Young, P., Lee, J., 1995. SB 203580 is a specific inhibitor of a MAP kinase homologue which is stimulated by cellular stresses and interleukin-1. FEBS Letters 364, 229–233.

Dunford, J.E., Thomsom, K., Coxon, F.P., Luckman, S.P., Hahn, F.M., Poulter, C.D., Ebetino, F.H., Rogers, M.J., 2001. Structure-activity relationships for inhibition of farnesyl diphosphate synthase in vitro and inhibition of bone resorption in vivo by nitrogen-containing bisphopshonates. The Journal of Pharmacology and Experimental Therapeutics 297 (2), 235–242.

Favata, M., Horiuchi, K., Manos, E., Daulerio, A., Stradley, D., Feeser, W., Van Dyk, D., Pitts, W., Earl, R., Hobbs, F., et al., 1998. Identification of a novel inhibitor of mitogen-activated protein kinase kinase. Journal of Biological Chemistry 273, 18623–18632.

Goillot, E., Raingeaud, J., Ranger, A., Tepper, R., Davis, R., Harlow, E., Sanchez, I., 1997. Mitogen activated protein kinase-mediated Fas apoptotic signalling pathway. Proceedings of the National Academy of Sciences 94 (7), 3302–3307.

Hamdy, N.A.T., 1997. Pathophysiology of glucocorticoid-induced osteoporosis. Glucocorticoids and Bone: the Clinical Problem, Boerhaave Committee for Postgraduate Education of medicine. Leiden University, The Netherlands, pp. 11–17.

Jamieson, C.A.M., Yamamoto, K.R., 2000. Crosstalk pathway for inhibition of glucocorticoid-induced apoptosis by T cell receptor signalling. Proceedings of the National Academy of Sciences 97 (13), 7319–7324.

Kato, Y., Windle, J., Koop, B., Mundy, G., Bonewald, L., 1997. Establishment of an osteocyte-like cell line, MLO-Y4. Journal of Bone and Mineral Research 12, 2014–2023.

Lai, C.-F., Chaudhary, L., Fausto, A., Halstead, L.R., Ory, D.S., Avioli, L.V., Cheng, S.-L., 2001. Erk is essential for growth, differentiation, integrin expression, and cell function in human osteoblastic cells. Journal of Biological Chemistry 276 (17), 14443–14450.

Lee, D., Long, S., Adams, J., Chan, G., Vaidya, K., Francis, T., Kikly, K., Winkler, J., Sung, C., Debouck, C., et al., 2000. Potent and selective nonpeptide inhibitors of caspases 3 and 7 inhibit apoptosis and maintain cell functionality. Journal of Biological Chemistry 275 (21), 16007–16014.

Martin, D., Siegel, R., Zheng, L., Lenardo, M., 1998. Membrane oligomerisation and cleavage activates the caspase-8 (FLICE/MACHa1) death signal. Journal of Biological Chemistry 273 (8), 4345–4349.

Misceau, O., Solary, E., Hammann, A., Dimanche-Boitrel, M., 1999. Fas ligand-independent, FADD-mediated activation of the fas death pathway by anticancer drugs. Journal of Biological Chemistry 274, 7987–7992.

Nijweide, P.J., Mulder, R.J.P., 1986. Identification of osteocytes in osteoblast-like cultures using a monoclonal antibody specifically directed against osteocytes. Histochemistry 84, 342–347.

Nishida, S., Fujii, Y., Yoshioka, S., Kikuichi, S., Tsubaki, M., Irimajiri, K., 2003. A new bisphosphonate, YM529 induces apoptosis in HL60 cells by decreasing phosphorylation of single survival signal ERL. Life Sciences 73 (21), 2655–2664.

Noble, B., Milne, J., Loveridge, N., 1995. Apoptosis in growing rat bone: preliminary studies. Bone 16, 689.

Noble, B., Stevens, H., Reeve, J., Loveridge, N., 1997. Identification of apoptotic changes in osteocytes in normal and pathological human bone. Bone 20 (3), 273–282.

Patschan, D., Loddenkemper, K., Buttgereit, F., 2001. Molecular mechanisms of glucocorticoid-induced osteoporosis. Bone 29 (6), 498–505.

Plotkin, L.I., Weintein, R.S., Parfitt, A.M., Roberson, P.K., Manolagas, S.C., Bellido, T., 1999. Prevention of osteocytes and osteoblast apoptosis by bisphosphonates and calcitonin. Journal of Clinical Investigation 104, 1363–1374.

Robinson, M., Cobb, M., 1997. Mitogen-activated protein kinase pathways. Current Opinion in. Cell Biology 9, 180–186.

Rodan, G.A., 1998. Mechanisms of action of bisphosphonates. Annual Review of Pharmacology and Toxicology 38, 375–388.

Rogers, M.J., Frith, C., Luckman, P., Coxon, F.P., Benford, H.L., Monkkonen, J., Auriola, S., Chilton, K.M., Russel, R.G.G., 1999. Molecular mechanisms of action of bisphosphonates. Bone 24 (5), 73S–79S.

Schmidt, M., Lugering, N., Lugering, A., Pauels, H., Schulze-Osthoff, K., Domschke, W., Kucharzik, T., 2001. Role of the CD95/CD95 Ligand system in glucocorticoid-induced monocyte apoptosis. Journal of Immunology 166, 1344–1351.

Tran, S.E.F., Holstrom, T.H., Ahonen, M., Kahari, V.-L., Eriksson, J.E., 2001. MAPK/ERK overrides the apoptotic signalling from Fas, TNF, and TRAIL receptors. Journal of Biological Chemistry 276 (19), 16484–16490.

Van den Brink, M., Kapeller, R., Pratt, J., Chang, J., Burakoff, S., 1999. The extracellular signal-regulated kinase pathway is required for activation-induced cell death of T cells. Journal of Biological Chemistry 274 (16), 11178–11185.

Van der Plas, A., Nijweide, P.J., 1992. Isolation and purification of osteocytes. Journal of Bone and Mineral Research 7, 389–396.

Wang, X., Martindale, J., Holbrook, N., 2000. Requirement for ERK activation in cisplatin-induced apoptosis. Journal of Biological Chemistry 275 (50), 39435–39443.

Weinstein, R.S., Jilka, R.L., Parfitt, A.M., Manolagas, S.C., 1998. Inhibition of osteoblastogenesis and promotion of apoptosis of osteoblasts and osteocytes by glucocorticoids. Journal of Clinical Investigation 102 (2), 274–282.

Zar, J.H., 1984. Biostatistical Analysis, second ed. Prentice-Hall International Editions. Chapter 15.